Towards an intranasal influenza vaccine

Based on whole inactivated influenza virus with *N,N,N*-trimethyl chitosan as adjuvant

ISBN/EAN 978-94-90588-01-4

Department of Pharmaceutics, Utrecht Institute for Pharmaceutical Sciences, Utrecht University, Utrecht, The Netherlands

Cover design: Riesenkind, studio voor grafisch ontwerp, 's-Hertogenbosch, The Netherlands
Manuscript layout: Louis Versteeg, Digit@l Xpression, Bennekom, The Netherlands
Printing: Ridderprint, Ridderkerk, The Netherlands

Printing of this thesis was financially supported by the Schering-Plough corporation.

Towards an intranasal influenza vaccine

Based on whole inactivated influenza virus with *N,N,N*-trimethyl chitosan as adjuvant

Op weg naar een intranasaal griepvaccin
op basis van geïnactiveerd griepvirus geadjuveerd met *N,N,N*-trimethylchitosan
(met een samenvatting in het Nederlands)

Proefschrift

ter verkrijging van de graad van doctor aan de Universiteit Utrecht
op gezag van de rector magnificus, prof.dr. J.C. Stoof,
ingevolge het besluit van het college voor promoties
in het openbaar te verdedigen op maandag 21 december 2009
des ochtends te 10.30 uur

door

Niels Hagenaars

geboren op 1 september 1980 te Delft

Promotoren:	Prof.dr. H. Vromans
	Prof.dr. W. Jiskoot
Co-promotor:	Dr. E. Mastrobattista

De ontdekking

K. Schippers

Als je goed om je heen kijkt
zie je dat alles gekleurd is

Voor mijn ouders

Table of Contents

Appendices

Chapter 1

General introduction

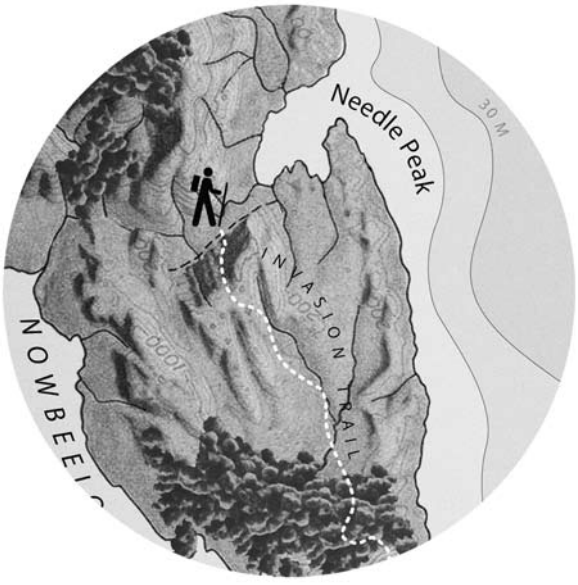

The influenza virus

The influenza virus is a negative sense, single stranded RNA virus from the family of orthomyxoviridae that was first identified in humans in 1933 [1]. The influenza viruses can be subdivided into the influenza A, B and C genera. Influenza viruses are classified by a uniform code, like Influenza A/Puerto Rico/8/34 in which A is the virus type, followed by the place of isolation, strain serial number and year of isolation [2, 3], as illustrated in Figure 1.

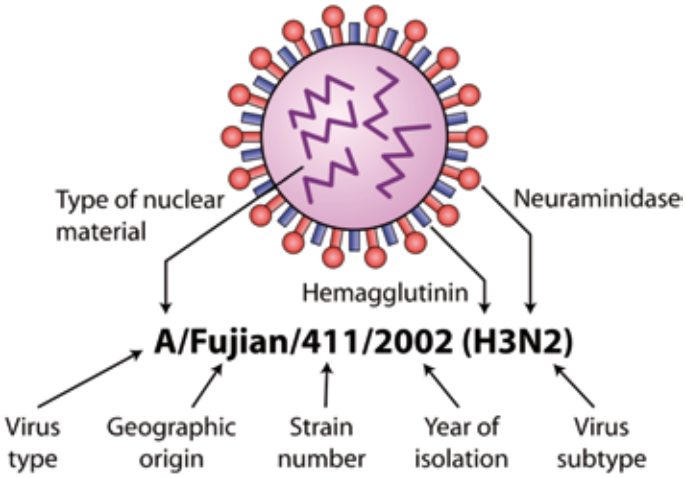

Figure 1: The nomenclature of influenza viruses

Influenza A viruses are the most virulent of the human influenza viruses and cause the most severe disease in humans and animal species. They are further subdivided into different serotypes, based on the antibody responses that are elicited against the hemagglutinin (HA) and neuraminidase (NA), the two most abundant surface proteins of the influenza virus (eg. Influenza A/Puerto Rico/8/34 (H1N1)).

The influenza A virus is a pleiotropic, enveloped virus [4]. The outer membrane consists of a lipid bilayer derived from the host cell [5] with the spike proteins HA and NA sticking out of the membrane [6] as trimers [7] and tetramers [8], respectively. Another, smaller protein, called M2 protein, is also present in the viral membrane [9, 10] and acts as an ion channel [11]. Within the enveloped virus, a layer of matrix protein (M1) forms a capsid that covers the viral genome [12]. This genome, bound to ribonuclear proteins, consists of 8 segments of single stranded, negative sense RNA encoding the 11 proteins of influenza. In contrast to Influenza B and C viruses, which are almost exclusively found in humans, Influenza A viruses can be found in a wide range of species, including humans, pigs, horses, aquatic mammals and birds. Whereas all mammalian species are host for a subset of HA subtypes (e.g. H1; H2 and H3 in humans), almost all known influenza A subtypes can be found in aquatic birds, which are considered the natural reservoir for all influenza viruses.

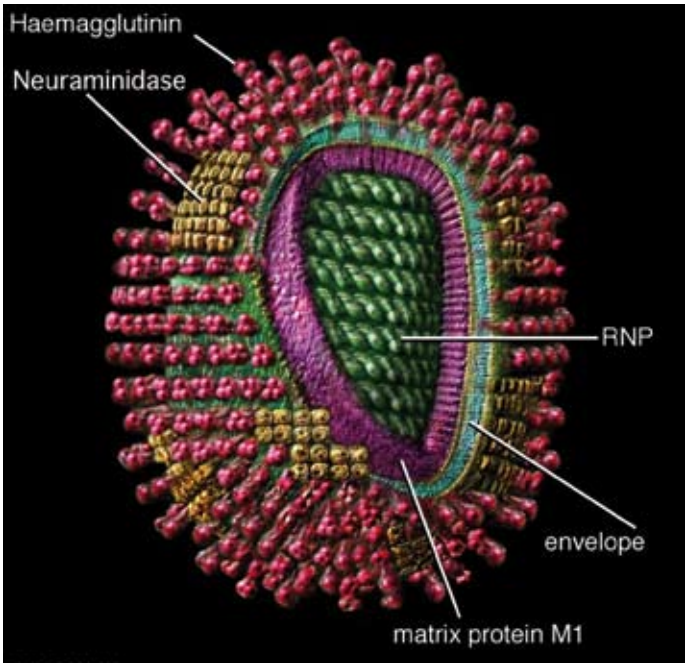

Figure 2: Schematic representation of the structure of influenza virus

Seasonal influenza epidemics and pandemics

Seasonal outbreaks of influenza, commonly known as "the flu", are caused by influenza viruses that are circulating through the human population, peaking each winter season. At this moment, the yearly influenza outbreaks are mainly caused by circulating Influenza A H3N2, H1N1 and Influenza B virus strains that undergo antigenic drift through the accumulation of point mutations in the surface proteins, allowing the virus to escape from the host's existing immunity, as illustrated in Figure 3. These viruses cause yearly epidemics with varying severity. These yearly influenza outbreaks are a substantial cause of morbidity and mortality worldwide each year, especially in the elderly and people with underlying diseases, such as chronic pulmonary, cardiovascular, renal, hepatic, hematologic or metabolic disorders, and people who are immunocompromised [13]. A more dramatic change in surface antigens called antigenic shift can be the result of genetic reassortment of two or more virus strains that are infecting the same cell. When two virus strains infect the same cell, this cell may produce new viruses that contain a combination of the genes of the two original strains. In this way, reassorted viruses with a new combination of surface antigens can be formed. When this occurs in a host that can be infected by influenza viruses from different species, like avian and human influenza strains, (as illustrated in Figure 4), new influenza viruses can be introduced to the human population, against which no pre-existing immunity exists.
Such an introduction can potentially cause a pandemic. Influenza pandemics have occurred every 10-40 years in the last century, with the "Spanish Flu" of 1918 being the most severe recorded

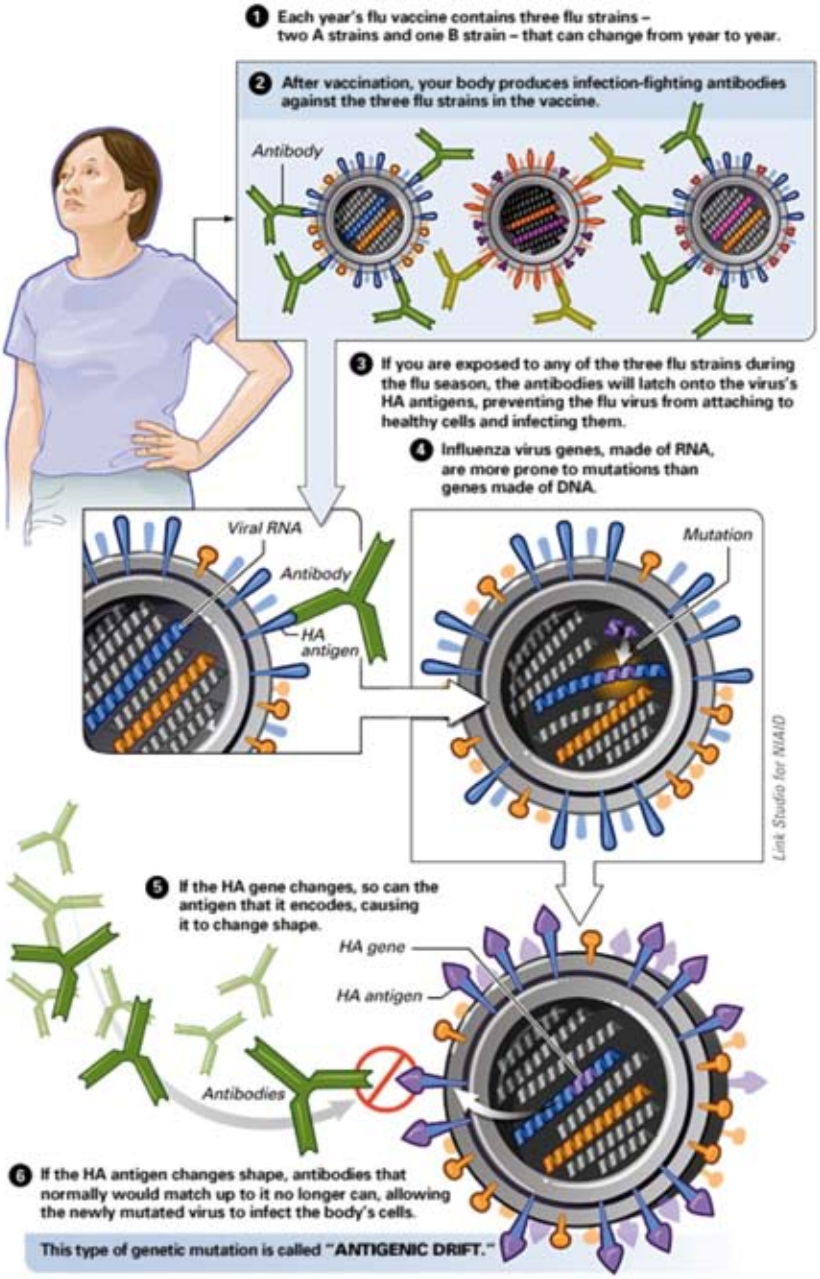

Figure 3. Antigenic drift

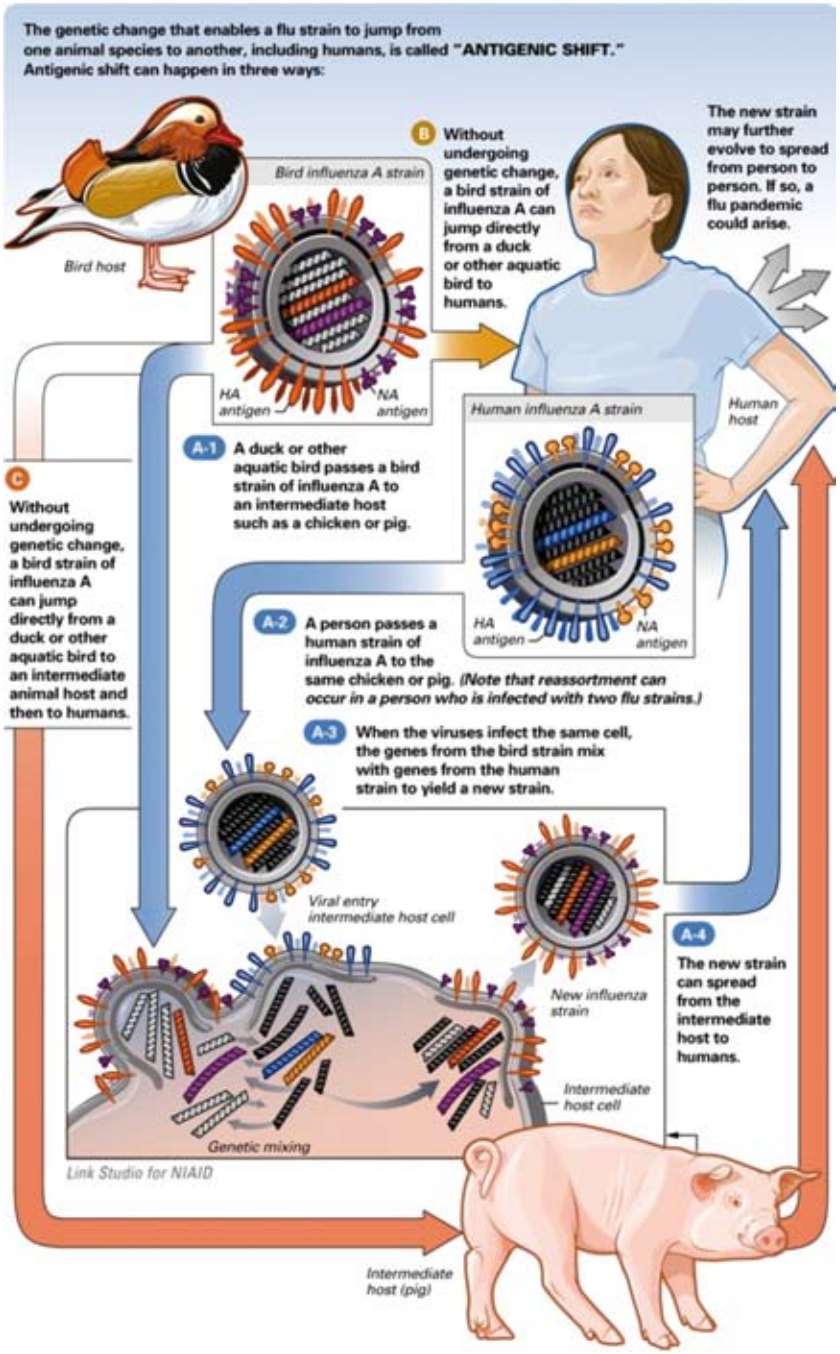

Figure 4: Antigenic shift

pandemic. The 1918 Spanish flu could have such a devastating effect, as the human population was immunologically naïve (i.e. unprotected), and the virus was highly pathogenic in combination with an ability to replicate well in a human host.

The new H1N1 influenza virus of swine origin that was introduced in the human population this year in Mexico [14], is currently rapidly spreading worldwide and was declared a pandemic by the WHO in June 2009. This pandemic strain, with genes from swine, human and avian derived origin [15], is apparently very fit for the human host. However, it is not very pathogenic [16, 17]. Therefore, it is likely that this pandemic will be relatively mild. In contrast to the mild, new H1N1 influenza virus, the H5N1 avian influenza virus that was first identified in China in 1996, is highly pathogenic to humans upon infection, resulting in a mortality rate of 60% [18]. This virus, however, is not very compatible with the human host, as evidenced by low human to human transmission thus far. The pandemic threat by H5N1 can not be ruled out, as the virus may acquire the ability to spread among humans without losing its pathogenicity.

Taken altogether, the impact of a potential pandemic virus depends on its pathogenicity and its compatibility with the human host. When a highly pathogenic and compatible new virus emerges in the human population, the impact on worldwide health, economy and everyday life can be immense. It is however, unknown what factors determine these characteristics of newly emerging viruses.

The history of influenza vaccination

Although antiviral drugs exist for the treatment of influenza, vaccination provides the best form of protection and has been shown to be highly cost-efficient [19-22]. Already in the 1930s, the first vaccination studies were done in humans [23] and in the early 40s the efficacy of influenza vaccination was unequivocally demonstrated [24, 25]. In the following years vaccines consisting of inactivated influenza viruses were administered parenterally and hemagglutination inhibition (HI) assays to assess the protective efficacy of a vaccination were developed [26]. In the 1940s, it was noticed that some persons were protected despite low systemic antibody titers [27], likely by the presence of virus-inactivating substances, later identified as sIgA [28]. In the 1960s, the adverse reaction of whole inactivated virus vaccines in small children after i.m. administration was the incentive for the development of split and subunit vaccines [29, 30], which showed less reactogenicity but were also less immunogenic [31]. At the same time, it became clear that local vaccine administration via the nasal route induced more respiratory antibodies, mainly sIgA, than i.m. vaccination [32].

Currently, most influenza vaccines on the market are split or subunit vaccines produced on henn's eggs in the same manner as the 1960s. It was discovered by Kilbourne, that influenza strains could be genetically reassorted with a high-growth Influenza A/PR/8/34 strain to optimize their growth for vaccine production, but with HA and NA variants of the circulating variant strains [33]. This technique was applied for most influenza vaccines on the market from the 1970s. Genetic reassortment allowed fast and high yield production of vaccines that closely match the circulating viruses that continuously undergo antigenic drift. The specific virus strains included in the vaccines

are adjusted each year for the upcoming influenza season upon recommendation of the WHO.

Improvement of influenza vaccines

There are several drawbacks to the current seasonal influenza vaccines. First of all, the production in fertilized henn's eggs requires extensive planning because of the large amounts of egg's that are needed, which leads to problems in upscaling when the vaccine demand suddenly increases [34]. Furthermore, the procurement of henn's eggs is sensitive to avian infectious diseases, and impurities in egg-based vaccines can lead to allergic reactions.,Additionally, egg-grown viruses do not antigenically match the isolated circulating virus strain due to changes in glycosylation patterns [35], potentially leading to decreased protection. Another drawback of current seasonal split and subunit vaccines only provide a narrow protection against homologous virus strains. Therefore, protection by these vaccines is very sensitive to antigenic drift and every season the selection of vaccine strains has to be critically selected to match the circulating virus strains as closely as possible. Furthermore, the efficacy of these vaccines is generally lower in elderly [36], the most important target population. Finally, these vaccines require trained personnel for administration and their invasive character is a hurdle in increasing vaccine coverage.

Advances in immunology, biotechnology, virology and pharmaceutical sciences have opened new opportunities to further optimize these influenza vaccines. Spurred by the recent pandemic threats of highly pathogenic avian H5N1 flu and the outbreak of the pandemic H1N1 2009 flu, the development of improved seasonal and pandemic vaccines have gained interest from pharmaceutical companies and health institutions [37, 38]. Vaccine developers have focused on increased, cell-based production capacity [34, 39]; antigen sparing strategies [38, 40, 41] and the induction of broader protection [42, 43].

In parallel, the efforts to control seasonal and pandemic influenza outbreaks through vaccination campaigns [44-47] and pandemic preparedness plans have increased [48-50]. Nevertheless, target vaccination coverage rates for the seasonal flu set by the WHO for at-risk populations, e.g. 75% for the elderly, are not realized in most European countries [51, 52]. At high vaccination coverage rates, not only vaccinees are protected but herd protection can be established by reducing the capabilities for influenza to spread in the non-vaccinated population.

Non-invasive immunization routes

Among the numerous efforts to improve influenza vaccination, the development of vaccines for alternative routes of administration is a promising approach, mostly for their noninvasive character [53], but also for the potential induction of mucosal immune responses. Among the non-invasive immunization routes, dermal (e.g. [54-58]), sublingual (e.g [59]), oral (e.g. [60-62]), pulmonary (e.g. [63]), nasal (e.g [64-69]), and ocular (e.g. [70]) routes for influenza vaccination have been described.

From these non-invasive routes, the nasal route is particularly attractive for vaccine administration.

Intranasal vaccines can induce strong mucosal immune responses, in the form of sIgA (e.g. [71]). Mucosal immunity may provide broader protection against influenza than systemic humoral antibodies [68, 72-75] and is rarely developed after parenteral vaccination. Furthermore, the nose is easily accessible, the administration is needle-free and there is no need for trained personnel. It is likely that nasal influenza vaccines will receive greater acceptance than influenza vaccines administered via i.m. injection, owing to their nonvasive character. In this way, nasal vaccines may also contribute to reaching the target vaccination coverage rates set by the WHO.

Nasal influenza vaccines

The influenza vaccines that for i.n. administration can be divided in live, attenuated (cold-adapted) influenza virus (LAIV) vaccines and inactivated influenza vaccines. The main objective for influenza vaccine manufacturers is to develop an influenza vaccine formulation that has the ideal safety/efficacy profile in all target populations, including the elderly.

LAIV

LAIV vaccines for intranasal administration have been developed in Russia in the 1960s and since then have been successfully used in millions of individuals over the last decades [76]. More recently, a similar LAIV vaccine, based on a different master donor virus, has been successfully introduced to the American market. This LAIV vaccine is an intranasal vaccine based on live, reassorted, cold-adapted, temperature sensitive, influenza virus that can only replicate in limited amounts at lower temperatures in the upper respiratory tract. LAIV can induce mucosal humoral and cellular immune responses in addition to systemic antibody response [77], in a similar way to natural infection. The induction of sufficient HI titers, currently set as a correlate of protection for i.m. vaccines, were not reached [78, 79]. As a result, extensive testing for clinical effectiveness in a large number of individuals was necessary for marketing approval. These tests revealed that LAIV is comparable or even more effective than conventional intramuscular vaccines in healthy individuals and children with respect to clinical outcome, regardless of low HI titers [80].

There are two major concerns with the use of LAIV. The first one is that the live attenuated influenza virus can undergo genetic reversion into a transmissible, pathogenic virus, either by mutation or by reassortment with circulating wildtype influenza viruses [81, 82]. However, despite the extensive use of LAIV, no cases of pathogenic reversion have been described so far. It is highly unlikely that LAIV will reverse into a potentially harmful virus [83].

The other safety concern is that heavily immunocompromised patients are much more sensitive to LAIV. Therefore, vaccination of these patients is contraindicated and concerns have been raised about vaccinating people that are in close contact with immunocompromized patients. A high rate of shedding of LAIV and a low rate of secondary transmissions in children attending daycare have been described [84, 85]. It is therefore advised that health care workers and other close contacts of heavily immunocompromised patients should be vaccinated with an inactivated influenza vaccine

[86, 87]. Taken altogether, these concerns could be the explanation that the LAIV vaccine has not gained widespread acceptance by prescribers [78, 83, 88]. Recent studies in immunocompromised ferrets, however, suggest that LAIV may also be safe and immunogenic in immunocompromised patients [89].
The LAIV vaccine has not been registered for use in patients above 50 years old, because, the efficacy of LAIV has not been demonstrated in elderly yet. This may be a consequence of overattenuation of the virus strain [90], resulting in a decreased efficacy, especially in elderly with a senescent immune system. In the case of LAIV, the balance of safety/efficacy could be tailored by changing the degree of attenuation, although this may be a difficult, trial and error based approach, as evidenced from the unsuccesful attempts to develop a safe and effective live, attenuated respiratory syncytial virus (RSV) vaccine [91]. It is not clear yet whether this can result in a safe and effective influenza vaccine for the elderly, the most important at risk target population for influenza vaccination.

Inactivated influenza vaccines for i.n. immunization

The other group of i.n. influenza vaccines are based on antigens from inactivated influenza virus. In general, inactivated vaccines, especially soluble proteins, are not immunogenic enough to induce strong immune responses. Therefore, immunostimulatory adjuvants and/or delivery systems have been used to develop a vaccine formulation that is both safe and effective. Several promising results have been obtained in preclinical studies with i.n. inactivated influenza vaccines. However, no inactivated influenza vaccine formulation is currently available on the market, likely because of safety issues from the adjuvants that have been used or because the vaccines could not meet the efficacy criteria that were formulated for the parenteral vaccines. Therefore it is an ongoing challenge to develop an i.n. inactivated vaccine formulation that is safe and effective.
Immunostimulatory molecules can strongly enhance the immunogenicity of i.n. vaccination and the growing knowledge of the innate immune system raised the interest in this group of adjuvants. Toxin-based adjuvants, cytokines and stimulants of the innate immune system, like Toll-like receptor (TLR) ligands, have all shown promising results as nasal vaccine adjuvants. Moreover, the only i.n influenza vaccine that has made it to the market was a virosomal vaccine formulation with *Escherizia coli* (E. coli) enterotoxin. However, it was withdrawn from the market after its use was associated with Bell's palsy [92, 93]. This case stressed the importance of the safety of vaccines. Efforts are being made to develop safer immunostimulatory adjuvants for i.n. vaccines, but none have made it to the market yet.

Another strategy to enhance the potency of inactivated i.n. influenza vaccines is the use of antigen delivery systems that improve the delivery of antigens to the immune system, either by increasing their nasal residence time, protecting antigens against enzymatic degradation, or enhancing antigen uptake from the nasal cavity or by antigen-presenting cells. Influenza virus antigens have been formulated in delivery systems like ISCOMs [94, 95], lipid- [96] and (mucoadhesive) polymer-based, nano- and microparticulate systems [97-100] as well as with solutions of mucoadhesive

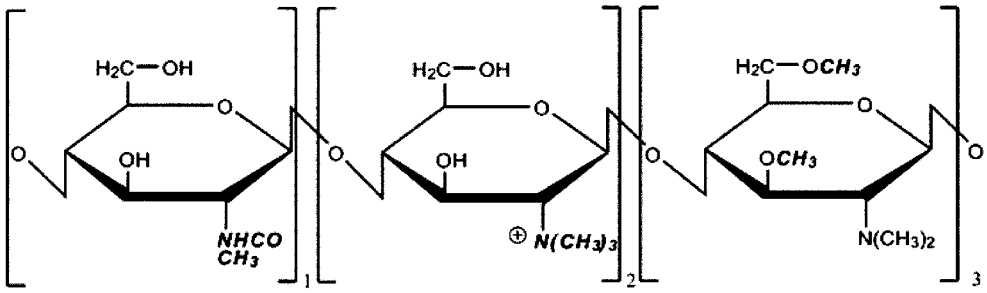

Scheme 1. General structure of TMC. The structural properties of TMC can be characterized by the degree of N-acetylation (DAc) (see block 1), quaternization (DQ) (see block 2), and O-methylation (DOM) (see block 3).

polymers, like chitosan [101, 102]. Chitosan is a mucoadhesive polysaccharide that is obtained from chitin, found in shells of crustaceans, by deacetylation. Although chitosan showed promising results as a mucosal vaccine adjuvant, its insolubility at physiological pH has led to the synthesis of its quaternized derivative *N,N,N*-trimethylchitosan (TMC), which is cationic and water soluble over a wide pH range. In addition to the molecular weight, TMC can be structurally characterized by the degree of quaternization (DQ), the degree of O-methylation (DOM) and degree of N-acetylation (DAc), as shown in Scheme 1. These properties can be varied during synthesis [102-104]. Several studies have shown that TMC can strongly enhance the immunogenicity of mucosal vaccines, including influenza vaccines [102, 105-107]

Previous results show that inactivated influenza vaccines can be effective and safe when formulated with the proper delivery systems. However, a better understanding of the efficacy-determining steps in nasal vaccination is necessary to further improve i.n. vaccine formulations. Furthermore, the mode of action of vaccine delivery systems should be investigated in more detail, which requires a good physicochemical characterization of the vaccine formulations.

Aim and outline of thesis

The development of a safe and effective i.n. influenza vaccine for human use is still an ongoing challenge. In case of developing LAIV vaccines, the key is to find the ideal balance between efficacy and attenuation, which may be very difficult. In comparison, for the development of an inactivated i.n. influenza vaccine a multitude of approaches are possible which may provide the ideal balance between efficacy and safety. This, however, requires a better understanding of the mechanism of action of these adjuvants, which has led to the research described in this thesis.

The principal aim of this work is to rationally design an inactivated influenza vaccine for i.n. administration, as outlined in the following section.

In order to facilitate this principle aim, several subaims were formulated. First, the main physiological hurdles that limit the immunogenicity of i.n. vaccines should be identified. Next, it should be investigated wether vaccine composition and formulation with adjuvants can overcome

these hurdles and result in a promising platform for further vaccine development. Finally, the mode of action of these improved i.n. influenza vaccines should be studied.

Thesis outline

Chapter 2 reviews the literature describing the main hurdles of nasal vaccine delivery and provides a roadmap for the rational design of nasal vaccines. Recent progress in the field of nasal delivery of inactivated vaccines is described and emerging opportunities for improving nasal vaccines are discussed.

Chapter 3 describes a direct comparison of whole inactivated influenza virus (WIV), split vaccine, subunit vaccine and virosomes, in a murine vaccination-challenge model. The influence of composition, spatial organization and route of administration on the immunogenicity is studied with these four commonly used influenza vaccines. Vaccine formulations are prepared and characterized and mice are vaccinated intramuscularly (i.m.) or intranasally (i.n.) with these vaccine formulations. Humoral immune responses are determined in serum and nasal washes collected 3 weeks after prime and boost vaccination. The protective efficacy of the vaccination schedule is determined by a homologous aerosol challenge.

In **chapter 4**, WIV is formulated with N,N,N-trimethylchitosan (TMC) to evaluate the feasibility of TMC-adjuvanted WIV vaccines for i.n. administration. The TMC-WIV formulations are physicochemically characterized and administered to mice. The immunogenicity and protection of the vaccination are evaluated.

In **chapter 5,** WIV is formulated with different TMCs with varying DOM, DQ and DAc and at different TMC:WIV (w/w) ratios. These formulations are characterized physicochemically and tested as i.n. vaccines in a murine vaccination-challenge model to determine the role of these properties on the adjuvant properties of TMC.

To further understand the mechanisms by which TMCs exert their adjuvant effect, plain WIV and TMC-WIV formulations are visualized after i.n. administration using *in vivo* optical imaging and immunohistochemistry on nasal cross-sections, as described in **chapter 6**. The nasal clearance and distribution of these vaccines are compared and related to the *in vivo* adjuvant properties. The local toxicity of plain WIV and TMC-WIV formulation is also evaluated.

In the **appendix to chapter 6,** additional studies are described to explain the increase in fluorescence intensity of fluorescently labeled WIV formulations in the stomach and to a lesser extent in the nose, as observed in the optical imaging experiments in chapter 6.

The role of reacetylation on the adjuvanticity of TMC is studied in **Chapter 7.** The effect of

reacetylation of TMC is determined at potentially critical steps in nasal vaccination, including degradation by mucosal enzymes, nasal clearance, distribution in the nasal cavity, cellular uptake and interaction with dendritic cells.
The structural properties of TMC and the TMC-WIV ratio may also influence the colloidal stability of the nanoparticulate TMC-WIV vaccine formulations, which is addressed in **chapter 8**. Also, the influence of ionic strength on the colloidal stability is studied and the feasibility of freeze drying TMC-WIV vaccines is assessed.

Chapter 9 summarizes the findings and conclusions of this thesis and discusses the perspectives for further research towards inactivated influenza vaccines for intranasal administration.

References

[1] Smith W, Andrewes C, Laidlaw P. A virus obtained from influenza patients. Lancet 1933;222(5732):66-68.

[2] WHO. WHO expert committee on Influenza. World Health organization technical report series 1953(64).

[3] A revision of the system of nomenclature for influenza viruses: a WHO memorandum. Bull World Health Organ 1980;58(4):585-91.

[4] Horne RW, Waterson AP, Wildy P, Farnham AE. The structure and composition of the myxoviruses. I. Electron microscope studies of the structure of myxovirus particles by negative staining techniques. Virology 1960;11:79-98.

[5] Kates M, Allison AC, Tyrell DA, James AT. Origin of lipids in influenza virus. Cold Spring Harb Symp Quant Biol 1962;27:293-301.

[6] Laver WG, Valentine RC. Morphology of the isolated hemagglutinin and neuraminidase subunits of influenza virus. Virology 1969;38(1):105-19.

[7] Wiley DC, Skehel JJ, Waterfield M. Evidence from studies with a cross-linking reagent that the haemagglutinin of influenza virus is a trimer. Virology 1977;79(2):446-8.

[8] Varghese JN, Laver WG, Colman PM. Structure of the influenza virus glycoprotein antigen neuraminidase at 2.9 A resolution. Nature 1983;303(5912):35-40.

[9] Lamb RA, Choppin PW. Identification of a second protein (M2) encoded by RNA segment 7 of influenza virus. Virology 1981;112(2):729-37.

[10] Lamb RA, Zebedee SL, Richardson CD. Influenza virus M2 protein is an integral membrane protein expressed on the infected-cell surface. Cell 1985;40(3):627-33.

[11] Pinto LH, Holsinger LJ, Lamb RA. Influenza virus M2 protein has ion channel activity. Cell 1992;69(3):517-28.

[12] Schulze IT. The structure of influenza virus. II. A model based on the morphology and composition of subviral particles. Virology 1972;47(1):181-96.

[13] Center for Disease control and prevention. Recommendations for Using TIV and LAIV During the 2009–10 Influenza Season. Morbidity and Mortality Weekly Report 2009(58):1-52.

[14] Dawood FS, Jain S, Finelli L, Shaw MW, Lindstrom S, Garten RJ, et al. Emergence of a novel swine-origin influenza A (H1N1) virus in humans. N Engl J Med 2009;360(25):2605-15.

[15] Smith GJ, Vijaykrishna D, Bahl J, Lycett SJ, Worobey M, Pybus OG, et al. Origins and evolutionary genomics of the 2009 swine-origin H1N1 influenza A epidemic. Nature 2009;459(7250):1122-5.

[16] Gilsdorf A, Poggensee G. Influenza A(H1N1)v in Germany: the first 10,000 cases. Euro Surveill 2009;14(34).

[17] Itoh Y, Shinya K, Kiso M, Watanabe T, Sakoda Y, Hatta M, et al. In vitro and in vivo characterization of new swine-origin H1N1 influenza viruses. Nature 2009;460(7258):1021-5.

[18] Gambotto A, Barratt-Boyes SM, de Jong MD, Neumann G, Kawaoka Y. Human infection with highly pathogenic H5N1 influenza virus. Lancet 2008;371(9622):1464-75.

[19] Drummond M, Chevat C, Lothgren M. Do we fully understand the economic value of vaccines? Vaccine 2007;25(32):5945-57.

[20] Nichol KL. The efficacy, effectiveness and cost-effectiveness of inactivated influenza virus vaccines. Vaccine 2003;21(16):1769-75.

[21] Postma MJ, Baltussen RM, Heijnen ML, de Berg LT, Jager JC. Pharmacoeconomics of influenza vaccination in the elderly: reviewing the available evidence. Drugs Aging 2000;17(3):217-27.

[22] Postma MJ, Jansema P, van Genugten ML, Heijnen ML, Jager JC, de Jong-van den Berg LT. Pharmacoeconomics of influenza vaccination for healthy working adults: reviewing the available evidence. Drugs 2002;62(7):1013-24.

[23] Francis Tj, Magill T. The Antibody response of human subjects vaccinated woth the virus of human influenza J Exp Med 1937;65:251-59.

[24] Francis T, Salk JE, Pearson HE, Brown PN. Protective Effect of Vaccination against Induced Influenza A. J Clin Invest 1945;24(4):536-46.

[25] Salk JE, Pearson HE, Brown PN, Francis T. Protective Effect of Vaccination against Induced Influenza B. J Clin Invest 1945;24(4):547-53.

[26] Hirst G. The quantitative determinationof influenzavirus and antibodies by means of red cell agglutination. J Exp Med 1942;75(1):49-64.

[27] Francis T, Jr. , Brightman IJ. Virus-inactivating capacity of nasal secretions in the acute and convalescent stages of influenza. Proc Soc Exp Biol

Med 1941;48:116-17.

[28] Bellanti JA, Artenstein MS, Buescher EL. Characterization of Virus Neutralizing Antibodies in Human Serum and Nasal Secretions. J Immunol 1965;94:344-51.

[29] Brandon FB, Barrett CD, Jr., Hook AE, Lease GO. Human febrile response to influenza virus or its ether isolated hemagglutinins. Proc Soc Exp Biol Med 1967;125(3):683-6.

[30] Davenport FM, Hennessy AV, Brandon FM, Webster RG, Barrett CD, Jr., Lease GO. Comparisons of Serologic and Febrile Responses in Humans to Vaccination with Influenza a Viruses or Their Hemagglutinins. J Lab Clin Med 1964;63:5-13.

[31] Gross PA, Ennis FA, Gaerlan PF, Denson LJ, Denning CR, Schiffman D. A controlled double-blind comparison of reactogenicity, immunogenicity, and protective efficacy of whole-virus and split-product influenza vaccines in children. J Infect Dis 1977;136(5):623-32.

[32] Kasel JA, Fulk RV, Togo Y, Hornick RB, Heiner GG, Dawkins AT, Jr., et al. Influenza antibody in human respiratory secretions after subcutaneous or respiratory immunization with inactivated virus. Nature 1968;218(5141):594-5.

[33] Kilbourne ED, Murphy JS. Genetic studies of influenza viruses. I. Viral morphology and growth capacity as exchangeable genetic traits. Rapid in ovo adaptation of early passage Asian strain isolates by combination with PR8. J Exp Med 1960;111:387-406.

[34] Audsley JM, Tannock GA. Cell-based influenza vaccines: progress to date. Drugs 2008;68(11):1483-91.

[35] Govorkova EA, Kodihalli S, Alymova IV, Fanget B, Webster RG. Growth and immunogenicity of influenza viruses cultivated in Vero or MDCK cells and in embryonated chicken eggs. Dev Biol Stand 1999;98:39-51; discussion 73-4.

[36] Goodwin K, Viboud C, Simonsen L. Antibody response to influenza vaccination in the elderly: a quantitative review. Vaccine 2006;24(8):1159-69.

[37] Hehme N, Colegate T, Palache B, Hessel L. Influenza vaccine supply: building long-term sustainability. Vaccine 2008;26 Suppl 4:D23-6.

[38] Stephenson I, Nicholson KG, Wood JM, Zambon MC, Katz JM. Confronting the avian influenza threat: vaccine development for a potential pandemic. Lancet Infect Dis 2004;4(8):499-509.

[39] Cox MM. Cell-based protein vaccines for influenza. Curr Opin Mol Ther 2005;7(1):24-9.

[40] Lin J, Zhang J, Dong X, Fang H, Chen J, Su N, et al. Safety and immunogenicity of an inactivated adjuvanted whole-virion influenza A (H5N1) vaccine: a phase I randomised controlled trial. Lancet 2006;368(9540):991-7.

[41] Wood J, McCaw J, Becker N, Nolan T, MacIntyre CR. Optimal dosing and dynamic distribution of vaccines in an influenza pandemic. Am J Epidemiol 2009;169(12):1517-24.

[42] Tamura S, Tanimoto T, Kurata T. Mechanisms of broad cross-protection provided by influenza virus infection and their application to vaccines. Jpn J Infect Dis 2005;58(4):195-207.

[43] Carrat F, Flahault A. Influenza vaccine: the challenge of antigenic drift. Vaccine 2007;25(39-40):6852-62.

[44] Peddecord KM, Jacobson IG, Engelberg M, Kwizera L, Macias V, Gustafson KW. Can movie theater advertisements promote health behaviors? Evaluation of a flu vaccination pilot campaign. J Health Commun 2008;13(6):596-613.

[45] Malmvall BE, Franzen I, Abom PE, Hugosson MB. The rate of influenza immunization to people aged 65 years and older was increased from 45% to 70% by a primary health care-based multiprofessional approach. Qual Manag Health Care 2007;16(1):51-9.

[46] Noakes K, Salisbury D. Immunization campaigns in the UK. Curr Top Microbiol Immunol 2006;304:53-70.
[47] Stenqvist K, Hellvin MA, Hellke P, Hoglund D, von Sydow H. Influenza work on the regional level in Sweden: an integrated program for vaccination of risk groups, surveillance and pandemic planning which focuses on the role of the health care worker. Vaccine 2006;24(44-46):6712-6.
[48] Monto AS. The risk of seasonal and pandemic influenza: prospects for control. Clin Infect Dis 2009;48 Suppl 1:S20-5.
[49] Morse SS. The US pandemic influenza implementation plan at six months. Nat Med 2007;13(6):681-4.
[50] (ECDC) It. Pandemic preparedness in the European Union--multi-sectoral planning needed. Euro Surveill 2007;12(2):E070222 1.
[51] Blank PR, Schwenkglenks M, Szucs TD. Influenza vaccination coverage rates in five European countries during season 2006/07 and trends over six consecutive seasons. BMC Public Health 2008;8:272.
[52] Blank PR, Schwenkglenks M, Szucs TD. Vaccination coverage rates in eleven European countries during two consecutive influenza seasons. J Infect 2009;58(6):446-58.
[53] Kersten G, Hirschberg H. Needle-free vaccine delivery. Expert Opin Drug Deliv 2007;4(5):459-74.
[54] Chen D, Endres R, Maa YF, Kensil CR, Whitaker-Dowling P, Trichel A, et al. Epidermal powder immunization of mice and monkeys with an influenza vaccine. Vaccine 2003;21(21-22):2830-6.
[55] Denis F, Alain S, Ploy MC. [New routes of administration: epidermal, transcutaneous mucosal ways of vaccination]. Med Sci (Paris) 2007;23(4):379-85.
[56] Frech SA, Kenney RT, Spyr CA, Lazar H, Viret JF, Herzog C, et al. Improved immune responses to influenza vaccination in the elderly using an immunostimulant patch. Vaccine 2005;23(7):946-50.
[57] Koutsonanos DG, del Pilar Martin M, Zarnitsyn VG, Sullivan SP, Compans RW, Prausnitz MR, et al. Transdermal influenza immunization with vaccine-coated microneedle arrays. PLoS One 2009;4(3):e4773.
[58] Zhu Q, Zarnitsyn VG, Ye L, Wen Z, Gao Y, Pan L, et al. Immunization by vaccine-coated microneedle arrays protects against lethal influenza virus challenge. Proc Natl Acad Sci U S A 2009;106(19):7968-73.
[59] Song JH, Nguyen HH, Cuburu N, Horimoto T, Ko SY, Park SH, et al. Sublingual vaccination with influenza virus protects mice against lethal viral infection. Proc Natl Acad Sci U S A 2008;105(5):1644-9.
[60] Mann JF, Shakir E, Carter KC, Mullen AB, Alexander J, Ferro VA. Lipid vesicle size of an oral influenza vaccine delivery vehicle influences the Th1/Th2 bias in the immune response and protection against infection. Vaccine 2009;27(27):3643-9.
[61] Pang GT, Clancy RL, O'Reilly SE, Cripps AW. A novel particulate influenza vaccine induces long-term and broad-based immunity in mice after oral immunization. J Virol 1992;66(2):1162-70.
[62] Lazzell V, Waldman RH, Rose C, Khakoo R, Jacknowitz A, Howard S. Immunization against influenza in humans using an oral enteric-coated killed virus vaccine. J Biol Stand 1984;12(3):315-21.
[63] Amorij JP, Saluja V, Petersen AH, Hinrichs WL, Huckriede A, Frijlink HW. Pulmonary delivery of an inulin-stabilized influenza subunit vaccine prepared by spray-freeze drying induces systemic, mucosal humoral as well as cell-mediated immune responses in BALB/c mice. Vaccine 2007;25(52):8707-17.
[64] Kasel JA, Hume EB, Fulk RV, Togo Y, Huber M, Hornick RB. Antibody responses in nasal secretions and serum of elderly persons following local or parenteral administration of inactivated influenza virus vaccine. J Immunol 1969;102(3):555-62.
[65] Fukumi H. Experience of nasal application of inactivated influenza vaccine. Dev Biol Stand 1976;33:155-61.
[66] Minor TE, Dick EC, Dick CR, Inhorn SL. Attenuated influenza A vaccine (Alice) in an adult population: vaccine-related illness, serum and nasal antibody production, and intrafamily transmission. J Clin Microbiol 1975;2(5):403-9.
[67] Read RC, Naylor SC, Potter CW, Bond J, Jabbal-Gill I, Fisher A, et al. Effective nasal influenza vaccine delivery using chitosan. Vaccine 2005;23(35):4367-74.
[68] Tamura SI, Asanuma H, Ito Y, Hirabayashi Y, Suzuki Y, Nagamine T, et al. Superior cross-protective effect of nasal vaccination to subcutaneous inoculation with influenza hemagglutinin vaccine. Eur J Immunol 1992;22(2):477-81.

[69] Greenbaum E, Furst A, Kiderman A, Stewart B, Levy R, Schlesinger M, et al. Mucosal [SIgA] and serum [IgG] immunologic responses in the community after a single intra-nasal immunization with a new inactivated trivalent influenza vaccine. Vaccine 2002;20(7-8):1232-9.

[70] Tannock GA, Paul JA, Barry RD. Immunization against influenza by the ocular route. Vaccine 1985;3(3 Suppl):277-80.

[71] Treanor J, Nolan C, O'Brien D, Burt D, Lowell G, Linden J, et al. Intranasal administration of a proteosome-influenza vaccine is well-tolerated and induces serum and nasal secretion influenza antibodies in healthy human subjects. Vaccine 2006;24(3):254-62.

[72] Asahi Y, Yoshikawa T, Watanabe I, Iwasaki T, Hasegawa H, Sato Y, et al. Protection against influenza virus infection in polymeric Ig receptor knockout mice immunized intranasally with adjuvant-combined vaccines. J Immunol 2002;168(6):2930-8.

[73] Asahi-Ozaki Y, Yoshikawa T, Iwakura Y, Suzuki Y, Tamura S, Kurata T, et al. Secretory IgA antibodies provide cross-protection against infection with different strains of influenza B virus. J Med Virol 2004;74(2):328-35.

[74] Brandtzaeg P. Induction of secretory immunity and memory at mucosal surfaces. Vaccine 2007;25(30):5467-84.

[75] Ichinohe T, Tamura S, Kawaguchi A, Ninomiya A, Imai M, Itamura S, et al. Cross-protection against H5N1 influenza virus infection is afforded by intranasal inoculation with seasonal trivalent inactivated influenza vaccine. J Infect Dis 2007;196(9):1313-20.

[76] Kendal AP. Cold-adapted live attenuated influenza vaccines developed in Russia: can they contribute to meeting the needs for influenza control in other countries? Eur J Epidemiol 1997;13(5):591-609.

[77] Petukhova G, Naikhin A, Chirkova T, Donina S, Korenkov D, Rudenko L. Comparative studies of local antibody and cellular immune responses to influenza infection and vaccination with live attenuated reassortant influenza vaccine (LAIV) utilizing a mouse nasal-associated lymphoid tissue (NALT) separation method. Vaccine 2009;27(19):2580-7.

[78] Ambrose CS, Luke C, Coelingh K. Current status of live attenuated influenza vaccine in the United States for seasonal and pandemic influenza. Influenza Other Respi Viruses 2008;2(6):193-202.

[79] Treanor JJ, Kotloff K, Betts RF, Belshe R, Newman F, Iacuzio D, et al. Evaluation of trivalent, live, cold-adapted (CAIV-T) and inactivated (TIV) influenza vaccines in prevention of virus infection and illness following challenge of adults with wild-type influenza A (H1N1), A (H3N2), and B viruses. Vaccine 1999;18(9-10):899-906.

[80] Rhorer J, Ambrose CS, Dickinson S, Hamilton H, Oleka NA, Malinoski FJ, et al. Efficacy of live attenuated influenza vaccine in children: A meta-analysis of nine randomized clinical trials. Vaccine 2009;27(7):1101-10.

[81] Beyer WE, Palache AM, de Jong JC, Osterhaus AD. Cold-adapted live influenza vaccine versus inactivated vaccine: systemic vaccine reactions, local and systemic antibody response, and vaccine efficacy. A meta-analysis. Vaccine 2002;20(9-10):1340-53.

[82] Cox RJ, Brokstad KA, Ogra P. Influenza virus: immunity and vaccination strategies. Comparison of the immune response to inactivated and live, attenuated influenza vaccines. Scand J Immunol 2004;59(1):1-15.

[83] Tosh PK, Boyce TG, Poland GA. Flu myths: dispelling the myths associated with live attenuated influenza vaccine. Mayo Clin Proc 2008;83(1):77-84.

[84] Vesikari T, Karvonen A, Korhonen T, Edelman K, Vainionpaa R, Salmi A, et al. A randomized, double-blind study of the safety, transmissibility and phenotypic and genotypic stability of cold-adapted influenza virus vaccine. Pediatr Infect Dis J 2006;25(7):590-5.

[85] Izurieta HS, Haber P, Wise RP, Iskander J, Pratt D, Mink C, et al. Adverse events reported following live, cold-adapted, intranasal influenza vaccine. Jama 2005;294(21):2720-5.

[86] Kamboj M, Sepkowitz KA. Risk of transmission associated with live attenuated vaccines given to healthy persons caring for or residing with an immunocompromised patient. Infect Control Hosp Epidemiol 2007;28(6):702-7.

[87] Smith NM, Bresee JS, Shay DK, Uyeki TM, Cox NJ, Strikas RA. Prevention and Control of Influenza: recommendations of the Advisory Committee on Immunization Practices (ACIP). MMWR Recomm Rep 2006;55(RR-10):1-42.

[88] Glezen WP. Cold-adapted, live attenuated influenza vaccine. Expert Rev Vaccines 2004;3(2):131-9.

[89] Huber VC, McCullers JA. Live attenuated influenza vaccine is safe and immunogenic in immunocompromised ferrets. J Infect Dis 2006;193(5):677-84.

[90] Wareing MD, Watson JM, Brooks MJ, Tannock GA. Immunogenic and isotype-specific responses to Russian and US cold-adapted influenza a vaccine donor strains A/Leningrad/134/17/57, A/Leningrad/134/47/57, and A/Ann Arbor/6/60 (H2N2) in mice. J Med Virol 2001;65(1):171-7.

[91] Meyer G, Deplanche M, Schelcher F. Human and bovine respiratory syncytial virus vaccine research and development. Comp Immunol Microbiol Infect Dis 2008;31(2-3):191-225.

[92] Couch RB. Nasal vaccination, Escherichia coli enterotoxin, and Bell's palsy. N Engl J Med 2004;350(9):860-1.

[93] Mutsch M, Zhou W, Rhodes P, Bopp M, Chen RT, Linder T, et al. Use of the inactivated intranasal influenza vaccine and the risk of Bell's palsy in Switzerland. N Engl J Med 2004;350(9):896-903.

[94] Coulter A, Harris R, Davis R, Drane D, Cox J, Ryan D, et al. Intranasal vaccination with ISCOMATRIX adjuvanted influenza vaccine. Vaccine 2003;21(9-10):946-9.

[95] Ben Ahmeida ET, Gregoriadis G, Potter CW, Jennings R. Immunopotentiation of local and systemic humoral immune responses by ISCOMs, liposomes and FCA: role in protection against influenza A in mice. Vaccine 1993;11(13):1302-9.

[96] el Guink N, Kris RM, Goodman-Snitkoff G, Small PA, Jr., Mannino RJ. Intranasal immunization with proteoliposomes protects against influenza. Vaccine 1989;7(2):147-51.

[97] von Hoegen P. Synthetic biomimetic supra molecular Biovector (SMBV) particles for nasal vaccine delivery. Adv Drug Deliv Rev 2001;51(1-3):113-25.

[98] Amidi M, Romeijn SG, Borchard G, Junginger HE, Hennink WE, Jiskoot W. Preparation and characterization of protein-loaded N-trimethyl chitosan nanoparticles as nasal delivery system. J Control Release 2006;111(1-2):107-16.

[99] Illum L, Jabbal-Gill I, Hinchcliffe M, Fisher AN, Davis SS. Chitosan as a novel nasal delivery system for vaccines. Adv Drug Deliv Rev 2001;51(1-3):81-96.

[100] Higaki M, Takase T, Igarashi R, Suzuki Y, Aizawa C, Mizushima Y. Enhancement of immune response to intranasal influenza HA vaccine by microparticle resin. Vaccine 1998;16(7):741-5.

[101] Bacon A, Makin J, Sizer PJ, Jabbal-Gill I, Hinchcliffe M, Illum L, et al. Carbohydrate biopolymers enhance antibody responses to mucosally delivered vaccine antigens. Infect Immun 2000;68(10):5764-70.

[102] Boonyo W, Junginger HE, Waranuch N, Polnok A, Pitaksuteepong T. Chitosan and trimethyl chitosan chloride (TMC) as adjuvants for inducing immune responses to ovalbumin in mice following nasal administration. J Control Release 2007;121(3):168-75.

[103] Verheul RJ, Amidi M, van der Wal S, van Riet E, Jiskoot W, Hennink WE. Synthesis, characterization and in vitro biological properties of O-methyl free N,N,N-trimethylated chitosan. Biomaterials 2008;29(27):3642-9.

[104] Verheul RJ, Amidi M, van Steenbergen MJ, van Riet E, Jiskoot W, Hennink WE. Influence of the degree of acetylation on the enzymatic degradation and in vitro biological properties of trimethylated chitosans. Biomaterials 2009;30(18):3129-35.

[105] Amidi M, Romeijn SG, Verhoef JC, Junginger HE, Bungener L, Huckriede A, et al. N-trimethyl chitosan (TMC) nanoparticles loaded with influenza subunit antigen for intranasal vaccination: biological properties and immunogenicity in a mouse model. Vaccine 2007;25(1):144-53.

[106] Amidi M, Pellikaan HC, Hirschberg H, de Boer AH, Crommelin DJ, Hennink WE, et al. Diphtheria toxoid-containing microparticulate powder formulations for pulmonary vaccination: preparation, characterization and evaluation in guinea pigs. Vaccine 2007;25(37-38):6818-29.

[107] Baudner BC, Verhoef JC, Giuliani MM, Peppoloni S, Rappuoli R, Del Giudice G, et al. Protective immune responses to meningococcal C conjugate vaccine after intranasal immunization of mice with the LTK63 mutant plus chitosan or trimethyl chitosan chloride as novel delivery platform. J Drug Target 2005;13(8-9):489-98.

Chapter 2

Rational design of nasal vaccines

Niels Hagenaars[#], Bram Slütter[#], Wim Jiskoot

[#] Authors contributed equally

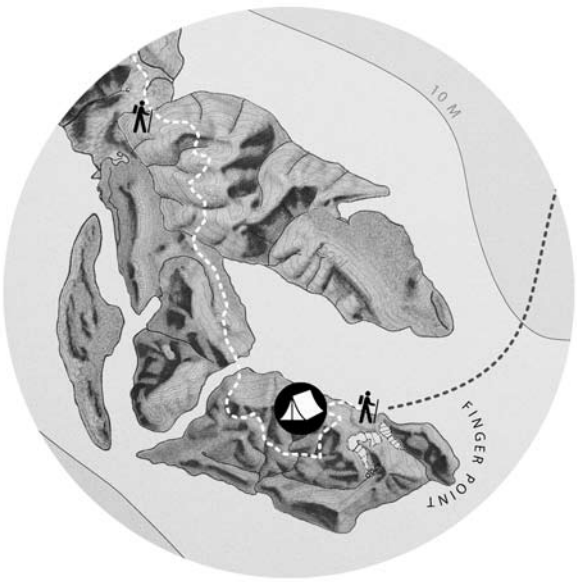

Journal of Drug Targeting 2008; 16(1), 1-17

Abstract

Nasal vaccination is a promising alternative to classical parental vaccination, as it is non-invasive and, in principle, capable of eliciting strong systemic and local immune responses. However, the protective efficacy of nasally administered antigens is often impaired because of delivery problems: free antigens are readily cleared from the nasal cavity, poorly absorbed by nasal epithelial cells, and generally have low intrinsic immunogenicity. In this review paper we describe the main physiological hurdles to nasal vaccine delivery, survey the progress made in technological approaches to overcome these hurdles, and discuss emerging opportunities for improving nasal vaccines. According to current insights, encapsulation of the antigen into bioadhesive (nano) particles is a promising approach towards successful nasal vaccine delivery. These antigen-loaded particles can be tailor made by supplying them with targeting ligands, adjuvants or endosomal escape mediators to form the desired vaccine that provides long-lasting protective immunity.

Introduction

Vaccination is the most cost effective way of fighting infectious diseases. Although some vaccination strategies have been very successful, novel approaches are needed to develop safe and effective vaccines against diseases like HIV/AIDS, malaria, influenza and cancer. Additionally, adverse reactions, like pain, fever, headaches, nausea and allergic reactions have led to declined patient compliance [1-6] and have prompted governments and health organizations to enlarge their funds for research and development of non-invasive vaccines [7-9]. Hence, alternative routes of application have been investigated in the search for safe, effective vaccines (Table I). Among the potential needle free routes, nasal vaccination is particularly attractive. The nasal cavity had been the preferred delivery site until the introduction of the hollow needle in the 19th century [10]. In the search for alternatives to the needle, the interest in nasal vaccination has reemerged.

This paper will review the main physiological hurdles that have to be overcome to render nasal vaccination successful, describe the progress made in the field of nasal delivery of subunit vaccines, and discuss emerging opportunities for improving nasal vaccines.

Nasal vaccination

Advantages and disadvantages of nasal and other types of vaccination are summarized in Table II. Nasal vaccination has several interesting advantages. The nose is easily accessible and the nasal cavity is equipped with a high density of dendritic cells (DC) that can mediate strong systemic and local immune responses against pathogens that invade the human body through the respiratory

Table I. Examples of oral and nasal vaccines currently on the market or at different stages of development.*

Immunization route	Disease	Pathogen	Vaccine type	Phase
Oral	Polio	Poliovirus	Live attenuated	On market
	Typhus	Salmonella typhi	Live attenuated	On market
	Cholera	Vibrio cholerae	Live attenuated	On market
	Acute gastroenteritis	Rotavirus	Live attenuated	On market
	Diarrhea	Escherichia coli	Killed/inactivated	Phase III
	Dysentery	Shigella sonnei	Live attenuated	Phase III
	Peptic ulcer, gastric cancer	Helicobacter pylori	Killed/inactivated	Phase I
	Anthrax	Bacillus anthracis	Subunit vaccine	Preclinical
Nasal	Influenza	Influenza virus	Live attenuated	On market
	Hepatitis B	Hepatitis B virus	Subunit vaccine	Phase I
	Influenza	Parainfluenza virus type 3	Live attenuated	Preclinical
	Anthrax	Bacillus anthracis	Killed/inactivated	Preclinical
	Herpes	Herpes simplex virus	Killed/inactivated	Preclinical
	Bronchiolitis/ Pneumonia	Respiratory syncytial virus	Killed/inactivated	Preclinical
	Cervical cancer	Human papillomavirus	Subunit vaccine	Preclinical
	SARS	SARS corona virus	Subunit vaccine	Preclinical

* Based on (Giudice and Campbell 2006) and (New Vaccines against Infectious Diseases: Research and Development Status 2005)

tract [11, 12, 13]. Mucosal immunity is mediated by secretory immunoglobulin A (sIgA) antibodies, which prevent pathogens from colonizing mucosal epithelia (e.g. respiratory tract, gastro intestinal tract) and hence clear the organisms before they invade the underlying tissue. Furthermore, the enzymatic activity in the nose is relatively low, which is favorable for antigen stability at the administration site.

Local immunity in the upper airways, as well as systemic immunity, is mainly mediated by the lymphoid tissue referred to as nasal associated lymphoid tissue (NALT). NALT is comprised of agglomerates of cells involved in the initiation and execution of an immune response, like DC, T-cells and B-cells [14], situated underneath the nasal epithelium. NALT is most pronounced in the nasopharynx and the Waldeyer's ring, which includes the nasopharyngeal, tubal, palatine and lingual tonsils, making the adenoids an important part of the NALT. Indeed some studies have shown that sIgA excretion is dependent on these areas and tonsillectomy has been associated with decreased immunity [15, 16]. Moreover, Zuercher *et al* [17] showed the presence of germinal centers (places where plasma cells are located) in the NALT after challenge with a reovirus, and Shimoda *et al* [18] showed that B-cells in the subepithelial region of the nose are prone to switch from IgM to IgA, indicating a role for the NALT as inductive site for immune responses. Mucosal immunity after nasal vaccination is, however, not restricted to the upper airways. Via a system called the common mucosal immune system, after nasal immunization sIgA antibodies also can be detected also in other mucosal secretions.

Despite the advantages of nasal vaccine delivery, only one nasal vaccine is currently on the market, whereas four different oral vaccines have been approved (Table I). All these approved vaccines are live attenuated vaccines, which are administered via the same route as the natural infection route of the corresponding pathogen and closely mimic the original pathogen. Although live attenuated vaccines are generally very effective, they may induce more adverse reactions than subunit vaccines. Additionally, in contrast to inactivated vaccines, live attenuated vaccines carry the risk of reassortment with wildtype pathogens, thereby regaining their pathogenicity, and not all pathogens can be attenuated for live vaccines. Subunit vaccines, however, have the disadvantage of being less immunogenic and therefore require potent delivery systems [19, 20]. They contain fewer stimulants of the immune system and are cleared from the nasal mucosa much faster than attenuated vaccines. Furthermore, nasal vaccine delivery may be compromised in patients with respiratory infections and the need for an effective delivery device should not be overlooked. In attempts made to improve the immunogenicity of nasal subunit vaccines, the vaccine formulation plays a crucial role, as will be further discussed below.

Roadmap to successful nasal vaccine delivery

After nasal administration of a vaccine, a number of successive steps should lead to a protective immune response (Fig. 1). In this section we will describe these steps and discuss how a vaccine delivery system can enhance the immune response by promoting these steps.

Table II. Advantages and disadvantages of different routes of immunization.

Immunization route	Advantages	Disadvantages
Parenteral	Powerful systemic immune response	Invasive
	Accurate dosing	Limited mucosal immune response
Nasal	Non invasive	Mucociliary clearance
	Mucosal & systemic immune response	Inefficient uptake of soluble antigens
	Easily accessible	Application device needed (Bryant el al. 1999)
	Little degradation (compared to oral)	
Oral	Non invasive	Vaccine digestion in stomach and gut
	Mucosal & systemic immune response	Inefficient uptake of soluble antigens
	Large surface area	Mucosal tolerance
Pulmonary	Non invasive	Delivery of antigen highly variable from person to person
	Mucosal & systemic immune response	Dry powder inhaler or nebulizer needed
	Little degradation (compared to oral)	Clearance from lungs
Dermal	Non or minimally invasive	May require (minimally) invasive technology (e.g. tattooing, microneedles)
	Large, easily accessible application area	Patch or application device needed
	High density of immune cells in skin	Less established technology
	Mucosal immune response possible	

Prolonging the nasal residence time

After intranasal (i.n.) administration, the first step in the trajectory towards an immune response is that the antigen reaches the NALT. In principle, there is no direct contact between DC in the subepithelial regions of the nose and the antigen in the lumen, although it has been suggested that DC can partially penetrate the epithelium making them capable of sampling the mucosal surface [21]. Therefore, during the limited nasal residence time of the vaccine, the antigen must cross the nasal epithelium. Increasing the residence time of the vaccine (normally ca. 20 minutes), with use of mucoadhesive substances, may therefore be a possible approach to improve the efficacy of a vaccine (Fig. 1).

M-cell targeting

The mechanism of antigen uptake through the epithelium is somewhat controversial. The epithelium is composed of only a thin layer of pseudostratified epithelial cells, connected by tight junctions. Since the diameter of tight junctions is only a few Ångstroms [22], it is very unlikely that (killed) bacteria or viruses, bulky antigens, or particulate vaccine delivery systems are able to penetrate this barrier by paracellular transport even if the tight junctions are widened up [23]. Transcellular transport is a more likely route by which (particulate) antigens reach the NALT. In particular, microfold cells (M-cells) serve as a portal for particulate antigens to enter the subepithelial region [12, 24, 25]; [26]. M-cells are part of the NALT and cover the subepithelial dome containing DC, B-cells and T-cells. M-cells do not contain cilia and have relatively high concentrations of cytoskeleton protein vimentin [27, 28], making M-cells easily accessible and flexible, respectively, to be involved in transmembranous transport [29]. Indeed, after recognition and internalization,

M-cells can transport particulate antigens to the NALT, by transcytosis [30]. Unlike epithelial cells, M-cells have been reported to efficiently take up antigens with a particulate nature and deliver them to a lymphatic environment rather than to the systemic circulation. This may explain why the increased efficiency of particulate antigens is undisputed, whereas increased drug transport using particles is still under discussion [31]. Hence, improving the uptake of a vaccine through M-cells would target the antigen to the underlying immune cells, and may thereby contribute to higher immune responses (Fig. 1).

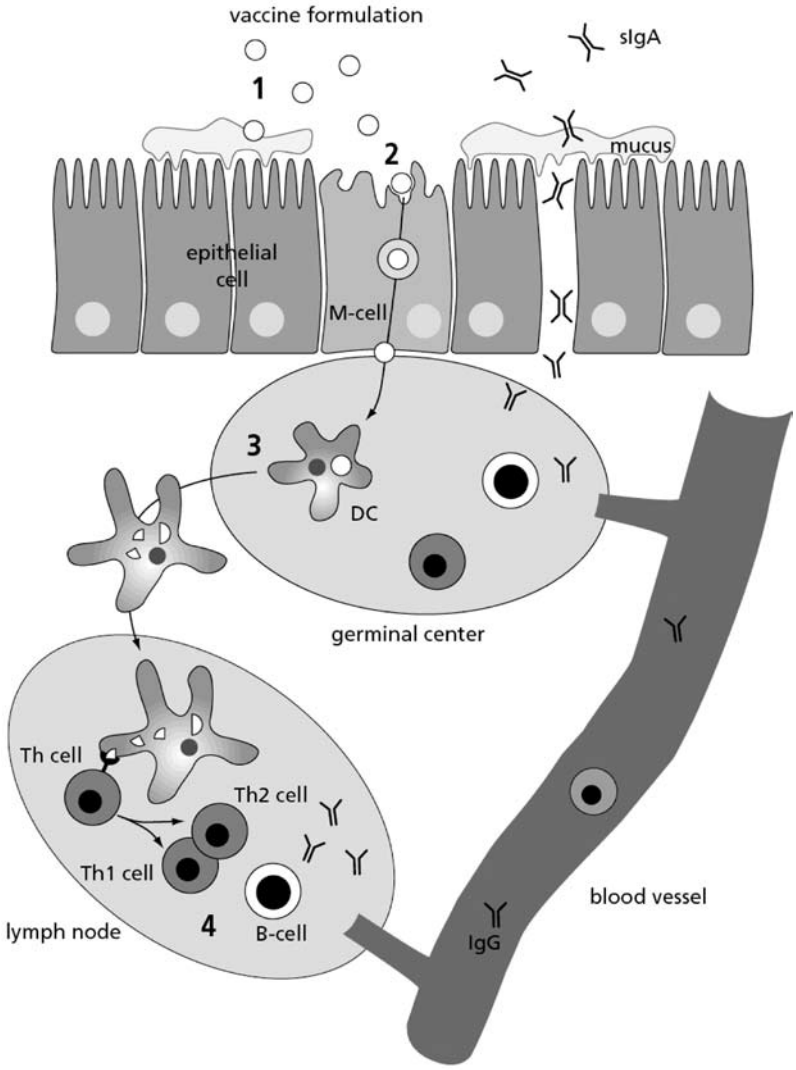

Figure 1. Schematic overview of the consecutive steps towards successful nasal vaccine delivery: 1) mucoadhesion; 2) antigen uptake, by M-cell transport; 3) delivery to and subsequent activation/maturation of DC; 4) induction of B-cell and T-cell responses. DC = dendritic cell, M-cell = microfold cell, Th cell = helper T cell.

DC signaling

After antigen uptake, DC mature and migrate to the nearby cervical lymph nodes, where they present the peptides on MHC class 2 (MHC II) molecules to helper T (Th) cells. Upon recognition of the MHC II-peptide complex and costimulation from APC, naïve Th cells differentiate into effector Th cells, which can be divided in two major subtypes: Th1 and Th2 cells. Th1 cells are mainly involved in activation and proliferation of the cellular immune system, whereas Th2 cells are involved in stimulation and increase of the humoral immune responses. The DC signaling determines the fate of the naïve Th cell and can be influenced by the use of delivery systems and adjuvants. So, not only can delivery systems and adjuvants increase immune responses, they can also influence the Th1/Th2 balance, i.e. the type of immune response. Since the optimal balance of the immune reaction is dependent on the pathogen in question, induction of the desired type of immune response should be tailored for each specific vaccine, which can be achieved by the use of proper delivery systems and adjuvants.

Induction of CTL immune responses

Obtaining immunity against intracellular pathogens like intracellular bacteria and viruses often requires the induction of CTL responses. The induction of CTL with a vaccine can only be achieved when a number of requirements are fulfilled. Firstly, the vaccine should contain class 1 (MHC I) epitopes. Secondly, an MHC II epitope must be present in the vaccine, since a strong induction of CTL responses is only possible when Th cells are co-activated. Thirdly, the MHC I epitope should enter the MHC I presentation pathway. DC copulsed with a Th1 and a Th2 inducing antigen were shown to direct these antigens to distinct compartments, leading to different, antigen dependent polarization of the immune response[32]. Presentation of exogeneous antigens by MHC I molecules is called cross presentation [33, 34]. Recently, it was described that the mechanism of antigen uptake, which dictates the intracellular destination compartment, is not only involved in the activation and polarization of Th cells, but also determines whether the antigen is presented to either $CD4^+$ Th cells or $CD8^+$ CTL. This would suggest that a DC itself is not polarized upon ingestion of an antigen; rather, each intracellular compartment can prepare different instructions that can be presented to different T cells by one DC [35, 36]. Targeting mediators in the vaccine formulation could be employed to facilitate the delivery of endocytosed antigens to the desired intracellular compartments and thereby promote cross presentation (Figure 2).

Adjuvant targets

Adjuvants can be classified according to their mechanisms of action. One group of adjuvants acts through binding to pathogen recognition receptors (PRR) on cells of the innate immune system. PRR recognize pathogen associated molecular patterns (PAMP) that are highly conserved throughout evolution [37, 38]. The binding of PAMP to PRR activates an intracellular signaling cascade in the innate immune cells, which eventually leads to DC maturation, cytokine production and costimulatory signaling to Th cells (Fig. 2).

The Toll-like receptor (TLR) family is a group of PRR that has been characterized in detail [39].

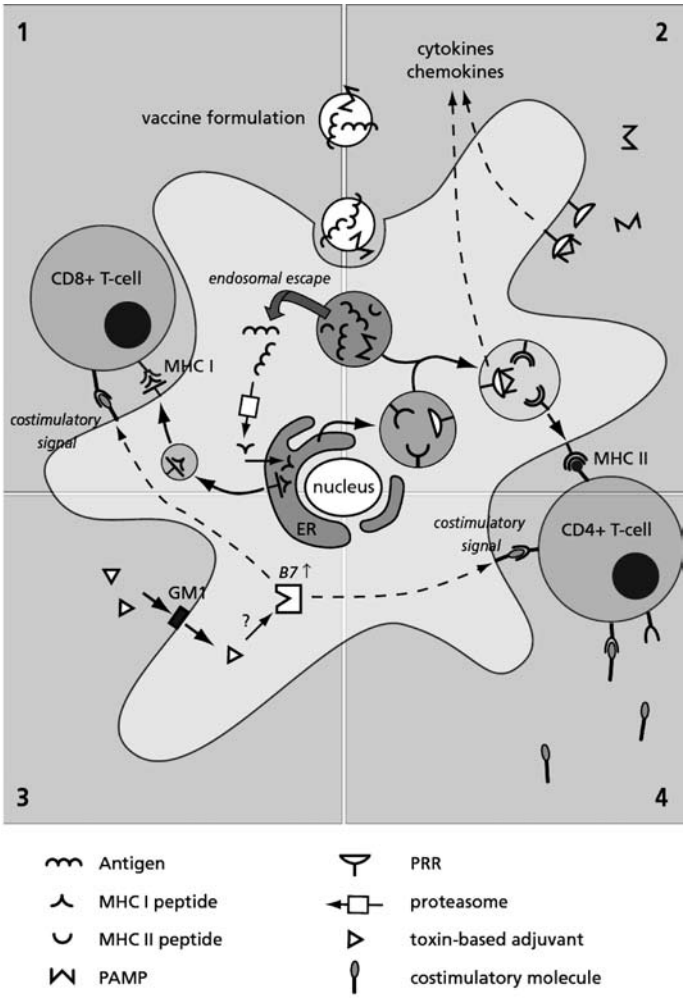

Figure 2. Various mechanisms a vaccine formulation can exploit to induce the desired immune response. 1) cytosolic delivery for targeting the antigen to MHC class I presentation; 2) targeting the innate immune system through pathogen recognition receptors (PRR); 3) the use of toxin-based adjuvants; 4) incorporation of cytokines or other costimulatory molecules. See text for further details.

TLR are expressed by DC and recognize PAMP (Fig. 2) like lipopolysaccharide (LPS), dsRNA, CpG motifs and bacterial lipoproteins [40, 41]. Simultaneous stimulation of these innate immune receptors and antigen delivery to the DC generally leads to Th1 responses and Th1 dependent antibody isotypes [39], but some TLR ligands induce Th2 cytokines upon activation of the TLR [42]).

Another group of adjuvants are toxin based adjuvants. Enterotoxins like the cholera toxin (CT) and the *Escherichia coli* heat labile toxin (LT) are strong mucosal adjuvants that induce mucosal as well as serum antibody responses [43, 44]. LT and CT consist of a toxic A subunit with ADP-ribosyltransferase activity, which is linked non-covalently to a pentamer of B subunits that bind to ganglioside GM-1 receptors found on most cells [45]. Since the use of LT has been associated with neurological toxicity, efforts have been made to develop non-toxic mutants of LT and CT. The exact mechanism of adjuvanticity of toxin-based adjuvants is not fully understood, but the toxins

CT and LT induce expression of B7 molecules on DC that can subsequently deliver costimulatory signals to Th cells (Fig. 2) [46].
Cytokines are probably the critical communication molecules of most classical adjuvants [47]. Therefore cytokines and other costimulatory molecules have been evaluated as adjuvants to promote T-cell activation (Fig. 2). Similary, antibodies mimicking the binding of these molecules to receptors on the T-cells have been tested as adjuvants.

Approaches to improve nasal vaccine delivery

In this section we discuss, based on the roadmap described in the previous section, several approaches that have been described in the literature to improve the delivery and immunogenicity of nasally administered antigens.

Mucoadhesives

Subunit antigens, having little affinity for the nasal epithelium, are generally cleared within minutes. Prolonging the residence time is commonly accomplished by coadministering the antigen with mucoadhesives, usually polymers. The term mucoadhesive does not discriminate between the interaction with either the mucosal cell surface or the mucus covering this surface. If the adhesive also interacts with the antigen, both interactions can lead to a decreased mucociliary clearance of antigens.
Recently, Smart gave an overview of the basics and mechanisms of mucoadhesion [48]. Briefly, properties like hydrophilicity, crosslinking, charge, molecular weight and the presence of acidic or alkaline functional groups influence the mucoadhesion of a polymer. Mucoadhesive polymers can be divided in 3 categories according to their mechanism of interaction. The first category includes hydrophilic polymers that adsorb to the mucus by forming hydrogen bonds, like sodium alginate, sodium carboxymethylcellulose, hydroxypropyl methylcellulose and carbopol. The second class comprises cationic polymers, like chitosan-derived polymers interacting with the negatively charged mucin mainly by ionic interactions, although hydrogen bonds could also play a role [49, 50]. Additionally, chitosan derivatives can open tight junctions and thereby can increase the permeability of the epithelium [51], but its significance for improved antigen delivery is questionable. The third class of mucoadhesives involves thiolated polymers, thiomers, that can form covalent disulfide bonds with the cystein groups in mucin [52]. Recent studies show that thiomers are the strongest mucoadhesives [53].
Antigens coadministered with mucoadhesive polymers, like hyaluronic acid [54], chitosan [55] and carboxylmethylcellulose [56] have indeed shown increased antibody responses as compared to application of the antigen without any additives. However, serum antibody levels reached by coadministration of *Bordetella pertussis* hemagglutinin vaccine [55], diphtheria toxoid [57], tetanus toxoid [58], anthrax protective protein [58], inactivated influenza virus [59] or herpesvirus 1 glycoprotein [60] with chitosan never exceeded levels reached by intramuscular (i.m.) injection, despite the capability of chitosan to increase the nasal residence time [61]. Clearly, a prolonged residence time is not the sole determinant for a successful vaccine.

Particulate antigen carriers

Uptake of antigens through the nasal epithelium can be increased by incorporation into particles [62]. For instance, i.n. administration in mice of antigens incorporated in nanoparticles composed of poly lactide-co-glycolide (PLGA), a biodegradable polymer, led to over 100 fold increased antibody responses in comparison with aqueous solution of parainfluenza virus proteins [63], hepatitis B soluble antigen [64], *Bordetella bronchiseptica* dermonecrotoxin [65] and recombinant HIV proteins [66]. Polystyrene beads loaded with hemagglutinin led to increased protection against influenza in mice [67], probably due to enhanced antigen uptake [68]. Nasal application of liposomes loaded with killed measles virus [69], formaldehyde-killed *Yersinia pestis* [70], or influenza A hemagglutinin [71] even elicited superior IgG antibody levels than i.m. administered alum adsorbed antigen.

Mucoadhesive particles

Particles composed of mucoadhesive polymers are even more effective antigen carriers, as they combine prolonged residence time in the nasal cavity with the beneficial properties of particulate systems. Chitosan particles are well-known mucoadhesive antigen carriers. Coadministration of soluble chitosan with cholera toxoid or ovalbumin (OVA) induced higher immune responses than administration of antigen alone, but incorporation of the CT or OVA antigen into chitosan nanoparticles resulted in superior serum antibody levels in rats [72]. Similarly, Amidi *et al* showed that nasally applied influenza antigens incorporated in trimethylated chitosan (TMC) nanoparticles elicited superior IgG and sIgA antibody response as compared to naked antigen or antigen coadministered with TMC [73].

Alternatively, particulate antigen carriers can be rendered mucoadhesive by coating them with mucoadhesive polymers. Intranasal vaccination with hepatitis B surface antigen (HBsAg) encapsulated in chitosan coated PLGA particles resulted in a 30 fold increase of serum IgG levels in comparison with uncoated HBsAg loaded PLGA particles [74]. Vila *et al* showed that chitosan coating of tetanus toxoid-containing PLA particles increases transport through the nasal epithelium in comparison with uncoated particles [75]. The increased transport was accompanied by higher IgG responses against tetanus toxoid, indicating a positive effect of epithelial transport on vaccine efficacy.

Particle characteristics

The physicochemical properties of the particles most likely are critical to the effectiveness of the vaccine. For instance, particle size and zeta potential can impact the transport by M-cells as well as subsequent events, but the ideal particle characteristics are still under discussion.

The effect of particle size has not been thoroughly investigated for nasal vaccination. It has been determined that M-cells in Peyer's patches in the gut selectively take up particles with a diameter up to 10 μm [76] and that the particle size influences the type of immune response [77]. Xiang *et al* stated that particles resembling the size of viruses (20-200 nm) will be handled by the immune system as being a virus and elicit a cellular biased response, whereas particles with the size of a

bacterium (between 0.5-5 μm) will favor a humoral response [78]. For nasal vaccination, several studies pointed to small (nano)particles being more rapidly absorbed by nasal M-cells [62, 72, 79-81], but no boundaries have been determined. Fujimura *et al* [82] showed that particles coated with the cationic polymers chitosan or poly-L-lysine were taken up by the NALT in a size range from 0.2 μm to 2 μm, with an increased uptake of smaller particles. Unfortunately, these particles did not carry an antigen, making it impossible to determine the effect of increased uptake on resulting immune responses.

As the cell membrane of M-cells is negatively charged, one can argue that a positive zeta potential is beneficial for M-cell transport. However, mucus and epithelial cells carry a negative charge as well, making electrostatic interactions very unspecific. Still, nasal application of a *Yersinia pestis* antigen in positively charged liposomes induced significantly stronger antibody responses than the same antigen in negatively charged liposomes [71, 83]. Likewise, nasal administration of HBsAg in positively charged PLGA microparticles resulted in significantly higher antibody levels than the same antigen in negatively charged PLGA microparticles[84]. Although negatively charged or neutral particles have been reported to drastically increase antibody response after nasal immunisation [79, 85], positively charged particles seem to be superior to their negatively charged counterparts.

Improved mechanistic insight into the role of particle characteristics on antigen uptake will be necessary to resolve the ideal characteristics of a particulate carrier for uptake by the nasal epithelium.

M-cell targeting approaches

Specific M-cell targeting could further enhance vaccine efficacy. A variety of microorganisms, e.g. influenza viruses and group A streptococci, have been found to target themselves to M-cells [12, 24, 25]. Complete bacteria can be used as vaccine carrier, exploiting their M-cell targeting mechanisms. Expression of *Streptococcus pneumoniae* antigens on live lactobacillus led to high IgG and sIgA titers in mice after i.n. administration [86]. Since live and inactivated lactobacilli induced similar protective immunity after nasal administration [87], the positive effect of lactobacillus is likely not due to prolonged residence time, but rather to increased bioadhesion or (M-cell mediated) uptake.

Virosomes are reconstituted virus envelopes, including a lipid bilayer and surface proteins. For instance, influenza virosomes (containing hemagglutinin and neuraminidase surface antigen) can be used as carriers to transport antigens to the cytosol of cells that overexpress sialic acid residues [88, 89] and might be exploited to target DC [90], but could target M-cells by the same mechanism. Virosomes have been shown to be excellent nasal carriers for several antigens like the F-protein of RSV [91] and DNA vaccines [92].

M-cells express several adhesion molecules on their cell surface that can bind pathogens. However, most work has been done on intestinal M-cells [93-95] and regional differences between M-cells exist [96, 97]. For instance, the plant lectin *Ulex europaeus* 1 lectin (UEA-1) [98] as well as lectins from other species [99-101] have been successfully used for targeting particles to intestinal M-cells in mice, but the specificity of UEA-1 for nasal M-cells is lower, as it also has affinity for nasal

epithelial and goblet cells [102]. Despite this shortcoming, UEA-1 has been shown to increase M-cell transport and able to raise serum antibody levels when coadministered i.n. with DNA encoding HIV envelope protein [103].

Putative ligands that selectively target nasal M-cells include isolectin B_4 and *Maackia amurensis I* lectin [102], which recognize α-(1-3)-linked galactose and sialic acid, respectively [104]. Interestingly, sialic acid and galactose residues are involved in the initial binding of influenza virion to the host cell [105] and influenza A type viruses adhere efficiently to nasal M-cells *in vitro* [24]. Adherence of *Streptococcus pneumoniae* to the tracheal epithelium in chinchillas is dependent on the expression of sialic acid [106], showing the importance of these carbohydrate residues on the nasal epithelium for the entrance of these airborne pathogens. Nasal application of the model antigen HRP with isolectin B_4 significantly enhanced the antibody (IgG and sIgA) response to HRP in comparison with administration of HRP alone [104].

Besides lectin binding domains, several other receptors have recently been identified as potential M-cell targeting ligands, especially β_1-integrin [107]. Several pathogens use β_1-integrins to cross the intestinal epithelium, such as *Yersinia pestis* [108] and *Escherichia coli* [109, 110]. Recently Gullberg *et al* showed that uptake of latex particles by human intestinal M-cells *in vitro* was increased when the particles were coated with a β_1-integrin ligand [111]. Hicks *et al* [112] showed that β_1-integrin is also readily expressed on nasal isolectin B_4 positive epithelial cells, i.e. most probably M-cells.

Intracellular targeting, induction of cytotoxic T cells

After antigen uptake through the nasal epithelium, their uptake and processing by DC are the next critical steps that determine the immune response. Antigen delivery systems that are capable of disrupting the DC's endosomal membrane and thereby promote endosomal escape can in principle be used to induce CTL responses. It has been shown that antigens incorporated in particulate antigen delivery systems are more effectively cross-presented than soluble antigens [113-115]. The efficiency of cross-presentation can vary between different types of particulate antigen delivery systems.

ISCOMs and ISCOMATRIX adjuvant are 40-nm cage-like structures composed of Quillaja saponins, cholesterol, and lipids that can incorporate or associate membrane antigens and DNA. ISCOMs are well-studied nasal and parenteral adjuvants that induce not only mucosal and systemic humoral responses, but also CTL responses [116-120]. It is thought that ISCOMs can deliver antigens to the APC's cytosol due to their membrane-disrupting properties [119], triggering endosomal escape. Additionally, it has been shown that CTL induction is markedly stronger when the antigen is physically attached to the ISCOMATRIX rather than administered unbound [117].

Virosomes can also induce strong CTL responses in addition to humoral and Th cell responses [88, 121] Influenza virosomes have been most extensively investigated. These virosomes contain influenza hemagglutinin, which binds to sialic acid residues on the cell surface and initiates receptor mediated endocytosis. Conformational changes in the influenza hemagglutinin due to acidification of the endosomes triggers the fusion of the endosomal membrane and the virosomal

membrane, which enables release of the virosomal contents from the endosome into the cytosol. Subsequently the released antigens are degraded by the proteasome and presented through MHC I molecules [122]. Influenza virosomes have shown increased CTL responses against virosomal influenza [123-126], hepatitis C [127] and cancer antigens [128]. Virosomal influenza vaccines are the only virosomal vaccines that have been tested via the nasal route [129-132].
In addition to lipid based antigen delivery systems, polymeric biodegradable nanoparticles can enhance CTL induction *in vitro* [133] and *in vivo* after nasal vaccination [134], as well as other routes [135-138]. Antigen loaded biodegradable PLGA nanoparticles are superior to nondegradable antigen adsorbed to latex nanoparticles [139], most likely due to hydrolysis of these polymeric nanoparticles in the acidic environment of endosomes. This facilitates endosomal escape [139-141] and antigen delivery into the cytosol, leading to enhanced MHC I presentation. The charge and structure of polymeric nanoparticles can also affect the uptake into DC. For instance, a positive charge has shown to increase phagocytic activity [140].
To summarize, vaccine delivery systems and endosomal escape mediators can be used for MHC I antigen presentation and thereby could increase CTL responses to an antigen.

Adjuvants

TLR ligands
CpG motifs in bacterial dsDNA are recognized by TLR 9. CpG oligodeoxynucleotides (ODN) have been tested in mice as adjuvant for nasal vaccines against several pathogens. Table III gives an overview of the results from studies in which TLR ligands have been tested as adjuvants for nasal vaccines. In general, the addition of CpG ODN to a nasal vaccine results in increased serum and mucosal antibody levels as well as increased cellular responses [142-144]. Generally, the addition of CpG ODN shifts the immune response from Th2 biased to a balanced Th1/Th2 response, i.e. it increases the production of Th1 cytokines and IgG2a.
Double stranded RNA and poly (I:C) are ligands for TLR 3. Poly (I:C) has been tested in mice as an adjuvant in a nasal influenza vaccine, resulting in protective immunity against influenza [145]. Poly (I:C) also increased humoral immune responses to two antigen formulations of *Bacillus anthracis*, inducing maturation and migration of DC and directing the immune response from mainly Th2 to a more balanced Th1/Th2 response. Moreover, sIgA was detected in broncheo alveolar lavage fluid [146, 147].
TLR 3 and TLR 9 are located in endosomal membranes. Storni *et al* suggested therefore that TLR 3 and 9 ligands should be taken up by the same DC as the antigen to exert their adjuvant effect [148]. Following this hypothesis, Joseph *et al* encapsulated CpG motifs in liposomes with influenza antigen, which on nasal administration in mice led to an increased anti-influenza IgG2a response, cellular responses (splenocyte proliferation, CTL response and IFN-γ production), and protection against influenza virus challenge [149]. This is likely due to enhanced liposomal delivery of CpG motifs to the endosomal compartment.
LPS, a major component of the outer membrane of Gram-negative bacteria, is a ligand for TLR 2

Table III. Examples of nasal vaccination studies using Toll like receptor ligands.

Ligand	TLR	Formulation	Pathogen	Response*			Protection	Reference
				Mucosal sIgA	Serum Ab	CMI		
MALP-2	2-6	ß-galactosidase with admixed MALP-2	none	Vaginal and bronchial IgA†	IgG†, IgG1†>IgG2a†	IL-10† (Th2), IL-2 (Th1) only detectable with MALP-2	Not applicable	(Rharbaoui et al. 2002; Rharbaoui et al. 2004)
Poly (I:C)	3	Poly (I:C) + recombinant protective antigen (rPA), or capsular poly-γ-d-glutamic acid (PGA)–BSA conjugate	Anthrax (Bacillus anthracis)	Brochial sIgA †	Balanced IgG1/ IgG2a, but shift to Th1	Expression of CD80 and CD86 and TNF-α secretion in DC	Anthrax lethal toxin neutalizing activity in vitro	(Sloat and Cui 2006a,b)
Poly (I:C)	3	Poly (I:C) + Ethyl ether split virus	Influenza A virus	Nasal sIgA†	IgG†	Th1 and Th2 cytokines† (IFN-α,-β, -γ, IL-4, IL-6 and IL-12p40)	Cross-protection against nasal challenge	(Ichinohe et al. 2005)
LPS	4	Invaplex (LPS + Ipa proteins from Shigella flexneri 2a) admixed with OVA	none	Lung bronchial IgA†	IgG1† (Th2), no α-OVA IgG2a	Proliferation of CLN and spleen cells, Th2 cytokines IL-4, IL-5 and IL-10 produced	Not applicable	(Kaminski et al. 2006)
LPS	2-4	Proteoliposomes from Neisseria meningitidis B; cochleate structure with incorporated ovalbumin or Leishmania antigens	Leishmania, Neisseria meningitidis	IgA in saliva†	α-PL IgG1† <IgG2a†	MHCII † in DC, IFNγ production in spleen cells	Smaller lesions after leishmania major infection	(Perez et al. 2004)
LPS	2-4	Liposomal OpaB and OpaJ formulations with admixed LPS	Neisseria meningitidis	Nasal sIgA†	IgG2b†>IgG2a† (mixed Th1/Th2) LPS> Mono-phosphoryl lipid A	Not described	Bactericidal serum antibody titers	(de Jonge et al. 2004)
Mono-phosphoryl lipid A	4	Liposomal OpaB and OpaJ formulations with admixed LPS	Neisseria meningitidis	Nasal sIgA†	IgG2b†>IgG2a† (mixed Th1/Th2)	Not described	Bactericidal serum antibody titers	(de Jonge et al. 2004)
flagellin from *Vibrio vulnificus*	5	Tetanus toxoid with admixed flagellin	Clostridium tetani	Nasal sIgA†	IgG1>IgG2a	Increased TLR 5 expression in lymph nodes and spleen	Yes	(Lee et al. 2006)
CpG ODN	9	non-toxic CRM197 conjugated Hib–PRP with admixed CpG ODN	*Haemophilus influenzae* type b	A-PRP and α-CRM197 IgA in saliva and BAL	A-PRP and α-CRM179 IgG2a† and IgG3†, shift to Th1	Not described	Not mentioned	(Mariotti et al. 2002)

Table III. Continued

Ligand	TLR	Formulation	Pathogen	Response*			Protection	Reference
				Mucosal sIgA	Serum Ab	CMI		
CpG ODN	9	P6 outer membrane protein non-typable *Haemophilus influenzae* (NTHI) with admixed CpG ODN	Nontypeable *Haemophilus influenzae*	sIgA† in nasal wash (similar to CT)	IgG1†, IgG2a† balanced to Th1 (CT more IgG1)	IFNγ †in CD 8+ T-cells, IL-6† and IFNγ† in CD4+ T-cells	Increased clearance of NTHI nasal washes after challenge	(Abe et al. 2006; Kodama et al. 2006)
CpG ODN	9	Liposomal formulation of CpG ODN with admixed or co-encapsulated subunit vaccine	Influenza A virus	Nasal and bronchial IgA†, coencapsulated >admixed	IgG1† and IgG2a†, more balanced IgG1/ IgG2a than after i.m. (Th1)	IFNγ †(Th1), Spleen proliferation†	Lung titers↓, lowest in co-encapsulated formulation	(Joseph et al. 2002)
CpG ODN	9	Formaldehyde inactivated influenza virus with admixed CpG 1826 or *E. coli* DNA	Influenza A virus	sIgA in saliva or vaginal washes ↔	Abs† at higher antigen dose, not significant for lower doses, *E. coli* DNA has stronger effect	Low proliferative responses from spleen of CLN isolated cells after *in vitro* restimulation	Not described	(Moldoveanu et al. 1998)
CpG ODN	9	Live Ankara virus vector with admixed CpG ODN	Vaccinia virus	Not described	No difference in virus neutralizing antibodies	CD8+ Tcell response †, CpG can substitute for CD4+ help	Protective dosage ↓, mediated primarily by CD8+ in lungs	(Belyakov et al. 2006)
CpG ODN	9	Whole cell sonicate with admixed CpG ODN	*Helicobacter pylori*	Not detected	IgG and IgG1 no difference, IgG2a†(Th1)	IFNγ-producing CD4+ and CD8+ T-cells	Protection associated with Th1 and IFN-γ	(Shi et al. 2005)
CpG ODN	9	Recombinant M type 6 with admixed CPG ODN	*Streptococcus pyogenes*	IgA† in BAL	Total IgG†, IgG1†, IgG2a†, IgG2b, Th1 type response CpG ODN< CT	Not described	Not described	(Teloni et al. 2004)
CpG ODN	9	Thelper-CTL epitope fusion peptides (pp65)	Cytomegalo-virus	Not described	Not described	CTL stimulation †	Not described	(La Rosa et al. 2002)

*As compared to the same formulation without the TLR ligand.
Abbreviations: Ab = antibody, CMI= cell-mediated immunity, CFU = colony-forming unit, † = increased, ↓ = decreased, ↔ = unchanged, α- = anti-, CLN = cervical lymph node, < = to a lesser extent than, > = to a higher extent than, BAL = bronchio alveolar lavage.

and TLR 4, and its adjuvant potential has been tested in various studies. Both Th1 [150, 151] and Th2 responses [152-155] have been found after nasal administration of LPS-containing vaccines. These contrary results are not yet fully understood. Iwasaki and Metzhitov suggested that a lower dose of administered LPS corresponds to environmental antigens and induces Th2 responses and allergic inflammation, whereas a high dose corresponds to responses against infection and induces Th1 responses [39]. Monophosphoryl lipid A, a derivative of LPS and ligand for TLR 4, has similar adjuvant effects as LPS in nasal vaccines [150]. Increased mucosal sIgA and serum antibodies were found by using monophosphoryl lipid A as an adjuvant [150, 156] when compared to LPS [150].
Bacterial flagellins are ligands for TLR 5 and have been tested in nasal vaccines [157-159]. They induce mucosal and serum humoral responses. *Vibrio vulnificus* derived flagellin has thus far been the only flagellin tested as an adjuvant and induced mainly Th2 responses against model antigen tetanus toxoid [157]. Further research should clarify the potential of this group of TLR ligands as adjuvants for nasal vaccines.
Other PRR include the intracellular NOD1 and NOD2 proteins, scavenger receptors, macrophage mannose receptors and other C-type lectin receptors as well as type 3 complement receptors [39]. For instance, targeting of the C-type lectin, mannose receptor, on DC significantly increased antigen presentation on MHC II molecules [160]; [40].
Altogether, it seems that many TLR ligands, and possibly other PRR ligands, can act as adjuvant for nasal vaccines. However, the shift towards Th1 immune responses as observed with parenteral vaccinations seems to be less evident with nasal vaccination where balanced Th1/Th2 immune responses are mostly observed with these adjuvants. Further research in the immunological mechanisms involved in eliciting mucosal immune responses is necessary to understand the role these adjuvants can play in future (nasal) vaccines.

Toxin-based adjuvants
Enterotoxins like CT and LT are strong mucosal adjuvants that induce mucosal as well as serum antibody responses [43, 44]. In 1997 the first commercial nasal virosomal influenza vaccine adjuvanted with LT became available. Although the vaccine yielded a high percentage of protection, it was withdrawn from the market because its use was associated with an increased risk of developing Bell's palsy [161]. The cause of the Bell's palsy was linked to LT [162] and consequently LT and CT have no longer been used intensively in humans as an adjuvant for nasal vaccines. It has been reported that the coadministration of CT or LT redirects the antigen into the olfactory neuroepithelium, likely the cause of the neurological toxicity [163]. In an effort to make safe adjuvants based on CT and LT, several mutants of the toxins have been developed and tested [164]. Amino acid mutations in the ADP-ribosyltransferase domain in the A subunit from CT and LT resulted in effective nontoxic mutants [165-172].
Nasal application of vaccines adjuvanted with CT and its nontoxic mutants induces Th2 type immune responses as well as mucosal sIgA production, whereas the differentiation of Th1 cells is suppressed [173-176]. On the other hand, LT and some mutants like LT(K63) [44, 177] induce a more balanced Th1/Th2 response [178, 179]. Some mutants of LT, like LT(R72) induce a specific

Th2 response [44, 177], while other LT mutants like induce a more Th1 polarized response [166]. A clear correlation between mutation and type of induced immune response has not been established. A construct of CT with a synthetic dimer of the D-fragment of *Staphylococcus aureus* protein A, which targets to B-cell Ig receptors, resulted in a strong nontoxic adjuvant that induced a balanced Th1/Th2 response against several tested antigens [180].

Cytokines and costimulatory molecules

Cytokines like IL-1 [181, 182], IL-12 [183-185], and type 1 IFN [186, 187] have been used as adjuvants for nasal vaccines to induce stronger and regulated Th1/Th2 immune responses [164]. Especially IFN type 1 and IL-12 are promising nasal adjuvants promoting Th1 type immune responses.

Costimulatory signals are non-antigen specific signals delivered by activated APC to T-cells or by Th cells to B-cells. Several pathways can be exploited as target for adjuvants. CD28, CD40, CD134 and CD137 have been investigated as adjuvant targets [188]. Monoclonal antibodies that mimic the agonistic binding of costimulatory molecules have been tested as ligands for these CD molecules. Anti-CD40 monoclonal antibodies were coadministered as an adjuvant with a liposomal formulation of an influenza CTL epitope in subcutaneous and i.n. vaccination in mice. A decrease of lung viral titers after non-lethal challenge was observed after i.n. but not after subcutaneous vaccination or nasal vaccination without anti-CD40 [189].

Conclusions

Although research and development of nasal vaccines has gained momentum over the last years, only one nasal vaccine is currently approved for human use, indicating that advances towards new effective vaccines have been slow, in particular for inactivated/subunit vaccines. However, the various attempts that have failed can teach us not to bet on one single horse. The opportunities in nasal vaccination are not in a single research field, but require the integration of immunology, biotechnology, microbiology and pharmaceutical sciences. Mechanistic insight into the hurdles that limit the efficacy of nasal vaccination will create opportunities for rationally designed nasal vaccines that can overcome these barriers. A concerted approach, combining various targeting techniques discussed in this paper, includes the use of particulate antigen carriers, which can be furnished with distinct functionalities such as mucoadhesive polymers, M-cell or DC targeting ligands, adjuvants and endosomal escape promoters. This could lead to "tailor made" vaccines that provide similar or even superior protection to diseases as provided by classical parental vaccines. The biggest challenge will be to combine these techniques in such a way that they do not interfere with one another, but synergistically enhance vaccine efficacy.

Acknowledgements

The authors thank Elly van Riet for critically reading the manuscript and her helpful suggestions, and Martijn Pieck for making the illustrations.

References

[1] Rumke HC, Visser HK. [Childhood vaccinations anno 2004. I. Effectiveness and acceptance of the Dutch National Vaccination Programme]. Ned Tijdschr Geneeskd 2004;148(8):356-63.

[2] Crockett M, Keystone J. "I hate needles" and other factors impacting on travel vaccine uptake J Travel Med 2005;12 Suppl 1:S41-6.

[3] Bitsori M, Ntokos M, Kontarakis N, Sianava O, Ntouros T, Galanakis E. Vaccination coverage among adolescents in certain provinces of Greece Acta Paediatr 2005;94(8):1122-5.

[4] Kalies H, Grote V, Schmitt HJ, von Kries R. Immunisation status of children in Germany: temporal trends and regional differences Eur J Pediatr 2006;165(1):30-6.

[5] Szucs TD, Muller D. Influenza vaccination coverage rates in five European countries-a population-based cross-sectional analysis of two consecutive influenza seasons Vaccine 2005;23(43):5055-63.

[6] Hak E, Schonbeck Y, De Melker H, Van Essen GA, Sanders EA. Negative attitude of highly educated parents and health care workers towards future vaccinations in the Dutch childhood vaccination program Vaccine 2005;23(24):3103-7.

[7] President Requests 2.6 Percent NIH Budget Increase in 2005 In, National Health Institute, 2005.

[8] Enserink M. Radical Steps Urged to Help Underserved In, Science/AAAS, 2000.

[9] Harrington M. To Double, or Not to Double? Bioterror Buys a Budget Boost In, aidsinfonyc.org, 2002.

[10] Brandtzaeg P. History of oral tolerance and mucosal immunity Ann N Y Acad Sci 1996;778:1-27.

[11] Kyd JM, Foxwell AR, Cripps AW. Mucosal immunity in the lung and upper airway Vaccine 2001;19(17-19):2527-33.

[12] Neutra MR, Frey A, Kraehenbuhl JP. Epithelial M cells: gateways for mucosal infection and immunization Cell 1996;86(3):345-8.

[13] van der Ven I, Sminia T. The development and structure of mouse nasal-associated lymphoid tissue: an immuno- and enzyme-histochemical study Reg Immunol 1993;5(2):69-75.

[14] Jeong KI, Suzuki H, Nakayama H, Doi K. Ultrastructural study on the follicle-associated epithelium of nasal-associated lymphoid tissue in specific pathogen-free (SPF) and conventional environment-adapted (SPF-CV) rats J Anat 2000;196 (Pt 3):443-51.

[15] Morag A, Morag B, Bernstein JM, Beutner K, Ogra PL. In vitro correlates of cell-mediated immunity in human tonsils after natural or induced Rubella virus infection J Infect Dis 1975;131(4):409-16.

[16] Ogra PL. Effect of tonsillectomy and adenoidectomy on nasopharyngeal antibody response to poliovirus N Engl J Med 1971;284(2):59-64.

[17] Zuercher AW, Coffin SE, Thurnheer MC, Fundova P, Cebra JJ. Nasal-associated lymphoid tissue is a mucosal inductive site for virus-specific humoral and cellular immune responses J Immunol 2002;168(4):1796-803.

[18] Shimoda M, Nakamura T, Takahashi Y, Asanuma H, Tamura S, Kurata T, et al. Isotype-specific selection of high affinity memory B cells in nasal-associated lymphoid tissue J Exp Med 2001;194(11):1597-607.

[19] Poland GA, Neff JM. Smallpox vaccine: problems and prospects Immunol Allergy Clin North Am 2003;23(4):731-43.

[20] Favre D, Viret JF. Biosafety evaluation of recombinant live oral bacterial vaccines in the context of European regulation Vaccine 2006;24(18):3856-64.

[21] Neutra MR, Pringault E, Kraehenbuhl JP. Antigen sampling across epithelial barriers and induction of mucosal immune responses Annu Rev Immunol 1996;14:275-300.

[22] Watson CJ, Rowland M, Warhurst G. Functional modeling of tight junctions in intestinal cell monolayers using polyethylene glycol oligomers Am J Physiol Cell Physiol 2001;281(2):C388-97.

[23] Illum L. Nanoparticulate systems for nasal delivery of drugs: A real improvement over simple systems? . J Pharm Sci 2007;96(3):473-83.

[24] Fujimura Y, Takeda M, Ikai H, Haruma K, Akisada T, Harada T, et al. The role of M cells of human nasopharyngeal lymphoid tissue in influenza virus sampling. Virchows Arch 2004;444(1):36-42.

[25] Fujimura Y. Evidence of M cells as portals of entry for antigens in the nasopharyngeal lymphoid tissue of humans Virchows Arch 2000;436(6):560-6.

[26] Park HS, Francis KP, Yu J, Cleary PP. Membranous cells in nasal-associated lymphoid tissue: a portal of entry for the respiratory mucosal pathogen group A streptococcus J Immunol 2003;171(5):2532-7.

[27] Gebert A. Identification of M-cells in the rabbit tonsil by vimentin immunohistochemistry and in vivo protein transport Histochem Cell Biol 1995;104(3):211-20.

[28] Gebert A, Willfuhr B, Pabst R. The rabbit M-cell marker vimentin is present in epithelial cells of the tonsil crypt Acta Otolaryngol 1995;115(5):697-700.

[29] Styers ML, Kowalczyk AP, Faundez V. Intermediate filaments and vesicular membrane traffic: the odd couple's first dance? . Traffic 2005;6(5):359-65.

[30] Brooking J, Davis SS, Illum L. Transport of nanoparticles across the rat nasal mucosa. J Drug Target 2001;9(4):267-79.

[31] Illum L. Nanoparticulate systems for nasal delivery of drugs: A real improvement over simple systems? J Pharm Sci 2006.

[32] Cervi L, MacDonald AS, Kane C, Dzierszinski F, Pearce EJ. Cutting edge: dendritic cells copulsed with microbial and helminth antigens undergo modified maturation, segregate the antigens to distinct intracellular compartments, and concurrently induce microbe-specific Th1 and helminth-specific Th2 responses. J Immunol 2004;172(4):2016-20.

[33] Ackerman AL, Cresswell P. Cellular mechanisms governing cross-presentation of exogenous antigens. Nat Immunol 2004;5(7):678-84.

[34] Ackerman AL, Kyritsis C, Tampe R, Cresswell P. Access of soluble antigens to the endoplasmic reticulum can explain cross-presentation by dendritic cells. Nat Immunol 2005;6(1):107-13.

[35] Blander JM, Medzhitov R. Toll-dependent selection of microbial antigens for presentation by dendritic cells. Nature 2006;440(7085):808-12.

[36] Burgdorf S, Kautz A, Bohnert V, Knolle PA, Kurts C. Distinct pathways of antigen uptake and intracellular routing in CD4 and CD8 T cell activation. Science 2007;316(5824):612-6.

[37] Gordon S. Pattern recognition receptors: doubling up for the innate immune response. Cell 2002;111(7):927-30.

[38] Kaisho T, Akira S. Toll-like receptors as adjuvant receptors. Biochim Biophys Acta 2002;1589(1):1-13.

[39] Iwasaki A, Medzhitov R. Toll-like receptor control of the adaptive immune responses. Nat Immunol 2004;5(10):987-95.

[40] Pashine A, Valiante NM, Ulmer JB. Targeting the innate immune response with improved vaccine adjuvants. Nat Med 2005;11(4 Suppl):S63-8.

[41] Akira S, Takeda K. Toll-like receptor signalling. Nat Rev Immunol 2004;4(7):499-511.

[42] Wang Q, McLoughlin RM, Cobb BA, Charrel-Dennis M, Zaleski KJ, Golenbock D, et al. A bacterial carbohydrate links innate and adaptive responses through Toll-like receptor 2. J Exp Med 2006;203(13):2853-63.

[43] Imaoka K, Miller CJ, Kubota M, McChesney MB, Lohman B, Yamamoto M, et al. Nasal immunization of nonhuman primates with simian immunodeficiency virus p55gag and cholera toxin adjuvant induces Th1/Th2 help for virus-specific immune responses in reproductive tissues. J Immunol 1998;161(11):5952-8.

[44] Ryan EJ, McNeela E, Pizza M, Rappuoli R, O'Neill L, Mills KH. Modulation of innate and acquired immune responses by Escherichia coli heat-labile toxin: distinct pro- and anti-inflammatory effects of the nontoxic AB complex and the enzyme activity. J Immunol 2000;165(10):5750-9.

[45] Arce S, Nawar HF, Russell MW, Connell TD. Differential binding of Escherichia coli enterotoxins LT-IIa and LT-IIb and of cholera toxin elicits differences in apoptosis, proliferation, and activation of lymphoid cells. Infect Immun 2005;73(5):2718-27.

[46] Yamamoto M, McGhee JR, Hagiwara Y, Otake S, Kiyono H. Genetically manipulated bacterial toxin as a new generation mucosal adjuvant Scand J Immunol 2001;53(3):211-7.

[47] Schijns VE. Immunological concepts of vaccine adjuvant activity. Curr Opin Immunol 2000;12(4):456-63.
[48] Smart JD. The basics and underlying mechanisms of mucoadhesion. Adv Drug Deliv Rev 2005;57(11):1556-68.
[49] Bogataj M, Vovk T, Kerec M, Dimnik A, Grabnar I, Mrhar A. The correlation between zeta potential and mucoadhesion strength on pig vesical mucosa. Biol Pharm Bull 2003;26(5):743-6.
[50] Ugwoke MI, Agu RU, Verbeke N, Kinget R. Nasal mucoadhesive drug delivery: background, applications, trends and future perspectives. Adv Drug Deliv Rev 2005;57(11):1640-65.
[51] Dodane V, Amin Khan M, Merwin JR. Effect of chitosan on epithelial permeability and structure Int J Pharm 1999;182(1):21-32.
[52] Bernkop-Schnurch A, Kast CE, Richter MF. Improvement in the mucoadhesive properties of alginate by the covalent attachment of cysteine J Control Release 2001;71(3):277-85.
[53] Grabovac V, Guggi D, Bernkop-Schnurch A. Comparison of the mucoadhesive properties of various polymers. Adv Drug Deliv Rev 2005;57(11):1713-23.
[54] Singh M, Briones M, O'Hagan DT. A novel bioadhesive intranasal delivery system for inactivated influenza vaccines J Control Release 2001;70(3):267-76.
[55] Jabbal-Gill I, Fisher AN, Rappuoli R, Davis SS, Illum L. Stimulation of mucosal and systemic antibody responses against Bordetella pertussis filamentous haemagglutinin and recombinant pertussis toxin after nasal administration with chitosan in mice. Vaccine 1998;16(20):2039-46.
[56] Hilfenhaus J, Moser H, Herrmann A, Mauler R. Herpes simplex virus subunit vaccine: characterization of the virus strain used and testing of the vaccine Dev Biol Stand 1982;52:321-31.
[57] McNeela EA, O'Connor D, Jabbal-Gill I, Illum L, Davis SS, Pizza M, et al. A mucosal vaccine against diphtheria: formulation of cross reacting material (CRM(197)) of diphtheria toxin with chitosan enhances local and systemic antibody and Th2 responses following nasal delivery Vaccine 2000;19(9-10):1188-98.
[58] Coeshott CM, Smithson SL, Verderber E, Samaniego A, Blonder JM, Rosenthal GJ, et al. Pluronic F127-based systemic vaccine delivery systems Vaccine 2004;22(19):2396-405.
[59] Read RC, Naylor SC, Potter CW, Bond J, Jabbal-Gill I, Fisher A, et al. Effective nasal influenza vaccine delivery using chitosan. Vaccine 2005;23(35):4367-74.
[60] Gogev S, de Fays K, Versali MF, Gautier S, Thiry E. Glycol chitosan improves the efficacy of intranasally administrated replication defective human adenovirus type 5 expressing glycoprotein D of bovine herpesvirus 1 Vaccine 2004;22(15-16):1946-53.
[61] Soane RJ, Hinchcliffe M, Davis SS, Illum L. Clearance characteristics of chitosan based formulations in the sheep nasal cavity Int J Pharm 2001;217(1-2):183-91.
[62] Koping-Hoggard M, Sanchez A, Alonso MJ. Nanoparticles as carriers for nasal vaccine delivery Expert Rev Vaccines 2005;4(2):185-96.
[63] Shephard MJ, Todd D, Adair BM, Po AL, Mackie DP, Scott EM. Immunogenicity of bovine parainfluenza type 3 virus proteins encapsulated in nanoparticle vaccines, following intranasal administration to mice Res Vet Sci 2003;74(2):187-90.
[64] Feng L, Qi XR, Zhou XJ, Maitani Y, Wang SC, Jiang Y, et al. Pharmaceutical and immunological evaluation of a single-dose hepatitis B vaccine using PLGA microspheres J Control Release 2006;112(1):35-42.
[65] Kang ML, Kang SG, Jiang HL, Shin SW, Lee DY, Ahn JM, et al. In vivo induction of mucosal immune responses by intranasal administration of chitosan microspheres containing Bordetella bronchiseptica DNT Eur J Pharm Biopharm 2006;63(2):215-20.
[66] Moore A, McGuirk P, Adams S, Jones WC, McGee JP, O'Hagan DT, et al. Immunization with a soluble recombinant HIV protein entrapped in biodegradable microparticles induces HIV-specific CD8+ cytotoxic T lymphocytes and CD4+ Th1 cells Vaccine 1995;13(18):1741-9.
[67] Higaki M, Takase T, Igarashi R, Suzuki Y, Aizawa C, Mizushima Y. Enhancement of immune response to intranasal influenza HA vaccine by microparticle resin. Vaccine 1998;16(7):741-5.

[68] Brooking J, Davis SS, Illum L. Transport of nanoparticles across the rat nasal mucosa J Drug Target 2001;9(4):267-79.

[69] de Haan A, Tomee JF, Huchshorn JP, Wilschut J. Liposomes as an immunoadjuvant system for stimulation of mucosal and systemic antibody responses against inactivated measles virus administered intranasally to mice Vaccine 1995;13(14):1320-4.

[70] Baca-Estrada ME, Foldvari MM, Snider MM, Harding KK, Kournikakis BB, Babiuk LA, et al. Intranasal immunization with liposome-formulated Yersinia pestis vaccine enhances mucosal immune responses Vaccine 2000;18(21):2203-11.

[71] Joseph A, Itskovitz-Cooper N, Samira S, Flasterstein O, Eliyahu H, Simberg D, et al. A new intranasal influenza vaccine based on a novel polycationic lipid--ceramide carbamoyl-spermine (CCS) I. Immunogenicity and efficacy studies in mice. Vaccine 2006;24(18):3990-4006.

[72] Nagamoto T, Hattori Y, Takayama K, Maitani Y. Novel chitosan particles and chitosan-coated emulsions inducing immune response via intranasal vaccine delivery Pharm Res 2004;21(4):671-4.

[73] Amidi M, Romeijn SG, Verhoef JC, Junginger HE, Bungener L, Huckriede A, et al. N-Trimethyl chitosan (TMC) nanoparticles loaded with influenza subunit antigen for intranasal vaccination: Biological properties and immunogenicity in a mouse model Vaccine 2007;25(1):144-53.

[74] Jaganathan KS, Vyas SP. Strong systemic and mucosal immune responses to surface-modified PLGA microspheres containing recombinant hepatitis B antigen administered intranasally Vaccine 2006;24(19):4201-11.

[75] Vila A, Sanchez A, Tobio M, Calvo P, Alonso MJ. Design of biodegradable particles for protein delivery J Control Release 2002;78(1-3):15-24.

[76] Shakweh M, Besnard M, Nicolas V, Fattal E. Poly (lactide-co-glycolide) particles of different physicochemical properties and their uptake by peyer's patches in mice Eur J Pharm Biopharm 2005;61(1-2):1-13.

[77] Matsunaga Y, Wakatsuki Y, Tabata Y, Kawasaki H, Usui T, Yoshida M, et al. Oral immunization with size-purified microsphere beads as a vehicle selectively induces systemic tolerance and sensitization Vaccine 2000;19(4-5):579-88.

[78] Xiang SD, Scholzen A, Minigo G, David C, Apostolopoulos V, Mottram PL, et al. Pathogen recognition and development of particulate vaccines: does size matter? . Methods 2006;40(1):1-9.

[79] Vila A, Sanchez A, Evora C, Soriano I, McCallion O, Alonso MJ. PLA-PEG particles as nasal protein carriers: the influence of the particle size Int J Pharm 2005;292(1-2):43-52.

[80] Jung T, Kamm W, Breitenbach A, Hungerer KD, Hundt E, Kissel T. Tetanus toxoid loaded nanoparticles from sulfobutylated poly(vinyl alcohol)-graft-poly(lactide-co-glycolide): evaluation of antibody response after oral and nasal application in mice Pharm Res 2001;18(3):352-60.

[81] Sandri G, Bonferoni MC, Rossi S, Ferrari F, Gibin S, Zambito Y, et al. Nanoparticles based on N-trimethylchitosan: evaluation of absorption properties using in vitro (Caco-2 cells) and ex vivo (excised rat jejunum) models Eur J Pharm Biopharm 2007;65(1):68-77.

[82] Fujimura Y, Akisada T, Harada T, Haruma K. Uptake of microparticles into the epithelium of human nasopharyngeal lymphoid tissue Med Mol Morphol 2006;39(4):181-6.

[83] Baca-Estrada ME, Foldvari M, Snider M. Induction of mucosal immune responses by administration of liposome-antigen formulations and interleukin-12 J Interferon Cytokine Res 1999;19(5):455-62.

[84] Jaganathan KS, Vyas SP. Strong systemic and mucosal immune responses to surface-modified PLGA microspheres containing recombinant hepatitis B antigen administered intranasally. Vaccine 2006;24(19):4201-11.

[85] Tafaghodi M, Sajadi Tabassi SA, Jaafari MR. Induction of systemic and mucosal immune responses by intranasal administration of alginate microspheres encapsulated with tetanus toxoid and CpG-ODN Int J Pharm 2006;319(1-2):37-43.

[86] Oliveira ML, Areas AP, Campos IB, Monedero V, Perez-Martinez G, Miyaji EN, et al. Induction of systemic and mucosal immune response and decrease in Streptococcus pneumoniae colonization by nasal inoculation

of mice with recombinant lactic acid bacteria expressing pneumococcal surface antigen A Microbes Infect 2006;8(4):1016-24.

[87] Audouy SA, van Selm S, van Roosmalen ML, Post E, Kanninga R, Neef J, et al. Development of lactococcal GEM-based pneumococcal vaccines Vaccine 2006.

[88] Huckriede A, Bungener L, Stegmann T, Daemen T, Medema J, Palache AM, et al. The virosome concept for influenza vaccines. Vaccine 2005;23 Suppl 1:S26-38.

[89] Bron R, Ortiz A, Wilschut J. Cellular cytoplasmic delivery of a polypeptide toxin by reconstituted influenza virus envelopes (virosomes) Biochemistry 1994;33(31):9110-7.

[90] Cusi MG. Applications of influenza virosomes as a delivery system. Hum Vaccin 2006;2(1):1-7.

[91] Cusi MG, Zurbriggen R, Correale P, Valassina M, Terrosi C, Pergola L, et al. Influenza virosomes are an efficient delivery system for respiratory syncytial virus-F antigen inducing humoral and cell-mediated immunity. Vaccine 2002;20(29-30):3436-42.

[92] Cusi MG. The response to plasmid DNA-virosome vaccination: a role for circulating antibodies? Trends Immunol 2001;22(7):355.

[93] Owen RL, Bhalla DK. Cytochemical analysis of alkaline phosphatase and esterase activities and of lectin-binding and anionic sites in rat and mouse Peyer's patch M cells Am J Anat 1983;168(2):199-212.

[94] Hultgren SJ, Abraham S, Caparon M, Falk P, St Geme JW, 3rd, Normark S. Pilus and nonpilus bacterial adhesins: assembly and function in cell recognition Cell 1993;73(5):887-901.

[95] Sharma R, van Damme EJ, Peumans WJ, Sarsfield P, Schumacher U. Lectin binding reveals divergent carbohydrate expression in human and mouse Peyer's patches Histochem Cell Biol 1996;105(6):459-65.

[96] Clark MA, Jepson MA, Hirst BH. Lectin binding defines and differentiates M-cells in mouse small intestine and caecum Histochem Cell Biol 1995;104(2):161-8.

[97] Lee YS. Lectin reactivity in human large bowel Pathology 1987;19(4):397-401.

[98] Foster N, Clark MA, Jepson MA, Hirst BH. Ulex europaeus 1 lectin targets microspheres to mouse Peyer's patch M-cells in vivo Vaccine 1998;16(5):536-41.

[99] Carreno-Gomez B, Woodley JF, Florence AT. Studies on the uptake of tomato lectin nanoparticles in everted gut sacs Int J Pharm 1999;183(1):7-11.

[100] Hussain N, Jani PU, Florence AT. Enhanced oral uptake of tomato lectin-conjugated nanoparticles in the rat Pharm Res 1997;14(5):613-8.

[101] Russell-Jones GJ, Veitch H, Arthur L. Lectin-mediated transport of nanoparticles across Caco-2 and OK cells Int J Pharm 1999;190(2):165-74.

[102] Takata S, Ohtani O, Watanabe Y. Lectin binding patterns in rat nasal-associated lymphoid tissue (NALT) and the influence of various types of lectin on particle uptake in NALT Arch Histol Cytol 2000;63(4):305-12.

[103] Wang X, Kochetkova I, Haddad A, Hoyt T, Hone DM, Pascual DW. Transgene vaccination using Ulex europaeus agglutinin I (UEA-1) for targeted mucosal immunization against HIV-1 envelope. Vaccine 2005;23(29):3836-42.

[104] Giannasca PJ, Boden JA, Monath TP. Targeted delivery of antigen to hamster nasal lymphoid tissue with M-cell-directed lectins Infect Immun 1997;65(10):4288-98.

[105] Rogers GN, Paulson JC. Receptor determinants of human and animal influenza virus isolates: differences in receptor specificity of the H3 hemagglutinin based on species of origin Virology 1983;127(2):361-73.

[106] Tong HH, Liu X, Chen Y, James M, Demaria T. Effect of neuraminidase on receptor-mediated adherence of Streptococcus pneumoniae to chinchilla tracheal epithelium Acta Otolaryngol 2002;122(4):413-9.

[107] Tyrer P, Foxwell AR, Cripps AW, Apicella MA, Kyd JM. Microbial pattern recognition receptors mediate M-cell uptake of a gram-negative bacterium Infect Immun 2006;74(1):625-31.

[108] Clark MA, Hirst BH, Jepson MA. M-cell surface beta1 integrin expression and invasin-mediated targeting of Yersinia pseudotuberculosis to mouse Peyer's patch M cells Infect Immun 1998;66(3):1237-43.

[109] Frankel G, Lider O, Hershkoviz R, Mould AP, Kachalsky SG, Candy DC, et al. The cell-binding domain of intimin from enteropathogenic Escherichia coli binds to beta1 integrins J Biol Chem 1996;271(34):20359-64.

[110] Cruz N, Alvarez X, Specian RD, Berg RD, Deitch EA. Role of mucin, mannose, and beta-1 integrin receptors in Escherichia coli translocation across Caco-2 cell monolayers Shock 1994;2(2):121-6.

[111] Gullberg E, Keita AV, Salim SY, Andersson M, Caldwell KD, Soderholm JD, et al. Identification of cell adhesion molecules in the human follicle-associated epithelium that improve nanoparticle uptake into the Peyer's patches. J Pharmacol Exp Ther 2006;319(2):632-9.

[112] Hicks W, Jr., Hall L, 3rd, Sigurdson L, Stewart C, Hard R, Winston J, et al. Isolation and characterization of basal cells from human upper respiratory epithelium Exp Cell Res 1997;237(2):357-63.

[113] Foged C, Sundblad A, Hovgaard L. Targeting vaccines to dendritic cells. Pharm Res 2002;19(3):229-38.

[114] Rock KL, Clark K. Analysis of the role of MHC class II presentation in the stimulation of cytotoxic T lymphocytes by antigens targeted into the exogenous antigen-MHC class I presentation pathway. J Immunol 1996;156(10):3721-6.

[115] Harding CV, Song R. Phagocytic processing of exogenous particulate antigens by macrophages for presentation by class I MHC molecules. J Immunol 1994;153(11):4925-33.

[116] Lenarczyk A, Le TT, Drane D, Malliaros J, Pearse M, Hamilton R, et al. ISCOM based vaccines for cancer immunotherapy. Vaccine 2004;22(8):963-74.

[117] Malliaros J, Quinn C, Arnold FH, Pearse MJ, Drane DP, Stewart TJ, et al. Association of antigens to ISCOMATRIX adjuvant using metal chelation leads to improved CTL responses. Vaccine 2004;22(29-30):3968-75.

[118] Stewart TJ, Drane D, Malliaros J, Elmer H, Malcolm KM, Cox JC, et al. ISCOMATRIX adjuvant: an adjuvant suitable for use in anticancer vaccines; 2004 Sep 9.

[119] Pearse MJ, Drane D. ISCOMATRIX adjuvant for antigen delivery. Adv Drug Deliv Rev 2005;57(3):465-74.

[120] Sanders MT, Brown LE, Deliyannis G, Pearse MJ. ISCOM-based vaccines: the second decade. Immunol Cell Biol 2005;83(2):119-28.

[121] Daemen T, de Mare A, Bungener L, de Jonge J, Huckriede A, Wilschut J. Virosomes for antigen and DNA delivery. Adv Drug Deliv Rev 2005;57(3):451-63.

[122] Bungener L, Huckriede A, de Mare A, de Vries-Idema J, Wilschut J, Daemen T. Virosome-mediated delivery of protein antigens in vivo: efficient induction of class I MHC-restricted cytotoxic T lymphocyte activity. Vaccine 2005;23(10):1232-41.

[123] Huckriede A, Bungener L, Daemen T, Wilschut J. Influenza virosomes in vaccine development. Methods Enzymol 2003;373:74-91.

[124] Lambkin R, Oxford JS, Bossuyt S, Mann A, Metcalfe IC, Herzog C, et al. Strong local and systemic protective immunity induced in the ferret model by an intranasal virosome-formulated influenza subunit vaccine. Vaccine 2004;22(31-32):4390-6.

[125] Durrer P, Gluck U, Spyr C, Lang AB, Zurbriggen R, Herzog C, et al. Mucosal antibody response induced with a nasal virosome-based influenza vaccine. Vaccine 2003;21(27-30):4328-34.

[126] Schumacher R, Adamina M, Zurbriggen R, Bolli M, Padovan E, Zajac P, et al. Influenza virosomes enhance class I restricted CTL induction through CD4+ T cell activation. Vaccine 2004;22(5-6):714-23.

[127] Amacker M, Engler O, Kammer AR, Vadrucci S, Oberholzer D, Cerny A, et al. Peptide-loaded chimeric influenza virosomes for efficient in vivo induction of cytotoxic T cells. Int Immunol 2005;17(6):695-704.

[128] Schwaninger R, Waelti E, Zajac P, Wetterwald A, Mueller D, Gimmi CD. Virosomes as new carrier system for cancer vaccines. Cancer Immunol Immunother 2004;53(11):1005-17.

[129] Glueck R. Review of intranasal influenza vaccine. Adv Drug Deliv Rev 2001;51(1-3):203-11.

[130] Gluck U, Gebbers JO, Gluck R. Phase 1 evaluation of intranasal virosomal influenza vaccine with and without Escherichia coli heat-labile toxin in adult volunteers. J Virol 1999;73(9):7780-6.

[131] de B, Zanasi A, Ragusa S, Gluck R, Herzog C. An open-label comparison of the immunogenicity and tolerability of intranasal and intramuscular formulations of virosomal influenza vaccine in healthy adults. Clin Ther 2002;24(1):100-11.

[132] Cusi MG, Lomagistro MM, Valassina M, Valensin PE, Gluck R. Immunopotentiating of mucosal and systemic

antibody responses in mice by intranasal immunization with HLT-combined influenza virosomal vaccine. Vaccine 2000;18(25):2838-42.

[133] Kwon YJ, Standley SM, Goodwin AP, Gillies ER, Frechet JM. Directed antigen presentation using polymeric microparticulate carriers degradable at lysosomal pH for controlled immune responses. Mol Pharm 2005;2(1):83-91.

[134] Partidos CD, Vohra P, Steward MW. Induction of measles virus-specific cytotoxic T-cell responses after intranasal immunization with synthetic peptides. Immunology 1996;87(2):179-85.

[135] Partidos CD, Vohra P, Jones D, Farrar G, Steward MW. CTL responses induced by a single immunization with peptide encapsulated in biodegradable microparticles. J Immunol Methods 1997;206(1-2):143-51.

[136] Partidos CD, Vohra P, Jones DH, Farrar G, Steward MW. Induction of cytotoxic T-cell responses following oral immunization with synthetic peptides encapsulated in PLG microparticles. J Control Release 1999;62(3):325-32.

[137] Partidos CD, Vohra P, Anagnostopoulou C, Jones DH, Farrar GH, Steward MW. Biodegradable microparticles as a delivery system for measles virus cytotoxic T cell epitopes. Mol Immunol 1996;33(6):485-91.

[138] Nixon DF, Hioe C, Chen PD, Bian Z, Kuebler P, Li ML, et al. Synthetic peptides entrapped in microparticles can elicit cytotoxic T cell activity. Vaccine 1996;14(16):1523-30.

[139] Shen H, Ackerman AL, Cody V, Giodini A, Hinson ER, Cresswell P, et al. Enhanced and prolonged cross-presentation following endosomal escape of exogenous antigens encapsulated in biodegradable nanoparticles. Immunology 2006;117(1):78-88.

[140] Kwon YJ, Standley SM, Goh SL, Frechet JM. Enhanced antigen presentation and immunostimulation of dendritic cells using acid-degradable cationic nanoparticles. J Control Release 2005;105(3):199-212.

[141] Kwon YJ, James E, Shastri N, Frechet JM. In vivo targeting of dendritic cells for activation of cellular immunity using vaccine carriers based on pH-responsive microparticles. Proc Natl Acad Sci U S A 2005;102(51):18264-8.

[142] Abe N, Kodama S, Hirano T, Eto M, Suzuki M. Nasal vaccination with CpG oligodeoxynucleotide induces protective immunity against non-typeable Haemophilus influenzae in the nasopharynx Laryngoscope 2006;116(3):407-12.

[143] Kodama S, Abe N, Hirano T, Suzuki M. Safety and efficacy of nasal application of CpG oligodeoxynucleotide as a mucosal adjuvant Laryngoscope 2006;116(2):331-5.

[144] Joseph A, Louria-Hayon I, Plis-Finarov A, Zeira E, Zakay-Rones Z, Raz E, et al. Liposomal immunostimulatory DNA sequence (ISS-ODN): an efficient parenteral and mucosal adjuvant for influenza and hepatitis B vaccines Vaccine 2002;20(27-28):3342-54.

[145] Ichinohe T, Watanabe I, Ito S, Fujii H, Moriyama M, Tamura S, et al. Synthetic double-stranded RNA poly(I:C) combined with mucosal vaccine protects against influenza virus infection. J Virol 2005;79(5):2910-9.

[146] Sloat BR, Cui Z. Nasal immunization with a dual antigen anthrax vaccine induced strong mucosal and systemic immune responses against toxins and bacilli. Vaccine 2006;24(40-41):6405-13.

[147] Sloat BR, Cui Z. Nasal immunization with anthrax protective antigen protein adjuvanted with polyriboinosinic-polyribocytidylic acid induced strong mucosal and systemic immunities. Pharm Res 2006;23(6):1217-26.

[148] Storni T, Kundig TM, Senti G, Johansen P. Immunity in response to particulate antigen-delivery systems. Adv Drug Deliv Rev 2005;57(3):333-55.

[149] Joseph A, Louria-Hayon I, Plis-Finarov A, Zeira E, Zakay-Rones Z, Raz E, et al. Liposomal immunostimulatory DNA sequence (ISS-ODN): an efficient parenteral and mucosal adjuvant for influenza and hepatitis B vaccines. Vaccine 2002;20(27-28):3342-54.

[150] de Jonge MI, Hamstra HJ, Jiskoot W, Roholl P, Williams NA, Dankert J, et al. Intranasal immunisation of mice with liposomes containing recombinant meningococcal OpaB and OpaJ proteins. Vaccine 2004;22(29-30):4021-8.

[151] Perez O, Bracho G, Lastre M, Mora N, del Campo J, Gil D, et al. Novel adjuvant based on a proteoliposome-

derived cochleate structure containing native lipopolysaccharide as a pathogen-associated molecular pattern. Immunol Cell Biol 2004;82(6):603-10.

[152] Redecke V, Hacker H, Datta SK, Fermin A, Pitha PM, Broide DH, et al. Cutting edge: activation of Toll-like receptor 2 induces a Th2 immune response and promotes experimental asthma. J Immunol 2004;172(5):2739-43.

[153] Pulendran B, Kumar P, Cutler CW, Mohamadzadeh M, Van Dyke T, Banchereau J. Lipopolysaccharides from distinct pathogens induce different classes of immune responses in vivo. J Immunol 2001;167(9):5067-76.

[154] Agrawal S, Agrawal A, Doughty B, Gerwitz A, Blenis J, Van Dyke T, et al. Cutting edge: different Toll-like receptor agonists instruct dendritic cells to induce distinct Th responses via differential modulation of extracellular signal-regulated kinase-mitogen-activated protein kinase and c-Fos. J Immunol 2003;171(10):4984-9.

[155] Kaminski RW, Turbyfill KR, Oaks EV. Mucosal adjuvant properties of the Shigella invasin complex. Infect Immun 2006;74(5):2856-66.

[156] Childers NK, Miller KL, Tong G, Llarena JC, Greenway T, Ulrich JT, et al. Adjuvant activity of monophosphoryl lipid A for nasal and oral immunization with soluble or liposome-associated antigen. Infect Immun 2000;68(10):5509-16.

[157] Lee SE, Kim SY, Jeong BC, Kim YR, Bae SJ, Ahn OS, et al. A bacterial flagellin, Vibrio vulnificus FlaB, has a strong mucosal adjuvant activity to induce protective immunity. Infect Immun 2006;74(1):694-702.

[158] Strindelius L, Filler M, Sjoholm I. Mucosal immunization with purified flagellin from Salmonella induces systemic and mucosal immune responses in C3H/HeJ mice. Vaccine 2004;22(27-28):3797-808.

[159] Sbrogio-Almeida ME, Ferreira LC. Flagellin expressed by live Salmonella vaccine strains induces distinct antibody responses following delivery via systemic or mucosal immunization routes. FEMS Immunol Med Microbiol 2001;30(3):203-8.

[160] Lanzavecchia A. Mechanisms of antigen uptake for presentation Curr Opin Immunol 1996;8(3):348-54.

[161] Mutsch M, Zhou W, Rhodes P, Bopp M, Chen RT, Linder T, et al. Use of the inactivated intranasal influenza vaccine and the risk of Bell's palsy in Switzerland. N Engl J Med 2004;350(9):896-903.

[162] Couch RB. Nasal vaccination, Escherichia coli enterotoxin, and Bell's palsy. N Engl J Med 2004;350(9):860-1.

[163] van Ginkel FW, Jackson RJ, Yoshino N, Hagiwara Y, Metzger DJ, Connell TD, et al. Enterotoxin-based mucosal adjuvants alter antigen trafficking and induce inflammatory responses in the nasal tract. Infect Immun 2005;73(10):6892-902.

[164] Yuki Y, Kiyono H. New generation of mucosal adjuvants for the induction of protective immunity. Rev Med Virol 2003;13(5):293-310.

[165] Douce G, Giuliani MM, Giannelli V, Pizza MG, Rappuoli R, Dougan G. Mucosal immunogenicity of genetically detoxified derivatives of heat labile toxin from Escherichia coli. Vaccine 1998;16(11-12):1065-73.

[166] Takahashi H, Sasaki K, Takahashi M, Shigemori N, Honda S, Arimitsu H, et al. Mutant Escherichia coli enterotoxin as a mucosal adjuvant induces specific Th1 responses of CD4+ and CD8+ T cells to nasal killed-bacillus calmette-guerin in mice. Vaccine 2006;24(17):3591-8.

[167] Kende M, Del Giudice G, Rivera N, Hewetson J. Enhancement of intranasal vaccination in mice with deglycosylated chain A ricin by LTR72, a novel mucosal adjuvant. Vaccine 2006;24(12):2213-21.

[168] Bowe F, Lavelle EC, McNeela EA, Hale C, Clare S, Arico B, et al. Mucosal vaccination against serogroup B meningococci: induction of bactericidal antibodies and cellular immunity following intranasal immunization with NadA of Neisseria meningitidis and mutants of Escherichia coli heat-labile enterotoxin. Infect Immun 2004;72(7):4052-60.

[169] Yamamoto M, Briles DE, Yamamoto S, Ohmura M, Kiyono H, McGhee JR. A nontoxic adjuvant for mucosal immunity to pneumococcal surface protein A. J Immunol 1998;161(8):4115-21.

[170] Yamamoto M, Kiyono H, Yamamoto S, Batanero E, Kweon MN, Otake S, et al. Direct effects on antigen-presenting cells and T lymphocytes explain the adjuvanticity of a nontoxic cholera toxin mutant. J Immunol 1999;162(12):7015-21.

[171] Yamamoto S, Kiyono H, Yamamoto M, Imaoka K, Fujihashi K, Van Ginkel FW, et al. A nontoxic mutant of cholera toxin elicits Th2-type responses for enhanced mucosal immunity. Proc Natl Acad Sci U S A 1997;94(10):5267-72.

[172] Pine S, Barackman J, Ott G, O'Hagan D. Intranasal immunization with influenza vaccine and a detoxified mutant of heat labile enterotoxin from Escherichia coli (LTK63). J Control Release 2002;85(1-3):263-70.

[173] Ohmura M, Yamamoto M, Kiyono H, Fujihashi K, Takeda Y, McGhee JR. Highly purified mutant E112K of cholera toxin elicits protective lung mucosal immunity to diphtheria toxin. Vaccine 2001;20(5-6):756-62.

[174] Periwal SB, Kourie KR, Ramachandaran N, Blakeney SJ, DeBruin S, Zhu D, et al. A modified cholera holotoxin CT-E29H enhances systemic and mucosal immune responses to recombinant Norwalk virus-virus like particle vaccine. Vaccine 2003;21(5-6):376-85.

[175] Yamamoto M, McGhee JR, Hagiwara Y, Otake S, Kiyono H. Genetically manipulated bacterial toxin as a new generation mucosal adjuvant. Scand J Immunol 2001;53(3):211-7.

[176] Braun MC, He J, Wu CY, Kelsall BL. Cholera toxin suppresses interleukin (IL)-12 production and IL-12 receptor beta1 and beta2 chain expression. J Exp Med 1999;189(3):541-52.

[177] Ryan EJ, McNeela E, Murphy GA, Stewart H, O'Hagan D, Pizza M, et al. Mutants of Escherichia coli heat-labile toxin act as effective mucosal adjuvants for nasal delivery of an acellular pertussis vaccine: differential effects of the nontoxic AB complex and enzyme activity on Th1 and Th2 cells. Infect Immun 1999;67(12):6270-80.

[178] Takahashi I, Marinaro M, Kiyono H, Jackson RJ, Nakagawa I, Fujihashi K, et al. Mechanisms for mucosal immunogenicity and adjuvancy of Escherichia coli labile enterotoxin. J Infect Dis 1996;173(3):627-35.

[179] Yamamoto M, Kiyono H, Kweon MN, Yamamoto S, Fujihashi K, Kurazono H, et al. Enterotoxin adjuvants have direct effects on T cells and antigen-presenting cells that result in either interleukin-4-dependent or -independent immune responses. J Infect Dis 2000;182(1):180-90.

[180] Lycke N. Targeted vaccine adjuvants based on modified cholera toxin. Curr Mol Med 2005;5(6):591-7.

[181] Egan MA, Chong SY, Hagen M, Megati S, Schadeck EB, Piacente P, et al. A comparative evaluation of nasal and parenteral vaccine adjuvants to elicit systemic and mucosal HIV-1 peptide-specific humoral immune responses in cynomolgus macaques. Vaccine 2004;22(27-28):3774-88.

[182] Staats HF, Ennis FA, Jr. IL-1 is an effective adjuvant for mucosal and systemic immune responses when coadministered with protein immunogens. J Immunol 1999;162(10):6141-7.

[183] Boyaka PN, Marinaro M, Jackson RJ, Menon S, Kiyono H, Jirillo E, et al. IL-12 is an effective adjuvant for induction of mucosal immunity. J Immunol 1999;162(1):122-8.

[184] Marinaro M, Boyaka PN, Jackson RJ, Finkelman FD, Kiyono H, Jirillo E, et al. Use of intranasal IL-12 to target predominantly Th1 responses to nasal and Th2 responses to oral vaccines given with cholera toxin. J Immunol 1999;162(1):114-21.

[185] Boyaka PN, Lillard JW, Jr., McGhee J. Interleukin 12 and innate molecules for enhanced mucosal immunity. Immunol Res 1999;20(3):207-17.

[186] Bracci L, Canini I, Puzelli S, Sestili P, Venditti M, Spada M, et al. Type I IFN is a powerful mucosal adjuvant for a selective intranasal vaccination against influenza virus in mice and affects antigen capture at mucosal level. Vaccine 2005;23(23):2994-3004.

[187] Proietti E, Bracci L, Puzelli S, Di Pucchio T, Sestili P, De Vincenzi E, et al. Type I IFN as a natural adjuvant for a protective immune response: lessons from the influenza vaccine model. J Immunol 2002;169(1):375-83.

[188] Barr TA, Carlring J, Heath AW. Co-stimulatory agonists as immunological adjuvants. Vaccine 2006;24(17):3399-407.

[189] Ninomiya A, Ogasawara K, Kajino K, Takada A, Kida H. Intranasal administration of a synthetic peptide vaccine encapsulated in liposome together with an anti-CD40 antibody induces protective immunity against influenza A virus in mice. Vaccine 2002;20(25-26):3123-9.

Chapter 3

Head-to-head comparison of four nonadjuvanted inactivated cell culture-derived influenza vaccines

Effect of composition, spatial organization and immunization route on the immunogenicity in a murine challenge model

Niels Hagenaars, Enrico Mastrobattista, Harrie Glansbeek, Jacco Heldens, Han van den Bosch, Virgil Schijns, Didier Betbeder, Herman Vromans, Wim Jiskoot

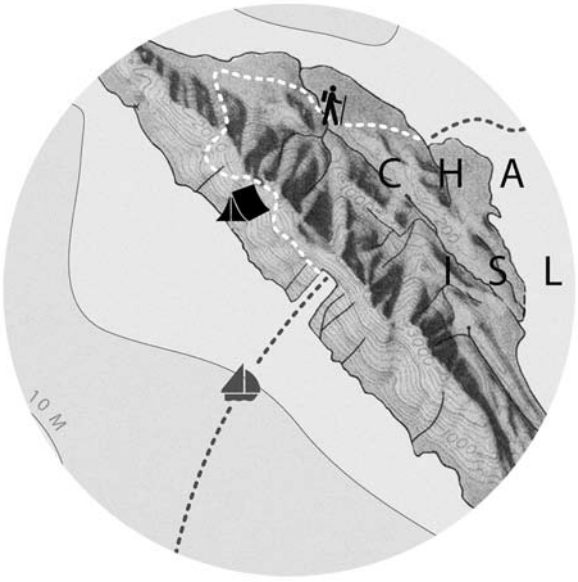

Vaccine 2008, 26(51), 6555-63

Abstract

In order to study the influence of antigen composition, spatial organization of antigen and the route of administration, four cell culture derived, inactivated, nonadjuvanted influenza vaccine formulations, i.e. whole inactivated virus (WIV), split, subunit and virosome vaccines were prepared from a single antigen batch. We directly compared the immunogenicity and efficacy of these vaccine formulations after intramuscular (i.m.) or intranasal (i.n.) administration in mice. Prime and boost vaccination were followed by a potentially lethal homologous aerosol challenge. For all vaccines, the i.m. route induced higher serum humoral immune responses as compared to the i.n. route and protected all mice against challenge at a dose of 5 μg. Upon i.n. immunization only WIV and split vaccines induced detectable IgG titers and partial protection against challenge but only very low HI titers were induced in almost all mice. WIV induced mainly IgG2a/c titers via both routes, whereas split vaccine induced exclusively IgG1 titers via both routes. Subunit and virosome vaccines induced exclusively IgG1 via the i.m. route. Mucosal sIgA levels were only detected after i.n. vaccination with WIV. Furthermore, vaccines containing all viral components (WIV and split vaccine) induced higher serum HI titers and serum antibody titers than subunit and virosome vaccines. The differences in magnitude and quality of immune responses of split and WIV, having the same composition, are likely related to their distinct spatial organization. In conclusion, the direct comparison between WIV, split, subunit and virosomes, shows that the differences in immune responses between these well known influenza vaccines can be explained by both the composition and particulate structure of these vaccine formulations.

Introduction

Since the outbreaks of highly pathogenic avian influenza (H5N1) in poultry in 1996 in Southeast Asia, resulting in lethal human infections [1], the threat of a new influenza pandemic has become real. This has prompted efforts to produce more effective influenza vaccines. In addition to adjuvant research, needle-free immunization routes are being explored [2].

There are several types of nonadjuvanted, inactivated influenza vaccines, like whole inactivated virus (WIV), split, subunit and virosome vaccines. Split and subunit influenza vaccines are widely used for seasonal intramuscular (i.m.) vaccination, generally well tolerated and considered to induce similar immune responses [3, 4]. Nonadjuvanted virosomes demonstrate comparable tolerability and immunogenicity to subunit and split vaccines in humans [5]. WIV induces strong immune responses after i.m. immunization and is superior to split and subunit vaccines in naïve human populations [6-8]. However, whole inactivated influenza virus (WIV), used as a vaccine until the 1980s, was withdrawn form the market because side effects like fever and headache were more frequently observed than with split and subunit vaccines [8]. These adverse reactions were attributed to the presence of impurities derived from production in eggs and have mainly been observed in influenza B strains [9]. However, it has been suggested that WIV may work best in case of a pandemic [10].

Currently, most influenza vaccines are still produced in eggs. This has major disadvantages like the prompt need for eggs, especially in a pandemic situation, limited production capacity and varying vaccine yields. Furthermore, these vaccines have induced allergic reactions to egg-derived protein impurities. Several companies aim to overcome these disadvantages of egg-derived vaccine production by using mammalian cell lines for vaccine production.

When compared to vaccines administered via i.m. injection, intranasal (i.n.) vaccination offers several advantages [11] such as simple, needle-free administration and less adverse reactions. Furthermore, i.n. vaccines can induce mucosal immune responses which may play an important role in the first line of defense against pathogens transmitted via the airways like influenza virus [12]. Regarding i.n. immunization, the immunogenic properties of nonadjuvanted, inactivated influenza vaccines are less clear and only a live attenuated influenza vaccine is currently licensed in the US and Russia and seems to be equally or more effective than current i.m. vaccines [13, 14]. From the nonadjuvanted inactivated influenza vaccines, WIV seems the most immunogenic one [15, 16].

All inactivated influenza vaccines are dosed on the amount of hemagglutinin (HA), but the total antigen composition and spatial organization of the vaccine components is different for WIV, split, subunit and virosome vaccines, as illustrated in figure 1. WIV and split vaccine contain all viral components, including all viral proteins and the viral genomic single-stranded RNA (ssRNA), which is complexed with viral nucleoprotein (NP) and viral polymerase proteins into ribonucleoprotein particles (RNPs). Subunit and virosomes on the other hand, contain mainly HA and small amounts of neuraminidase, another envelope glycoprotein. When comparing the spatial organization, WIV and virosomes have their antigens organized in vesicles resembling the

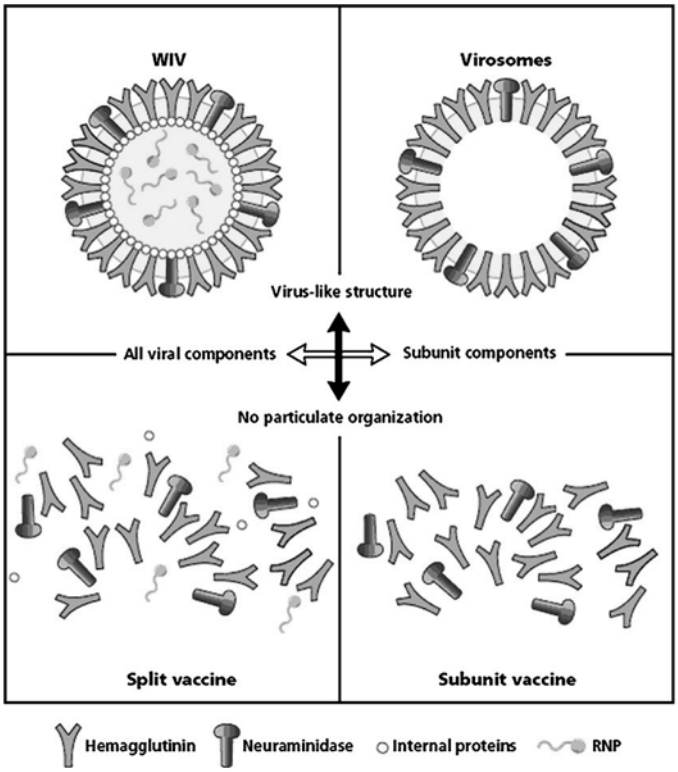

Figure 1: Schematic presentation of composition and spatial organization of WIV, split, subunit and virosome vaccines.

size of the original virus (100-300 nm), whereas subunit vaccine does not contain this particulate structure and split vaccines consist of a mixture of solubilized membrane proteins and viral internal components (figure 1).

Although several reports have been published on the immunogenicity of various influenza vaccines via i.m. and/or i.n. vaccination in humans and mice, (eg. [3, 4, 7, 17-20]), a direct comparison of these vaccine formulations is missing.

When studying the influences of antigen composition, spatial organization of vaccine components and route of administration on the magnitude and quality of induced immune responses, the antigen source, and the fact that human subjects have varying histories of influenza infections may bias the results. Therefore we made a head-to-head comparison of these four types of nonadjuvanted, cell culture-derived, inactivated influenza vaccines, prepared from the same antigen batch in unprimed mice.

Materials & methods

Materials

n-Octyl-ß-D-glucopyranoside (OG), octaethylene glycol monododecylether ($C_{12}E_8$) and sucrose were purchased from Sigma (St Louis, MO,USA). PO-labeled goat anti mouse -IgG (H+L), -IgG1,

-IgG2a/c and -IgA(Fc) were purchased from Nordic Immunological Laboratories (Tilburg, The Netherlands). Live, egg-grown, mouse adapted influenza A/PR/8/34 virus (A/PR/8/34) and purified, cell culture-grown (MDCK), β-propiolacton (BPL) inactivated influenza A/PR/8/34 virus, as well as polyclonal rabbit anti- A/PR/8/34 serum were kindly provided by Nobilon, part of Schering Plough, Boxmeer, the Netherlands

Preparation of vaccine formulations

Purified, BPL inactivated A/PR/8/34 suspended in a 10 mM phosphate buffered saline (150 mM NaCl, pH=7) (PBS) was used as WIV. This vaccine was concentrated by centrifugation at 22,000 x g for 30 min at 4 °C and resuspended in the desired volume of PBS. Split vaccine was produced by incubating the concentrated WIV with 60 mM OG for 40 min at room temperature. Isolation of membrane associated proteins (almost exclusively HA) by centrifugation of the split vaccine for 30 min at 22,000 x g at 4°C resulted in the subunit vaccine. Virosomes were prepared as described earlier [21]. Shortly, concentrated WIV was solubilized with C12E8 and centrifuged for 30 min at 22,000 x g. Biobeads (Bio-Rad, Hercules, CA,USA) were added to the clear supernatant (275 mg/5 mg total viral proteins) and incubated for 1 hr at room temperature while stirring. Then 138 mg additional Biobeads were added and the mixture was incubated for another 10 min while stirring. The obtained virosomes were purified by ultracentrifugation (33,000 x g for 2 hrs) on a sucrose block gradient (40% (w/v) + 10% (w/v)). The isolated virosome band was dialyzed against PBS in 0.5-3.0 ml Slide-A-Lyzer® 10K dialysis cassettes (Pierce, Rockford, IL, USA) with a 10 kDa MW cut off. The virosomes vaccine was then concentrated by ultrafiltration for 5-10 min at 4000 x g at 4°C using a Millipore Amicon ultra spinning ultracentrifugation device (Millipore Corp., Billerica, MA, USA). Obtained concentrated vaccines were quantified and diluted when necessary with PBS to obtain the appropriate concentration for vaccination. All i.n. vaccines had a volume of 10 µl and the i.m. vaccines had a volume of 100 µl, containing 0.13; 0.5; 2.0 or 5.0 µg HA.

Characterization of vaccine formulations

The total protein content was quantified by DC protein assay (Bio-Rad, Hercules, CA, USA) and the HA content of the vaccine formulations was determined by SDS-PAGE under nonreducing conditions and silver staining. Gels were scanned and analyzed afterwards with Totallab TL100 software. After background subtraction, intensity profiles were created of each lane. The HA content was estimated by the percentage of the HA peak in relation to the total peak area.

Particle size was measured by dynamic light scattering (DLS) using a Malvern ALV CGS-3 (Malvern Instruments, Malvern, UK). DLS results are given as a z-average particle size diameter and a polydispersity index (PDI). The PDI can range from 0 (indicating monodisperse particles) and 1 (a completely heterodisperse system).

Immunization protocol

Animal experiments were conducted according to the guidelines provided by the Dutch Animal Protection Act and were approved by a Committee for Animal Experimentation (DEC). For all

experiments 6-8 weeks old female C57-BL/6 mice (Charles River) were used. Mice were housed in groups of 3-10 mice and food was provided ad libitum. Prime and boost immunizations at day 0 and 21 respectively, were performed without anesthesia. Mice were vaccinated with WIV, split, subunit or virosome vaccine at various dosages HA. Control mice were immunized with PBS. For i.n. immunization, mice were held in supine position and the vaccine was administered to the left and right nostril (5 µl each). For i.m. vaccination, mice were injected with a volume of 100 µl in the left and right quadriceps for prime and boost vaccination, respectively.

Blood sampling and nasal washes

Blood samples were collected by orbital puncture in MINICOLLECT® serum separator tubes coated with SiO_2 (Greiner Bio-One, Alphen a/d Rijn, the Netherlands) 1 day before and 3 weeks after boost vaccination, on day 20 and 49. Coagulated blood samples were centrifuged at 6,500 x g for 8 min at room temperature to obtain serum samples. Individual serum samples were stored at -20°C until further analysis.

On day 28 after boost vaccination, 3 mice immunized with each formulation at a dose of 5.0 µg HA were anesthetized with diethyl ether and bled by orbital puncture. The trachea was cannulated towards the nasopharyngeal duct with a PVC tube (inner/outer diameter 0.5/1.0 mm). 500 µl PBS containing complete Mini, EDTA free protease inhibitor (Roche Diagnostics, Indianapolis, IN, USA) at a concentration of 1 tablet / 7 ml PBS was flushed through the nasal cavity and collected from the nostrils.

Challenge

35 days after the boost vaccination, mice were randomly divided into groups of 30-35 mice and challenged with 50 ml (8.8×10^8 x the 50% egg infectious dose (EID50)/ml) aerosolized, egg-grown influenza A/PR/8/34 using a DeVilbiss Ultra-Neb 2000 ultrasonic nebulizer (Direct Medical Ltd, Lecarrow, Ireland) for 25 min. After challenge, mice were put back in their cages and their body weight was monitored daily for two weeks. Mice were sacrificed when more than 25 % body weight was lost. 5 mice per group were challenged, except for the groups immunized with i.n. WIV at a dose of 2.0 µg (n=3) and 0.5 µg (n=4) and i.m. WIV at a dose of 2.0 µg (n=4). In these groups, 1 or 2 mice, respectively, died earlier in the experiment due to handling.

Hemagglutination inhibition test

First, 25 µl serum was incubated for 18 hrs at 37°C with 75 µl Receptor Destroying Enzyme (RDE) solution (Denka Seiken UK Ltd, Coventry, UK) to suppress nonspecific hemagglutination inhibition. RDE was then inactivated by incubating the mixture for 30 min at 56°C. Next, 150 µl PBS was added to obtain a final serum dilution of 1:10. 50 µl diluted serum was transferred in duplicate to V-bottom 96-wells plates (Greiner, Alphen a/d Rijn, The Netherlands) and serially diluted twofold in PBS. Next, 4 hemagglutination units (HAU) Influenza A/PR/8/34 (in 25 µl PBS) were added to all wells and the mixtures were incubated for 40 min at room temperature. Finally, 50 µl 0.5% (v/v) chicken erythrocytes in PBS were added to all wells and plates were incubated for

1 hr at room temperature. The HI titer was expressed as the reciprocal value of the highest serum dilution capable of completely inhibiting the virus-induced agglutination of chicken erythrocytes. If no complete inhibition could be detected in the first lane, serum was arbitrarily scored 10. Comparison between different experimental groups from the same dose was made by a one-way ANOVA test and the Bonferroni correction for multiple comparisons on the log transformed HI titers.

Enzyme linked immunosorbent assay (ELISA)

Antigen specific serum antibody responses were determined by a sandwich ELISA. Maxisorp ELISA plates (Nunc, Roskilde, Denmark) were coated overnight with polyclonal rabbit anti-A/PR/8/34 serum (dilution 1:1620). Plates were washed in between all prescribed steps using a Skanwasher 300 (Molecular Devices, Sunnyvale, CA, USA). Next, plates were incubated for 1 hr at 37°C with blocking buffer (0.2% (w/w) casein, sucrose 4% (w/w), Triton X-100 0.05% (w/w) and sodium azide 0.01% (w/w) in 30 mM TRIS pH=7.4), followed by incubation with a 1:20 dilution of egg-grown, BPL inactivated A/PR/8/34 (8 HAU/50 µl) for 1 hr at 37°C. Plates were then incubated with twofold serially diluted sera (100 µl/well) for 1 hr at 37°C. Next, plates were incubated with 100 µl of a 1:2500 dilution of horseradish peroxidase linked goat anti mouse -IgG (H+L), -IgG1, -IgG2a/c or -IgA(Fc) (Nordic Laboratories, Tilburg, the Netherlands) for 30 min, and washed twice. Finally, 100 µl 3,3',5,5'-tetramethylbenzidine (TMB) substrate solution was added and plates were incubated for 15 min at room temperature before enzymatic conversion was stopped by adding 50 µl 2 M sulfuric acid. Optical density (OD) was then measured at 450 nm using a Tecan Sunrise plate reader (Tecan Trading AG, Zurich Switzerland). Titers are given as the reciprocal of the sample dilution corresponding to 20% of the maximal ELISA signal above background.

The levels of sIgA in nasal washes are given as the OD of undiluted nasal wash samples, since the undiluted samples were too dilute to obtain a maximum plateau signal in the ELISA. Comparison between different experimental groups was made by a one-way ANOVA test and the Bonferroni correction for multiple comparisons.

Results

Characterization of vaccine formulations

Dynamic light scattering (DLS) showed that WIV had an average diameter of 220 nm with a PDI of 0.14. Virosomes had an average diameter of 275 nm and a PDI of 0.32, while the subunit vaccine had an average diameter of 18 nm with a PDI of 0.44. Split vaccine could not be reproducibly measured by DLS, since this formulation contained a cloudy precipitate.

SDS-PAGE analysis showed that the subunit and virosome vaccines contained mainly HA, whereas WIV and split vaccines contained all viral proteins, of which HA, nucleoprotein (NP), and matrix protein are the most abundant ones (fig. 2). The purity of the vaccines was confirmed by SDS-PAGE, which did not reveal any protein bands that originated from cell line impurities.

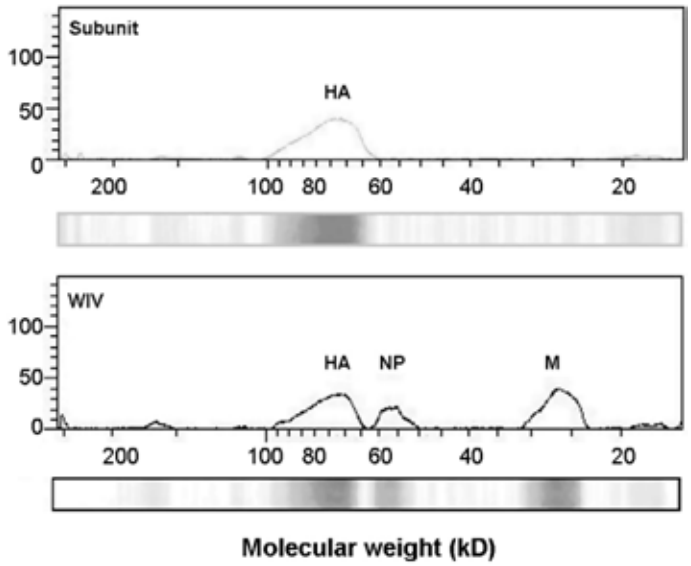

Figure 2: Silver stained SDS-PAGE gel of subunit vaccine (top) and WIV (bottom). For each lane the original stained gel and the intensity profile is shown. In the graphs, band intensity is plotted against Mw in kDa. HA=hemagglutinin, NP=nucleoprotein, M=M-protein.

Influence of antigen dose on serum immune responses

Initially, the optimal dose for a comparison between all four vaccines was determined. Therefore, WIV and subunit, being opposites in particulate structure and composition, were tested at different doses (0.13; 0.5; 2.0 and 5.0 μg HA) via the i.n. and i.m. route of administration. As shown in figure 3, after boost vaccination i.m. WIV had induced higher HI titers than subunit vaccine, showing increasing HI titers, ranging from a geometric mean titer (GMT) of 41 for the 0.13 μg dose to 1149 for the 5.0 μg dose. For the i.m. subunit vaccine, the GMT varied from ≤10 (0.13 μg dose) to 65.8 (5.0 μg dose).

When compared to i.m. vaccination, significantly lower HI titers were measured after i.n. vaccination. Subunit vaccine did not induce detectable HI titers in any of the tested doses, whereas WIV only induced HI titers ≥10 in at most 1 out of 5 mice per dose group. I.n. and i.m. control groups developed no HI titers. These results show that the i.m. route of vaccination is more efficient in inducing HI antibodies than the i.n. route and that WIV induces dose dependent HI titers that are significantly higher than those after i.m. administration of the subunit vaccine.

Influence of antigen dose on protection

To determine the protective efficacy of these vaccinations, mice were challenged 35 days after boost vaccination with a potentially lethal dose of homologous influenza A/PR/8/34 virus. After i.m. vaccination with WIV, all dosage groups were completely protected. As shown in figure 4a, all mice in these groups had a nearly constant weight over the 2 week period. In the i.m. subunit groups, a dose dependent protection was seen, as shown in figure 4b. In the lowest (0.13 μg) dose group, all mice lost a considerable amount of body weight between day 4 and 9, and only 3 out of 5 mice survived the challenge. In the 0.5 μg group, body weight loss was less, but still only 3

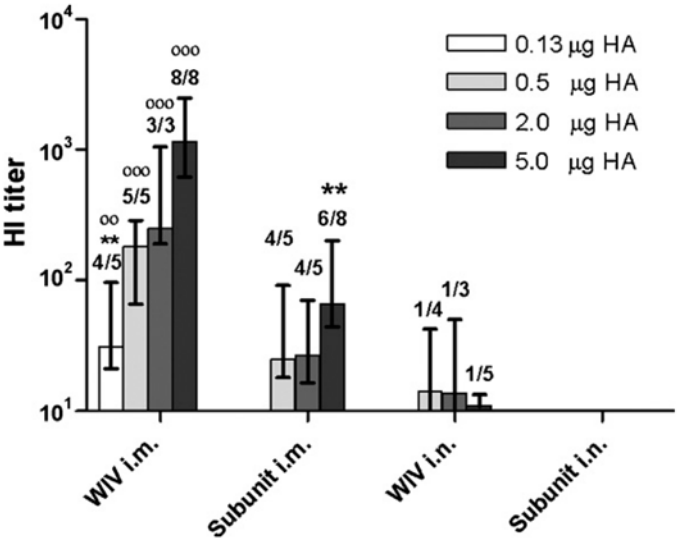

Figure 3: Geometric mean HI titers 3 weeks after i.m. or i.n. boost vaccinations with various doses of WIV or subunit vaccines. Negative samples were assigned a titer of 10 for calculation purposes. Error bars indicate 95% confidence interval. Indicated above the bars is the number of mice that developed detectable HI titers after boost vaccination (e.g. 6/8= 6 out of 8 mice). n=5 for the 0.13; 0.5 and 2.0 µg HA groups and n=8 for the 5.0 µg HA groups, except for WIV i.m. 2.0 µg (n=4), WIV i.n. 0.5 µg (n=4) and WIV i.n. 2.0 µg (n=3). All formulations of the same dose were compared using a one-way ANOVA test and Bonferroni's correction for multiple comparisons. Asterisks indicate titers are significantly (**P<0.05) higher than those of the control group. Circles indicate that titers are significantly (^{oo}P<0.01; ^{ooo}P<0.001) higher than those immunized i.m. with subunit vaccine at the same dose.

out of 5 mice survived the challenge. All mice vaccinated with 2.0 µg subunit vaccine survived the challenge, although a clear drop in body weight was still observed. At the highest (5.0 µg) dose tested, the subunit vaccine provided complete protection to all mice, resulting in 5/5 mice surviving the challenge without significant loss of body weight. In some groups (e.g.0.13; 0.5 or 2.0 µg subunit) the average body weight increases after day 7-9, due to a combined effect of sacrificing animals that lost over 25% body weight (only in the 0.13 and 0.5 µg groups) and recovery of other mice from the challenge infection.

After i.n. vaccination, 0/4 mice in the 0.125µg WIV group survived the challenge, while 1 out of 4, 3 out of 3 and 3 out of 5 mice in the WIV 0.5, 2.0 and 5.0 µg HA dosages survived, respectively (fig 4c). In the subunit group, only 1 out of 5 mice survived the challenge in the 2.0 µg group as well as the 5.0 µg group (fig. 4d).

Based on the outcome of this dose-response study, further experiments were performed at a dose of 5 µg, since this dose could provided protection against a potentially lethal challenge without weight loss for both the i.m. and the i.n.route.

HI titers

To further study the influence of the vaccine composition and their spatial organization on their immunogenicity, mice were immunized i.n. or i.m. with WIV, split, subunit and virosomes at a dose of 5 µg HA. As shown in figure 5, i.m. priming with WIV induced substantial HI titers in all mice. In contrast, detectable HI titers were absent in most mice after i.m. priming with split, subunit or

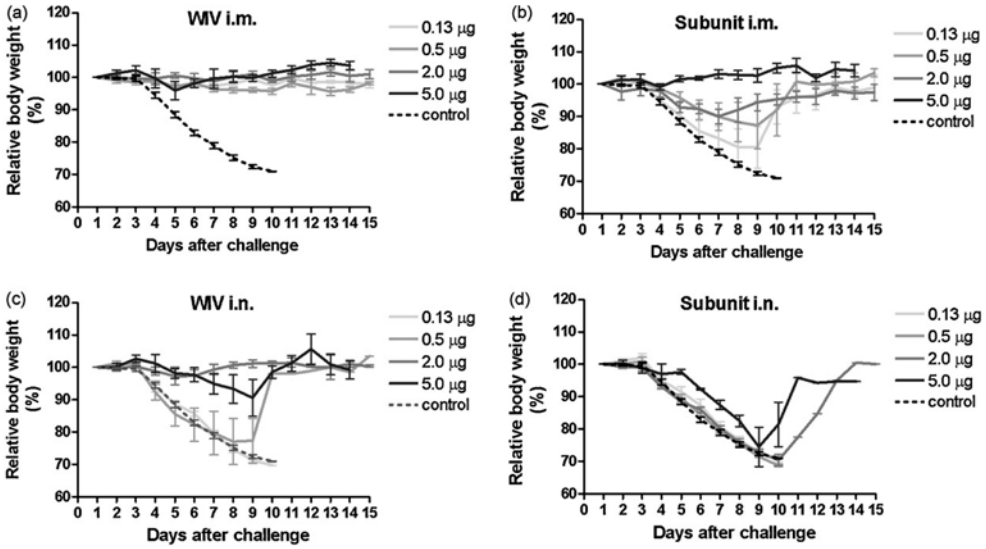

Figure 4: Average relative weight curves mice vaccinated with WIV i.m. (a), subunit i.m. (b), WIV i.n. (c) and subunit i.n. (d) after challenge.

virosome vaccines. After boost vaccination, the i.m. WIV group displayed even higher HI titers in all mice. The i.m. boost vaccination with split vaccine induced lower but substantial HI titers. Subunit and virosome vaccines induced HI titers to a lower extent after i.m. boost vaccination.
No vaccine formulation induced a detectable HI titer after a single vaccination via the i.n. route. Boost HI titers were developed after i.n. vaccination with split vaccine (4 out of 8) and WIV (1 out of 8), although all very low (ranging from 20 to 40). Subunit and virosome vaccines did not induce HI titers after i.n. vaccination.

Serum IgG titers

In addition to the HI titers, the antigen-specific IgG titers in serum were determined by ELISA, as shown in figure 6. The serum IgG titers after boost i.m. vaccination largely corresponded with HI titers. Highest serum IgG titers were induced by i.m. vaccination with WIV. IgG titers were lower after i.m. vaccinations with split, subunit and virosomes. In the control groups no IgG could be detected. After i.n. vaccination, IgG titers could be detected in all mice vaccinated with WIV and in 6 out of 8 mice vaccinated with split vaccine. Serum IgG titers of mice vaccinated with WIV or split vaccine via the i.n. route were not significantly different from the serum IgG titers developed in mice i.m. immunized with subunit or virosomes. Subunit and virosome vaccines did not induce serum IgG titers after two i.n. vaccinations.

IgG isotype profiling

To assess the isotype of IgG elicited by the various vaccine formulations, IgG subtypes were further characterized. IgG1 and IgG2a/c titers were determined by ELISA.

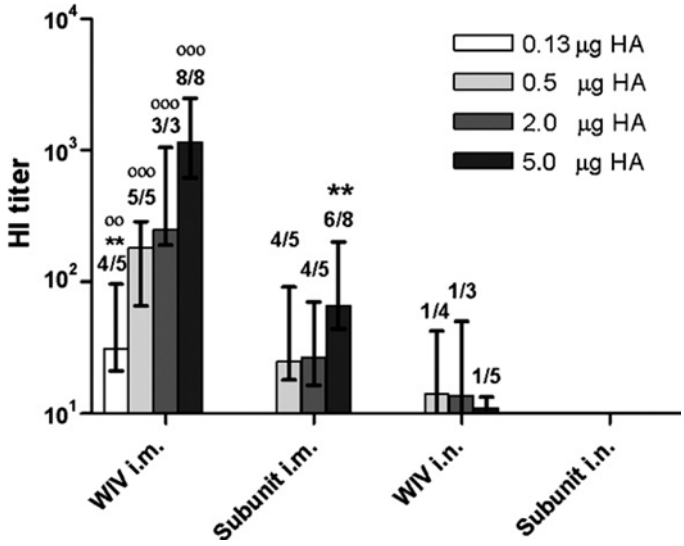

Figure 5: Geometric mean HI titers 3 weeks after prime and 3 weeks after boost vaccinations via the i.n. or i.m. route with WIV, split, subunit and virosomes containing 5 µg HA. Negative samples were assigned a titer of 10 for calculation purposes. Error bars indicate 95% confidence interval. Indicated above the bars for boost HI titers is the number of mice that developed detectable HI titers after boost vaccination (e.g. 6/8= 6 out of 8 mice). N=8 for all groups. All groups were compared using a one-way ANOVA test and Bonferroni's correction for multiple comparisons. Asterisks indicate titers are significantly (*P<0.05; ***P<0.001) higher than those of the group immunized i.m. with virosomes. Circles indicate that titers are significantly (^{ooo}P<0.001) higher than those of the group immunized i.m. with split vaccine.

As shown in figure 7, mice vaccinated i.m. with WIV developed both high IgG1 (fig.7a) and IgG2a/c (fig 7b) titers in all mice, indicative of a mixed Th1/Th2 immune response. In contrast, i.m. administered split, subunit and virosome vaccines induced exclusively IgG1 titers in almost all mice. Differences were also observed after i.n. vaccination, although overall immune responses were substantially lower than after i.m. vaccination with the same vaccine formulation. WIV induced exclusively IgG2a/c titers in 4 out of 8 mice and exclusively IgG1 titers in 2 out of 8 mice. Split vaccine on the other hand induced exclusively IgG1 titers in 6 out of 8 mice and IgG2a/c in only 1 out of 8 mice.

Mucosal immune responses

To investigate the induction of mucosal immune responses by these vaccines via the i.n. and i.m. route of administration, sIgA levels were determined in nasal washes from 3 mice in each group that were sacrificed 28 days after boost vaccination. As shown in figure 8, only mice immunized i.n. with WIV developed substantial levels of antigen specific sIgA in the nasal cavity.

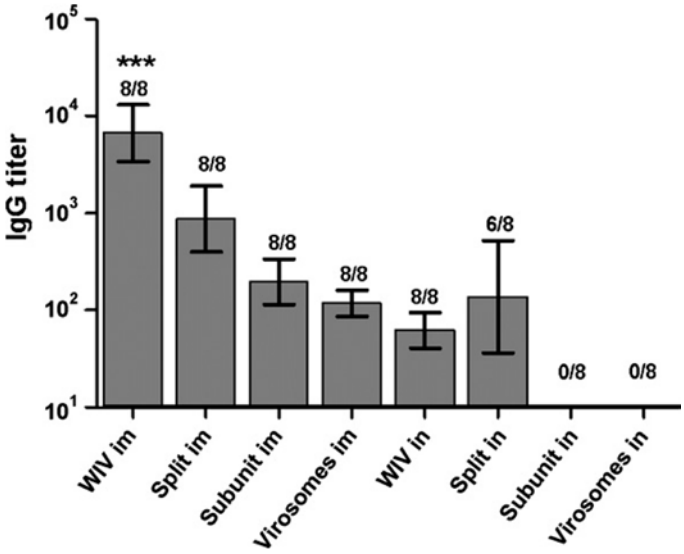

Figure 6: Geometric mean antigen specific serum IgG titers of seropositive mice 3 weeks after boost vaccination via the i.m. or i.n. route with WIV, split, subunit and virosomes containing 5µg HA. Error bars indicate the 95% confidence interval. Indicated above the bars is the number of mice that developed detectable IgG titers after boost vaccination (e.g. 6/8= 6 out of 8 mice). N=8 for all groups. All formulations were compared using a one-way ANOVA test and Bonferroni's correction for multiple comparisons. Asterisks indicate titers are significantly (***P<0.001) higher than those of the group immunized i.n. with WIV.

Protection after challenge infection

Thirty five days after boost vaccination, 5 mice in each group were challenged with a potentially lethal dose of aerosolized, egg-grown influenza A/PR/8/34. Body weight was monitored during 2 weeks after challenge. Mice that were not protected against challenge lost over 25% body weight between day 6 and 10 after challenge and had to be sacrificed before the end of the experiment. Table 1 shows the numbers of surviving mice in each group.

All mice vaccinated via the i.m. route with WIV, split, subunit and virosome vaccines were protected against challenge, as illustrated in figure 9a. All i.m. vaccinated mice had a fairly constant weight after challenge, in contrast to the control group that was administered PBS i.m.

None of the mice in the control group and the virosome group survived the challenge. Only 1 out of 5 mice vaccinated with subunit vaccine survived the challenge but still lost weight significantly. I.n. vaccination with WIV protected 3 out of 5 mice against a potentially lethal challenge while the split vaccine protected 4 out of 5 mice after i.n. vaccination. The surviving mice had a relatively constant body weight after challenge.

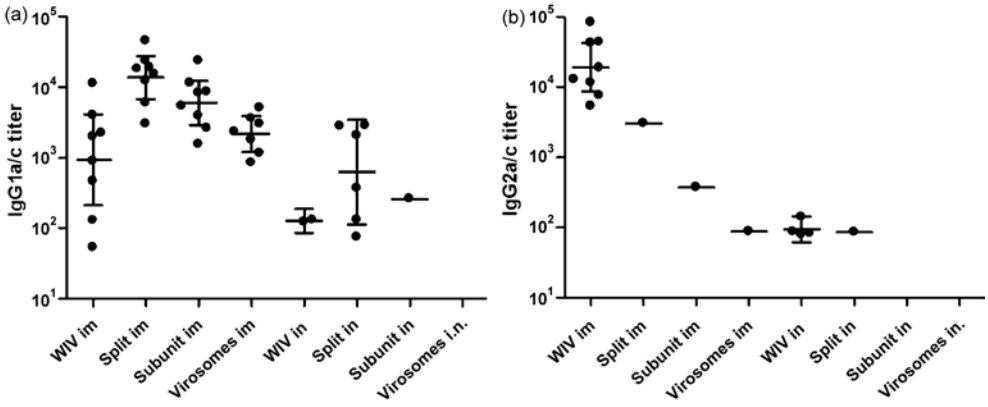

Figure 7: Antigen specific serum IgG1 (a) and IgG2a/c (b) titers of seropositive mice 3 weeks after boost vaccinations via the i.n. or i.m. route with WIV, split, subunit and virosome vaccines containing 5 µg HA. Each dot represents the individual titer of a seropositive mouse. Horizontal bars indicate the geometric mean titers and error bars indicate the 95% confidence interval. N=8 for all groups.

Discussion

In contrast to many other reports on the comparative immunogenicity of influenza vaccines, the nonadjuvanted vaccines compared in this study were prepared from the same virus batch. This avoids biased results due to different antigenic origin of vaccines from different manufacturers as well as varying impurities such as nonviral proteins from the production process [22]. Moreover, influenza virus production in mammalian cells could decrease the pyrogenic adverse reactions observed with WIV vaccines in the 1970s, since these vaccines contain no egg derived impurities and can have different glycosylation patterns than the egg-derived influenza vaccines [23]. Based on this idea, several companies aim to reintroduce WIV produced on mammalian cells to the market as a seasonal and/or pandemic influenza vaccine.

We used 6-8 weeks old female C57-BL/6 mice that were naïve to influenza infections prior to the first vaccination in order to avoid biases in immune responses due to varying histories of influenza infections and vaccination, as is often the case when human individuals are used. Disadvantage of this approach is that the results may not have a direct predictive value for the use in primed humans, but our experimental setup may be very relevant for vaccination against a pandemic influenza virus, for which the human population is not primed. Other authors have also demonstrated that priming can have a big impact on the response to influenza vaccines [24].

We initially compared WIV, by definition containing all viral components in a particulate structure, and subunit vaccine, containing only solubilized HA, at different doses administered i.m. and i.n. We showed that these vaccines induce dose dependent immune responses and protection after i.m. administration. After i.n. administration, however, only WIV induced dose dependent immune responses and protection, while the subunit vaccine was not immunogenic at any of the tested doses. These findings are supported by earlier findings that WIV is more immunogenic than

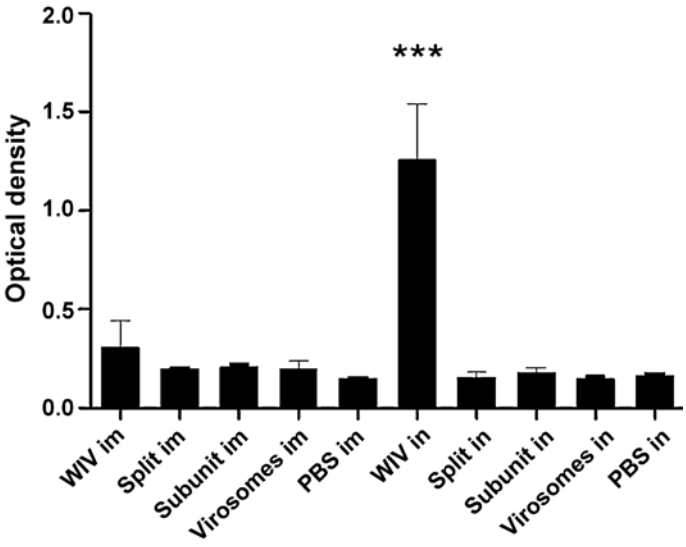

Figure 8: Antigen specific sIgA levels in nasal washes of mice 28 days after boost vaccination via the i.n. or i.m. route with WIV, split, subunit or virosome vaccines containing 5 μg HA. PBS was administered as a negative control. N=3 for all groups. All formulations were compared using a one-way ANOVA test and Bonferroni's correction for multiple comparisons. Asterisks indicate titers are significantly (***P<0.001) higher than those of all other groups.

subunit vaccine via either route [16, 19] and that a 10 fold higher dose is needed via i.n. vaccination to induce protection [25].

To further study the role of vaccine composition and organized particulate structure on the immunogenicity, mice were vaccinated with WIV, split, subunit and virosome vaccines. Clearly, WIV and split vaccine, both containing all viral components, were more immunogenic than subunit and virosome vaccines, containing only subunit components. Internal proteins and ssRNA, present in WIV and split vaccine but not in subunit and virosome vaccines, likely contribute to the overall immunogenicity and efficacy of these vaccine formulations.

The spatial organization, surprisingly, does not seem to influence the immunogenicity of the subunit vaccine, since subunit and virosome vaccines induced comparable immune responses via both routes. It seems that formulation of HA in virosomes, although effective as a vaccine in

Table 1. Number of mice per group that were protected against infection by a potentially lethal, homologous challenge with A/PR/8/34.

Formulation	Route of administration	Survival rate[a]
WIV	i.m.	5/5
Split	i.m.	5/5
Subunit	i.m.	5/5
Virosomes	i.m.	5/5
PBS	i.m.	0/5
WIV	i.n.	3/5
Split	i.n.	4/5
Subunit	i.n.	1/5
Virosomes	i.n.	0/5
PBS	i.n.	0/5

[a] Indicated by the number of mice per group survived for 2 weeks after challenge.
4/5 indicates that 4 out of 5 challenged mice survived.

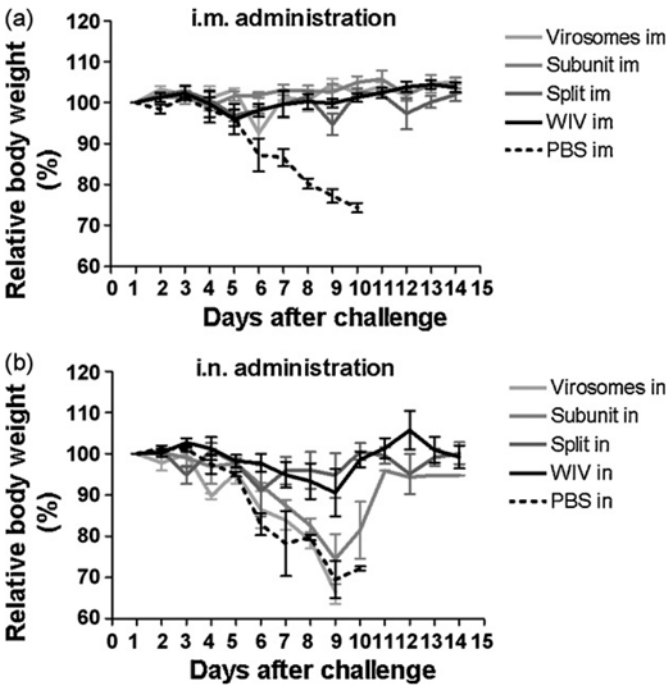

Figure 9: Average relative weight curves after challenge of mice vaccinated with WIV, split, subunit and virosomes via the i.m. (a) or i.n. (b) route of administration.

combination with adjuvants or as delivery system for encapsulated antigens or DNA [26], does not improve the immunogenicity of influenza subunit vaccines via the i.m. or i.n. route in mice. Interestingly, also for i.n. administration, the vaccine composition appeared more important than the organized particulate structure, although it is generally believed that antigens are taken up from the nasal cavity through M-cells [27], which preferably take up particles [28]. Apparently, a nonadjuvanted influenza vaccine containing only HA is not immunogenic enough to induce immune responses via the i.n. route.

When comparing the WIV and split vaccines, both containing all viral components, the spatial organization does affect the strength and type of the immune responses. WIV induced higher HI and serum IgG titers than the split vaccine after i.m. vaccination. Additionally, mixed serum IgG2a/c and IgG1 titers were obtained with WIV vaccine, whereas split vaccine induced mainly IgG1. The IgG2a/c isotype, indicative of a Th1 immune response, is the strongest isotype in response to viral infection [29] and is expected to be involved in cellular immune responses [30-33]. Th1 responses are desired in influenza vaccination because they are superior to Th2 responses in inducing cross-protection [34].

One of the components that is present in the WIV and split vaccine is the viral genomic, negative, ssRNA, a ligand for the murine and human toll like receptor 7 [35, 36]. Live as well as heat inactivated influenza virus induces plasmacytoid dendritic cells to produce IFN-α upon binding of ssRNA to endosomal TLR7 [37], which in turn bridges the innate and adaptive immune compartments and induces Th1 type immune responses. Moreover, direct activation of TLRs 7 and 9 on B-cells by

ssRNA [38] and CpG [39], respectively, induces a class switch to IgG2a. Our results indicate that an isotype switch to IgG2a/c occurs only when all viral components are present in an organized particulate system such as a viral envelope. The exclusive induction of IgG1 observed for the subunit and virosomal vaccine may be explained by the absence of ssRNA. However, this does not explain the differences observed between WIV and split vaccine, since their viral composition is identical. So, both the spatial organization of proteins and viral ssRNA must be responsible for these differences.
Firstly, the ssRNA in WIV is protected from RNases until cellular uptake because of its encapsulation in the viral envelope, whereas the ssRNA in a split vaccine is accessible to RNases [40]. Secondly, these differences may be explained by a more efficient delivery of ssRNA to TLR7, present within the endosomal compartment [41, 42]. Thirdly, delivery of ssRNA and antigens to the same APC, even to the same endosome, could increase the adjuvant effects of ssRNA. Co-delivery of antigen and TLR ligands as adjuvants, by incorporation in the same particle or by covalent linkage, leads to improved immune responses when compared to administration of co-administered antigen and soluble adjuvant [33, 43, 44]. WIV co-delivers the TLR7 ligand ssRNA and the influenza antigens to the same cell, even the same endosome, whereas for split vaccine this would be less likely, even in the case ssRNA is present.
In addition to different serum IgG immune responses, differences in mucosal immune responses were observed. WIV was the only vaccine that induced mucosal sIgA, and only after i.n. vaccination. These results are in agreement with earlier findings that sIgA development depends on the route of administration [25]. Several reports suggest that the induction of sIgA after i.n. vaccination mediates cross-protection against heterologous influenza strains [45-47]. Furthermore, i.n. vaccination with WIV adjuvanted with poly(I):poly(C_{12}U) provided superior cross-protection in mice to a subcutaneous administration of the same vaccine formulation [48].
For i.m. influenza vaccinations, HI titers are used as the correlate of protection against influenza in humans. In our experiments, the HI titers also correlated with protection after i.m. vaccination. Remarkably, this correlation could not be found after i.n. vaccination. Most mice that were protected against challenge had not developed HI titers, in line with results published by others [48]. Moreover, WIV and split vaccine were both protective but induced qualitatively distinct immune responses. Although one should be cautious translating results of mice to humans, it is possible that HI titers will not correlate with protection in human i.n. vaccinations either. Future research should reveal which roles individual components of the immune response, including mucosal and systemic humoral responses as well as cellular immune responses, play in vaccine-induced protection against influenza infection. Cytotoxic T lymphocytes and sIgA may be especially important in protection against heterologous influenza infection, like in a pandemic situation, since pre-existing serum antibodies fail to recognize a newly introduced influenza A subtype [48, 49].
This report directly compares WIV, split, subunit and virosomes, and shows for the first time that the differences in immune responses between these well known influenza vaccines can be explained by both the composition and particulate structure of these vaccine formulations.
Our results show that of the vaccine formulations tested here, the best formulation is the organized particulate WIV, containing all viral components, when administered via the i.m. route.

For the i.n. route, all tested vaccines require better formulation or higher dosing. Since worldwide the vaccine production capacities are limited and the demand for influenza vaccines is increasing, especially in the case of a pandemic, there is a need for a cell culture-derived, antigen sparing, cross-protective vaccine formulation. Although WIV and split vaccine were comparable in efficacy in this challenge model after i.n. vaccination, WIV seems the best candidate for such an i.n. vaccine, since the type of immune responses that were induced are more likely to mediate cross-protection.

Acknowledgements

The authors thank the people of the Animal Services Department of Nobilon, part of Schering-Plough, for their help with the animal experiments and Frouke Kuijer for making figure 1.

References

[1] de Jong JC, Claas EC, Osterhaus AD, Webster RG, Lim WL. A pandemic warning? Nature 1997;389(6651):554.

[2] Details of new influenza research projects announced today. Press release. Brussels: European Union; 2007 11 September 2007. Report No.: MEMO/07/348.

[3] Morales A, Arias Salazar J, Salazar Y, Garcia A, Arnoux S, Arancibia A, et al. A randomized controlled trial comparing split and subunit influenza vaccines in adults in Colombia. Medicina (B Aires) 2003;63(3):197-204.

[4] Beyer WEP, Palache AM, Osterhaus ADME. Comparison of serology and reactogenicity between influenza subunit vaccines and whole virus or split vaccines - A review and meta-analysis of the literature. Clinical Drug Investigation 1998;15(1):1-12.

[5] de Bruijn IA, Nauta J, Cramer WC, Gerez L, Palache AM. Clinical experience with inactivated, virosomal influenza vaccine. Vaccine 2005;23 Suppl 1:S39-49.

[6] Samdal HH, Bakke H, Oftung F, Holst J, Haugen IL, Korsvold GE, et al. A non-living nasal influenza vaccine can induce major humoral and cellular immune responses in humans without the need for adjuvants. Hum Vaccin 2005;1(2):85-90.

[7] Hovden AO, Cox RJ, Haaheim LR. Whole influenza virus vaccine is more immunogenic than split influenza virus vaccine and induces primarily an IgG2a response in BALB/c mice. Scand J Immunol 2005;62(1):36-44.

[8] Gross PA, Ennis FA, Gaerlan PF, Denson LJ, Denning CR, Schiffman D. A controlled double-blind comparison of reactogenicity, immunogenicity, and protective efficacy of whole-virus and split-product influenza vaccines in children. J Infect Dis 1977;136(5):623-32.

[9] Gwaltney JM, DeSanctis AN, Metzgar DP, Hendley JO. Systemic reactions to influenza B vaccine. Am J Epidemiol 1977;105(3):252-60.

[10] Jefferson TO, Rivetti D, Di Pietrantonj C, Rivetti A, Demicheli V. Vaccines for preventing influenza in healthy adults. Cochrane Database Syst Rev 2007(2):CD001269.

[11] Slütter B, Hagenaars N, Jiskoot W. Rational design of nasal vaccines. J Drug Target 2008;16(1):1-17.

[12] Renegar KB, Small PA, Jr. Passive transfer of local immunity to influenza virus infection by IgA antibody. J Immunol 1991;146(6):1972-8.

[13] Belshe RB, Mendelman PM, Treanor J, King J, Gruber WC, Piedra P, et al. The efficacy of live attenuated, cold-adapted, trivalent, intranasal influenzavirus vaccine in children. N Engl J Med 1998;338(20):1405-12.

[14] Ambrose CS, Walker RE, Connor EM. Live attenuated influenza vaccine in children. Semin Pediatr Infect Dis 2006;17(4):206-12.

[15] Takada A, Matsushita S, Ninomiya A, Kawaoka Y, Kida H. Intranasal immunization with formalin-inactivated virus vaccine induces a broad spectrum of heterosubtypic immunity against influenza A virus infection in mice. Vaccine 2003;21(23):3212-8.

[16] Minne A, Jaworska J, Gerhold K, Ahrens B, Avagyan A, Vanbever R, et al. Intranasal delivery of whole influenza vaccine prevents subsequent allergen-induced sensitization and airway hyper-reactivity in mice. Clin Exp Allergy 2007;37(8):1250-8.

[17] Barry DW, Staton E, Mayner RE. Inactivated influenza vaccine efficacy: diminished antigenicity of split-product vaccines in mice. Infect Immun 1974;10(6):1329-36.

[18] Ben-Yehuda A, Joseph A, Zeira E, Even-Chen S, Louria-Hayon I, Babai I, et al. Immunogenicity and safety of a novel liposomal influenza subunit vaccine (INFLUSOME-VAC) in young adults. J Med Virol 2003;69(4):560-7.

[19] Bright RA, Carter DM, Daniluk S, Toapanta FR, Ahmad A, Gavrilov V, et al. Influenza virus-like particles elicit broader immune responses than whole virion inactivated influenza virus or recombinant hemagglutinin. Vaccine 2007;25(19):3871-8.

[20] Greenbaum E, Furst A, Kiderman A, Stewart B, Levy R, Schlesinger M, et al. Mucosal [SIgA] and serum [IgG] immunologic responses in the community after a single intra-nasal immunization with a new inactivated trivalent influenza vaccine. Vaccine 2002;20(7-8):1232-9.

[21] Stegmann T, Morselt HW, Booy FP, van Breemen JF, Scherphof G, Wilschut J. Functional reconstitution of influenza virus envelopes. Embo J 1987;6(9):2651-9.

[22] Chaloupka I, Schuler A, Marschall M, Meier-Ewert H. Comparative analysis of six European influenza vaccines. Eur J Clin Microbiol Infect Dis 1996;15(2):121-7.

[23] Govorkova EA, Kodihalli S, Alymova IV, Fanget B, Webster RG. Growth and immunogenicity of influenza viruses cultivated in Vero or MDCK cells and in embryonated chicken eggs. Dev Biol Stand 1999;98:39-51; discussion 73-4.

[24] Potter CW, Jennings R. Effect of priming on subsequent response to inactivated influenza vaccine. Vaccine 2003;21(9-10):940-5.

[25] Bizanov G, Janakova L, Knapstad SE, Karlstad T, Bakke H, Haugen IL, et al. Immunoglobulin-A antibodies in upper airway secretions may inhibit intranasal influenza virus replication in mice but not protect against clinical illness. Scand J Immunol 2005;61(6):503-10.

[26] Huckriede A, Bungener L, Daemen T, Wilschut J. Influenza virosomes in vaccine development. Methods Enzymol 2003;373:74-91.

[27] Neutra MR, Frey A, Kraehenbuhl JP. Epithelial M cells: gateways for mucosal infection and immunization. Cell 1996;86(3):345-8.

[28] Brooking J, Davis SS, Illum L. Transport of nanoparticles across the rat nasal mucosa. J Drug Target 2001;9(4):267-79.

[29] Nimmerjahn F, Ravetch JV. Fcgamma receptors: old friends and new family members. Immunity 2006;24(1):19-28.

[30] Klaus GG, Pepys MB, Kitajima K, Askonas BA. Activation of mouse complement by different classes of mouse antibody. Immunology 1979;38(4):687-95.

[31] Heusser CH, Anderson CL, Grey HM. Receptors for IgG: subclass specificity of receptors on different mouse cell types and the definition of two distinct receptors on a macrophage cell line. J Exp Med 1977;145(5):1316-27.

[32] Kipps TJ, Parham P, Punt J, Herzenberg LA. Importance of immunoglobulin isotype in human antibody-dependent, cell-mediated cytotoxicity directed by murine monoclonal antibodies. J Exp Med 1985;161(1):1-17.

[33] Huleatt JW, Jacobs AR, Tang J, Desai P, Kopp EB, Huang Y, et al. Vaccination with recombinant fusion proteins incorporating Toll-like receptor ligands induces rapid cellular and humoral immunity. Vaccine 2007;25(4):763-75.

[34] Moran TM, Park H, Fernandez-Sesma A, Schulman JL. Th2 responses to inactivated influenza virus can be converted to Th1 responses and facilitate recovery from heterosubtypic virus infection. J Infect Dis 1999;180(3):579-85.

[35] Heil F, Hemmi H, Hochrein H, Ampenberger F, Kirschning C, Akira S, et al. Species-specific recognition of single-stranded RNA via toll-like receptor 7 and 8. Science 2004;303(5663):1526-9.

[36] Lund JM, Alexopoulou L, Sato A, Karow M, Adams NC, Gale NW, et al. Recognition of single-stranded RNA viruses by Toll-like receptor 7. Proc Natl Acad Sci U S A 2004;101(15):5598-603.

[37] Diebold SS, Kaisho T, Hemmi H, Akira S, Reis e Sousa C. Innate antiviral responses by means of TLR7-mediated recognition of single-stranded RNA. Science 2004;303(5663):1529-31.

[38] Heer AK, Shamshiev A, Donda A, Uematsu S, Akira S, Kopf M, et al. TLR signaling fine-tunes anti-influenza B cell responses without regulating effector T cell responses. J Immunol 2007;178(4):2182-91.

[39] Jegerlehner A, Maurer P, Bessa J, Hinton HJ, Kopf M, Bachmann MF. TLR9 signaling in B cells determines class switch recombination to IgG2a. J Immunol 2007;178(4):2415-20.

[40] Ye Z, Liu T, Offringa DP, McInnis J, Levandowski RA. Association of influenza virus matrix protein with ribonucleoproteins. J Virol 1999;73(9):7467-73.

[41] Heil F, Ahmad-Nejad P, Hemmi H, Hochrein H, Ampenberger F, Gellert T, et al. The Toll-like receptor 7 (TLR7)-specific stimulus loxoribine uncovers a strong relationship within the TLR7, 8 and 9 subfamily. Eur J Immunol 2003;33(11):2987-97.

[42] Lee J, Chuang TH, Redecke V, She L, Pitha PM, Carson DA, et al. Molecular basis for the immunostimulatory activity of guanine nucleoside analogs: activation of Toll-like receptor 7. Proc Natl Acad Sci U S A 2003;100(11):6646-51.

[43] Joseph A, Louria-Hayon I, Plis-Finarov A, Zeira E, Zakay-Rones Z, Raz E, et al. Liposomal immunostimulatory DNA sequence (ISS-ODN): an efficient parenteral and mucosal adjuvant for influenza and hepatitis B vaccines. Vaccine 2002;20(27-28):3342-54.

[44] Zhang XQ, Dahle CE, Weiner GJ, Salem AK. A comparative study of the antigen-specific immune response induced by co-delivery of CpG ODN and antigen using fusion molecules or biodegradable microparticles. J Pharm Sci 2007;96(12):3283-92.

[45] Brandtzaeg P. Induction of secretory immunity and memory at mucosal surfaces. Vaccine 2007;25(30):5467-84.

[46] Asahi-Ozaki Y, Yoshikawa T, Iwakura Y, Suzuki Y, Tamura S, Kurata T, et al. Secretory IgA antibodies provide cross-protection against infection with different strains of influenza B virus. J Med Virol 2004;74(2):328-35.

[47] Asahi Y, Yoshikawa T, Watanabe I, Iwasaki T, Hasegawa H, Sato Y, et al. Protection against influenza virus infection in polymeric Ig receptor knockout mice immunized intranasally with adjuvant-combined vaccines. J Immunol 2002;168(6):2930-8.

[48] Ichinohe T, Tamura S, Kawaguchi A, Ninomiya A, Imai M, Itamura S, et al. Cross-protection against H5N1 influenza virus infection is afforded by intranasal inoculation with seasonal trivalent inactivated influenza vaccine. J Infect Dis 2007;196(9):1313-20.

[49] Rimmelzwaan GF, Fouchier RA, Osterhaus AD. Influenza virus-specific cytotoxic T lymphocytes: a correlate of protection and a basis for vaccine development. Curr Opin Biotechnol 2007;18(6):529-36.

Chapter 4

Physicochemical and immunological characterization of *N,N,N*-trimethyl chitosan-coated whole inactivated influenza virus vaccine for intranasal administration

Niels Hagenaars, Enrico Mastrobattista, Rolf Verheul, Imke Mooren, Harrie Glansbeek, Jacco Heldens, Han van den Bosch, Wim Jiskoot

Pharmaceutical Research 2009, 26(6), 1353-64

Abstract

Purpose: The purpose of this study was the development and physicochemical and immunological characterization of intranasal (i.n.) vaccine formulations of whole inactivated influenza virus (WIV) coated with N,N,N-trimethyl chitosan (TMC).

Methods: Synthesized TMCs with a degree of quarternization of 15% (TMC15) or 37% (TMC37) were tested *in vitro* for their ability to decrease the transepithelial resistance (TEER) of an epithelial cell monolayer. TMC15- and TMC37-coated WIV (TMC15-WIV and TMC37-WIV) were characterized by zeta potential measurements, dynamic light scattering, electron microscopy and gel permeation chromatography. Mice were vaccinated i.n. with selected vaccine formulations and immunogenicity was determined by measuring serum hemagglutination inhibition (HI) and serum IgG, IgG1 and IgG2a/c titers. Also a pulse-chase study with TMCs in solution administered i.n. 2 h prior to WIV was performed. Protective efficacy of vaccination was determined by an aerosol virus challenge.

Results: TMC37 induced a reversible decrease in TEER, suggesting the opening of tight junctions, whereas TMC15 did not affect TEER. Simple mixing of (negatively charged) WIV with TMC15 or TMC37 resulted in positively charged particles with TMCs being partially bound. Intranasal immunization with TMC37-WIV or TMC15-WIV induced stronger HI, IgG, IgG1 and IgG2a/c titers than WIV alone. TMC37-WIV induced the highest immune responses. Both TMC15-WIV and TMC37-WIV provided protection against challenge, whereas WIV alone was not protective. Intranasal administration of TMC prior to WIV did not result in significant immune responses, indicating that the immunostimulatory effect of TMC is primarily based on improved i.n. delivery of WIV.

Conclusions: Coating of WIV with TMC is a simple procedure to improve the delivery and immunogenicity of i.n. administered WIV and may enable effective i.n. vaccination against influenza.

Introduction

Currently most inactivated influenza vaccines on the market are administered via the intramuscular (i.m.) or subcutaneous (s.c.) route. Although these routes of administration can induce strong systemic humoral immune responses, the intranasal (i.n.) route has several advantages when compared to i.m. vaccination [1]. It allows simple, non-invasive, needle-free administration which decreases infection risks due to the reuse of needles, enables large scale vaccinations without trained personnel and increases compliance. Furthermore, the i.n. route theoretically induces less local adverse effects than i.m. needle injections and is easily accessible, making administration by a trained professional unnecessary. Furthermore, i.n. immunization has the potential of inducing mucosal immunity, and it has been suggested that nasal vaccination may induce broader protection against heterologous influenza viruses, a feature that is very important in providing protection against seasonal as well as pandemic influenza [2, 3].

Live attenuated influenza virus (LAIV) has been researched extensively and is currently on the market as i.n. seasonal influenza vaccine in the US and Russia. The efficacy of i.n. LAIV is comparable to or even better than that of i.m. split vaccines [4]. Nonadjuvanted inactivated i.n. influenza vaccines on the other hand, are generally not as immunogenic as i.m. vaccines or as promising as LAIV for i.n. vaccination. On the other hand, inactivated vaccines are generally regarded as safer than LAIV, especially for infants and immunocompromised individuals [5].

From the inactivated influenza vaccines, whole inactivated virus (WIV) formulations seem to be the most promising [5-8]. In comparison to subunit and split influenza vaccines, WIV induces much stronger humoral and cellular immune responses via various immunization routes [5, 9-11]. Furthermore, WIV can induce cross-protection, especially when administered via the mucosal route, which may be especially important in the development of a pandemic vaccine [2, 6, 12, 13]. The superior, Th1-biased immune responses can be explained by the presence of viral RNA inside the particulate viral structure of WIV, a TLR 7 ligand, which acts as an adjuvant [10].

Although these features of WIV are promising, the immunogenicity of plain WIV after i.n. administration, especially the systemic humoral immune responses, can still be improved [14]. The use of adjuvants is a common approach to improve vaccination and different types of adjuvants have been tested for i.n. vaccination, like *Escherichia coli* heat labile enterotoxin (LT), and cholera toxin (CT) derivatives, various toll-like receptor ligands like CpG motifs, LPS and poly I:C (as reviewed in [1]). In the case of i.n. vaccination, however, the induction of relatively low systemic immune responses cannot be fully explained by a lack of intrinsic immunogenicity of the vaccine, illustrated by the strong immune responses induced by these vaccines after i.m. administration, especially in the case of WIV [10, 15-17]. It is therefore likely that inefficient delivery of antigens to antigen presenting cells, caused by mucosal barriers and rapid clearance from the nasal cavity, is a limiting factor in the induction of stronger immune responses. Use of mucoadhesive polymers may overcome these problems by their interaction with the mucosal surfaces in the nasal cavity, leading to an increased residence time and enhanced uptake of the antigen [18].

Chitosan is a mucoadhesive polymer that has been studied for many applications [19] [20], including

mucosal vaccine delivery [21-23]. The unfavorable pH-dependent water solubility of chitosan has prompted the development of chitosan derivatives [24], like *N,N,N*-trimethyl chitosan (TMC) [25, 26]. TMC is a cationic and mucoadhesive polymer that has been tested as additive in mucosal vaccines, both as solution in oral, pulmonary and nasal vaccination [27] and as nanoparticles with associated antigen [28-32]. TMC can be characterized by the degree of quaternization (DQ) of amines, which determines the charge density of TMC. The DQ of TMC can be tailored during synthesis and influences chemical and biological properties of TMC. Amidi et al. demonstrated the superior immunogenicity of i.n. administered influenza antigens that are encapsulated in TMC nanoparticles when compared to antigens admixed with TMC solutions [28].

Because WIV vaccines were found to be the most immunogenic of the nonadjuvanted influenza vaccines [14, 16, 17, 33], it is a logical step to use WIV vaccines for optimization with TMC for i.n. vaccination. In this study, we propose TMC-coated WIV (TMC-WIV) as i.n. influenza vaccine by combining the mucoadhesive properties of TMC with the particulate structure of WIV. This approach exploits the ability of TMC to interact not only with negatively charged mucus and mucosal surfaces, but also with negatively charged virus particles. We used *O*-methylated TMCs with a DQ of 15% (TMC15) and 37% (TMC37) to coat WIV. The preparation and characterization of TMC15-coated WIV (TMC15-WIV) and TMC37-coated WIV (TMC37-WIV) vaccines are presented and it is analyzed whether these novel vaccine formulations significantly improve the immunogenicity and protective efficacy of i.n. administered whole inactivated influenza virus. Additionally, a pulse-chase study is performed with TMCs in solution and WIV to determine if TMC requires coadministration with WIV to exert its adjuvant effect.

Materials & methods

Materials

Chitosan was purchased from Primex (Siglufjordur, Iceland). N-Methyl-2-pyrrolidone (NMP), thiazolyl blue tetrazolium bromide (MTT), sodium acetate, acetic acid (anhydrous), sodium hydroxide and hydrochloric acid were obtained from Sigma–Aldrich Chemical Co (Zwijndrecht, the Netherlands). Dulbecco's modified Eagle's medium (DMEM) and Hank's balanced salt solution (HBSS) were purchased from Invitrogen (Breda, the Netherlands). Sodium dodecyl sulfate (SDS) was ordered from Merck (Darmstadt, Germany). Linear polyethylene imine (PEI) was kindly provided by S. van der Wal (Utrecht University, the Netherlands). Iodomethane 99% stabilized with copper was obtained from Acros Organics (Geel, Belgium). Live, egg-grown, mouse adapted influenza A/PR/8/34 virus (A/PR/8/34) and purified, cell culture-grown (Madin-Darby Canine Kidney (MDCK) cells), β-propiolacton (BPL)-inactivated influenza A/PR/8/34 virus, as well as polyclonal rabbit anti-A/PR/8/34 serum were kindly provided by Nobilon, part of Schering-Plough, Boxmeer, the Netherlands. PO-labeled goat anti mouse -IgG (H+L), -IgG1, -IgG2a/c and -IgA(Fc) were purchased from Nordic Immunological Laboratories (Tilburg, The Netherlands). All other chemicals were analytical grade.

Synthesis of TMC15 and TMC37

TMC15 was synthesized by methylation of chitosan as described previously [26, 34]. Briefly, 1.0 g of chitosan (number average molecular weight (Mn) =25 kDa, weight average molecular weight (Mw) =42 kDa, determined by gel permeation chromatography (GPC), as described in the next section) and 2.4 g of sodium iodide were added to 60 ml NMP and 6.0 ml 15% weight/weight (w/w) NaOH solution and stirred for 20 min. Then, 6.0 ml of methyl iodide was added and the mixture was refluxed for 60 minutes. The obtained TMC with a DQ of 15 was precipitated in diethyl ether and washed thoroughly with diethyl ether. Finally, the precipitated TMC was dissolved in 10% (w/v) NaCl solution and stirred for at least 18 hrs for ion-exchange. This solution was dialyzed afterwards at room temperature against deionized water for 3 days by changing buffer twice daily, filtered through a 0.8 μm filter and freeze dried. TMC37 was synthesized from chitosan (Mn=46 kDa, Mw=75 kDa, determined by GPC) in a similar way, but in an extra step, 3.0 ml 15% (w/w) NaOH solution and 3.0 ml iodomethane were added and stirred for another 60 minutes before the TMC was precipitated and washed with diethyl ether. In addition to trimethylation of the amines, these reaction conditions lead to substantial methylation of the C3 and C6 hydroxyl groups [34]. Polymers were characterized by GPC and NMR as described previously [26, 34]. Polymer characteristics are summarized in Table I.

GPC analysis of chitosans and TMCs

The Mn and Mw of chitosans and the synthesized TMC15 and TMC37 were determined by GPC on a Viscotec triple detection system using a Shodex OHPak SB806 column (30 cm) and 0.3 M sodium acetate buffer pH=4.4 as running buffer as described earlier [34]. Briefly, polymer samples were dried overnight in a vacuum oven at 40°C. Then, samples were dissolved overnight in running buffer at a concentration of 5 mg/ml, filtered through a 0.2 μm filter and injected (50 μl) onto the GPC column. Flow was 0.7 ml/min. Mw and Mn were determined using the Viscotec analysis software that integrates refractive index, viscosity and right (90°) and low angle (7°) scattering data.

MTT cell toxicity assay

MTT cell toxicity assay was performed according to Mosmann [35]. Caco-2 cells were seeded in a 96-well plate at a density of 4 x10^4 cells per well and incubated for 2 days at 37 °C and 5% CO2 in culture medium (DMEM, high glucose,10% FCS, L-glutamine, pyruvate, non-essential amino

Table 1. Polymer characteristics of synthesized TMC15 and TMC37[1)]

Polymer	DQ[2)] (%)	DOM[2)] C3 (%) / C6 (%)	DAc[2)] (%)	Mn[3)] (kDa)	Mw[3)] (kDa)
TMC37	37 %	(9 / 14)	4	44	94
TMC15	15 %	(4 / 6)	16	30	63

[1)]Abbreviations: DQ= degree of quarternization; DOM= degree of *O*-methylation; DAc= degree of acetylation; Mn= number average molecular weight; Mw= weight average molecular weight
[2)]As determined by NMR
[3)]As determined by GPC

acids). The medium was removed and the cells were incubated for 2.5 h with 100 µl TMC solutions in HBSS (TMC concentrations were 0.1, 1 and 10 mg/ml, pH set at 7 with 0.1 M NaOH). SDS (10 mg/ml) was used as positive control and HBSS as reference for 100% cell viability. Then, the HBSS was removed and the cells were washed with phosphate buffered saline. The cells were incubated with 100µl freshly prepared solution of 0.5 mg/ml MTT in DMEM, without any additions for 3 h at 37 °C and 5% CO2. Subsequently, the wells were emptied, the formed formazan crystals were dissolved with 100 µl of DMSO and the absorbance was read at 595 nm.

Transepithelial electrical resistance (TEER) measurements

TEER measurements were performed as described earlier [34, 36]. Shortly, Caco-2 cells were cultured on 12-transwell plates with a microporous membrane in Dulbecco's modified Eagle's medium (DMEM) until a confluent cell layer was formed. The medium was replaced by Hank's balanced salt solution (HBSS) at the basolateral side 10 min before the start of the experiments. Then, 0.5 ml solution of TMC15 and TMC37 (2 mg/ml in HBSS, pH adjusted to 7 with 0.1 M NaOH) was applied at the apical side of the cell monolayers. SDS (10 mg/ml) was used as positive control and HBSS as reference. The TEER of the Caco-2 cells was measured with a Millicell-ERS (Millipore, Billerica, USA) measuring device at certain time points (0, 15, 30, 45, 60 and 90 min) after addition of the stimuli. After 90 min, the cells were washed with HBSS and incubation of the cells was continued in DMEM for 24 h at 37 °C and 5% CO2 to determine the recovery of the TEER.

Preparation of vaccine formulations

Purified, cell culture-derived, BPL-inactivated A/PR/8/34 suspended in a 10 mM phosphate buffered saline solution (150 mM NaCl, pH=7) (PBS) was concentrated by centrifugation at 22,000 x g for 30 min at 4 °C and resuspended in 5 mM HEPES buffer (pH 7.4). The WIV concentration is expressed as mg total protein/ml as determined by DC protein assay (Bio-Rad, Hercules, CA, USA). The amount of hemagglutinin (HA) was approximately 35 % of the total protein content, as determined previously [14]. The TMC15-WIV and TMC37-WIV vaccines were prepared by simply adding equal volumes of TMC15 or TMC37 solution (in 5 mM HEPES, pH 7.4) to a WIV dispersion using a Gilson pipette while gently mixing for 5 seconds. The (w/w) ratio of TMC/WIV was varied between 0 and 12 by adding the TMCs at different concentrations while keeping the volume the same. The formulations were prepared at a final WIV concentration of 0.156 mg/ml for the initial characterization of TMC-coated WIV formulations over a broad range of TMC/WIV (w/w) ratios. For i.n. vaccination, the vaccine formulations were prepared at a concentration of 1.25 mg/ml in 5 mM HEPES, pH 7.4 and were also characterized at this concentration. The TMC solutions for the pulse-chase study were prepared at a concentration of 1.25 mg/ml in 5 mM HEPES, pH 7.4.

Characterization of vaccine formulations

Particle size was measured by dynamic light scattering (DLS) using a Malvern ALV CGS-3 (Malvern Instruments, Malvern, UK). DLS results are given as a z-average particle size diameter

and a polydispersity index (PDI). The PDI can range from 0 (indicating monodisperse particles) to 1 (a completely heterodisperse system).
Zeta potentials of WIV and TMC-WIV vaccines were measured using a Zetasizer Nano (Malvern Instruments, Malvern, UK). The integrity of the viral structure was investigated using negative stain transmission electron microscopy (TEM). Therefore WIV formulations (1.25 mg/ml) with and without TMC coating (TMC/WIV ratio of 1) were stained using 2% uranyl acetate as described previously [37].

The WIV-associated fraction of TMC15 and TMC37 was determined by quantification of the free TMC, present in the supernatant of centrifuged TMC-WIV vaccine, using the GPC method described above. Briefly, 75 µl TMC solution (in 5 mM HEPES buffer, pH7.4) was added to 75 µl WIV (2.5 mg protein/ml in 5 mM HEPES, pH 7.4) and mixed by pipeting and vortexing gently for 3 s. TMC-WIV formulations were centrifuged for 40 minutes at 22,000 x g at 4°C and the supernatant was collected. Prior to injection, 20 µl GPC running buffer was added to 100 µl supernatant to adjust the pH of the sample. The sample concentration was determined using the refractive index.
The WIV-associated TMC content as percentage of the total TMC in the formulation (TMC_{bound} (%)) was calculated as:

$$TMC_{bound}\ (\%) = 100 - \frac{(TMC_{free}\ (g) * 100)}{\text{total TMC (g)}}$$

The WIV-associated TMC as TMC/WIV (w/w) ratio (TMC_{bound}/WIV (w/w)) was calculated as:

$$TMC_{bound}/WIV\ (w/w) = \frac{(\text{total TMC (g)} - TMC_{free}\ (g))}{\text{WIV (g)}}$$

Immunization protocol
Animal experiments were conducted according to the guidelines provided by the Dutch Animal Protection Act and were approved by a Committee for Animal Experimentation. For all experiments 6-8 weeks old female C57-BL/6 mice (Charles River) were used. Mice were housed in groups of 8-11 mice and food and water were provided ad libitum. Prime and boost immunizations at day 0 and 21, respectively, were performed without anesthesia. Groups of 11 mice were vaccinated i.n. with WIV, TMC15-WIV or TMC37-WIV at a dose of 12.5 µg WIV (corresponding to approximately 4.3 µg HA). As a negative control, a group of 11 mice was vaccinated i.n. with PBS. TMC15-WIV and TMC37-WIV vaccines were freshly prepared from WIV dispersion and TMC15 or TMC37 solution. For i.n. immunization, mice were held in supine position without anesthesia and the vaccine was administered to the left and right nostril in a total volume of 10 µl. As a reference, one group of mice was vaccinated i.m. with WIV at a dose of 12.5 µg protein in a volume of 100 µl in the left and right quadriceps for prime and boost vaccination, respectively.
Additionally, a pulse-chase study was performed in which 2 groups of mice were first administered

10 µl of a 1.25 mg/ml TMC37 or TMC15 solution i.n., followed 2 h later by 10 µl of 1.25 mg/ml WIV i.n.

Blood sampling and nasal washes

Blood samples were collected by orbital puncture in MINICOLLECT® serum separator tubes coated with SiO_2 (Greiner Bio-One, Alphen a/d Rijn, the Netherlands) 20 days after prime vaccination and boost vaccination. Coagulated blood samples were centrifuged at 6,500 x g for 8 min at room temperature to obtain serum samples. Individual serum samples were stored at -20°C until further analysis. 20 days after boost vaccination, 3 mice from each group were anesthetized with diethyl ether and bled by orbital puncture. The trachea was cannulated towards the nasopharyngeal duct with a PVC tube (inner/outer diameter 0.5/1.0 mm). 500 µl PBS containing complete Mini, EDTA free protease inhibitor (Roche Diagnostics, Indianapolis, IN, USA) at a concentration of 1 tablet / 7 ml PBS was flushed through the nasal cavity and collected from the nostrils.

Challenge

22 days after the boost vaccination, mice challenged with 50 ml (8.8×10^8 x the 50% egg infectious dose (EID50)/ml) aerosolized, egg-grown influenza A/PR/8/34 using a DeVilbiss Ultra-Neb 2000 ultrasonic nebulizer (Direct Medical Ltd, Lecarrow, Ireland) for 25 min. After challenge, mice were put back in their cages and any observed signs of illness like lethargy, standing fur and curved back were recorded. Additionally, their body weight was monitored daily for 15 days. For comparison of loss in body weight, the average area under the curve (AUC) was calculated for each group from body weight curves of individual mice. All i.n. groups were compared to the negative control group (PBS i.n.) and the positive control group (WIV i.m.) by the average (AUC) of individual mice using a one-way ANOVA and Bonferroni's correction for multiple comparisons.

Hemagglutination inhibition test

First, 25 µl serum was incubated for 18 h at 37°C with 75 µl Receptor Destroying Enzyme (RDE) solution (Denka Seiken UK Ltd, Coventry, UK) to suppress nonspecific hemagglutination inhibition. RDE was then inactivated by incubating the mixture for 30 min at 56°C. Next, 150 µl PBS was added to obtain a final 10-fold serum dilution. 50 µl diluted serum was transferred in duplicate to V-bottom 96-wells plates (Greiner, Alphen a/d Rijn, The Netherlands) and serially diluted twofold in PBS. Next, 4 hemagglutination units (HAU) Influenza A/PR/8/34 (in 25 µl PBS) were added to all wells and the mixtures were incubated for 40 min at room temperature. Finally, 50 µl 0.5% (v/v) chicken erythrocytes in PBS were added to all wells and plates were incubated for 1 h at room temperature. The HI titer was expressed as the reciprocal value of the highest serum dilution capable of completely inhibiting the virus-induced agglutination of chicken erythrocytes. If no complete inhibition could be detected in the first lane, serum was arbitrarily scored 5. Comparison between different experimental groups from the same dose was made by a one-way ANOVA test and the Bonferroni correction for multiple comparisons on the log transformed HI titers.

Antibody assays

Antigen specific serum antibody responses were determined by a sandwich ELISA. Maxisorp ELISA plates (Nunc, Roskilde, Denmark) were coated overnight with polyclonal rabbit anti-A/PR/8/34 serum (dilution 1:1620). Plates were washed in between all prescribed steps with wash buffer (0.64 M NaCl, 3mM KCl, 0.15% polysorbate 20 in 10mM phosphate buffer pH=7.2) using a Skanwasher 300 (Molecular Devices, Sunnyvale, CA, USA). Next, plates were incubated for 1 h at 37°C with blocking buffer (0.2% (w/w) casein, sucrose 4% (w/w), Triton X-100 0.05% (w/w) and sodium azide 0.01% (w/w) in 30 mM TRIS pH=7.4), followed by incubation with egg-grown, BPL-inactivated A/PR/8/34 (8 HAU/ml) for 1 h at 37°C. Plates were then incubated with twofold serially diluted sera (100 µl/well) for 1 h at 37°C. Next, plates were incubated with 100 µl of a 1:2500 dilution of horseradish peroxidase linked goat anti mouse -IgG (H+L), -IgG1, -IgG2a/c or -IgA(Fc) (Nordic Laboratories, Tilburg, the Netherlands) for 30 min, and washed twice. Finally, 100 µl 3,3',5,5'-Tetramethylbenzidine (TMB) substrate solution was added and plates were incubated for 15 min at room temperature before enzymatic conversion was stopped by adding 50 µl 2 M sulfuric acid. Optical density (OD) was then measured at 450 nm using a Tecan Sunrise plate reader (Tecan Trading AG, Zurich Switzerland). Titers are given as the reciprocal sample dilution corresponding to 20% of the maximal ELISA signal above background. Comparison between different experimental groups was made by a one-way ANOVA test and the Bonferroni correction for multiple comparisons.

Results

Effect of TMCs on epithelial cell toxicity and TEER in vitro

The *in vitro* cell toxicity of the TMCs was determined using the MTT cell toxicity assay. The results (Figure 1) show that TMC37 was slightly more toxic than TMC15, but far less than PEI. Even at the highest concentration (10 mg/ml) tested, the TMCs were less toxic than PEI at 0.2 mg/ml.

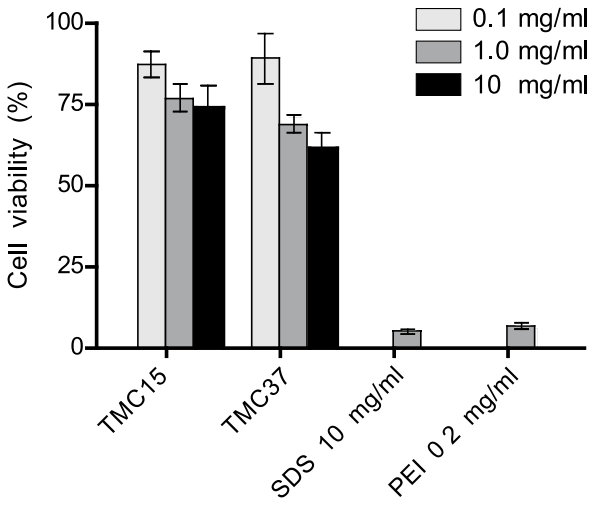

Figure 1. Effect of TMC15 and TMC37 on the viability of Caco-2 cells (MTT assay) at different concentrations. Error bars represent 95% confidence intervals (n=6). For comparison, polyethylene imine (PEI) (0.2 mg/ml) and SDS (10 mg/ml) were used as controls known to be toxic.

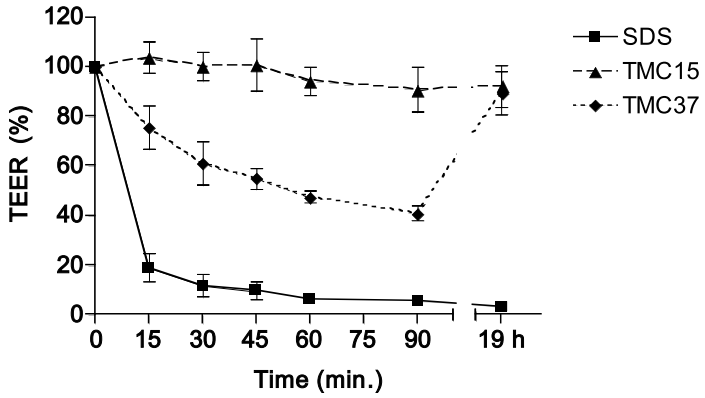

Figure 2. Effect of TMC15 and TMC37 on the TEER of Caco-2 cells at a concentration of 2 mg/ml. 10 mg/ml sodium dodecyl sulfate (SDS) was used as a control known to be toxic. After 90 min, the cells were washed with HBSS and incubation of the cells was continued in DMEM to determine the recovery of the TEER. The TEER of cells treated with HBSS was set at 100%. Error bars represent 95% confidence intervals (n=6).

TEER measurements were performed to investigate the ability to open tight junctions. As shown in Figure 2, TMC37 induced a reversible decrease in TEER, suggesting that TMC37 has the ability to open tight junctions. TMC15 on the other hand, did not decrease the TEER at any measured time point, indicating that TMC15 cannot open tight junctions.

Zeta potential and particle size of TMC-WIV

TMC15 and TMC37 were mixed with WIV at different (w/w) ratios and the zeta potential and particle size were determined. Uncoated WIV, with an average diameter of 160 nm (PDI 0.11), had a negative zeta potential of approximately -20 mV, as shown in Figure 3. By increasing the concentration of TMC, the zeta potential of the TMC15-WIV and TMC37-WIV increased, initially resulting in a neutral zeta potential and instant aggregation. This indicates that the colloidal WIV formulation is stabilized by repulsive electrostatic forces between the particles. At higher TMC/WIV (w/w) ratios, above 0.9 and 0.2 for TMC15 and TMC37, respectively, positively charged particles were formed with an average diameter between 260 and 350 nm for TMC15-WIV and 400-500 nm for TMC37-WIV (PDI ≤0.23, indicating fairly homogeneous particle sizes). A maximum zeta potential was reached above +30 mV at a TMC/WIV (w/w) ratio of 12 for TMC15-WIV and TMC37-WIV. Figure 3 also shows that less TMC37 was needed to obtain positively charged particles as compared to TMC15.

Binding of TMC15 and TMC37 to WIV

The binding of TMCs to WIV was quantified using GPC. The percentage of TMC that is associated to WIV depended strongly on the amount of TMC added (Figure 4a). On the other hand, the amount of TMC15 and TMC37 that is associated to WIV was rather constant between 0.15 and 0.25 g/g WIV, at TMC/WIV ratios ranging from 0.25 to 2 (Figure 4b). At higher (w/w) ratios the WIV-associated fraction of TMC15 and TMC37 was very small. Therefore the data points were less reliable, because the standard deviations, derived from measurements of the supernatant, were

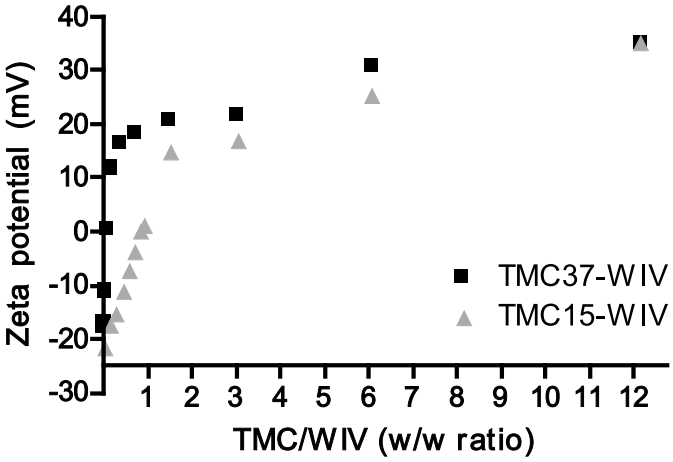

Figure 3. Zeta potential of WIV at a concentration of 0.156 mg/ml, formulated with TMC15 or TMC37 at different TMC/WIV (w/w) ratios in 5 mM HEPES pH 7.4.

relatively large (see calculation in Materials & Methods), leading to unreliable results. At increasing TMC/WIV ratios, the excess TMC appeared to remain in solution. The constant amount of WIV-associated TMC suggests that the amount of TMC bound to WIV had reached saturation levels. The zeta potential did not decrease when TMC15-WIV or TMC37-WIV (1:1 (w/w)) formulated at

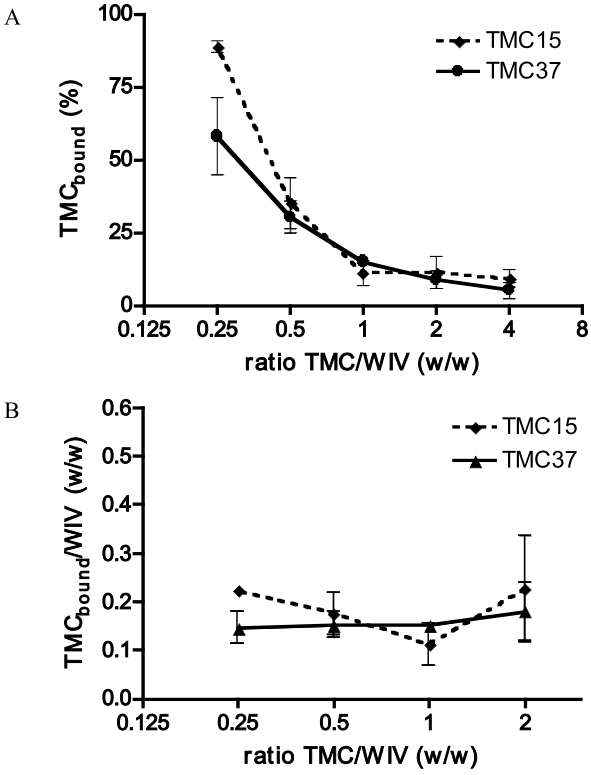

Figure 4. WIV-associated TMC expressed (A) as percentage of total TMC content in the formulation and (B) as TMC/WIV (w/w) ratio. TMC-WIV formulations were prepared at a WIV concentration of 1.25 mg/ml. Error bars indicate the 95% confidence intervals of three independent measurements.

Table 2. Properties of i.n. administered vaccine formulations

Formulation	Concentration WIV (mg protein/ml)	TMC:WIV ratio (w/w)	TMC bound[1)] w/w (±sd)	Zeta potential[2)] (mV)	radius (PDI)
WIV	1.25	0	–	-13.3 (±0.9)	93.2 (0.18)
TMC15-WIV	1.25	1	0.112 (±0.017)	15.6 (±0.4)	196.0 (0.24)
TMC37-WIV	1.25	1	0.151 (±0.002)	15.1 (±0.9)	269.1 (0.32)

[1)] Average of three batches, three measurements per batch
[2)] Average of three measurements

a WIV concentration of 1.25 mg/ml was diluted up to 32-fold with 5 mM HEPES buffer (Figure 5). This indicates that the WIV-associated TMC does not readily dissociate and that the association of TMC with WIV is not strongly dependent on the free TMC concentration in solution. The slight increase in zeta potential upon dilution, especially in the TMC37 sample, may be caused by the dilution of residual ions from residual PBS after pelleting and resuspending the WIV.

Based upon these results, TMC15-WIV and TMC37-WIV formulations with a TMC/WIV (w/w) ratio of 1.0 were selected for an immunization study. At this (w/w) ratio, the particles were positively charged and the WIV seemed maximally coated with the cationic polymers. Moreover, the physicochemical characteristics of these formulations were comparable, as shown in Table II. TMC induced no observable changes to the viral ultra structure visualized by TEM (Figure 6). In our setting the TMC coating could not be observed, likely due to the nature of the negative stain or the limitations of the microscope. TMC coated grids stained with uranyl acetate did not show any recognizable structure (data not shown).

Immunization study

The novel TMC-WIV vaccines were compared to plain WIV in a vaccination study. Mice were vaccinated twice with a 3 week interval and sera were sampled 20 days after prime and boost vaccination. Although i.m. vaccination with plain WIV induced higher HI titers than any of the i.n. vaccinations, coating of WIV with TMC37 significantly enhanced the induction of HI titers

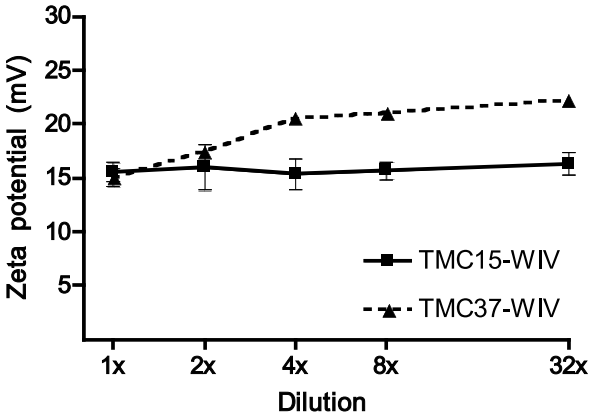

Figure 5. Zeta potential of TMC15-WIV and TMC37-WIV formulated at 1.25 mg/ml WIV at a TMC/WIV (w/w) ratio of 1.0, after different dilution steps with 5 mM HEPES pH 7.4. Error bars indicate the standard deviations of 3 measurements.

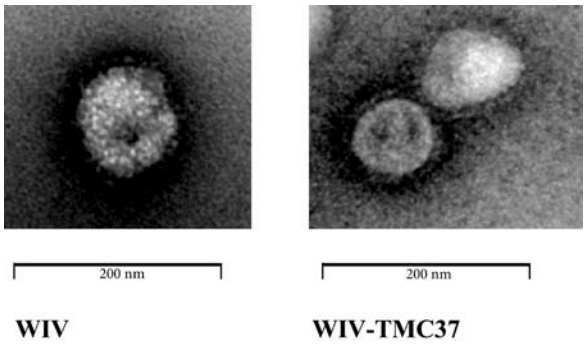

Figure 6. Negative stain transmission electron microscopy picture of WIV (left) and TMC37-WIV (right).

after i.n. administration (Figure 7). Coating with TMC15, on the other hand, hardly improved the induction of HI titers of plain WIV.

In contrast to WIV, strong antigen-specific IgG responses were developed after i.n. prime vaccination with TMC37-WIV in all mice, which were further increased after boost vaccination (Figure 8a). TMC15-WIV also induced substantial antigen-specific IgG responses, especially after boost vaccination, though not as pronounced as TMC37.

To determine the influence of TMC15 and TMC37 on the type of immune responses against WIV, IgG1 and IgG2a/c titers were determined by ELISA (Figure 8b and c, respectively). For the formulations that showed detectable HI and IgG responses (i.m. WIV, i.n. TMC37-WIV and i.n. TMC15-WIV), IgG2a titers after prime vaccination were higher and detectable in a larger number of mice than IgG1 titers. After boost vaccination with these three vaccines, more mice developed IgG1 as well as IgG2a titers. These findings indicate that coating of WIV with TMC15 or TMC37 does not influence the quality of humoral systemic immune responses, but rather improves the delivery of WIV after i.n. administration.

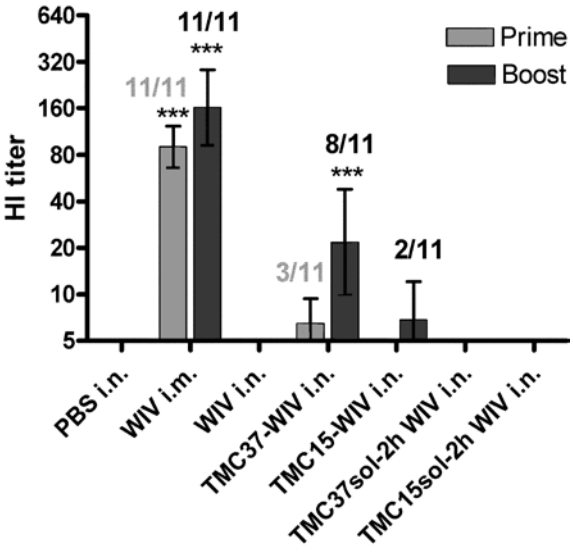

Figure 7. Geometric mean HI titers 20 days after prime and boost vaccinations. Negative serum samples were arbitrarily assigned a titer of 5 for calculation purposes. Error bars indicate 95% confidence intervals. Indicated above the bars are the number of mice that developed detectable HI titers (e.g. 3/11 indicates 3 out of 11 mice). n=11 for all groups. All HI titers after prime and boost vaccination were compared using a one-way ANOVA test and Bonferroni's correction for multiple comparisons. Asterisks indicate titers that are significantly (***P<0.001) higher than those of the WIV i.n. group.

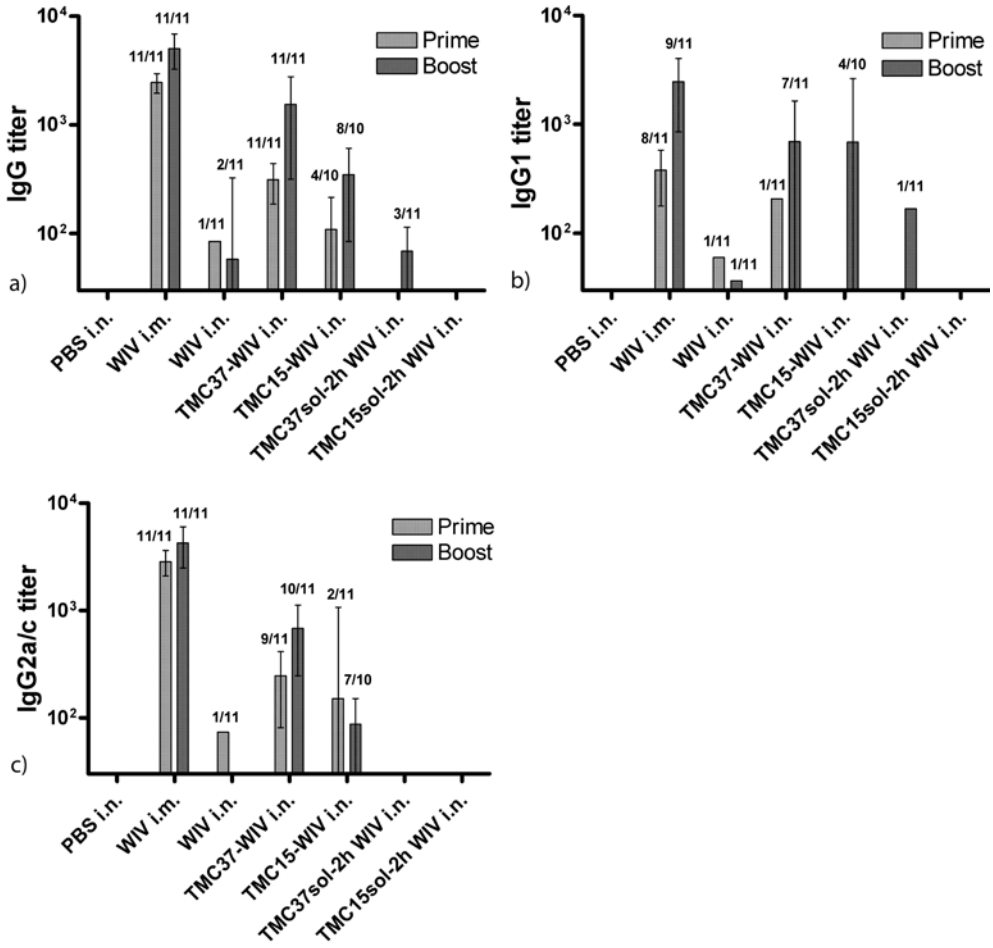

Figure 8: Geometric mean antigen specific serum IgG titers (a), IgG1 (b) and IgG2a/c (c) of seropositive mice 3 weeks after prime and boost vaccination. Error bars indicate 95% confidence intervals. Indicated above the bars is the number of mice that developed detectable IgG titers after boost vaccination (e.g. 3/11 indicates 3 out of 11 mice). All formulations were compared using a one-way ANOVA test and Bonferroni's correction for multiple comparisons.

Additionally, a pulse-chase study was performed to study whether the adjuvant activity was only observed when TMCs were coadministered with WIV. In this study the time between the administration of TMC and WIV should be as short as possible, but long enough to avoid interaction between TMC and WIV after administration. Therefore, as opposed to others who used a time period of 24 h (22), we chose 2 h. This should be sufficiently long to prevent WIV and TMC to interact after administration, anticipating that the cationic TMC will be rapidly neutralized by the abundantly present negatively charged mucins and/or cleared by mucociliary activity. In the pulse-chase study with TMC15 and TMC37 (indicated in Figure 7 and 8 with "TMC37sol-

2h WIV" and "TMC15-2h WIV", respectively), none of the mice developed detectable HI titers (Figure 7) and only a few mice that received TMC37 solution i.n. 2 h before the WIV developed weak IgG titers after boost vaccination (Figure 8a-c). Mice that received TMC15 solution prior to WIV i.n. vaccination were unresponsive. These results clearly indicate that TMC37 and TMC15 are not effective when administered 2 h prior to the i.n. administration of WIV, confirming our conclusion that the adjuvant effect is mainly based on improved delivery and less on immune stimulation by TMC.

Challenge with live, aerosolized virus

To determine the protective effect of vaccination, 8 mice in each group were challenged with homologous, egg grown influenza virus. Mice were monitored for signs of illness like standing fur, grouping together and lethargic behavior. Additionally, body weight was recorded daily for 15 days after challenge as a measurable sign of illness. As shown in Figure 9, all mice in the positive control group, vaccinated i.m. with WIV, were protected. Mice did not show any signs of illness and maintained body weight over the period of 2 weeks after challenge. On the other hand, mice in negative control group that received PBS i.n., lost weight from day 2 to day 10, became lethargic and had a curved back and standing fur. Two mice in this group were sacrificed at day 9 and the other mice regained weight from this day, indicating recovery from viral infection. Mice vaccinated i.n. with WIV alone (Figure 9a) were also not protected. They lost body weight in a similar pattern as the control group but started to regain body weight 2 days earlier than the control group. Furthermore, all mice vaccinated with WIV i.n. showed signs of illness from day 6 and 8, respectively, until day 13.

In contrast, i.n. vaccination with TMC37-WIV protected all mice against signs of illness and loss of body weight (Figure 9b). Furthermore, all challenged mice in the TMC15-WIV i.n. group that were seropositive (6 out of 7) were also protected against symptoms of illness (Figure 9c). Like the i.m. WIV group, both groups had a significantly higher average relative body weight than the PBS i.n. group.

In the pulse-chase study with TMC37, all mice lost a considerable amount of body weight. Body weight loss was more severe in the pulse-chase study with TMC15 (Figure 9e) than with TMC37 (Figure 9d). Moreover, most mice in the pulse-chase study with TMC15 and one mouse in the pulse-chase study with TMC37 developed clear signs of illness. These results may suggest that the TMC37 solution reduced the severity of infection slightly, although the AUC data of the TMC15 and the TMC37 group were not significantly different from that of the negative control group that received PBS i.n. So, TMC should be administered i.n. together with WIV to provide complete protection against weight loss and clinical signs of illness.

Discussion

In a previous study we have shown that the most promising inactivated nonadjuvanted i.n. influenza vaccines are based on WIV [14]. To further optimize WIV for i.n. vaccination, the use of the

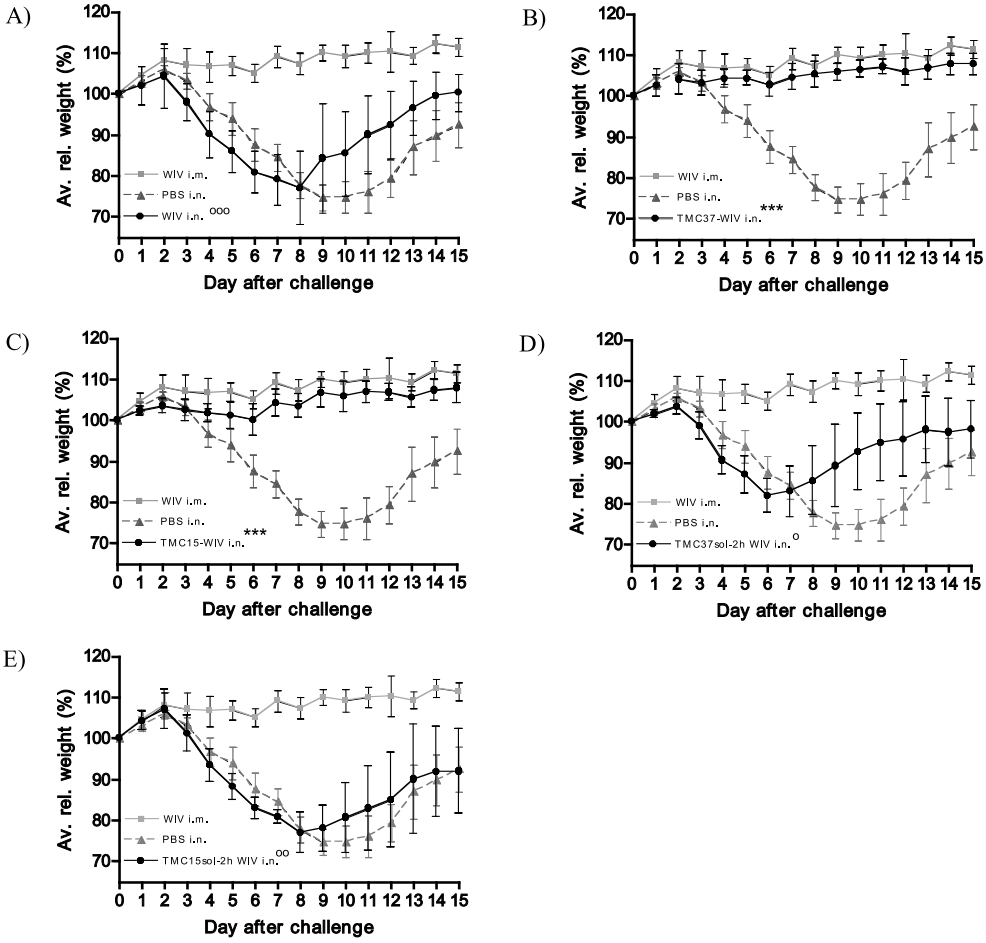

Figure 9(a-e): Average relative body weight curves after challenge of mice vaccinated with:.(a) WIV i.n.; (b) TMC37-WIV; (c) TMC15-WIV; (d) TMC37sol-2h WIV i.n. and (e) TMC15sol-2h WIV i.n.. For comparison, each panel contains the curves of WIV i.m. and PBS i.n.. During the study some mice were sacrificed (§) or died due to handling (†): (a) WIV i.n., 1 mouse (day 9,§); (b) TMC37-WIV i.n., 1 mouse (day 0, †); (c)TMC15-WIV i.n., 1 mouse (day 14, §); PBS i.n., 2 mice (day 10, §). N=8 for all groups except for TMC15sol–2h WIV (n=7). One nonresponding mouse in the TMC15-WIV group that lost weight and showed signs of illness, was sacrificed at day 15 and not included in the average body weight curve. Error bars indicate the 95% confidence intervals. Asterisks indicate average AUCs significantly (***P<0.001) higher than the PBS i.n. group. Circles indicate that average AUC is significantly (^{o}P<0.05; ^{oo}P<0.01 and ^{ooo}P<0.001) lower than the WIV i.m. group.

cationic mucoadhesive polymer TMC was explored in this study. We demonstrated that coating of WIV with TMC substantially improves the immunogenicity of i.n. WIV vaccine. Although some reports have been published on TMC as a nasal adjuvant [28, 31], this is the first time that TMC in solution was formulated with WIV as an antigen, resulting in TMC-coated WIV. Because of the

particulate character of WIV, soluble TMC can simply be added to obtain a positively charged, nanoparticulate antigen delivery system. The way to produce TMC-coated WIV formulations is extremely simple and fast, making this procedure very suitable for upscaling to large scale production. For other nanoparticulate vaccines, the large scale production can be too difficult or costly to make it to the market [38]. A simple formulation procedure is especially important in the case of seasonal and pandemic flu, since the timelines for development and production of flu vaccines are extremely short [39]. Future studies should be performed to determine the stability upon storage.

The presented TMC-WIV vaccines contain both WIV-associated TMC and TMC in solution. It should be further investigated what the role of free TMC is in the induction of immune responses as well as stabilization of the formulation. Both the soluble fraction and the coated TMC may contribute to the adjuvant effect, since both TMC solution and TMC nanoparticles have been reported to increase immune responses [28, 31, 36].

TMC15-WIV and TMC37-WIV i.n. induced strong immune responses and complete protection, whereas WIV i.n. hardly induced detectable HI and antibody titers and was not protective. Although expected from other reports [27, 28, 30, 32] and from earlier observations in our own lab, no sIgA could be detected in the nasal washes. We can, however, not exclude the sampling and/or detection methods were suboptimal.

Our results show that TMC37-WIV induced superior immune responses to TMC15-WIV, indicating that the polymer characteristics determine their adjuvanticity. The TMC15 and TMC37 used had different molecular weights in addition to different DQs (see Table I). The differences in Mn and Mw are caused by differences in chain length of the chitosans used, chain scission during trimethylation and DQs [40]. Systematic studies about the influence of molecular weight on the adjuvant properties of TMC are lacking. However, the effect of the Mw of TMC and chitosan on cell toxicity, ability to open tight junctions and drug uptake has been descibed [41-45]. These studies indicate that small differences in Mw have a negligible influence on these parameters. Therefore, it can be anticipated that the observed differences between TMC15 and TMC37 regarding their effect on cell viability, TEER and adjuvant effect can be attributed to the different DQs.

The relation between the DQ of TMC and opening of tight junctions as well as toxicity has been studied thoroughly [29, 34, 46-48]. TMC with a DQ of ca. 40%, has been proposed to have the strongest effect on opening of tight junctions [46, 47] , the strongest adjuvant properties [27] and an acceptable toxicity profile. Our results, showing increased immunogenicity and stronger decrease in TEER for TMC37 when compared to TMC15, are in line with these findings.

The quality of serum humoral immune responses was hardly affected by TMC15 and TMC37. Both TMC15-WIV and TMC37-WIV induced a mix of IgG2a/c and IgG1 immune response, just like i.m. WIV. This is indicative of mixed Th1/Th2 immune responses, which are more favorable than biased Th2 immune responses typically elicited by nonadjuvanted subunit and split vaccines [14, 49]. Furthermore, these results are in line with the notion that TMC acts as an adjuvant by improving the delivery of antigens to the immune system rather than providing an immunostimulatory signal, which is the mechanism action of other adjuvants like TLR ligands and toxins. The results from the

pulse-chase study also support this idea. Mice that received either TMC15 or TMC37 i.n., 2h before WIV was administered i.n., hardly developed any immune responses. Likely, the TMC solution is already cleared from the nasal cavity or neutralized by the abundantly present, negatively charged mucus or mucosal surfaces, prior to the WIV administration. These findings are in line with the results of an earlier i.n. pulse-chase study where chitosan solution was administered 24 h prior to the antigen [23]. So, TMC exerts its adjuvant effect mainly by improving the antigen delivery and must therefore be formulated and/or administered together with WIV to enhance the induction of immune responses.

Recently, two papers were published on dry powder formulations of WIV with several mucoadhesive compounds including chitosan [50, 51]. In these studies, a spray freeze dried WIV-chitosan formulation induced significantly lower serum IgG titers after i.n. boost vaccination than plain WIV without any mucoadhesives. This might be due to the poor solubility of chitosan at physiological pH, the very reason why we used TMC instead. Also, TMC was recently shown to enhance immune responses elicited by a powder vaccine formulation after pulmonary delivery [30].

In conclusion, TMC-coated WIV elicited strong humoral immune responses in mice upon i.n. vaccination and provided protection against signs of illness after a homologous aerosol challenge. This, together with the ease of production and the clear advantages of the intranasal route of administration, holds great promise for the further development of effective inactivated i.n. influenza vaccines. Since WIV i.m. was more potent than any of the i.n. administered vaccines, these promising results call for more research. Studies should be performed to determine the influence of other polymer characteristics on the adjuvant properties of TMC. Recent developments in TMC synthesis facilitate this research [34]. Moreover, the design of TMC-WIV particles combined with other adjuvants like TLR-ligands may further improve the potency of i.n. WIV vaccines.

Acknowledgements

The authors thank Frits Flesch for making the TEM pictures, Nancy Ong and Shirley Sparla for their contributions to the physicochemical characterization of TMC-WIV and Elly van Riet for her assistance with the cell culture studies.

References

[1] Slütter B, Hagenaars N, Jiskoot W. Rational design of nasal vaccines. J Drug Target 2008;16(1):1-17.

[2] Tumpey TM, Renshaw M, Clements JD, Katz JM. Mucosal delivery of inactivated influenza vaccine induces B-cell-dependent heterosubtypic cross-protection against lethal influenza A H5N1 virus infection. J Virol 2001;75(11):5141-50.

[3] Ichinohe T, Tamura S, Kawaguchi A, Ninomiya A, Imai M, Itamura S, et al. Cross-protection against H5N1 influenza virus infection is afforded by intranasal inoculation with seasonal trivalent inactivated influenza vaccine. J Infect Dis 2007;196(9):1313-20.

[4] Belshe RB, Edwards KM, Vesikari T, Black SV, Walker RE, Hultquist M, et al. Live attenuated versus inactivated influenza vaccine in infants and young children. N Engl J Med 2007;356(7):685-96.

[5] Hagenaars N, Mastrobattista E, Glansbeek H, Heldens J, van den Bosch H, Schijns V, et al. Head-to-head comparison of four nonadjuvanted inactivated cell culture-derived influenza vaccines: Effect of composition, spatial organization and immunization route on the immunogenicity in a murine challenge model. Vaccine 2008;26(51):6555-63.

[6] Takada A, Matsushita S, Ninomiya A, Kawaoka Y, Kida H. Intranasal immunization with formalin-inactivated virus vaccine induces a broad spectrum of heterosubtypic immunity against influenza A virus infection in mice. Vaccine 2003;21(23):3212-8.

[7] Minne A, Jaworska J, Gerhold K, Ahrens B, Avagyan A, Vanbever R, et al. Intranasal delivery of whole influenza vaccine prevents subsequent allergen-induced sensitization and airway hyper-reactivity in mice. Clin Exp Allergy 2007;37(8):1250-8.

[8] Samdal HH, Bakke H, Oftung F, Holst J, Haugen IL, Korsvold GE, et al. A non-living nasal influenza vaccine can induce major humoral and cellular immune responses in humans without the need for adjuvants. Hum Vaccin 2005;1(2):85-90.

[9] Chen D, Weis KF, Chu Q, Erickson C, Endres R, Lively CR, et al. Epidermal powder immunization induces both cytotoxic T-lymphocyte and antibody responses to protein antigens of influenza and hepatitis B viruses. J Virol 2001;75(23):11630-40.

[10] Geeraedts F, Goutagny N, Hornung V, Severa M, de Haan A, Pool J, et al. Superior Immunogenicity of Inactivated Whole Virus H5N1 Influenza Vaccine is Primarily Controlled by Toll-like Receptor Signalling. PLoS Pathog 2008;4(8):e1000138.

[11] Sawai T, Itoh Y, Ozaki H, Isoda N, Okamoto K, Kashima Y, et al. Induction of cytotoxic T-lymphocyte and antibody responses against highly pathogenic avian influenza virus infection in mice by inoculation of apathogenic H5N1 influenza virus particles inactivated with formalin. Immunology 2008;124(2):155-65.

[12] Lipatov AS, Hoffmann E, Salomon R, Yen HL, Webster RG. Cross-protectiveness and immunogenicity of influenza A/Duck/Singapore/3/97(H5) vaccines against infection with A/Vietnam/1203/04(H5N1) virus in ferrets. J Infect Dis 2006;194(8):1040-3.

[13] Lu X, Edwards LE, Desheva JA, Nguyen DC, Rekstin A, Stephenson I, et al. Cross-protective immunity in mice induced by live-attenuated or inactivated vaccines against highly pathogenic influenza A (H5N1) viruses. Vaccine 2006;24(44-46):6588-93.

[14] Hagenaars N, Mastrobattista E, Glansbeek H, Heldens J, van den Bosch H, Schijns V, et al. Head-to-head comparison of four nonadjuvanted inactivated cell culture-derived influenza vaccines: Effect of composition, spatial organization and immunization route on the immunogenicity in a murine challenge model. Vaccine 2008.

[15] Gross PA, Ennis FA, Gaerlan PF, Denson LJ, Denning CR, Schiffman D. A controlled double-blind comparison of reactogenicity, immunogenicity, and protective efficacy of whole-virus and split-product influenza vaccines in children. J Infect Dis 1977;136(5):623-32.

[16] Hovden AO, Cox RJ, Haaheim LR. Whole influenza virus vaccine is more immunogenic than split influenza virus vaccine and induces primarily an IgG2a response in BALB/c mice. Scand J Immunol 2005;62(1):36-44.

[17] Beyer WEP, Palache AM, Osterhaus ADME. Comparison of serology and reactogenicity between influenza subunit vaccines and whole virus or split vaccines - A review and meta-analysis of the literature. Clinical Drug Investigation 1998;15(1):1-12.

[18] Read RC, Naylor SC, Potter CW, Bond J, Jabbal-Gill I, Fisher A, et al. Effective nasal influenza vaccine delivery using chitosan. Vaccine 2005;23(35):4367-74.

[19] Kumar MN, Muzzarelli RA, Muzzarelli C, Sashiwa H, Domb AJ. Chitosan chemistry and pharmaceutical perspectives. Chem Rev 2004;104(12):6017-84.

[20] Agnihotri SA, Mallikarjuna NN, Aminabhavi TM. Recent advances on chitosan-based micro- and nanoparticles in drug delivery. J Control Release 2004;100(1):5-28.

[21] van der Lubben IM, Kersten G, Fretz MM, Beuvery C, Coos Verhoef J, Junginger HE. Chitosan microparticles for mucosal vaccination against diphtheria: oral and nasal efficacy studies in mice. Vaccine 2003;21(13-14):1400-8.

[22] van der Lubben IM, van Opdorp FA, Hengeveld MR, Onderwater JJ, Koerten HK, Verhoef JC, et al. Transport of chitosan microparticles for mucosal vaccine delivery in a human intestinal M-cell model. J Drug Target 2002;10(6):449-56.

[23] Illum L, Jabbal-Gill I, Hinchcliffe M, Fisher AN, Davis SS. Chitosan as a novel nasal delivery system for vaccines. Adv Drug Deliv Rev 2001;51(1-3):81-96.

[24] Kotze AF, Luessen HL, de Boer AG, Verhoef JC, Junginger HE. Chitosan for enhanced intestinal permeability: prospects for derivatives soluble in neutral and basic environments. Eur J Pharm Sci 1999;7(2):145-51.

[25] Kotze AF, Luessen HL, de Leeuw BJ, de Boer BG, Verhoef JC, Junginger HE. N-trimethyl chitosan chloride as a potential absorption enhancer across mucosal surfaces: in vitro evaluation in intestinal epithelial cells (Caco-2). Pharm Res 1997;14(9):1197-202.

[26] Sieval AB, Thanou M, Kotze AF, Verhoef JE, Brussee J, Junginger HE. Preparation and NMR characterization of highly substituted N-trimethyl chitosan chloride. Carbohydrate Polymers 1998;36(2-3):157-65.

[27] Boonyo W, Junginger HE, Waranuch N, Polnok A, Pitaksuteepong T. Chitosan and trimethyl chitosan chloride (TMC) as adjuvants for inducing immune responses to ovalbumin in mice following nasal administration. J Control Release 2007;121(3):168-75.

[28] Amidi M, Romeijn SG, Verhoef JC, Junginger HE, Bungener L, Huckriede A, et al. N-trimethyl chitosan (TMC) nanoparticles loaded with influenza subunit antigen for intranasal vaccination: biological properties and immunogenicity in a mouse model. Vaccine 2007;25(1):144-53.

[29] Sayin B, Somavarapu S, Li XW, Thanou M, Sesardic D, Alpar HO, et al. Mono-N-carboxymethyl chitosan (MCC) and N-trimethyl chitosan (TMC) nanoparticles for non-invasive vaccine delivery. Int J Pharm 2008.

[30] Amidi M, Pellikaan HC, Hirschberg H, de Boer AH, Crommelin DJ, Hennink WE, et al. Diphtheria toxoid-containing microparticulate powder formulations for pulmonary vaccination: preparation, characterization and evaluation in guinea pigs. Vaccine 2007;25(37-38):6818-29.

[31] Baudner BC, Verhoef JC, Giuliani MM, Peppoloni S, Rappuoli R, Del Giudice G, et al. Protective immune responses to meningococcal C conjugate vaccine after intranasal immunization of mice with the LTK63 mutant plus chitosan or trimethyl chitosan chloride as novel delivery platform. J Drug Target 2005;13(8-9):489-98.

[32] Chen F, Zhang ZR, Yuan F, Qin X, Wang M, Huang Y. In vitro and in vivo study of N-trimethyl chitosan nanoparticles for oral protein delivery. Int J Pharm 2008;349(1-2):226-33.

[33] Geeraedts F, Bungener L, Pool J, ter Veer W, Wilschut J, Huckriede A. Whole inactivated virus influenza vaccine is superior to subunit vaccine in inducing immune responses and secretion of proinflammatory cytokines by DCs. Influenza and Other Respiratory Viruses 2008;2(2):41-51.

[34] Verheul RJ, Amidi M, van der Wal S, van Riet E, Jiskoot W, Hennink WE. Synthesis, characterization and in vitro biological properties of O-methyl free N,N,N-trimethylated chitosan. Biomaterials 2008;29(27):3642-9.

[35] Mosmann T. Rapid colorimetric assay for cellular growth and survival: application to proliferation and cytotoxicity assays. J Immunol Methods 1983;65(1-2):55-63.

[36] Amidi M, Romeijn SG, Borchard G, Junginger HE, Hennink WE, Jiskoot W. Preparation and characterization of protein-loaded N-trimethyl chitosan nanoparticles as nasal delivery system. J Control Release 2006;111(1-2):107-16.

[37] Schillemans JP, van Nostrum CF. Molecularly imprinted polymer particles: synthetic receptors for future medicine. Nanomedicine 2006;1(4):437-47.

[38] Müller RH, Jacobs C, Kayser O. Nanosuspensions as particulate drug formulations in therapy. Rationale for development and what we can expect for the future. Adv Drug Deliv Rev 2001;47(1):3-19.

[39] Gerdil C. The annual production cycle for influenza vaccine. Vaccine 2003;21(16):1776-9.

[40] Snyman D, Hamman JH, Kotze JS, Rollings JE, Kotze AF. The relationship between the absolute molecular weight and the degree of quaternisation of N-trimethyl chitosan chloride. Carbohydr Polym 2002;50(2):145-50.

[41] Huang M, Khor E, Lim LY. Uptake and cytotoxicity of chitosan molecules and nanoparticles: effects of molecular weight and degree of deacetylation. Pharm Res 2004;21(2):344-53.

[42] Mao S, Germershaus O, Fischer D, Linn T, Schnepf R, Kissel T. Uptake and transport of PEG-graft-trimethyl-chitosan copolymer-insulin nanocomplexes by epithelial cells. Pharm Res 2005;22(12):2058-68.

[43] Mao S, Shuai X, Unger F, Wittmar M, Xie X, Kissel T. Synthesis, characterization and cytotoxicity of poly(ethylene glycol)-graft-trimethyl chitosan block copolymers. Biomaterials 2005;26(32):6343-56.

[44] Mei D, Mao S, Sun W, Wang Y, Kissel T. Effect of chitosan structure properties and molecular weight on the intranasal absorption of tetramethylpyrazine phosphate in rats. Eur J Pharm Biopharm 2008.

[45] Schipper NG, Varum KM, Artursson P. Chitosans as absorption enhancers for poorly absorbable drugs. 1: Influence of molecular weight and degree of acetylation on drug transport across human intestinal epithelial (Caco-2) cells. Pharm Res 1996;13(11):1686-92.

[46] Hamman JH, Stander M, Kotze AF. Effect of the degree of quaternisation of N-trimethyl chitosan chloride on absorption enhancement: in vivo evaluation in rat nasal epithelia. Int J Pharm 2002;232(1-2):235-42.

[47] Thanou MM, Kotze AF, Scharringhausen T, Luessen HL, de Boer AG, Verhoef JC, et al. Effect of degree of quaternization of N-trimethyl chitosan chloride for enhanced transport of hydrophilic compounds across intestinal caco-2 cell monolayers. J Control Release 2000;64(1-3):15-25.

[48] van der Merwe SM, Verhoef JC, Verheijden JH, Kotze AF, Junginger HE. Trimethylated chitosan as polymeric absorption enhancer for improved peroral delivery of peptide drugs. Eur J Pharm Biopharm 2004;58(2):225-35.

[49] Moran TM, Park H, Fernandez-Sesma A, Schulman JL. Th2 responses to inactivated influenza virus can be converted to Th1 responses and facilitate recovery from heterosubtypic virus infection. J Infect Dis 1999;180(3):579-85.

[50] Garmise RJ, Staats HF, Hickey AJ. Novel dry powder preparations of whole inactivated influenza virus for nasal vaccination. AAPS PharmSciTech 2007;8(4):E81.

[51] Garmise RJ, Mar K, Crowder TM, Hwang CR, Ferriter M, Huang J, et al. Formulation of a dry powder influenza vaccine for nasal delivery. AAPS PharmSciTech 2006;7(1):E19.

Chapter 5

Relationship between structure and adjuvanticity of *N,N,N*-trimethyl chitosan (TMC) structural variants in a nasal influenza vaccine

Niels Hagenaars[*], Rolf Verheul[*], Imke Mooren, Pascal de Jong, Enrico Mastrobattista, Harrie Glansbeek, Jacco Heldens, Han van den Bosch, Wim Hennink, Wim Jiskoot

[*]Authors contributed equally

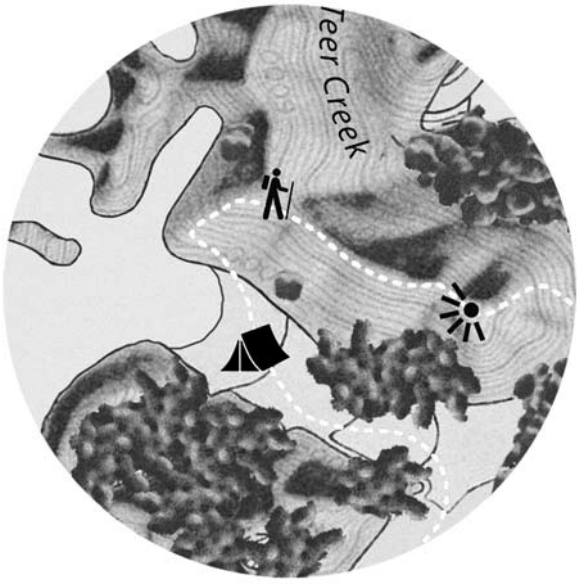

Journal of Controlled Release 2009, Epub ahead of print, August 25

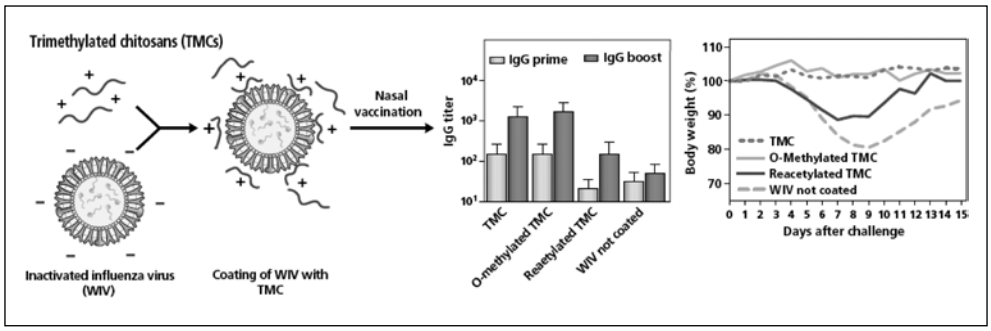

Graphical abstract

Abstract

Aim of this study was to assess the influence of structural properties of *N,N,N*-trimethyl chitosan (TMC) on its adjuvanticity. Therefore, TMCs with varying degrees of quaternization (DQ, 22-86%), *O*-methylation (DOM, 0-76%) and acetylation (DAc 9-54%) were formulated with whole inactivated influenza virus (WIV). The formulations were characterized physicochemically and evaluated for their immunogenicity in an intranasal (i.n.) vaccination/challenge study in mice.

Simple mixing of the TMCs with WIV at a 1:1 (w/w) ratio resulted in comparable positively charged nanoparticles, indicating coating of WIV with TMC. The amount of free TMC in solution was comparable for all TMC-WIV formulations. After i.n. immunization of mice with WIV and TMC-WIV on day 0 and 21, all TMC-WIV formulations induced stronger total IgG, IgG1 and IgG2a/c responses than WIV alone, except WIV formulated with reacetylated TMC with a DAc of 54% and a DQ of 44% (TMC-RA44). No significant differences in antibody titers were observed for TMCs that varied in DQ or DOM, indicating that these structural characteristics play a minor role in their adjuvant properties. TMC with a DQ of 56% (TMC56) formulated with WIV at a ratio of 5:1 (w/w) resulted in significantly lower IgG2a/c:IgG1 ratios compared to TMC56 mixed in ratios of 0.2:1 and 1:1, implying a shift towards a Th2 type immune response. Challenge of vaccinated mice with aerosolized virus demonstrated protection for all TMC-WIV formulations with the exception of TMC-RA44-WIV.

In conclusion, formulating WIV with TMCs strongly enhances the immunogenicity and induces protection against viral challenge in mice after i.n. vaccination. The adjuvant properties of TMCs as i.n. adjuvant are strongly decreased by reacetylation of TMC, whereas the DQ and DOM hardly affect the adjuvanticity of TMC.

Introduction

Intranasal (i.n.) vaccination offers several advantages over the intramuscular (i.m.) route, like simple, needle-free administration without the need for trained personnel, potentially less adverse effects and the induction of local mucosal immune responses [1]. On the other hand, vaccines administered via the i.n. route generally induce low systemic immune responses when compared to i.m. administration likely due to mucociliary clearance and low antigen uptake. Mucoadhesive polymers have been used to increase the immunogenicity of i.n. vaccines by increasing nasal residence time and enhancing antigen presentation [1].

Chitosan, a polysaccharide that is obtained by deacetylation of the natural polymer chitin, has mucoadhesive properties and showed promising results as an adjuvant in nasal vaccines [2-5]. However, the unfavorable pH-dependent solubility and charge density led to the synthesis of its quaternized derivative *N,N,N*-trimethyl chitosan (TMC) (Scheme 1), which is well soluble in aqueous solution at neutral pH.

TMC is traditionally synthesized by reaction of chitosan with excess iodomethane in strong alkaline conditions with *N*-methyl-2-pyrrolidone (NMP) as solvent and the degree of quaternization (DQ) can be varied by varying the number of reaction steps [6]. Besides *N*-methylation this synthesis method also introduces substantial *O*-methylation on the hydroxyl groups located at the C-3 and C-6 of the glucosamine unit. The degree of *O*-methylation (DOM) increases up to 80-90% with increasing DQ [7, 8]. Recently, *O*-methyl free TMC was synthesized using a novel two-step synthesis procedure, allowing good control of the DQ without altering other structural properties. Both DQ and DOM were found to influence toxicity and transepithelial electrical resistance (TEER), an indicator for opening of tight junctions, in a Caco-2 cell model. A higher DQ leads to more toxicity and a stronger TEER effect, with a maximum effect on TEER at a DQ above 60%. Furthermore, *O*-methyl free TMC has a much stronger effect on TEER than *O*-methylated TMC (TMC-OM) and shows more *in vitro* cell toxicity [8]. Another characteristic of TMCs is the degree of *N*-acetylation (DAc). Partial reacetylation of TMC (from 17 to 54%) decreased the *in vitro* cell

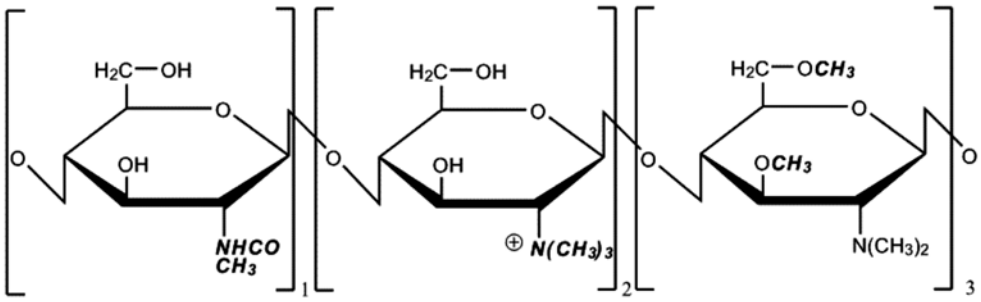

Scheme 1. General structure of TMC. Depending on the synthesis route TMCs can be varied in degree of acetylation (see block 1), quaternization (see block 2), and O-methylation (see block 3). The various substitutions are randomly distributed throughout the polymer; O-methylation (block 3) may also occur on the quaternized and acetylated units (blocks 1 & 2).

toxicity and effect on TEER but increased the enzymatic degradability of TMC by lysozyme [9]. Little is known about the relationship between the structural characteristics and adjuvant properties of TMCs *in vivo*. For TMC-OM solutions in i.n. vaccination with ovalbumin an optimal DQ of 40% was reported although differences were small [10]. Previously, whole inactivated influenza virus (WIV) vaccine was formulated with TMC-OM with a DQ of 15% or 37%. This resulted in positively charged nanoparticles with partially bound TMC-OM. These particles had an intact viral ultrastructure. Strong, protective immune responses were induced after i.n. vaccination [11]. No significant differences were observed between the two different TMC-OMs. Most likely, TMC exerts its adjuvant effect by an improved antigen delivery, through an increased nasal residence time and/or enhanced uptake through the epithelium and by antigen presenting cells.
Besides differences in DQ, the TMC-OMs used in these studies also differed in DOM and, likely, polymer molecular weight. So, the individual contributions of DQ, DAc and DOM on the adjuvant effect of TMC are unknown.
In the present study we investigated for i.n. administered WIV the adjuvant properties of *O*-methyl free TMCs with varying DQs and reacetylated *O*-methyl free TMC in comparison to conventional TMC-OMs with similar DQ. The TMC-WIV vaccines were physicochemically characterized and the immunogenicity and protectivity of the vaccines were assessed in a murine challenge model. Additionally, the influence of TMC:WIV ratio on the quality and quantity of humoral immune responses was investigated.

Materials & Methods

Materials

Chitosan with a DAc of 17% (determined with ^{1}H-NMR as described in [9]) and a number average molecular weight (M_n) and weight average molecular weight (M_w) of 28 and 43 kDa, as determined by gel permeation chromatography (GPC) as described in [8], respectively, was purchased from Primex (Siglufjordur, Iceland). Acetic anhydride, sodium borohydrate, formic acid, formaldehyde 37% (stabilized with methanol), deuterium oxide, sodium acetate, acetic acid (anhydrous), sodium hydroxide and hydrochloric acid were obtained from Sigma-Aldrich Chemical Co. Iodomethane 99% stabilized with copper was obtained from Acros Organics (Geel, Belgium). Live, egg-grown, mouse adapted influenza A/Puerto Rico/8/34 virus (A/PR/8/34) and purified, cell culture-grown (Madin-Darby Canine Kidney (MDCK) cells), β-propiolacton (BPL)-inactivated A/PR/8/34, as well as polyclonal rabbit anti-A/PR/8/34 serum were from Nobilon International BV, Boxmeer, The Netherlands. PO-labeled goat anti mouse -IgG (H+L), -IgG1, -IgG2a/c and -IgA(Fc) were purchased from Nordic Immunological Laboratories (Tilburg, The Netherlands). All other chemicals used were of analytical grade.

Synthesis and characterization of methylated chitosans

N,N,N-Trimethylated chitosans with varying DQ and DAc, and DOM were synthesized from chitosan as described previously [8, 9]. Briefly, *O*-methyl free TMCs were made with a two-step

method: first quantitative dimethylation of the free amino-groups of chitosan with formaldehyde and formic acid was carried out, followed by reaction of the dimethylated chitosan with an excess of iodomethane. By varying the reaction time the DQ of the TMCs could be tailored [8]. TMC-OMs, with substantial *O*-methylation of the hydroxyl groups on the C-3 and C-6 of the glucosamine units, were synthesized according to the method of Sieval et al. [6, 8]. Here, chitosan was trimethylated to various extents by reacting with iodomethane in the presence of a strong base (NaOH) for several times depending on the desired DQ. Finally, to obtain TMC with a high degree of acetylation, chitosan was first re-acetylated using acetic anhydride [9, 12]. Then, this re-acetylated chitosan was quantitatively dimethylated with formaldehyde and sodium borohydrate followed by complete trimethylation of the dimethylated amino groups with iodomethane [9]. All synthesized TMCs were dissolved in an aqueous 10% w/v NaCl solution, put on a shaker overnight for ion-exchange and the obtained solution was dialyzed at room temperature against deionized water for 3 days changing water twice daily, filtered through a 0.8 μm filter and freeze dried.
The DQ, DAc and DOM of the hydroxyl groups on C-3 and C-6 (DOM-3 and DOM-6, respectively) of the TMCs were determined with ^{1}H-NMR on a Varian INOVA 500MHz NMR spectrometer (Varian Inc., Palo Alto, Ca, USA) at 80 °C in D_2O [9]. Furthermore, M_n and M_w of the various TMCs were determined, as described previously [9, 13], by GPC on a Viscotek system detecting refractive index, viscosity and light scattering. A Shodex OHPak SB-806 column (30 cm) was used with 0.3 M sodium acetate pH 4.4 (adjusted with acetic acid) as running buffer. The structural characteristics of the synthesized TMCs are summarized in Table 1.

Preparation of TMC-WIV formulations

Purified, cell culture-derived, BPL-inactivated A/PR/8/34 suspended in a 10 mM phosphate buffered saline solution (150 mM NaCl, pH 7.4) (PBS) was concentrated by centrifugation at 22,000 x g for 30 min at 4 °C and resuspended in 5 mM HEPES buffer (pH 7.4). The WIV concentration is expressed as mg total protein/ml as determined by DC protein assay (Bio-Rad, Hercules, CA, USA). The amount of hemagglutinin (HA) was approximately 35 % of the total protein content, as determined previously [14]. The TMC-WIV vaccines were prepared by adding equal volumes of TMC solution (in 5 mM HEPES, pH 7.4) to a WIV dispersion (in 5 mM HEPES pH 7.4) at a 1:1 w/w ratio using a Gilson pipette while gently mixing for 5 seconds. TMC-WIV was formulated at a final WIV concentration of 1.25 mg/ml, except for the samples used for dynamic light scattering (DLS) and zeta-potential measurements, which were performed at lower concentrations (62.5 μg/ml) for optimal test-conditions. To study the immunogenicity of TMC-WIV at other ratios, TMC56 was also formulated with WIV at ratios of 0.2:1 (TMC56-WIV(0.2:1))and 5:1(TMC56-WIV(5:1)), by varying the TMC concentration added to WIV.

Particle size and zeta-potential measurements

WIV and TMC-WIV formulations were prepared at a final WIV concentration of 62.5 μg/ml in 5 mM HEPES buffer pH 7.4. Particle size was measured by dynamic light scattering (DLS) using a Malvern ALV CGS-3 (Malvern Instruments, Malvern, UK). DLS results are given as a z-average

particle size diameter and a polydispersity index (PDI). The PDI can range from 0 (indicating monodisperse particles) to 1 (a completely heterodisperse system). Zeta-potential was measured using a Zetasizer Nano (Malvern Instruments, Malvern, UK).

Quantification of unbound TMCs by GPC

The fraction of the various TMCs that was not bound to WIV was quantified in the supernatant of centrifuged TMC-WIV formulations, using the GPC method described earlier [11]. TMC-WIV formulations were centrifuged for 40 min at 22,000 x g at 4 °C and the supernatant was collected. Prior to injection, 20 µl GPC running buffer was added to 100 µl supernatant to adjust the pH of the sample to pH 4.4. The sample concentration was determined using refractive index detection.

Immunization protocol

Animal experiments were conducted according to the guidelines provided by the Dutch Animal Protection Act and were approved by a Committee for Animal Experimentation. For all experiments 6-8 weeks old female C57-BL/6 mice (Charles River) were used. Mice were housed in groups of 7-11 mice and food and water were provided ad libitum. Prime and boost immunizations at day 0 and 21, respectively, were performed without anesthesia. Groups of 11 mice were vaccinated i.n. with the various TMC-WIV formulations at a dose of 12.5 µg WIV (corresponding to approximately 4.3 µg HA). All TMC-WIV vaccines were freshly prepared by mixing WIV dispersion with solutions of the various TMCs, as described in section 2.3. Additionally, a group of 11 mice were vaccinated with WIV i.n. without TMC. As negative control groups, one group of 11 mice was treated i.n. with 5 mM HEPES and another with TMC56 solution (1.25 mg/ml in 5 mM HEPES pH 7.4) without WIV. For i.n. immunization, mice were held in supine position without anesthesia and the formulations were administered to the left and right nostril in a total volume of 10 µl. As a reference, one group of mice was vaccinated i.m. with WIV at a dose of 12.5 µg protein in a volume of 100 µl in the left and right quadriceps for prime and boost vaccination, respectively.

Blood sampling and nasal washes

Blood samples were collected by orbital puncture in MINICOLLECT® serum separator tubes coated with SiO_2 (Greiner Bio-One, Alphen a/d Rijn, the Netherlands) 20 days after prime vaccination and 17 days after boost vaccination. Coagulated blood samples were centrifuged at 6,500 x g for 8 min at room temperature to obtain serum samples. Individual serum samples were stored at -20 °C until further analysis. Seventeen days after boost vaccination, 4 mice from each group were sacrificed by a lethal intraperitoneal injection of 100 µl sodium pentobarbital (200 mg/ml). The trachea was then cannulated towards the nasopharyngeal duct with a PVC tube (inner/outer diameter 0.5/1.0 mm). PBS (500 µl) containing complete Mini, EDTA free protease inhibitor (Roche Diagnostics, Indianapolis, IN, USA) at a concentration of 1 tablet / 7 ml PBS was flushed through the nasal cavity and collected from the nostrils 3 times. The combined nasal washes were stored at -70 °C until further analysis.

Challenge

Twenty one days after the boost vaccination, mice were challenged with 50 ml (2×10^8 x the 50% egg infectious dose (EID50)/ml) aerosolized, egg-grown A/PR/8/34 using a DeVilbiss Ultra-Neb 2000 ultrasonic nebulizer (Direct Medical Ltd, Lecarrow, Ireland) for 25 min. After challenge, mice were put back in their cages and any observed signs of illness like lethargy, standing fur and curved back were recorded. Additionally, their body weight was monitored daily for 15 days. For comparison of loss in body weight, the average area under the curve (AUC) was calculated for each group from relative body weight curves of individual mice. All i.n. groups were compared to the negative control group (PBS i.n.) and the positive control group (WIV i.m.) by the average (AUC) of individual mice using a one-way ANOVA and Bonferroni's correction for multiple comparisons.

Hemagglutination inhibition test

First, 25 µl serum was incubated for 18 h at 37 °C with 75 µl Receptor Destroying Enzyme (RDE) solution (Denka Seiken UK Ltd, Coventry, UK) to suppress nonspecific hemagglutination inhibition. RDE was then inactivated by incubating the mixture for 30 min at 56 °C. Next, 150 µl PBS was added to obtain a final 10-fold serum dilution. Fifty µl diluted serum was transferred in duplicate to V-bottom 96-wells plates (Greiner, Alphen a/d Rijn, The Netherlands) and serially diluted twofold in PBS. Next, 4 hemagglutination units (HAU) of A/PR/8/34 (in 25 µl PBS) were added and the mixture was incubated for 40 min at room temperature. Finally, 50 µl 0.5% (v/v) chicken erythrocytes in PBS was added. Plates were incubated for 1 h at room temperature. The HI titer is expressed as the reciprocal value of the highest serum dilution capable of completely inhibiting the virus-induced agglutination of chicken erythrocytes. If no complete inhibition could be detected in the first lane, serum was arbitrarily scored 5. Comparison between different experimental groups from the same dose was made by a one-way ANOVA test and the Tukey post test on the log transformed HI titers.

Antibody assays

Antigen specific serum antibody responses were determined by a sandwich ELISA. Maxisorp ELISA plates (Nunc, Roskilde, Denmark) were coated overnight with polyclonal rabbit anti-A/PR/8/34 serum (dilution 1:1620). Plates were washed in between all prescribed steps with wash buffer (0.64 M NaCl, 3 mM KCl, 0.15% polysorbate 20 in 10 mM phosphate buffer pH 7.2) using a Skanwasher 300 (Molecular Devices, Sunnyvale, CA, USA). Next, plates were incubated for 1 h at 37 °C with blocking buffer (0.2% (w/w) casein, 4% (w/w) sucrose, 0.05% (w/w) Triton X-100 and 0.01% (w/w) sodium azide in 30 mM TRIS pH 7.4), followed by incubation for 1 h at 37 °C with egg-grown, BPL-inactivated A/PR/8/34 (25.6 HAU/ml). Plates were then incubated with twofold serially diluted sera (100 µl/well) for 1 h at 37 °C. Next, plates were incubated with 100 µl of a 1:2500 dilution of horseradish peroxidase linked goat anti mouse -IgG (H+L), -IgG1, -IgG2a/c or -IgA(Fc) (Nordic Laboratories, Tilburg, the Netherlands) for 30 min, and washed twice. Finally, 100 µl 3,3',5,5'-Tetramethylbenzidine (TMB) substrate solution was added and plates were incubated for 15 min at room temperature before enzymatic conversion was stopped by adding 50 µl 2 M

sulfuric acid. Optical density (OD) was then measured at 450 nm using a Tecan Sunrise plate reader (Tecan Trading AG, Zurich Switzerland). Titers are given as the reciprocal sample dilution corresponding to 20% of the maximal ELISA signal above background. Seronegative sera were arbitrarily scored with a titer of 15. Comparison between different experimental groups was made using the log transformed titers by a one-way ANOVA test and the Tukey post test.
Boost IgG2a/c:IgG1 ratios were calculated and compared using the log transformed data by a one-way ANOVA test and Bonferroni's correction for multiple comparison.

Results

Structural properties of TMCs

The structural properties of the TMCs used in this study are summarized in table 1. The DQ of the *O*-methyl free TMCs ranged between 30 and 68%, allowing us to selectively study the influence of trimethylation on adjuvant properties of TMC. With the TMC-OM group (DQ varying from 22 to 86%, *O*-methylation from 12 to 76% along with increasing DQ) the combined effect of charge density and *O*-methylation on adjuvanticity can be studied. The effect of *O*-methylation can be evaluated by comparing the *O*-methylated TMCs with *O*-methyl free TMCs. Finally, the re-acetylated TMC with a DAc of 54% and a DQ of 44% can be used to assess the role of *N*-acetylated units in the adjuvant properties of TMCs. Especially the comparison of TMC43, TMC-OM45 and TMC-RA44 will provide insight into the optimal structural properties of TMC for its use in nasal vaccine delivery. Importantly, it is unlikely that the minor differences in molecular weights between the various TMCs (table 1) caused by variation in the degrees of substitutions and/or synthesis methods will affect the biological properties of the polymers [15].

Characterization of TMC-WIV formulations

Various TMC-WIV formulations were prepared by mixing the two components at a 1:1 (w/w) ratio. For comparison, TMC56-WIV formulations were also prepared at 0.2:1 and 5:1 (w/w) ratios. Particle size and size distribution were determined and compared with those of plain WIV.

Table 1. Structural properties of synthesized TMCs.[1)]

Abbreviation	Mn (kDa)	Mw (kDa)	DQ (%)	DAc (%)	DOM-6 (%)	DOM-3 (%)
TMC30	33	59	30	17	–	–
TMC43	36	75	43	17	–	–
TMC56	37	78	56	17	–	–
TMC68	39	84	68	17	–	-
TMC-OM22	34	56	22	12	18	12
TMC-OM45	32	49	45	11	25	16
TMC-OM61	31	49	61	10	56	44
TMC-OM86	29	44	86	9	76	72
TMC-RA44	43	83	44	54	–	–

[1)] Degree of acetylation (DAc), quaternization (DQ), O-methylation on C-6 (DOM-6) and on C-3 (DOM-3) of TMCs were determined by 1H-NMR analysis. Mn, Mw were determined by GPC.

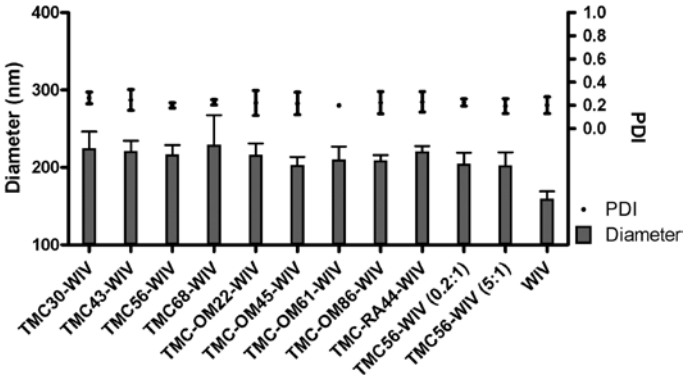

Figure 1. Diameter and size distribution (PDI) of TMC-WIV formulations as determined by dynamic light scattering. Error bars represent standard deviations of three measurements.

Figure 1 shows that plain WIV had a diameter of approximately 170 nm with a polydispersity index (PDI) of 0.2, indicating a fairly homogeneous particle size distribution. Formulating the WIV particles with the various TMCs led to a small increase in particle size (200-220 nm) and comparable size distributions, independent of the type of TMC used or the TMC/WIV ratio.

Furthermore, the zeta-potential of the TMC-WIV particles was analyzed in 5 mM HEPES pH 7.4. The addition of TMC to negatively charged WIV (-13 mV) in a 1:1 (w/w) ratio resulted in positively charged particles (+12 to +20 mV) as seen in Figure 2, suggesting that all TMCs adsorb onto WIV in a similar fashion. The zeta-potential increased slightly with increasing DQ and the lowest surface charge was observed with TMC-OM22-WIV. As expected, compared to the 1:1 ratio a lower TMC56:WIV ratio (0.2:1 (w/w)) resulted in a lower surface charge (+12 mV vs. +18 mV), but a higher ratio (5:1 (w/w)) did not result in a higher zeta-potential.

The amount of free TMC present in the TMC-WIV formulations was quantified using GPC. The concentration and relative amount of free TMC are depicted in Table 2. TMC-WIV formulations at a ratio of 1:1 (w/w) had an average free TMC content between 0.95 and 1.15 mg/ml (corresponding to 76 and 91% of total TMC in the formulation), independent of the DQ of the polymers. TMC-RA44 had the highest amount of TMC bound to the WIV particles. In the TMC56-WIV(0.2:1)

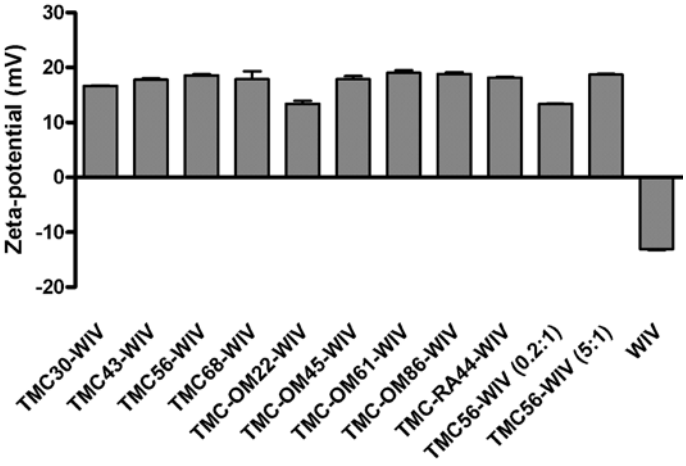

Figure 2. Zeta-potential of TMC-WIV formulations determined in 5 mM HEPES pH 7.4 Error bars indicate standard deviations of three samples.

Table 2. Specifications of TMC in various TMC-WIV formulations

Formulation	WIV (μg)	Total TMC in formulation (μg)	TMC:WIV (w/w) ratio	Unbound TMC (mg/ml)[ab]	Unbound TMC (% of total)[b]
TMC30-WIV	12.5	12.5	1:1	1.13± 0.04	90.0±3.3
TMC43-WIV	12.5	12.5	1:1	1.14± 0.03	91.2±2.6
TMC56-WIV	12.5	12.5	1:1	1.09± 0.01	87.1±0.8
TMC68-WIV	12.5	12.5	1:1	1.08± 0.08	86.1±6.2
TMC-OM22-WIV	12.5	12.5	1:1	1.02± 0.04	81.8±3.4
TMC-OM45-WIV	12.5	12.5	1:1	1.05± 0.06	83.9±4.4
TMC-OM61-WIV	12.5	12.5	1:1	1.01± 0.04	80.7±3.2
TMC-OM86-WIV	12.5	12.5	1:1	1.06± 0.01	85.1±0.9
TMC-RA44-WIV	12.5	12.5	1:1	0.95± 0.00	76.0±0.4
TMC56-WIV (0.2:1)	12.5	2.5	0.2:1	0.10± 0.05	49.3±1.5
TMC56-WIV (5:1)	12.5	62.5	5:1	6.11± 0.07	97.7±1.1
WIV	12.5	–	–	–	–

[a] Amount of free TMC in the TMC-WIV formulations determined by GPC
[b]Values are presented as the average of three samples ± standard deviation.

mixture about 50% of the TMC56 remained free in solution, whereas in the TMC56-WIV(5:1) almost 98% of the total TMC56 in the formulation remained unbound. These results, together with the results of the zeta-potential measurements, indicate that WIV is likely saturated with TMCs at TMC:WIV ratios 1:1 and 5:1 (w/w).

Summarizing, mixing WIV with various TMCs in a ratio of 1:1 resulted in particles with similar size, size distribution, surface charge and amount of free TMC, thus allowing a fair evaluation of the influence of the structural characteristics of the TMCs on their adjuvant properties. Altering the TMC:WIV ratio mostly changed the amount of free TMC present in the formulation and here the contribution of free TMC can be assessed.

Immunization study

Serum antigen specific total IgG after prime and boost vaccination

The TMC-WIV formulations were compared to WIV alone in an intranasal vaccination study. Serum samples were analyzed for antigen-specific total IgG responses three weeks after prime and boost vaccination (Fig. 3). IgG responses were induced by all formulations containing WIV after prime vaccination and had increased after boost vaccination. TMCs with a DAc ≤ 17% had a strong adjuvant effect that is not critically affected by DOM and DQ. All TMC-WIV formulations, except TMC-RA44-WIV, showed a higher number of responding mice and elicited significantly higher IgG titers than WIV alone. Interestingly, TMC-RA44-WIV induced significantly lower total IgG responses than all other TMC-WIV formulations with a TMC:WIV ratio of 1:1.

Additionally, no significant differences were observed between the various TMC56-WIV ratio formulations, indicating that free TMC does not strongly influence total IgG titers and that the lowest dose of TMC that was tested already significantly increased immune responses after i.n. vaccination with WIV.

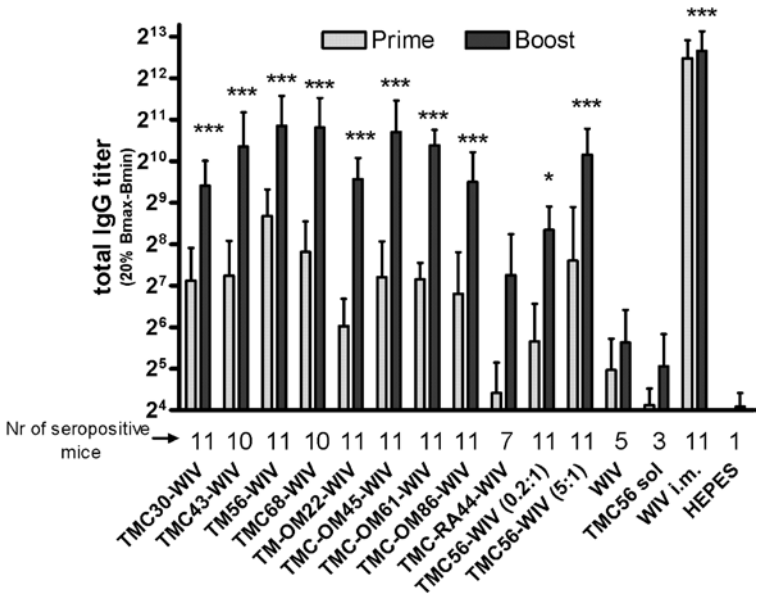

Figure 3. Geometric mean antigen specific total IgG titers three weeks after prime and boost vaccination. Error bars indicate 95% confidence intervals (n=11). Non-responding mice were arbitrarily given a total IgG serum titer of 15. Below the x-axis the number of seropositive mice per group after boost vaccination are depicted. All titers after boost vaccination were compared using a one-way ANOVA test and Tukey's post test. *** $p<0.001$ and * $p<0.05$ indicate titers that are significantly higher than those of WIV i.n.

Serum antigen-specific IgG1 and IgG2a/c after prime and boost vaccination

To determine the influence of the type and ratio of TMC on the quality of the humoral immune response elicited against WIV, serum was analyzed for antigen-specific IgG1 and IgG2a/c titers by ELISA. There were no significant differences observed in type of immune response for the various TMCs mixed with WIV at a TMC:WIV ratio of 1:1 (not shown). All induced a stronger IgG2a/c response than IgG1 after prime vaccination, but after boost vaccination IgG1 titers were strongly enhanced, as illustrated in Figure 4A for the 1:1 (w/w) TMC56-WIV formulation. Strikingly, the TMC56:WIV ratio did have an effect on the type of immune response; the IgG1 titers and the number of responding mice increased with increasing TMC:WIV ratio. In contrast, the number of IgG2a/c positive mice was the lowest at a TMC:WIV ratio of 5.

Plotting the IgG2a/c:IgG1 ratio per individual mouse illustrates that the Th1/Th2 balance of humoral immune responses shifts towards Th2 with increasing TMC:WIV ratio (Fig. 4B).

HI titers

After boost vaccination, HI titers were hardly detectable in any of the i.n. vaccinated groups (data not shown). Only WIV i.m. induced substantial HI titers (average HI titer of 160). This is in line with previous results [11, 14]

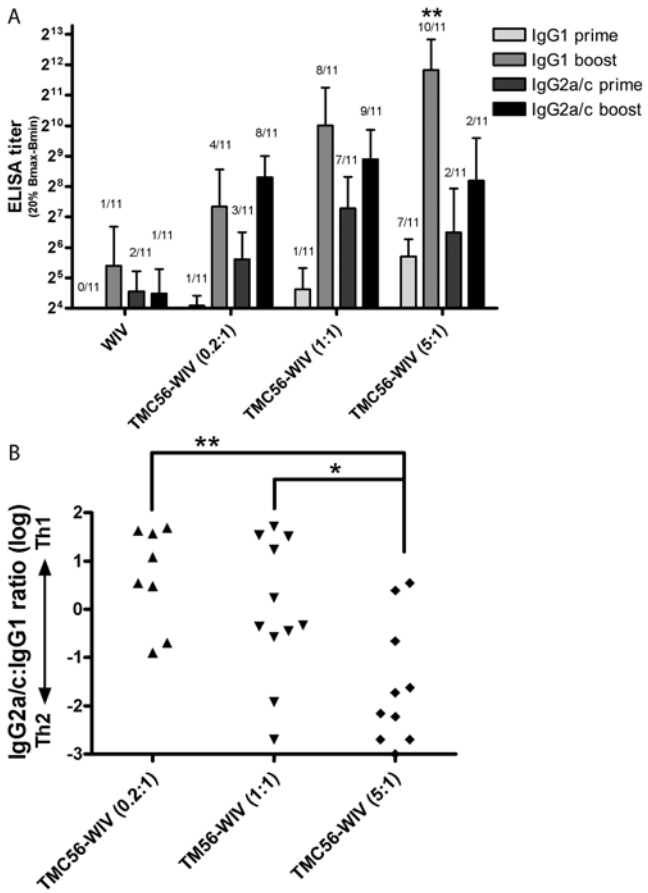

Figure 4. A) IgG1 and IgG2a/c titers elicited by WIV formulations with varying TMC56:WIV ratios after prime and boost vaccination. Error bars indicate 95% confidence intervals (n=11). Indicated above the bars is the number of mice that developed detectable IgG1 or IgG2a/c titers (e.g. 1/11 indicates one out of eleven mice). ** $p<0.01$ indicates that IgG1 boost titer was significantly higher than that of TMC56-WIV (0.2:1). B) IgG2a/c:IgG1 ratio of boost titers of individual mice elicited by WIV formulations with varying TMC56:WIV ratios. * $p<0.05$ and ** $p<0.01$ indicate that IgG2a/c:IgG1 ratio of TMC56-WIV(5:1) was significantly lower than those of the other TMC56-WIV formulations.

Antigen-specific secretory IgA (sIgA) in nasal washes

Nasal washes were performed 17 days after boost vaccination to determine whether antigen-specific sIgA were elicited by any of the various formulations. As shown in Figure 5 only in the TMC-WIV formulations some mice developed detectable sIgA responses in the nasal cavity. Interestingly, although WIV i.m. immunization showed the highest serum IgG titers, no sIgA was found in the nasal washes of any of these mice. Altogether, the determination of sIgA in the nasal mucus showed a relatively high variation within the formulation-groups (as observed by others [10]) likely due to the collection and detection methods.

Challenge with live, aerosolized virus

To assess the protective effect of the immunization, seven mice per group were challenged with potentially lethal, homologous, egg-grown influenza virus and loss of body weight as a measure of illness was monitored. All mice vaccinated i.n. with *O*-methyl free or *O*-methylated TMC-WIV formulations were protected against the live virus. As representative examples the average body

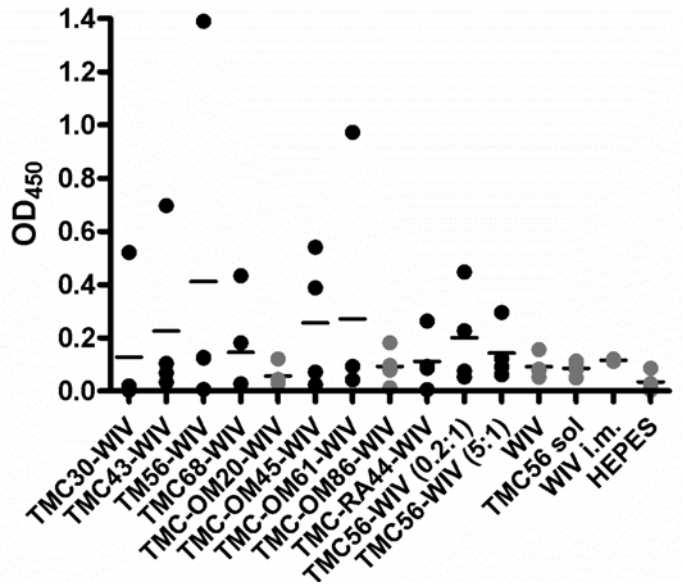

Figure 5. Antigen-specific secretory IgA levels in nasal washes of four individual mice per formulation 17 days after boost vaccination. Only in groups represented by black dots sIgA positive washes were found.

weight over 15 days after the challenge of the mice immunized with TMC43-WIV and TMC-OM45-WIV formulations are shown in Figure 6A and B.

Additionally, there were no signs of illness observed in these groups and the AUC of the average body weight was significantly higher ($p<0.001$) than the curve obtained with the HEPES group. No significant differences in AUC of the average body weight were observed between these i.n. groups and the WIV i.m. group. Furthermore, altering the TMC-WIV ratio did not result in differences in protection (results not shown). Interestingly, the mice treated with TMC-RA44-WIV formulation showed a significant drop in body weight and developed clinical signs of illness like lethargy and a curved back (Fig. 6C). The average AUC of the relative body weight in the TMC-RA44-WIV group was significantly lower than WIV after i.m. immunization ($p <0.05$). Nevertheless, the TMC-RA44-WIV group lost less body weight than the buffer control group (Fig. 6C) ($p<0.01$). In contrast, the WIV i.n. formulation without TMC did not provide significantly better protection against the live virus challenge than the buffer control (Fig. 6D) and all mice suffered from signs of illness.

Discussion

Novel synthesis methods allow to tailor the DQ and DAc of *N,N,N*-trimethyl chitosan without altering other structural properties [8, 9]. Alternatively, Sievals method [6] can be used to synthesize partially *O*-methylated TMC with varying DQs. *In vitro* characterization of the biological properties of the various TMCs showed that these structural characteristics affect cell toxicity and TEER of epithelial cell monolayers. Briefly, a higher DQ of TMC leads to a higher toxicity and a stronger effect on TEER. *O*-methylation and *N*-acetylation on the other hand decrease toxicity and effect on TEER [8, 9]. The polymer molecular weight of chitosan and its derivatives can also influence

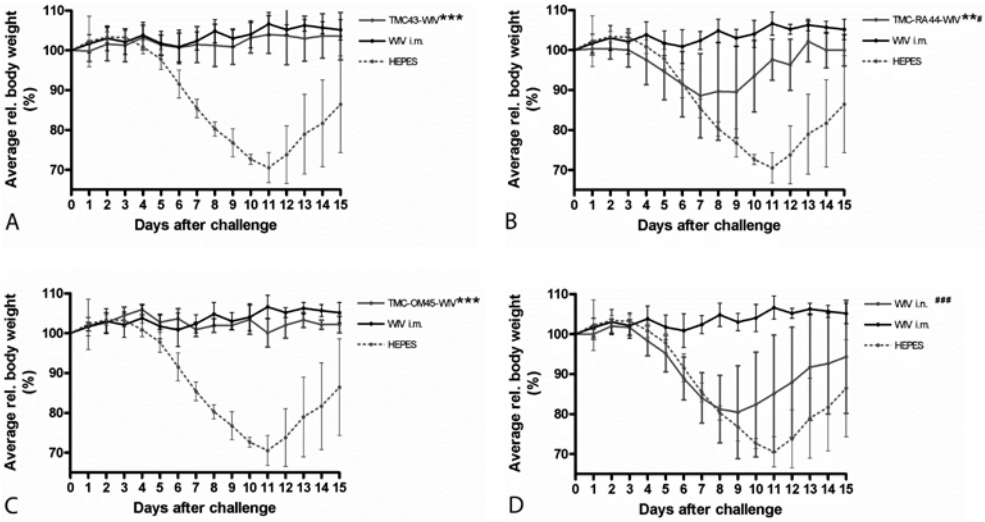

Figure 6. Average relative body weight curves after challenge of mice (n=7) vaccinated with A) TMC43-WIV; B) TMC-OM45-WIV; C) TMC-RA44-WIV and D) WIV i.n.. For comparison each panel contains the curves of WIV i.m. and HEPES i.n.. Error bars indicate the 95% confidence intervals. *** $p< 0.001$ and ** $p< 0.01$ indicate that average AUCs are significantly higher than the HEPES i.n. group. ### $p< 0.001$ and # $p <0.05$ indicate that average AUCs are significantly lower than the WIV i.m. group.

its biological properties *in vivo* [16] and *in vitro* [15, 17]. This effect can be neglected in our study because all TMCs have comparable chain lengths as confirmed with GPC.

Physicochemical characterization revealed that all TMC-WIV formulations were very similar in particle size, zeta-potential or fraction of unbound TMC. Any observed differences in immunogenicity can therefore be attributed to the structural differences between the various TMC polymers rather than to differences in the above parameters. Moreover, the TMC56-WIV formulations with different TMC:WIV (w/w) ratios mainly differed in the amount of free TMC and can therefore provide insight into the role of free TMC in the adjuvant effect.

The influence of the DQ on the adjuvant effect was not significant. All *O*-methyl free TMC-WIV vaccines induced comparable total IgG and IgG isotype titers and provided protection after challenge independent of the DQ. This is in line with earlier studies with TMC-OM [10, 11]. Furthermore, *O*-methylated TMCs had similar effects on both antibody titers and protection as *O*-methyl free TMCs, indicating that the DOM does not affect the adjuvant properties of TMC.

Interestingly, these findings do not correlate with the large influence of DQ and O-methylation *in vitro* on cell toxicity and TEER. This teaches us that DQ and DOM have a much more pronounced effect on *in vitro* cell toxicity and TEER assays than on mucosal adjuvant properties. It should be noted that the DOM and DQ may have an influence on the activity of TMC as a penetration enhancer in mucosal drug delivery, as suggested by reports on the influence of DQ [18-20]. As HA likely is too big to pass even fully opened tight junctions, it is unlikely that opening of tight junctions will directly improve antigen uptake from the nasal cavity.

The reacetylation of TMC on the other hand induced a strong decrease in adjuvant effect illustrated by lower antibody titers and poor protection against challenge with live influenza virus. Since the mucoadhesion of particulate systems can be attributed to positive charge and hydrophobic effect [3], it is likely that TMC-RA44-WIV has similar or even better mucoadhesive properties as the other TMC-WIV vaccines. Also, the zeta-potential of the particles was similar to the other TMC-coated particles, implying that the introduction of a positive surface charge alone is not sufficient to improve adjuvanticity. Therefore other factors must be responsible for the decreased adjuvant effect of reacetylated TMC.

The first explanation for the decreased adjuvant effect of TMC-RA44 is a difference in interaction with cells, illustrated by a much lower *in vitro* toxicity and TEER effect than most other TMCs on Caco-2 cells [9]. TMC-OM22, however, hardly induced a TEER effect or cell toxicity either but showed to be a good mucosal adjuvant. This indicates that TEER and toxicity studies, as carried out for these TMCs [8, 9] cannot fully explain the loss of adjuvant effect by reacetylation.

A second explanation for the poor adjuvant properties of TMC-RA44 is its enhanced enzymatic degradation by lysozyme compared to other TMCs. Previous research showed that the extent of lysozyme-catalyzed degradation of TMC is highly dependent on the DAc: TMC-RA44 showed a large decrease in molecular weight while TMCs with DAc of ≤17% were only slightly degraded in presence of lysozyme [9]. Lysozyme is a strong antibacterial cationic protein that is excreted in high concentrations in the nasal cavity [21]. This may result in rapid degradation of the TMC-RA44 after i.n. administration, thereby strongly limiting its adjuvant effect on the WIV vaccination.

Finally, chitin, an insoluble polysaccharide of *N*-acetylglucosamine units, which are also present in TMC-RA44, can be recognized by specific receptors of the innate immune system [22]. It has recently been suggested that chitin induces pro-inflammatory but also anti-inflammatory signals depending on its size [23]. Further studies should be done to investigate whether TMC-RA44 also induces anti-inflammatory signals through interaction with the innate immune system.

In addition to changes in the type of TMC, the influence of free TMC was studied by varying the TMC concentration in the formulation. An excess of free TMC induced a shift towards higher IgG1 titers after boost vaccination. Several studies investigated the influence of TMC on the quality of immune responses [24-26] while other studies determined the effect of adjuvant dose on the type of responses elicited, using different adjuvants [27, 28]. However, since the type of adjuvant, animal model used, route of administration and animal model can affect the quality of immune responses, it is difficult to compare these studies to our data. This is the first time that the effect of adjuvant dose was studied for TMC and additional studies should be performed to provide mechanistical insight.

Conclusions

All TMC-WIV formulations had comparable physicochemical properties, and therefore observed differences in immunogenicity are related to the various chemical structures of the TMCs. Formulating WIV with TMCs strongly enhances the immunogenicity and protection of i.n.

vaccination with WIV. The adjuvant properties of TMCs as i.n. adjuvant are strongly decreased by reacetylation of TMC, whereas the DQ and DOM did not significantly affect the adjuvant effect of TMC.

Acknowledgements

This research was partially performed under the framework of TI Pharma project D5-106; Vaccine delivery: alternatives for conventional multiple injection vaccines. The authors acknowledge Frouke Kuijer for making the graphical abstract.

References

[1] Slütter B, Hagenaars N, Jiskoot W. Rational design of nasal vaccines. J Drug Target 2008;16(1):1-17.

[2] Grabovac V, Guggi D, Bernkop-Schnurch A. Comparison of the mucoadhesive properties of various polymers. Adv Drug Deliv Rev 2005;57(11):1713-23.

[3] Harding SE. Mucoadhesive interactions. Biochem Soc Trans 2003;31(Pt 5):1036-41.

[4] Read RC, Naylor SC, Potter CW, Bond J, Jabbal-Gill I, Fisher A, et al. Effective nasal influenza vaccine delivery using chitosan. Vaccine 2005;23(35):4367-74.

[5] Vila A, Sanchez A, Janes K, Behrens I, Kissel T, Vila Jato JL, et al. Low molecular weight chitosan nanoparticles as new carriers for nasal vaccine delivery in mice. Eur J Pharm Biopharm 2004;57(1):123-31.

[6] Sieval AB, Thanou M, Kotze AF, Verhoef JE, Brussee J, Junginger HE. Preparation and NMR characterization of highly substituted N-trimethyl chitosan chloride. Carbohydrate Polymers 1998;36(2-3):157-65.

[7] Polnok A, Borchard G, Verhoef JC, Sarisuta N, Junginger HE. Influence of methylation process on the degree of quaternization of N-trimethyl chitosan chloride. Eur J Pharm Biopharm 2004;57(1):77-83.

[8] Verheul RJ, Amidi M, van der Wal S, van Riet E, Jiskoot W, Hennink WE. Synthesis, characterization and in vitro biological properties of O-methyl free N,N,N-trimethylated chitosan. Biomaterials 2008;29(27):3642-9.

[9] Verheul RJ, Amidi M, van Steenbergen MJ, van Riet E, Jiskoot W, Hennink WE. Influence of the degree of acetylation on the enzymatic degradation and in vitro biological properties of trimethylated chitosans. Biomaterials 2009;30(18):3129-35.

[10] Boonyo W, Junginger HE, Waranuch N, Polnok A, Pitaksuteepong T. Chitosan and trimethyl chitosan chloride (TMC) as adjuvants for inducing immune responses to ovalbumin in mice following nasal administration. J Control Release 2007;121(3):168-75.

[11] Hagenaars N, Mastrobattista E, Verheul RJ, Mooren I, Glansbeek HL, Heldens JG, et al. Physicochemical and Immunological Characterization of N,N,N-Trimethyl Chitosan-Coated Whole Inactivated Influenza Virus Vaccine for Intranasal Administration. Pharm Res 2009;26(6):1353-64.

[12] Kiang T, Wen J, Lim HW, Leong KW. The effect of the degree of chitosan deacetylation on the efficiency of gene transfection. Biomaterials 2004;25(22):5293-301.

[13] Jiang X, van der Horst A, van Steenbergen MJ, Akeroyd N, van Nostrum CF, Schoenmakers PJ, et al. Molar-mass characterization of cationic polymers for gene delivery by aqueous size-exclusion chromatography. Pharm Res 2006;23(3):595-603.

[14] Hagenaars N, Mastrobattista E, Glansbeek H, Heldens J, van den Bosch H, Schijns V, et al. Head-to-head comparison of four nonadjuvanted inactivated cell culture-derived influenza vaccines: Effect of composition, spatial organization and immunization route on the immunogenicity in a murine challenge model. Vaccine 2008;26(51):6555-63.

[15] Mao S, Shuai X, Unger F, Wittmar M, Xie X, Kissel T. Synthesis, characterization and cytotoxicity of poly(ethylene glycol)-graft-trimethyl chitosan block copolymers. Biomaterials 2005;26(32):6343-56.

[16] Mei D, Mao S, Sun W, Wang Y, Kissel T. Effect of chitosan structure properties and molecular weight on the intranasal absorption of tetramethylpyrazine phosphate in rats. Eur J Pharm Biopharm 2008.

[17] Huang M, Khor E, Lim LY. Uptake and cytotoxicity of chitosan molecules and nanoparticles: effects of molecular weight and degree of deacetylation. Pharm Res 2004;21(2):344-53.

[18] Thanou MM, Kotze AF, Scharringhausen T, Luessen HL, de Boer AG, Verhoef JC, et al. Effect of degree of quaternization of N-trimethyl chitosan chloride for enhanced transport of hydrophilic compounds across intestinal caco-2 cell monolayers. J Control Release 2000;64(1-3):15-25.

[19] Hamman JH, Stander M, Kotze AF. Effect of the degree of quaternisation of N-trimethyl chitosan chloride on absorption enhancement: in vivo evaluation in rat nasal epithelia. Int J Pharm 2002;232(1-2):235-42.

[20] Sandri G, Rossi S, Bonferoni MC, Ferrari F, Zambito Y, Di Colo G, et al. Buccal penetration enhancement properties of N-trimethyl chitosan: Influence of quaternization degree on absorption of a high molecular weight molecule. Int J Pharm 2005;297(1-2):146-55.

[21] Cole AM, Liao HI, Stuchlik O, Tilan J, Pohl J, Ganz T. Cationic polypeptides are required for antibacterial activity of human airway fluid. J Immunol 2002;169(12):6985-91.

[22] Lee CG, Da Silva CA, Lee JY, Hartl D, Elias JA. Chitin regulation of immune responses: an old molecule with new roles. Curr Opin Immunol 2008;20(6):684-9.

[23] Da Silva CA, Chalouni C, Williams A, Hartl D, Lee CG, Elias JA. Chitin is a size-dependent regulator of macrophage TNF and IL-10 production. J Immunol 2009;182(6):3573-82.

[24] Amidi M, Pellikaan HC, Hirschberg H, de Boer AH, Crommelin DJ, Hennink WE, et al. Diphtheria toxoid-containing microparticulate powder formulations for pulmonary vaccination: preparation, characterization and evaluation in guinea pigs. Vaccine 2007;25(37-38):6818-29.

[25] Amidi M, Romeijn SG, Verhoef JC, Junginger HE, Bungener L, Huckriede A, et al. N-trimethyl chitosan (TMC) nanoparticles loaded with influenza subunit antigen for intranasal vaccination: biological properties and immunogenicity in a mouse model. Vaccine 2007;25(1):144-53.

[26] Sayin B, Somavarapu S, Li XW, Thanou M, Sesardic D, Alpar HO, et al. Mono-N-carboxymethyl chitosan (MCC) and N-trimethyl chitosan (TMC) nanoparticles for non-invasive vaccine delivery. Int J Pharm 2008.

[27] McCluskie MJ, Weeratna RD, Clements JD, Davis HL. Mucosal immunization of mice using CpG DNA and/or mutants of the heat-labile enterotoxin of Escherichia coli as adjuvants. Vaccine 2001;19(27):3759-68.

[28] Riedl K, Riedl R, von Gabain A, Nagy E, Lingnau K. The novel adjuvant IC31 strongly improves influenza vaccine-specific cellular and humoral immune responses in young adult and aged mice. Vaccine 2008;26(27-28):3461-8.

Chapter 6

Role of *N*-trimethylated chitosan (TMC) in nasal residence time, local distribution and toxicity of an intranasal influenza vaccine

Niels Hagenaars, Marta Mania, Pascal de Jong, Ivo Que, Rob Nieuwland, Bram Slütter, Harrie Glansbeek, Jacco Heldens, Han van den Bosch, Clemens Löwik, Eric Kaijzel, Enrico Mastrobattista, Wim Jiskoot

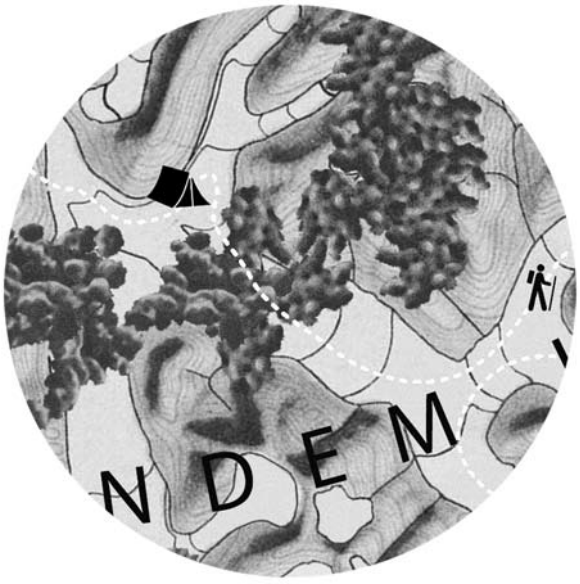

Submitted for publication

Abstract

The nose is a promising immunization site and intranasal (i.n.) vaccination studies with whole inactivated influenza virus (WIV) adjuvanted with N,N,N-trimethylchitosan (TMC-WIV) have shown promising results. In this study, the influence of TMC on the i.n. delivery of WIV was studied in mice by comparing the nasal residence time and the specific location in the nasal cavity of WIV and TMC-WIV. Additionally, the local toxicity profile of the WIV formulations was assessed. *In vivo* fluorescence imaging was used to study the nasal residence time and the fate of the bulk vaccine in mice that received vaccines fluorescently labeled with IRDye800CW®. An immunohistochemical (IHC) staining method for nasal cross-sections was developed to visualize the antigen in the nasal cavity. Therefore, mice were sacrificed at different time points after vaccination with various vaccine formulations and nasal cross-sections were made. The local toxicity was assessed using hematoxylin and eosin staining for the nasal cross-sections. No significant differences in the nasal residence time between WIV and TMC-WIV were observed. However, IHC revealed a striking difference in the location and distribution of WIV in the nasal cavity. When formulated as plain WIV, positive staining was mainly found in the nasal cavity, presumably in mucus blobs. TMC-coated WIV, on the other hand, was mostly present as a thin layer on the epithelial surfaces of the naso- and maxilloturbinates. This difference in staining pattern correlates with the observed differences in immunogenicity of these two vaccines and indicates that TMC-WIV results in a much closer interaction of WIV with the epithelial surfaces than WIV alone, potentially leading to enhanced uptake and induction of immune responses. This study further shows that both WIV and TMC-WIV formulations induce minimal local toxicity. Taken altogether, these results provide more insight in the mode of action and safety of TMC and justify further research to develop TMC adjuvanted nasal vaccines.

Introduction

Intranasal (i.n.) vaccination poses several advantages to the classical intramuscular (i.m.) route of vaccination. The simple, needle-free administration does not require trained personnel and i.n. immunization has the potential to evoke both mucosal as well as systemic immune responses. The major drawback of this route of administration is the relatively poor immunogenicity of nonadjuvanted vaccines when compared to the i.m. route. This is likely the result of inefficient delivery of antigens to the immune system via the nasal cavity, as illustrated by the strong immune responses that the same vaccines elicit after i.m. administration [1].

The delivery of vaccine antigens is impaired by the mucociliary clearance, which removes inhaled substances like dust and bacteria and viruses, entrapped in mucus, from the nasal cavity towards the throat, preventing that potentially harmful substances can penetrate the nasal epithelium.

Several strategies have been explored to improve the efficacy of i.n. vaccination [2]. In the case of influenza vaccines, the use of a live attenuated influenza virus vaccine, which replicates only locally in the upper respiratory tract, has been successful [3]. Furthermore, the use of adjuvants in combination with killed vaccines has shown promising results (as reviewed in [2]). Besides immunostimulatory adjuvants like TLR-ligands, toxin-derivatives and cytokines, the use of mucoadhesive polymers is of special interest in nasal vaccination as it may improve the delivery of i.n. administered antigens [4].

Promising results were obtained using N,N,N-trimethylchitosan (TMC), a water soluble derivative of chitosan, as an adjuvant in nasal vaccines [5-8]. TMC is a cationic mucoadhesive polymer that can be characterized by the degree of quaternization (DQ), the degree of O-methylation and the degree of acetylation (DAc).

We formulated whole inactivated influenza virus (WIV) with various TMCs to obtain positively charged TMC-coated WIV (TMC-WIV) formulations that induced significantly higher immune responses and provided protection against challenge with live influenza virus [7]. Furthermore, we showed that the DQ and DOM of TMC did not significantly influence the immunogenicity of TMC-WIV formulations [8].

It is generally believed that the mode of action of mucoadhesive adjuvants, including TMC in i.n. WIV vaccines, is the improvement of the mucoadhesion of the antigen, leading to an increased nasal residence time and/or an altered interaction of the antigen with the mucosal surfaces in the nasal cavity. However, the relationship between mucoadhesiveness, nasal residence time and immunogenicity has not been properly investigated *in vivo*. Mostly, *in vitro* methods have been employed to describe the mucoadhesive properties of polymers and vaccine formulations [9], including TMC [10] which is moderately mucoadhesive.

Gamma scintigraphy has been used to image the clearance of radiolabeled polymers and particles from the nasal cavity *in vivo* [11-14]. However, nuclear imaging has its drawbacks such as the need for trained personnel, expensive instrumentation and specialized facilities to work with radioactive materials. Recent advances in probe design and instrumentation have enabled *in vivo* fluorescence imaging using near infrared fluorescence (NIR) spectroscopy with improved spatial

resolution [15]. NIR fluorescence imaging is a cheap and practical alternative to nuclear imaging. Novel NIR fluorescent probes such as IRDye800CW® can be covalently coupled to any protein via simple procedures. Moreover, the deep tissue penetration of NIR light and the low tissue auto fluorescence enable *in vivo* fluorescence imaging.

Another approach to study the mechanism of action of TMCs as mucosal vaccine adjuvants is using microscopy techniques. Microscopic techniques have been used to locate i.n. administered nanoparticulate formulations[16], localize adjuvant targets [17] and visualize uptake of nanoparticles and micro-organisms through nasal epithelium [18, 19]. In fluorescence microscopy, fluorescent probes can be used to label administered particles or antigens prior to administration. Alternatively, the use of immunohistochemical (IHC) staining with antigen specific antibodies enables visualization of the administered antigen in isolated nasal cross-sections post administration without the need for labeling the antigen prior to administration.

Nasal cross-sections can also be used to study the local toxicity of i.n. administered vaccines and vaccine adjuvants. The safety of vaccines is key in the development of nasal vaccine adjuvants, as evidenced by the withdrawal of an inactivated i.n. influenza vaccine with LT as an adjuvant from the market because of adverse effects [20]. Although various TMCs have different *in vitro* cell toxicities, they are considered relatively nontoxic *in vitro* [21-24]. Nevertheless, the local toxicity of TMC solutions and TMC-WIV formulations may be different after i.n. administration and should therefore be determined.

The aim of this study was to compare the nasal residence time, the specific location in the nasal cavity and the local toxicity of WIV and TMC-WIV. Therefore, an *in vivo* fluorescence imaging approach was used and an IHC staining protocol was developed.

Materials & methods

Materials

Purified, cell culture-grown (Madin-Darby Canine Kidney (MDCK) cells), β-propiolacton (BPL)-inactivated influenza A/PR/8/34 virus (WIV), and polyclonal anti-WIV rabbit serum were from Nobilon International BV, (Boxmeer, The Netherlands). Alexa Fluor® 488-labeled goat anti-rabbit IgG and 4',6-diamidino-2-phenylindole dihydrochloride (DAPI) were purchased from Invitrogen (Breda, The Netherlands). Osteosoft decalcifier (10% EDTA) and ethanol were from Merck Serono BV (Schiphol, The Netherlands). Xylene was obtained from Mallinckrodt Baker (Deventer, The Netherlands). Citric acid, Triton-X, n-octyl-β-D-glucopyranoside (OG), trypsin from bovine pancreas, normal goat serum and normal rabbit serum were obtained from Sigma (Zwijndrecht, The Netherlands). Phosphate buffered saline (10 mM phosphate buffer, pH 7.4 150 mM NaCl) (PBS) was purchased from Braun (Melsungen, Germany). IRDye800CW®-labeled epidermal growth factor (EGF) and the IRDye800CW® protein labeling kit were from LI-COR Biosciences (Lincoln, NE, USA). Fixative (4% formalin in phosphate buffer pH 7.0) was purchased from Klinipath (Duiven, The Netherlands). All other chemicals used were of analytical grade.

TMCs

In the *in vivo* fluorescence imaging studies we used *O*-methyl free TMC with a DQ of 43% (TMC43) to compare the nasal residence time of TMC-coated WIV and plain WIV. For the immunostaining and toxicity studies, O-methyl free TMC68 and O-methylated TMCs (TMC-OM) with DQs of 15% (TMC-OM15) and 37% (TMC-OM37) were also included in the study. The various TMCs were produced and characterized as described earlier [7, 21]. The polymer characteristics of the TMCs are summarized in table 1.

Formulation of TMC-WIV

WIV in PBS was pelleted by centrifugation at 22,000 x g for 30 min at 4 °C and resuspended in 5 mM HEPES buffer (pH 7.4) at a final concentration of 2.5 mg total protein/ml. The amount of hemagglutinin (HA) was approximately 35 % of the total protein content, as determined previously [25].

For the *in vivo* fluorescence imaging experiments, WIV was labeled with the NIR fluorescent probe IRDye800 CW® according to the instructions provided by the manufacturer. Briefly, the pH of the WIV suspension with a final protein concentration of approximately 1 mg/ml was raised to pH=8.5 with 1M K_2PO_4, pH 9. To 450 µl of this suspension, 15 µl of IRDye800CW® Reactive Dye solution (4 mg/ml in DMSO) was added and the mixture was incubated for 2 h in the dark at room temperature while shaking. Next, labeled WIV was separated from the free label using a size-exclusion *Zeba*™ Desalting Spin Column. The purified IRDye800CW®-labeled WIV was then centrifuged for 45 minutes at 22,000 x g at 4°C and resuspended in 100 µl 5 mM HEPES buffer. The protein concentration was determined by a micro BCA protein assay from Pierce, part of Thermo Fisher Scientific (Rockford, IL, USA) using bovine serum albumin (BSA) as a reference protein and the IRDye800CW®-labeled WIV suspension was adjusted with approximately 50 µl 5mM HEPES to a WIV concentration of 2.5 mg/ml.

The TMC-WIV vaccines were prepared by simply adding equal volumes of a TMC solution (in 5 mM HEPES, pH 7.4) to a WIV dispersion at a 1:1 w/w ratio using a Gilson pipette while gently mixing for 5 seconds. A volume of 10 µl (5µl to each nostril) of TMC-WIV formulations was administered to mice at a final WIV concentration of 1.25 mg/ml.

Imaging and local toxicity studies after i.n. administration of WIV formulatons in mice

All animal experiments described in this study were conducted according to the guidelines

Table 1: Physicochemical characteristics of the TMCs used in this study.

Abbreviation	Mn (kDa)	Mw (kDa)	DQ (%)	DAc (%)	DOM-6 (%)	DOM-3 (%)
TMC43	36	75	43	17	-	-
TMC68	39	84	68	17	-	-
TMC-OM15	44	94	15	16	6	4
TMC-OM37	30	63	37	4	14	9

provided by the Dutch Animal Protection Act and were approved by a Committee for Animal Experimentation.

***In vivo* fluorescence imaging**

Female nude (Balb/c nu/nu) mice aged 6 weeks were obtained from Charles River (LÁrbresle, France) and housed in ventilated cages in groups of 3-6 mice. Chlorophyl-free food and water were provided *ad libitum*. The animals (n=9 for each formulation) received the IRDye800CW®-labeled WIV formulations under light anesthesia with isoflurane inhalation. Next, mice were scanned with an IVIS Spectrum imaging system from Caliper Life Sciences (Hopkinton, MA, USA). Scans were performed regularly over a time period of at least 2 h. In between scans, mice were put back in their cages to recover from anesthesia. Scanned images were analyzed using Living Image 3.1 software from Caliper Life Sciences (Hopkinton, MA, USA). The threshold was set using the background scan made from each mouse before administration of the IRDye800CW®-labeled formulations. The excitation wavelength was set at 710 nm and emitted light was measured at 760; 780; 800; 820 and 840 nm. Spectral unmixing was performed to decompose the emitted light into auto fluorescence and label-specific fluorescence. The obtained fluorescence represents the quantity of the fluorophore at each pixel. Regions of interest in the nasal cavity were detected and quantified over time. To compare the fluorescence in different mice and different groups, the absolute fluorescence was converted to relative fluorescence (% of the maximum fluorescence in the nasal cavity). The influence of TMC on the nasal residence time was studied by comparing the average area under the curves (AUC) of the relative fluorescence of individual mice in each group using a one way ANOVA test. At the end of the experimental period, animals were sacrificed by cervical dislocation and a postmortem scan was made of the abdomen after dissection.

Immunostaining of WIV in nasal cross-sections

For immunostaining experiments 6-8 weeks old female C57-BL/6 mice (Charles River) were used. Mice were housed in groups of 5 mice and food and water were provided *ad libitum*. They were i.n. vaccinated with various WIV formulations. As negative controls, mice received PBS or solutions of TMCs and 4 mice were left untreated. At different time points after dosing - i.e. 20 minutes, 1 h, 3 h or 24 h - animals were sacrificed by cervical dislocation and the nasal cavity was isolated by removing the brains, lower jaw, skin and muscle tissue. The nasal cavities were then fixed in 10% formalin for 24 h.

After fixation, nasal cavities were decalcified for 14 days in a solution of 10 % EDTA, pH 7.4, which was refreshed once between day 4 and 6. Next, nasal cavities were embedded in paraffin and 3.5 µm thick cross-sections were made at different depths of the nasal cavity using a Microm HM 355 S microtome from Thermo Fisher Scientific (Walldorf, Germany). Cross-sections for immunohistochemistry were mounted on superfrost plus glass slides from Menzel-Gläser (Braunschweig, Germany). On each glass slide, 2 cross-sections were placed.

Paraffin-embedded cross-sections were deparaffinized and hydrated by incubation with xylene followed by a series of graded alcohols and finally tap water. Next, the cross-sections were incubated

with preheated 10 mM citrate buffer, pH 6.0, at 95°C for 30 minutes for heat-induced epitope retrieval (HIER) step to improve the recognition of the antigen by the primary antibody. Cross-sections were allowed to cool down to room temperature.

Deparaffinized, HIER-treated cross-sections were washed 3 x 5 min with 0.2% Triton-X in PBS. Cross-sections were incubated first with normal goat serum for 15 minutes and then with a 1:500 dilution of polyclonal WIV-specific rabbit antiserum overnight at 4°C. As a negative control, one of the two paraffin sections was incubated with nonspecific rabbit serum as primary antibody. All sera and antibody solutions were centrifuged at 10,000 x g for 1 min at room temperature prior to application to remove any aggregates from the staining solution. After washing the slides 3x for 5 min with 0.2% Triton-X in PBS, a 1:200 dilution of Alexa Fluor® 488-labeled goat anti-rabbit IgG was applied. The samples were incubated for 45 minutes at room temperature. Next, the slides were washed 3x with PBS and stained with a 1:25000 dilution of DAPI for 6 min at room temperature and washed 3x with PBS again. Finally, the slides were mounted with Fluorosave™ from Calbiochem (San Diego, CA, USA).

All slides were examined using a fluorescence microscope (Nikon Eclipse TE-2000 Nikon, Amstelveen, the Netherlands) equipped with a Digital Sight DS-2Mv camera. Slides were blindly scored for the presence, location, pattern and intensity of antigen staining and pictures were taken with fixed camera settings for a fair comparison.

Determination of local toxicity

Sections, prepared as described above, were mounted on cut edge glass slides from Menzel-Gläser (Braunschweig, Germany) and stained with hematoxylin and eosin (H&E) for toxicological evaluation by a trained toxicologist. One slide per animal was routinely stained with Hematoxylin and Eosin (H&E) for microscopic examination. The presence of serous fluid, desquamated epithelial cells, and necrotic debris in the nasal cavity was examined. Furthermore, epithelial necrosis and congestion of the submucosa were scored. The microscopic findings were graded as absent, minimal, slight, moderate, marked or severe histological change.

Results and Discussion

In vivo fluorescence imaging

To study the effect of TMC on the nasal residence time of WIV, *in vivo* fluorescence imaging was used. The purified, IRDye800CW®-labeled WIV was formulated in HEPES 5 mM pH 7.4 with or without TMC43, a strong adjuvant for i.n. WIV vaccines [8], at a 1:1 (w/w) ratio. After i.n. administration, the fluorescence in the nasal cavity was monitored for at least 120 min. Figure 1 shows a representative example of the detected, IRDye800CW®-specific fluorescence in a mouse over time.

After administration, the fluorescence was originally only detected in the nasal cavity where it increased during the first half hour and later disappeared over time, as shown in figure 2. The initial increase in fluorescence is likely a result of a dequenching effect that may have occurred

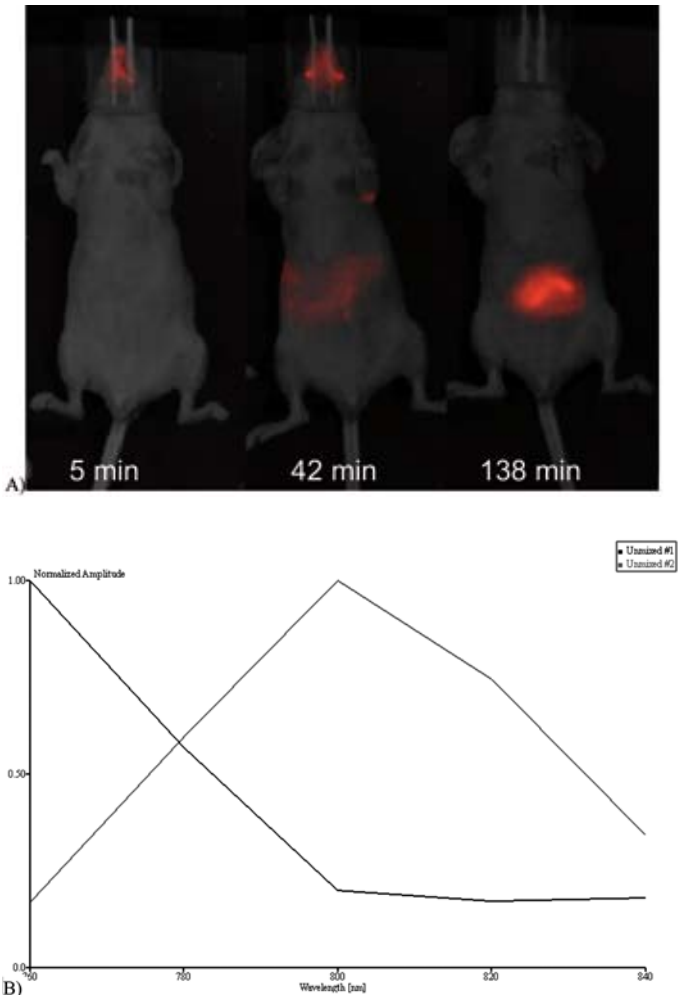

Figure 1. A) Fluorescence detected in a representative mouse after intranasal administration of IRDye800CW®-labeled WIV at different time points. Fluorescence, depicted in red, was initially only present in the nasal cavity. Over time, it was cleared from the nose via the nasopharyngeal duct towards the stomach and intestines. B) Emission spectrum of detected fluorescence after spectral unmixing. The grey spectrum with a peak at 800 nm represents the labeled-WIV-specific emission spectrum in the nasal cavity; the black spectrum represents the background fluorescence. Similar spectra were found in the stomach (data not shown).

in the nasal cavity. At later time points, fluorescence was observed in the stomach as well at total intensities that exceeded the maximum values in the nose. This is further studied in the appendix to this chapter.

The fluorescence profile in the nasal cavity was comparable over time for both plain WIV and TMC43-WIV, and was detectable for at least two hours after administration in 8 out of 9 mice in both groups. Furthermore, the AUCs of the relative fluorescence for WIV and TMC-WIV were not statistically different ($p > 0.05$), suggesting that the nasal residence time of the bulk vaccine was not strongly influenced by the addition of TMC.

These data suggest that the improved immunogenicity of TMC-WIV formulations cannot be ascribed to a difference in nasal residence time of the vaccine in the nasal cavity. In line with these findings, Garmise et al. could not find a correlation between nasal residence time and immunogenicity of WIV [26]. In that study, radioactive colloids as model virus particles to compare nasal clearance of

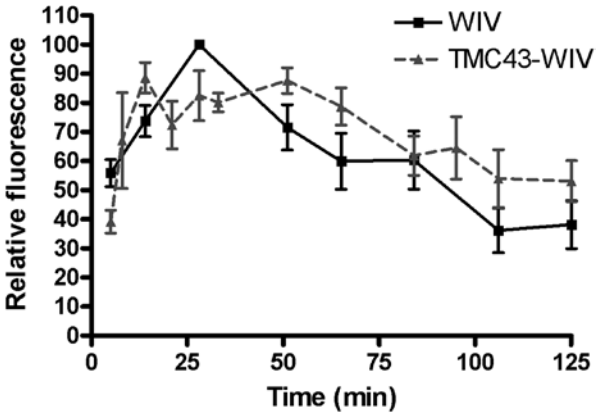

Figure 2. Average relative fluorescence in the nasal cavity over time. n=9 mice for each group. Error bars indicate the standard error of the mean.

A

B

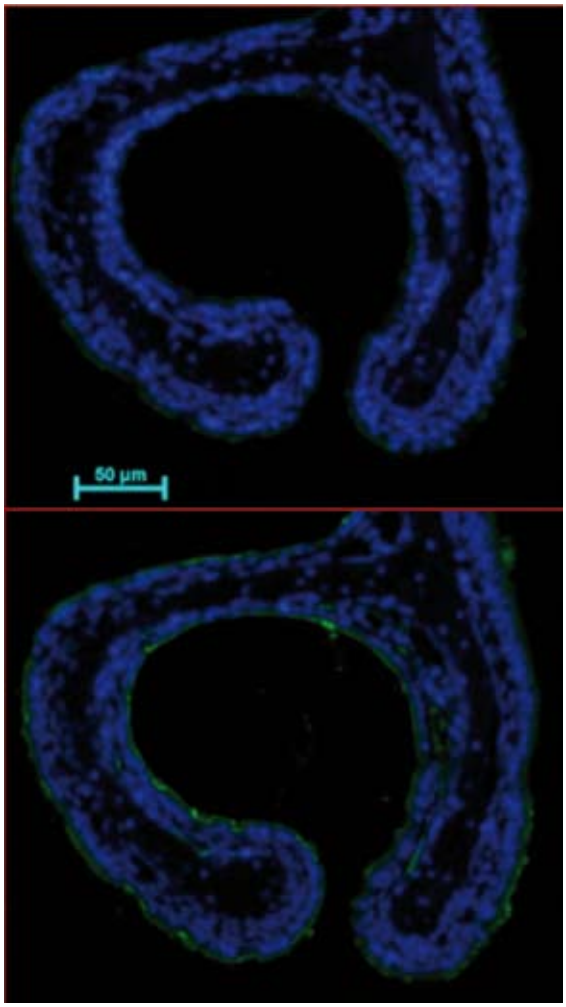

Figure 3: Antigen specificity of staining on the nasoturbinate. Representative sections of a mouse treated with TMC-OM37-WIV stained with nonspecific rabbit serum (A) or with WIV-specific rabbit serum (B). WIV-staining is shown in green and DAPI-stained cell nuclei in blue to visualize tissue anatomy.

dispersions and powder formulations of WIV with various mucoadhesive polymers, like chitosan, hydroxypropyl methylcellulose, carboxymethylcellulose and sodium alginate. These results suggest that mucoadhesive polymers may have a different mode of action as nasal vaccine adjuvants than purely prolonging the nasal residence time. Soane et al. found that chitosan solutions and chitosan particles are retained longer in the nasal cavities of sheep and humans than radiolabeled 99mTc, chelated with diethylene triamine pentaacetic acid (DTPA), as a control [12, 13]. It is likely that WIV itself already has an improved retention in the nasal cavity that is not further improved by TMCs, as it binds to cell surface sialic acid residues on epithelial cells in upper airways, the host cell receptors for influenza viruses [27].

While the fluorescence was cleared from the nasal cavity, a fluorescence signal became visible in the abdomen of the mice (See fig 1). This was observed for both WIV and TMC43-WIV formulations, indicating that the labeled WIV and TMC-WIV were cleared from the nasal cavity through the nasopharyngeal duct via the esophagus towards the gastrointestinal tract. Post mortem analysis revealed that almost all fluorescence was found back in the stomach and intestines after 4 h (Figure 3) and only trace amounts could be found in the kidneys, spleen and liver. Furthermore, no fluorescence could be detected in the lungs. This is especially important because immunogenicity of i.n. administered vaccine formulations can be strongly overestimated in a murine model when the antigens are delivered in the lower respiratory tract [28].

Immunostaining of nasal cross-sections

To further study the effect of TMC on the nasal delivery of WIV, nasal cross sections were prepared from mice that were sacrificed at different time points after administration of WIV or various TMC-WIV formulations. An IHC staining protocol was developed for these experiments. After fixation and decalcification, tissues were embedded in paraffin and sectioned. The deparaffinized sections required an antigen retrieval step to achieve optimal staining, likely because the fixation step with formalin induced antigen masking, as reviewed recently [29]. The best results were obtained with a heat induced epitope retrieval (HIER) step in citric acid, pH 6.0 for 30 minutes at 95°C, adapted from [30].

After HIER, sections could be stained specifically for WIV using a polyclonal rabbit serum against WIV, as evidenced by the low background fluorescence observed in nasal cross sections of non treated mice, mice treated with PBS and treated mice when the specific primary polyclonal serum was replaced by either PBS or nonspecific rabbit serum (Figure 4).

After 20 min, positive staining was found in the nasal cavities of almost all mice that had received either WIV or any of the TMC-WIV formulations. Three hours after administration, the staining was less clear and in some mice staining could no longer be detected. After 24 h, no positive staining was found in any of the mice, indicating that the vaccines were fully cleared from the nasal cavity.

The stained sections showed no evidence that TMC-WIV was retained longer in the nasal cavity than plain WIV, which supports the findings from the *in vivo* fluorescence imaging experiments. It is clear though, that the (microscopic) IHC technique logically is more sensitive than the

(macroscopic) *in vivo* fluorescence imaging: in most mice, the antigen was still detected by IHC 3 h after administration (both for plain WIV and TMC-WIV), whereas the vaccine could no longer be detected in the nasal cavity using *in vivo* fluorescence imaging.

In contrast to the similarity in bulk clearance between plain and TMC-coated WIV formulations, a striking difference in the location and pattern of staining was observed. As illustrated in figure 5, WIV was mainly found in the nasal cavity, presumably in blobs of mucus and was hardly present on the epithelial surfaces, especially at the 20 min time point. After 3 h, plain WIV was more attached to the epithelial surface than after 20 minutes, but positive staining on the naso- and maxilloturbinates was still not observed (data not shown)

All TMC-coated WIV formulations, on the other hand, revealed a clear staining pattern of WIV along the epithelial surfaces after 20 minutes, especially on the naso- and maxilloturbinates (see Fig 6).

Importantly, mice that received only TMC solution showed no positive staining, which demonstrates that the positive signal on the naso- and maxilloturbinates was not due to nonspecific interactions of the primary or secondary antibodies with the TMCs. After 1 h, 3 h and 4 h, WIV was still present on the naso- and maxilloturbinates of mice vaccinated with TMC-coated WIV formulations, although the staining became less intense over time (results not shown).

This staining pattern revealed that WIV, when formulated with TMC, had a much larger contact area with the epithelial surfaces of the turbinates. This pattern was comparable for all TMC-WIV formulations, whereas positive staining on the turbinates was hardly detected after administration of plain WIV. Table 2 shows the results of the stained sections that were blindly scored for the presence and location of WIV staining after various time points for different formulations.

Unlike the nasal residence time, this difference in location correlates with the enhanced immunogenicity and protection of TMC-WIV formulations that was observed in vaccination studies [7] This is the first time that a correlation between the location of antigens in the nasal cavity after i.n. administration and the immunogenicity of the vaccine formulation has been described. Moreover, these results provide insight into the mode of action of TMC as nasal vaccine adjuvant. It seems that the addition of TMC brings WIV in closer contact with the mucosal surfaces, especially on the naso- and maxilloturbinates, facilitating the interaction of antigen with the epithelial surfaces in the nasal cavity. This may facilitate the uptake of TMC-coated WIV through the epithelium, the next step towards the induction of an immune response.

Surprisingly, WIV was hardly detected on the epithelial layer covering the NALT (results not shown), the main immune inductive site for nasal immune responses [31] and a location with increased particulate uptake via specialized M-cells [32, 33]. Unfortunately, no uptake of antigen through the epithelium could be observed anywhere in the nasal cavity. It is likely that only a minute fraction of the administered antigens will reach the immune system and induce an immune response or that extensive degradation of the vaccine occurs prior to reaching the NALT, which hampers detection by IHC. *In vitro* cell uptake studies or incubation of the vaccine formulation with excised nasal tissue may be used to study the influence of TMC on the uptake of antigen through the epithelial layer.

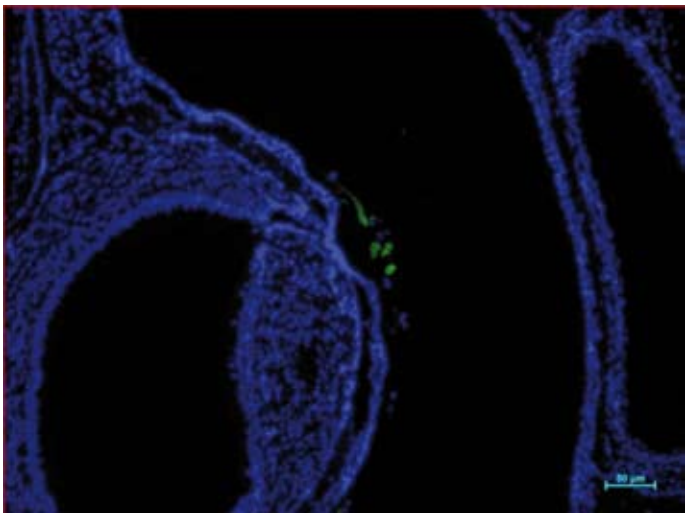

Figure 4. WIV (green) present as blobs in the nasal cavity after 20 min when administered in the absence of TMC. Cell nuclei were stained with DAPI (blue) to visualize tissue anatomy.

Assessment of local toxicity

In addition to the localization of the antigen in the nasal cavity, the safety profile of i.n. administered TMC- WIV vaccines was assessed, which is of crucial importance in the development of vaccine adjuvants. Signs of local toxicity were scored for individual mice by a trained pathologist, and the results are shown in Figure 7.

Local toxicity was either not observed or consisted of minimal to slight presence of serous fluid or a minimal presence of desquamated cells (shedding) in the nasal cavity. A minimal to slight congestion was also observed sometimes. Histopathological findings were comparable for mice vaccinated with plain WIV, all TMC-WIV formulations and all TMC solutions, suggesting that the addition of TMC does not increase the local adverse reactions of an i.n. WIV vaccine. Moreover, the local toxicity reactions were only marginally higher than observed with PBS.

Table 2. Scoring results for the presence of positive staining of various WIV formulation.

Timepoint	Treatment	Positive staining	Present on NT and/or MT
20 min	WIV	5/5	1/5
20 min	TMCOM15-WIV	5/5	4/5
20 min	TMCOM37-WIV	5/5	4/5
20 min	TMC43-WIV	4/4*	4/4*
20 min	TMC68-WIV	5/5	4/5
3 h	WIV	4/5	1/5
3 h	TMCOM15-WIV	5/5	4/5
3 h	TMCOM37-WIV	2/3*	2/3*
3 h	TMC68-WIV	2/5	1/5

NT=Nasoturbinate; MT=Maxilloturbinate

*Some mice were excluded from the scoring because blood was accidently introduced into the nasal cavity during the tissue preparation.

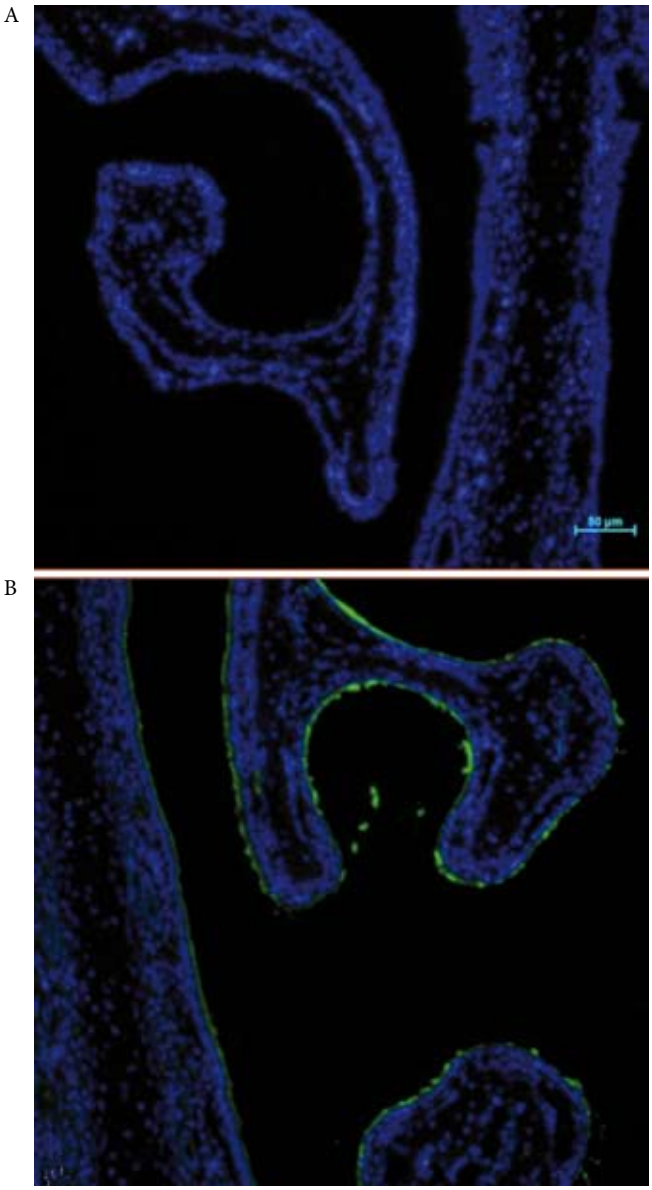

Figure 5. WIV-staining of nasoturbinates of mice that received WIV(A) or TMC68-WIV(B)20 minutes prior to sacrifice. WIV, stained in green, could only be found on epithelial surfaces of maxillo- and nasoturbinates when formulated with any of the TMCs (e.g. B) that were used, but not when administered alone (A). Cell nuclei were stained with DAPI (blue) to visualize tissue anatomy.

In contrast, mice that received a solution of PEI, a cationic polymer often used as a carrier for nonviral gene delivery via the pulmonary route [34], clearly developed more severe local adverse reactions, especially after 3 h and 24 h. The presence of serous fluid and desquamated cells as well as congestion increased over time in these mice. Furthermore, focal epithelial necrosis became evident after 24 h. This was not observed in plain WIV or any of the TMC-based formulations, indicating that the WIV-TMC formulations induce less local reactions than PEI.

These results were expected because the TMCs used were previously shown to be much less toxic

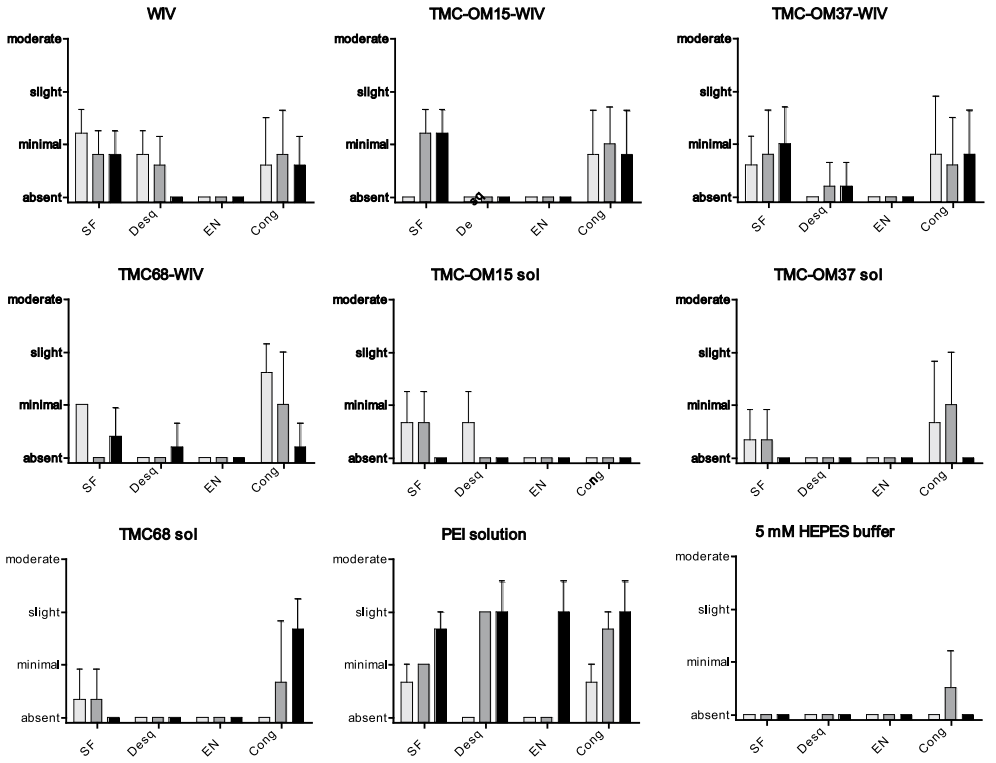

Figure 6. Local toxicity of WIV, TMC-WIV formulations and TMC solutions. Local toxicity is divided into the presence of serous fluid (SF); the presence of desquamated cells/necrotic debris (Desq); epithelial necrosis (EN) and congestion (Cong). Bars indicate average scored local toxicity at 20 min (light grey); 1 h (grey) and 24 h (black). n=5 for WIV; TMC-OM15-WIV; TMC-OM37-WIV and TM68-WIV and n=3 for all other groups). Error bars indicate the standard deviation.

in an *in vitro* cell toxicity assay [21]. Interestingly, the differences between the *in vitro* cell toxicity of *O*-methylated TMCs and *O*-methyl free TMCs [21], could not be observed *in vivo.* It appears that the *in vitro* cell toxicity experiments overestimate the toxicity induced after a single i.n. dose of TMC. Similarly, the differences in *in vitro* cell toxicity between TMCs with a high and a low DQ [21] could not be found *in vivo*. These promising results, combined with the earlier findings that TMCs have a marginal effect on the ciliary beat frequency [19, 23], justify further research to develop TMCs as nasal vaccine adjuvants.

Conclusions

Using *in vivo* fluorescence imaging and immunohistochemistry it was demonstrated that WIV and TMC-WIV had a comparable nasal clearance profile. Therefore, the adjuvant effect of TMC in i.n. WIV vaccine formulations cannot be ascribed to differences in nasal residence time of the

bulk vaccine. However, the addition of TMC resulted in an increased contact area between WIV and epithelium, which may explain the improved immunogenicity of TMC-adjuvanted WIV formulations. Moreover, the TMC-coated WIV vaccines induced minimal local toxicity, which is promising for further development.

Acknowledgements

The authors thank Isolde Debeijer for the toxicological examination of the nasal sections

References

[1] Hagenaars N, Mastrobattista E, Glansbeek H, Heldens J, van den Bosch H, Schijns V, et al. Head-to-head comparison of four nonadjuvanted inactivated cell culture-derived influenza vaccines: Effect of composition, spatial organization and immunization route on the immunogenicity in a murine challenge model. Vaccine 2008;26(51):6555-63.

[2] Slütter B, Hagenaars N, Jiskoot W. Rational design of nasal vaccines. J Drug Target 2008;16(1):1-17.

[3] Belshe RB, Edwards KM, Vesikari T, Black SV, Walker RE, Hultquist M, et al. Live attenuated versus inactivated influenza vaccine in infants and young children. N Engl J Med 2007;356(7):685-96.

[4] Davis SS. The use of soluble polymers and polymer microparticles to provide improved vaccine responses after parenteral and mucosal delivery. Vaccine 2006;24 Suppl 2:S2-7-10.

[5] Amidi M, Romeijn SG, Verhoef JC, Junginger HE, Bungener L, Huckriede A, et al. N-trimethyl chitosan (TMC) nanoparticles loaded with influenza subunit antigen for intranasal vaccination: biological properties and immunogenicity in a mouse model. Vaccine 2007;25(1):144-53.

[6] Boonyo W, Junginger HE, Waranuch N, Polnok A, Pitaksuteepong T. Chitosan and trimethyl chitosan chloride (TMC) as adjuvants for inducing immune responses to ovalbumin in mice following nasal administration. J Control Release 2007;121(3):168-75.

[7] Hagenaars N, Mastrobattista E, Verheul RJ, Mooren I, Glansbeek HL, Heldens JG, et al. Physicochemical and Immunological Characterization of N,N,N-Trimethyl Chitosan-Coated Whole Inactivated Influenza Virus Vaccine for Intranasal Administration. Pharm Res 2009;26(6):1353-64.

[8] Hagenaars N, Verheul RJ, Mooren I, de Jong PH, Mastrobattista E, Glansbeek HL, et al. Relationship between structure and adjuvanticity of N,N,N-trimethyl chitosan (TMC) structural variants in a nasal influenza vaccine. J Control Release 2009.

[9] Grabovac V, Guggi D, Bernkop-Schnurch A. Comparison of the mucoadhesive properties of various polymers. Adv Drug Deliv Rev 2005;57(11):1713-23.

[10] Snyman D, Hamman JH, Kotze AF. Evaluation of the mucoadhesive properties of N-trimethyl chitosan chloride. Drug Dev Ind Pharm 2003;29(1):61-9.

[11] Bryant ML, Brown P, Gurevich N, McDougall IR. Comparison of the clearance of radiolabelled nose drops and nasal spray as mucosally delivered vaccine. Nucl Med Commun 1999;20(2):171-4.

[12] Soane RJ, Frier M, Perkins AC, Jones NS, Davis SS, Illum L. Evaluation of the clearance characteristics of bioadhesive systems in humans. Int J Pharm 1999;178(1):55-65.

[13] Soane RJ, Hinchcliffe M, Davis SS, Illum L. Clearance characteristics of chitosan based formulations in the sheep nasal cavity Int J Pharm 2001;217(1-2):183-91.

[14] Washington N, McGlashan JA, Jackson SJ, Bush D, Pitt KG, Rawlins DA, et al. The effect of nasal patency on the clearance of radiolabeled saline in healthy volunteers. Pharm Res 2000;17(6):733-6.

[15] Ntziachristos V, Bremer C, Weissleder R. Fluorescence imaging with near-infrared light: new technological advances that enable in vivo molecular imaging. Eur Radiol 2003;13(1):195-208.

[16] Gao X, Chen J, Tao W, Zhu J, Zhang Q, Chen H, et al. UEA I-bearing nanoparticles for brain delivery following intranasal administration. Int J Pharm 2007;340(1-2):207-15.

[17] Giannasca PJ, Boden JA, Monath TP. Targeted delivery of antigen to hamster nasal lymphoid tissue with M-cell-directed lectins Infect Immun 1997;65(10):4288-98.

[18] Owen SJ, Batzloff M, Chehrehasa F, Meedeniya A, Casart Y, Logue CA, et al. Nasal-Associated Lymphoid Tissue and Olfactory Epithelium as Portals of Entry for Burkholderia pseudomallei in Murine Melioidosis. J Infect Dis 2009;199(12):1761-70.

[19] Amidi M, Romeijn SG, Borchard G, Junginger HE, Hennink WE, Jiskoot W. Preparation and characterization of protein-loaded N-trimethyl chitosan nanoparticles as nasal delivery system. J Control Release 2006;111(1-2):107-16.

[20] Mutsch M, Zhou W, Rhodes P, Bopp M, Chen RT, Linder T, et al. Use of the inactivated intranasal influenza vaccine and the risk of Bell's palsy in Switzerland. N Engl J Med 2004;350(9):896-903.

[21] Verheul RJ, Amidi M, van der Wal S, van Riet E, Jiskoot W, Hennink WE. Synthesis, characterization and *in vitro* biological properties of O-methyl free N,N,N-trimethylated chitosan. Biomaterials 2008;29(27):3642-9.

[22] Thanou MM, Kotze AF, Scharringhausen T, Luessen HL, de Boer AG, Verhoef JC, et al. Effect of degree of quaternization of N-trimethyl chitosan chloride for enhanced transport of hydrophilic compounds across intestinal caco-2 cell monolayers. J Control Release 2000;64(1-3):15-25.

[23] Thanou MM, Verhoef JC, Romeijn SG, Nagelkerke JF, Merkus FW, Junginger HE. Effects of N-trimethyl chitosan chloride, a novel absorption enhancer, on caco-2 intestinal epithelia and the ciliary beat frequency of chicken embryo trachea. Int J Pharm 1999;185(1):73-82.

[24] Verheul RJ, Amidi M, van Steenbergen MJ, van Riet E, Jiskoot W, Hennink WE. Influence of the degree of acetylation on the enzymatic degradation and in vitro biological properties of trimethylated chitosans. Biomaterials 2009;30(18):3129-35.

[25] Hagenaars N, Mastrobattista E, Glansbeek H, Heldens J, van den Bosch H, Schijns V, et al. Head-to-head comparison of four nonadjuvanted inactivated cell culture-derived influenza vaccines: Effect of composition, spatial organization and immunization route on the immunogenicity in a murine challenge model. Vaccine 2008.

[26] Garmise RJ, Staats HF, Hickey AJ. Novel dry powder preparations of whole inactivated influenza virus for nasal vaccination. AAPS PharmSciTech 2007;8(4):E81.

[27] Ito T. Interspecies transmission and receptor recognition of influenza A viruses. Microbiol Immunol 2000;44(6):423-30.

[28] Sanders MT, Deliyannis G, Pearse MJ, McNamara MK, Brown LE. Single dose intranasal immunization with ISCOMATRIX vaccines to elicit antibody-mediated clearance of influenza virus requires delivery to the lower respiratory tract. Vaccine 2009;27(18):2475-82.

[29] D'Amico F, Skarmoutsou E, Stivala F. State of the art in antigen retrieval for immunohistochemistry. J Immunol Methods 2009;341(1-2):1-18.

[30] Yamashita S. Heat-induced antigen retrieval: mechanisms and application to histochemistry. Prog Histochem Cytochem 2007;41(3):141-200.

[31] Cesta MF. Normal structure, function, and histology of mucosa-associated lymphoid tissue. Toxicol Pathol 2006;34(5):599-608.

[32] Brooking J, Davis SS, Illum L. Transport of nanoparticles across the rat nasal mucosa J Drug Target 2001;9(4):267-79.

[33] Takata S, Ohtani O, Watanabe Y. Lectin binding patterns in rat nasal-associated lymphoid tissue (NALT) and the influence of various types of lectin on particle uptake in NALT. Arch Histol Cytol 2000;63(4):305-12.

[34] Densmore CL. Polyethyleneimine-based gene therapy by inhalation. Expert Opin Biol Ther 2003;3(7):1083-92.

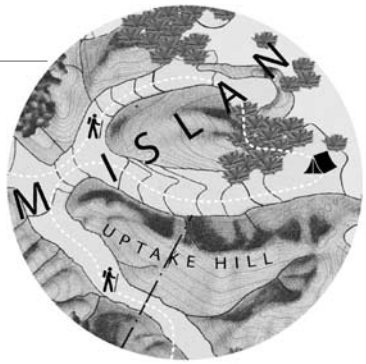

Appendix to Chapter 6

Increased dye fluorescence due to enzymatic degradation of IRDye800CW®-labeled WIV

Introduction

In the *in vivo* optical imaging experiments described in Chapter 6, a fluorescence signal was observed in the nasal cavity, that initially increased and then disappeared to show up in the stomach, 1 h after i.n. administration of the WIV formulations. This was observed for both WIV and TMC43-WIV formulations in a similar fashion, indicating that these formulations were cleared from the nasal cavity through the nasopharyngeal duct via the esophagus towards the gastrointestinal tract. Interestingly, the fluorescence signal in the stomach was even stronger than the signal that was observed in the nasal cavity, both for the TMC-WIV formulation (about 7-fold higher) and the plain WIV formulation (about 13-fold higher).

One explanation for the increase in fluorescence, first observed in the nasal cavity and later in the stomach, is that the fluorescent probe is quenched to a certain extent when labeled to WIV and dequenched in the nose and especially in the GI tract, resulting in a stronger fluorescence signal. Additional experiments were performed to investigate if dequenching can play a role in the observed increase in fluorescence.

Methods and Materials

To study the effect of viral disruption on the fluorescence signal of the label, 5 µl of a 1.25 µg IRDye800CW®-labeled WIV was diluted to a final volume of 800 µl in phosphate buffered saline (10 mM phosphate buffer, pH 7.4 150 mM NaCl) (PBS) with or without 30 mM octyl glucoside (OG) and measured at room temperature.
The effect of enzymatic degradation of WIV on the fluorescence was studied by adding 50 µl 2mg/ml trypsin from bovine pancreas to 6.25 µg of IRDye800CW®-labeled WIV and TMC43-WIV formulations in 750 µl 5 mM HEPES, pH 7.4. Subsequently, the samples were measured every 3 minutes for 90 min at 37°. Experiments were performed in triplicate.
Fluorescence intensity measurements were performed on a Fluorolog fluorometer (Horiba, Kyoto, Japan) at an angle of 90°, using Plastibrand® disposable cuvettes, an excitation wavelength of 764 nm, an emission wavelength of 800 nm, and 5-nm slit widths.

Results and discussion

First, we studied whether dilution of the vaccine formulation, which occurs after administration, induces dequenching. Figure 1 shows a linear correlation between concentration of the

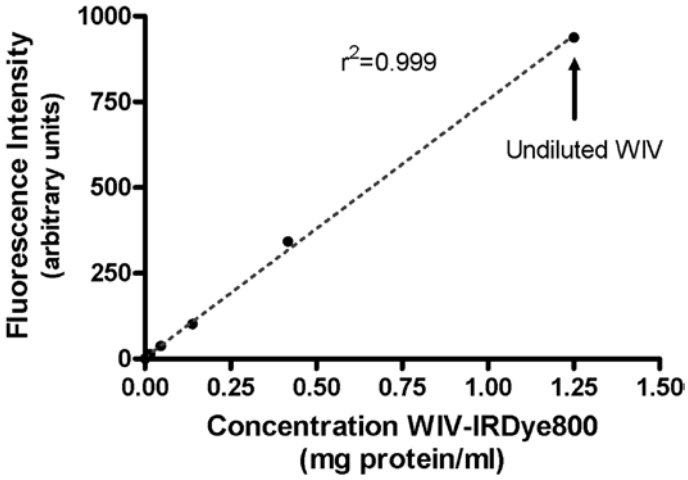

Figure 1: Fluorescence of a serially 3-fold diluted IRDye800CW®-labeled WIV formulation in PBS.

IRDye800CW®-labeled WIV and fluorescence, indicating that the dequenching effect cannot be explained by dilution of intact virus particles.

To find out if the fluorescence is quenched within the virus particles, the mild detergent OG was added to disrupt the viral envelope, but leaving the individual proteins intact (unpublished results). As shown in figure 2, viral detergent disruption induced a 3-fold increase in fluorescence. As a control, the same amount of detergent did not induce an increase in fluorescence of IRDye800CW®-labeled epidermal growth factor (EGF), a soluble protein (data not shown), indicating that disruption of the viral ultrastructure caused the increase in fluorescence rather than an interaction of the detergent with the fluorescent probe.

These results indicate that the fluorophores are quenched within the viral particles. Since these detergent concentrations are not found in the stomach and the maximal threefold increase in fluorescence by viral disruption is lower than that observed *in vivo*, other processes may contribute to the dequenching effect.

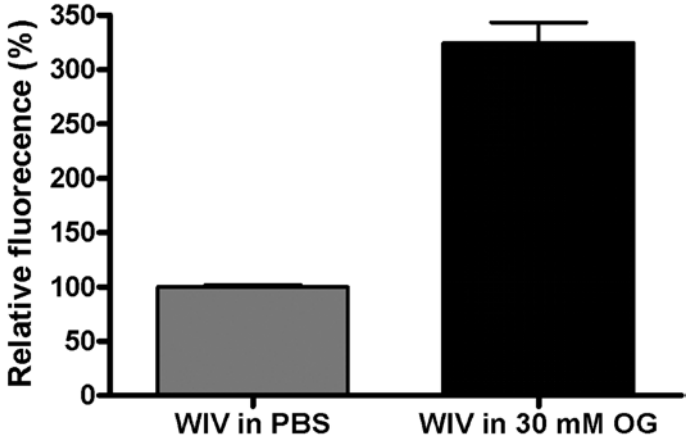

Figure 2: Dequenching of fluorescence of IRDye800CW®-labeled WIV by detergent disruption of the viral particles. (A) Fluorescence of WIV-IRDye800 formulation in PBS and in 30 mM OG in PBS.

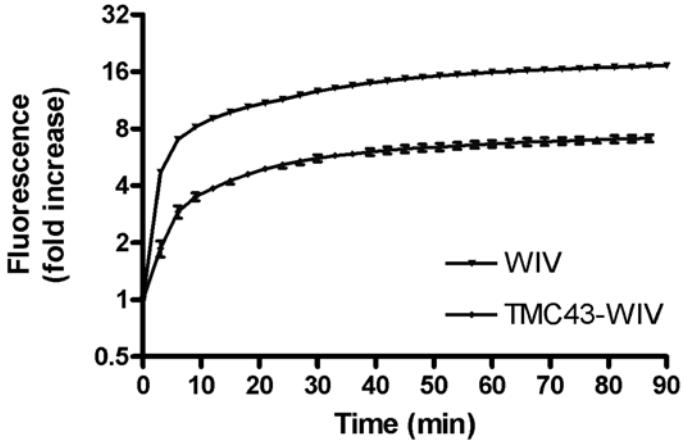

Figure 3: Fluorescence of IRDye800CW®-labeled WIV formulated with or without TMC when incubated with trypsin (PBS, 37°C).

Proteolytic enzymes, which are abundantly present in the stomach to digest food, can degrade proteins into amino acids and/or oligopeptides. Proteases can cleave peptide bonds of the protein backbone but not the stable amide bond between the fluorescent probe and the protein. Potentially, this may lead to dequenching of fluorophores that are present on the same protein. Therefore, we investigated whether incubation of IRDye800CW®-labeled WIV with proteolytic enzymes results in dequenching.
To study this, the IRDye800CW®-labeled WIV formulated with and without TMC were incubated with trypsin as a model protease.

Figure 3 shows that trypsin treatment induced a much larger increase in fluorescence than observed after viral disruption by a detergent (about 17-fold for WIV and about 7-fold increase for TMC-WIV), indicating that enzymatic degradation of the virus particles can explain the dequenching effect that was initially observed in the nose and later in the stomach. Furthermore, it appears that coating of WIV with TMC partially inhibited the dequenching by trypsin, as shown in Figure 3, as if TMC-coating protects the WIV for degradation. This difference in dequenching nicely correlates with the dequenching observed *in vivo*. It is not clear whether this mild protective effect of TMCs plays a role in the adjuvant effect of TMC.

Conclusion

Taken altogether, it is likely that i.n. administered IRDye800CW®-labeled WIV is enzymatically degraded, first to some extent in the nose and later, more rigorously, in the stomach. This would explain the enhanced fluorescence observed in the nose and later in the stomach after i.n. administration of IRDye800CW®-labeled WIV vaccines.

Chapter 7

A step-by-step approach to study the influence of *N*-acetylation on the adjuvanticity of TMC

Niels Hagenaars*, Rolf Verheul*, Thomas van Es, Ethlinn van Gaal, Sven Bruijns, Pascal de Jong, Enrico Mastrobattista, Ivo Que, Jacco Heldens, Han van den Bosch, Harrie Glansbeek, Yvette van Kooyk, Wim Hennink, Wim Jiskoot

*authors contributed equally

Manuscript in preparation

Abstract

In a previous study we observed that reacetylation of TMC abolishes its effect as an intranasal (i.n.) vaccine adjuvant in mice (chapter 5) The aim of the present study was to elucidate the reason for the lack of adjuvanticity of reacetylated TMC (TMC-RA) in a step-by-step approach by comparing TMC-RA with non-reacetylated TMC (TMC) at potentially critical steps in the induction of an immune response after i.n. administration. The biodegradation of the TMCs in nasal washes were determined and the clearance and local distribution of the TMC-WIV formulations were compared. Next, to study the uptake, fluorescently labeled beads and WIV, formulated with the TMCs were incubated with HeLa cells and 16-HBE14o, respectively. Finally, the effect of TMC and TMC-RA on murine and human dendritic cells was assessed.

TMC-RA was degraded slightly faster in a nasal wash than TMC. Fluorescently labeled beads and WIV were taken up less efficiently by HeLa cells and human bronchial epithelial cells (16-HBE14o), respectively, when formulated with TMC-RA compared to TMC. The local i.n. distribution and nasal clearance were similar for both TMC types. Preliminary studies in murine, bone marrow derived dendritic cells (DCs) suggest that DC activation and cytokine production is similar for plain WIV, and WIV formulated with TMC-RA or TMC. In contrast, studies on monocyte derived human DCs indicate that TMC-RA, as a solution or when formulated with WIV, induces a much stronger DC maturation and cytokine production than any of the other formulations. In conclusion, TMC-RA and TMC are functionally different in various aspects that are potentially critical for their adjuvant effect. Further studies should be done to further clarify these preliminary results.

Introduction

It was shown that the efficacy of intranasal vaccination against influenza with a whole inactivated influenza virus vaccine (WIV) can be greatly enhanced by formulation with *N,N,N*-trimethylchitosan (TMC) [1]. Cationic nanoparticles were formed with TMC being partially present as a coating on WIV and partially free in solution. The structural properties of TMC like the degree of quaternization (DQ), the degree of *O*-methylation, and the degree of N-acetylation (DAc) can be elegantly varied during synthesis [2, 3]. The influence of these structural properties on the adjuvant effect of TMC in i.n. WIV vaccines were recently investigated in mice [4], showing that the DQ and the DOM of TMC have no significant effect on the immunogenicity of the i.n. WIV vaccines, but a striking loss in adjuvanticity of TMC was observed when WIV was formulated with reacetylated TMC (TMC-RA) with a DAc of 54%, compared to a DAc of 17% for all other tested TMCs, like TMC43 (TMC). TMC-RA can be enzymatically degraded by lysozyme, has a low toxicity profile *in vitro* and has no effect on the transepithelial electrical resistance of Caco-2 cells, in contrast to TMC [3]. Logically, these differences must be a consequence of the higher DAc of the TMC-RA, since this is the only structural difference with TMC.
In an attempt to elucidate why TMC-RA does not work as an adjuvant for an i.n. WIV vaccine in mice, TMC-WIV and TMC-RA-WIV and WIV were compared at potentially critical steps in the induction of an immune response after i.n. administration. The consecutive steps that have to be taken to successfully induce an immune response are schematically presented in Figure 1 in **Chapter 2**.

First, a vaccine formulation has to adhere to the mucosal surfaces of the nasal cavity before it is cleared from the nasal cavity. The decreased adjuvant effect of TMC-RA might be due to its faster degradation in the nasal cavity, compared to TMCs with a lower DAc, because TMC-RA is more sensitive to enzymatic degradation by lysozyme (Chapter 6). In addition, local distribution and the clearance rate might be different for TMC-RA when compared to the other TMCs. A following step that could play a role in the decreased adjuvant effect of TMC-RA is the uptake of antigen through the epithelial barrier before it is degraded in the nasal cavity. After uptake through the epithelium, the antigen has to be taken up by dendritic cells (DCs), which subsequently should mature. The effect on DC maturation may be different for the TMCs. Moreover, the DAc of TMC may affect the cytokine profile that is produced by DCs, potentially leading to different B- and T-cell responses.
The preliminary results of a step-by-step approach to elucidate the mechanism by which the DAc affects the adjuvantivity of TMC are presented in this chapter.

Materials and methods

Materials

Chitosan with a DAc of 17% (determined with ^{1}H-NMR as described in [3] and a number average molecular weight (M_n) and weight average molecular weight (M_w) of 28 and 43 kDa, respectively, as determined by gel permeation chromatography (GPC) as described in [2], was purchased from

Primex (Siglufjordur, Iceland). Acetic anhydride, sodium borohydrate, formic acid, formaldehyde 37% (stabilized with methanol), deuterium oxide, sodium acetate, acetic acid (anhydrous), sodium hydroxide and hydrochloric acid were obtained from Sigma-Aldrich Chemical Co. Iodomethane 99% stabilized with copper was obtained from Acros Organics (Geel, Belgium). Live, egg-grown, mouse adapted influenza A/Puerto Rico/8/34 virus (A/PR/8/34) and purified, cell culture-grown (Madin-Darby Canine Kidney (MDCK) cells), β-propiolacton (BPL)-inactivated A/PR/8/34, as well as polyclonal rabbit anti-A/PR/8/34 serum were from Nobilon International BV (Boxmeer, The Netherlands). Yellow-green fluorescent FluoSpheres Size Kit #2, carboxylate-modified microspheres of 200 nm in diameter was purchased from Molecular Probes, Invitrogen Breda, The Netherlands.

Hela cells were a generous gift from Rob Roovers (Department of Cellular Architecture and Dynamics, Institute of Biomembranes, Utrecht University, Utrecht, The Netherlands).PO-labeled goat anti mouse -IgG (H+L), -IgG1, -IgG2a/c and -IgA(Fc) were purchased from Nordic Immunological Laboratories (Tilburg, The Netherlands). Virally transformed human bronchial epithelial cell line 16HBE14o- was a kind gift from Dr. D. Gruenert (University of California at San Francisco)., Trypsin/EDTA 10x, Plain DMEM (Dulbecco's modification of Eagle's medium, with 3.7 g/l sodium bicarbonate, 1 g/l L-glucose, L-Glutamine) and antibiotics/antimycotics (penicillin, streptomycin sulphate, amphotericin B) were from PAA Laboratories GmbH (Pasching, Austria) and propidium iodide (PI) and MEM with 0.292g/L L Glutamine, 1g /L Glucose, 2.2g/L NaHCO3 was from (Invitrogen, Breda, The Netherlands). All other chemicals used were of analytical grade.

Synthesis and characterization of methylated chitosans

O-methyl free *N,N,N*-trimethylated chitosans (TMCs) with a DQ of around 45% and varying DAc were synthesized from chitosan as described previously [3]. The DQ and DAc of the TMCs were determined with H-NMR on a Varian INOVA 500 MHz NMR spectrometer (Varian Inc., Palo Alto, Ca, USA) at 80 °C in D2O [3]. Furthermore, M_n and M_w of the TMCs were determined, as described previously [3, 5], by GPC on a Viscotek system detecting refractive index, viscosity and light scattering. A Shodex OHPak SB-806 column (30 cm) was used with 0.3 M sodium acetate pH 4.4 (adjusted with acetic acid) as running buffer. The structural characteristics of the synthesized TMCs are summarized in Table 1.

Degradation of TMCs in nasal wash

Six female 6-8 weeks old Balb/c nu/nu mice were sacrificed by a lethal intraperitoneal injection of 100 µl sodium pentobarbital (200 mg/ml). The trachea of each mouse was then cannulated towards the nasopharyngeal duct with a PVC tube (inner/outer diameter 0.5/1.0 mm). PBS (600 µl) was flushed

Table 1: polymer characteristics of used TMC and TMC-RA derivates.

Abbreviation	Mn (kDa)	Mw (kDa)	DQ (%)	DA (%)
TMC	36	75	43	17
TMC-RA	43	83	44	54

through the nasal cavity and collected from the nostrils 3 times; the collected samples were pooled. TMC and TMC-RA were dissolved in 5 mM HEPES at 2.5 mg/ml, mixed 1:1 (v/v) with nasal wash and the mixtures were incubated at 37 °C. Samples were taken after 4 and 24 hours and 5 and 9 days. Changes in M_n and M_w were determined by GPC on a Viscotek system detecting refractive index, viscosity and light scattering. A Shodex OHPak SB806 column (15cm) was used with 0.3 M sodium acetate, pH 4.4 (adjusted with acetic acid), as running buffer. Pullulan (M_n 102 kDa, M_n 106 kDa) obtained from Viscotek Benelux (Oss, The Netherlands) was used for calibration and polymer solutions mixed with PBS 1:1 (v/v) were used as controls. Prior to injection, 30 µl GPC running buffer was added to 120 µl sample to adjust the pH of the sample to pH 4.4.

In vivo imaging of nasal residence time of TMC-WIV formulations

Female nude (Balb/c nu/nu) mice were obtained from Charles River (L'Arbresle, France) and housed in ventilated cages in groups of 3-6 mice. Chlorophyl-free food and water were provided ad libitum. The animals received plain IRDye800CW®-labeled WIV (n=9) or formulated with TMC (n=9) or TMC-RA (n=3) or without TMC under light anesthesia with isoflurane inhalation. Next, mice were scanned with an IVIS Spectrum imaging system from Caliper Life Sciences (Hopkinton, MA, USA). Scans were performed regularly over a time period of at least 2 h. In between scans, mice were put back in their cages to recover from anesthesia. Scanned images were analyzed using Living Image 3.1 software from Caliper Life Sciences (Hopkinton, MA, USA). The threshold was set using the background scan made from each mouse before administration of the IRDye800CW®-labeled formulations. The excitation wavelength was set at 710 nm and emitted light was measured at 760; 780; 800; 820 and 840 nm. Spectral unmixing was performed to decompose the emitted light into auto fluorescence and label-specific fluorescence. The obtained fluorescence represents the quantity of the fluorophore at each pixel. Regions of interest in the nasal cavity were detected and quantified over time. To compare the fluorescence in different mice and different groups, the absolute fluorescence was converted to relative fluorescence (% of the maximal fluorescence in the nasal cavity). The areas under the curve (AUC) of the relative fluorescence of individual mice were used to compare the fluorescence over time for the different groups.

Immunostaining of TMC-WIV formulations in nasal cross-sections

For immunostaining experiments 6-8 weeks old female C57-BL/6 mice from Charles River (L'Arbresle, France) were used. Mice were housed in groups of 5 mice and food and water were provided ad libitum. They were i.n. vaccinated with TMC-RA-WIV or TMC-WIV or WIV formulations. As negative controls, mice received PBS or solutions of TMCs and 4 mice were left untreated. At 20 minutes and 1 hour animals were sacrificed by cervical dislocation and the nasal cavity was isolated by removing the brains, lower jaw, skin and muscle tissue. The nasal cavities were then fixed in 10% formalin for 24 h. After fixation, nasal cavities were decalcified for 14 days in a solution of 10 % EDTA, pH 7.4, which was refreshed once between day 4 and 6. Next, nasal cavities were embedded in paraffin and 3.5 µm thick cross-sections were made at different depths of the nasal cavity using a Microm HM 355 S microtome from Thermo Fisher Scientific (Walldorf,

Germany). Cross-sections for immunohistochemistry were mounted on superfrost plus glass slides from Menzel-Gläser (Braunschweig, Germany). On each glass slide, 2 cross-sections were placed. Paraffin-embedded cross-sections were deparaffinized and hydrated by incubation with xylene followed by a series of graded alcohols and finally tap water. Next, the cross-sections were incubated with preheated 10 mM citrate buffer, pH 6.0, at 95°C for 30 minutes for heat-induced epitope retrieval (HIER) step to improve the recognition of the antigen by the primary antibody. Cross-sections were allowed to cool down to room temperature. Deparaffinized, HIER-treated cross-sections were washed 3 x 5 min with 0.2% Triton-X in PBS. Cross-sections were incubated first with normal goat serum for 15 minutes and then with a 1:500 dilution of polyclonal WIV-specific rabbit antiserum overnight at 4°C. As a negative control, one of the two paraffin sections was incubated with nonspecific rabbit serum as primary antibody. All sera and antibody solutions were centrifuged at 10,000 x g for 1 min at room temperature prior to application to remove any aggregates from the staining solution. After washing the slides 3x for 5 min with 0.2% Triton-X in PBS, a 1:200 dilution of Alexa Fluor® 488-labeled goat anti-rabbit IgG was applied. The samples were incubated for 45 minutes at room temperature. Next, the slides were washed 3x with PBS and stained with a 1:25000 dilution of DAPI for 6 min at room temperature and washed 3x with PBS again. Finally, the slides were mounted with Fluorosave™ from Calbiochem (San Diego, CA, USA). All slides were examined using a fluorescence microscope (Nikon Eclipse TE-2000 Nikon, Amstelveen, the Netherlands) equipped with a Digital Sight DS-2Mv camera. Slides were blindly scored for the presence, location, pattern and intensity of antigen staining and pictures were taken with fixed camera settings for a fair comparison.

Uptake by HeLa cells of fluorescently labeled beads formulated with TMC and TMC-RA

HeLa cells were grown in DMEM supplemented with antibiotics/antimycotics and 10% heat-inactivated fetal calf serum (FCS) (Integro, Zaandam, The Netherlands). Cells were maintained at 37°C in a 5% CO_2 humidified air atmosphere and split twice a week.

Forty thousand cells were seeded per well into 24-well tissue culture plates 24 hours prior to treatment, such that 60–70% confluency was reached on the day of treatment. Immediately prior to the incubation step the culture medium was refreshed with 500 µl plain DMEM. Fluorescently labeled, carboxylate-modified FluoSpheres® beads with a diameter of 200 nm were mixed with TMC or TMC-RA at a TMC:bead (w/w) ratio of 0.6:1 and 1:1 in PBS. Cells were incubated with 100 µl plain beads or with TMC(-RA)-bead formulations at various concentrations (1.14×10^8; 2.28×10^7; 4.56×10^6 beads/well, corresponding with approximately 2840; 569 and 114 beads/cell) for 4 hours at 37°C. After incubation, cells were washed 1 x with fresh medium and medium was replaced with fresh DMEM supplemented with 10 % FCS and antibiotics. After another 1 h incubation in the absence of particles, cells were washed 2x with 200 µl PBS, trypsinized with 100 µl trypsin/EDTA and resuspended in 100 µl DMEM supplemented with 10% FCS to inactivate the trypsin. Cells were transferred into a U-shaped 96-well plate and centrifuged for 5 minutes at 250 g at 4°C. Medium was removed and cells were washed 2x with 200 µl phosphate-buffered albumin (PBA; 1% w/v albumin in PBS) and finally resuspended in 200 µl 0.4% trypan blue in PBA to quench the

extracellular fluorescence [6]. Immediately prior to measurement, 20 µl propidium iodide solution (PI; 1 µg/ml in water) was added for live/dead cell discrimination. Flow cytometric analysis was performed on a FACS Canto (Becton and Dickinson, Mountain View, CA, USA) using a 15 mW 488 nm, air-cooled argon-ion laser and data were analyzed using FACS Diva software (Becton and Dickinson, Mountain View, CA, USA). 10,000 cells were recorded per sample to determine bead-uptake (FL1-channel) and PI-staining (FL3-channel).

Uptake by human bronchial epithelial cells of fluorescently labeled TMC-WIV and TMC-RA-WIV

16HBE14o-cells were grown in (FBS; Integro, Zaandam, The Netherlands) MEM with 0.292 g/l L Glutamine, 1g/l Glucose, 2.2g/L NaHCO3 (Invitrogen, Breda, The Netherlands) supplemented with antibiotics/antimycotics and 10% heat-inactivated FCS. Cells were cultured in fibronectin-coated flasks and maintained at 37°C in a 5% CO2 humidified air atmosphere and split twice a week.

Flasks were coated by thoroughly rinsing the surface of the flask with fibronectin solution (1mg/ml; BD Laboratories 40008) and subsequent incubation for a minimum of 2-3 hours at 37 °C. For the uptake experiments, cells were resuspended in MEM supplemented with 10% FCS, counted and diluted to $1x10^6$ cells/ml. Subsequently, cells were transferred into a U-shaped 96-well plate (100,000 cells/well) and incubated with 100 µl of plain AlexaFluor-488®-labeled WIV or formulated with TMC or TMC-RA at a TMC:WIV (w/w) ratio of 5:1 and diluted as indicated (50µg WIV/ml diluted 10-160x) for 1h at 37°C. After incubation, cells were centrifuged (250 x g for 5 minutes at 4°C) and washed three times with 200 µl PBA and finally resuspended in 100 µl 0.4% trypan blue in PBA to quench the extracellular fluorescence. Immediately prior to measurement, 20 µl propidium iodide solution (PI; 1 µg/ml in water) was added for live/dead cell discrimination. Flow cytometric analysis was performed as described for HeLa cells.

Maturation of and cytokine production by murine bone marrow derived dendritic cells

The femur and tibia of C57-BL/6 mice were removed, both ends were cut and bone marrow was flushed with Iscove's Modified Dulbecco's Medium (IMDM; Gibco, CA, USA) using a syringe with 0.45 mm diameter needle. The bone marrow suspension was vigorously resuspended and passed over a 100 µm gauge to obtain a single cell suspension. After washing, cells were seeded $2x10^6$ cells per 100 mm petridish (Greiner Bio-One, Alphen aan den Rijn, The Netherlands) in 10 ml IMDM, supplemented with 2 mM L-glutamine, 50 U/ml penicillin, 50 ug/ml streptomycin and 50 µM β-mercaptoethanol (Merck, Darmstadt, Germany) and 30 ng/ml recombinant murine GM-CSF (rmGM-CSF). At day 2, 10 ml medium containing 30 ng/ml rmGM-CSF was added. At day 5 another 30 ng/ml rmGM-CSF was added to each plate. From day 6 onwards, the non-adherent DCs were harvested and used for subsequent experiments.

These immature DCs were seeded (50,000 cells/well) in a 96-well plate in a total volume of 100 µl RPMI 10% FCS in the presence of TMC (0.001-30 µg/ml), TMC-WIV formulations at a 1:1 or 5:1 (w/w) ratios or lipopolysaccharide (LPS) (0.01-1000 ng/ml) as a positive control. DCs were incubated for 16 h at 37 °C. DC maturation was determined by analyzing cell-surface expression

of co-stimulatory molecules (CD40) on FACS. After 16 h culture supernatants were harvested and frozen at −80 °C until analysis for the detection of cytokines. The supernatants were analyzed for the presence of the cytokines IL-10 and IL-12p40, IL12p70 and TNFα by ELISA (Biosource International, CA).

Maturation of and cytokine production by human monocyte derived dendritic cells

Immature DCs were cultured as described before [7]. In short, human blood monocytes were isolated from buffy coats by use of a Ficoll gradient and subsequently a Percoll gradient. Purified monocytes were differentiated into immature DCs in the presence of interleukin-4 (IL-4, 500 U/ml) and granulocyte-macrophage colony-stimulating factor (GM-CSF, 800 U/ml).

Immature DCs (day 6) were seeded (50,000 cells/well) in a 96-well plate in a total volume of 100 µl RPMI 10% FCS in the presence of TMC (30-0.001 µg/ml), TMC-WIV formulations at 1:1 and 5:1 (w/w) ratios or lipopolysaccharide (LPS) (0.01-1000 ng/ml) as a positive control. DCs were incubated for 16 h at 37 °C. DC maturation was determined by analyzing cell-surface expression of co-stimulatory molecules (CD86) on FACS. After 16 h culture supernatants were harvested and frozen at −80 °C until analysis for the detection of cytokines. The supernatants were analyzed for the presence of the cytokines IL-10 and IL-12p40, IL12p70 and TNFα by ELISA (Biosource International, CA). For the DC maturation studies, 4 donors were used. For the cytokine experiments, 2 donors were used.

Results and discussion

To elucidate why the reacetylated TMC is inferior as an adjuvant for an i.n. influenza vaccine in mice compared to the TMCs with a lower DAc, several experiments were performed. The effect of TMC and TMC-RA on various, potentially critical steps in successful i.n. vaccination were investigated.

Biodegradation

An important difference between TMC and TMC-RA that was observed *in vitro* is their enzymatic biodegradability by lysozyme [3], an enzyme which is present in the nasal cavity [8]. Potentially, TMC-RA-WIV could have a different fate because of a more rapid degradation in the nasal cavity. To study if TMC and TMC-RA are degraded at different rates in a nasal wash, solutions of these TMCs were incubated with murine nasal washes at 37°C. At different time points, the solutions were analyzed by GPC to determine the Mn/Mw of the TMCs. TMCs in PBS that were taken as controls, did not decrease in Mn/Mw. As shown in Figure 1, TMC-RA degraded faster than TMC in a nasal wash. However, the degradation of both TMC-RA and TMC was relatively slow in the nasal wash and up to 24 h of incubation, no significant differences were observed between the two TMCs. On the other hand, it is not clear whether the biodegradability of TMC in nasal wash accurately reflects the degradation in the nasal cavity after administration. It is likely that the concentration of lysozyme and other proteases in a nasal wash is much lower than the concentration in the nasal cavity because of a strong dilution effect in the wash and because lysozyme is mostly stored and excreted from submucosal glands and may not be efficiently extracted by a nasal wash. Therefore,

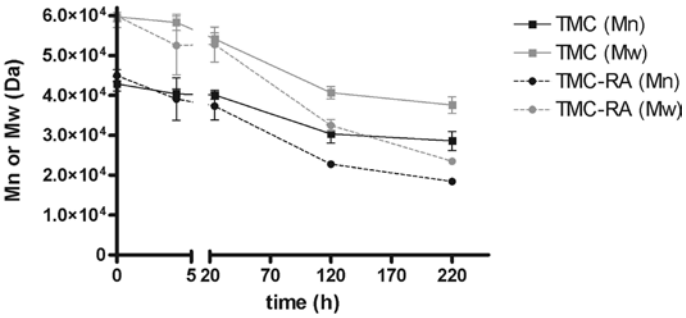

Figure 1: Biodegradation of TMC (squares) and TMC-RA (dots) in pooled nasal wash of mice. The Mw is presented in grey and the Mn in black.

the degradation rates may be highly underestimated when they are determined using a nasal wash. These results at least suggest that enzymatic degradation by substances in the nasal cavity is faster for TMC-RA, which might compromise the adjuvant activity of TMC-RA.

In vivo fluorescence imaging

In vivo fluorescence imaging was used to compare the nasal clearance of the TMC-WIV and TMC-RA-WIV formulations. Fluorescently labeled WIV was formulated with TMC and TMC-RA and the formulations were administered to mice. Imaging did not reveal a significant difference in fluorescence over time, as calculated from the AUC ($p>0.05$), as shown in figure 2. After an initial increase in fluorescence, likely due to fluorescence dequenching (see appendix to chapter 6), all formulations showed a comparable decrease in fluorescence over time. This suggests that the nasal clearance of TMC-WIV and TMC-RA-WIV is comparable. It is therefore unlikely that a difference in clearance is responsible for the decreased adjuvanticity of TMC-RA. Furthermore, if degradation of TMC-RA in the nose is faster than that of TMC, apparently it does not influence the nasal clearance of WIV.

Local distribution of vaccine formulations in the nasal cavity

The next factor studied was the local distribution of the antigen in the nasal cavity after i.n. administration. In chapter 4 it was shown that TMC-WIV formulations exhibit a completely different distribution pattern as plain WIV. To find out if the distribution pattern is different for

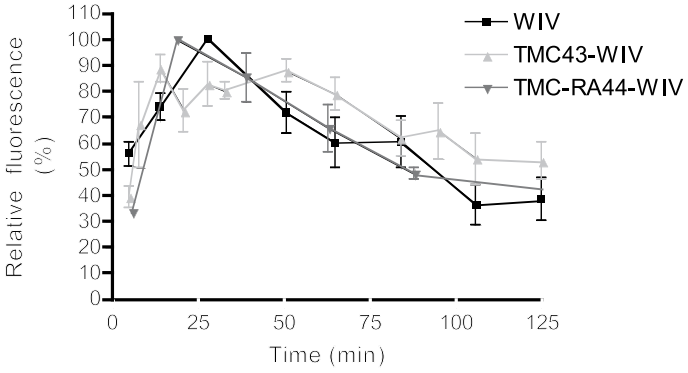

Figure 2: Average relative fluorescence in the nasal cavity over time. n=3 mice. Error bars indicate the standard deviation.

A

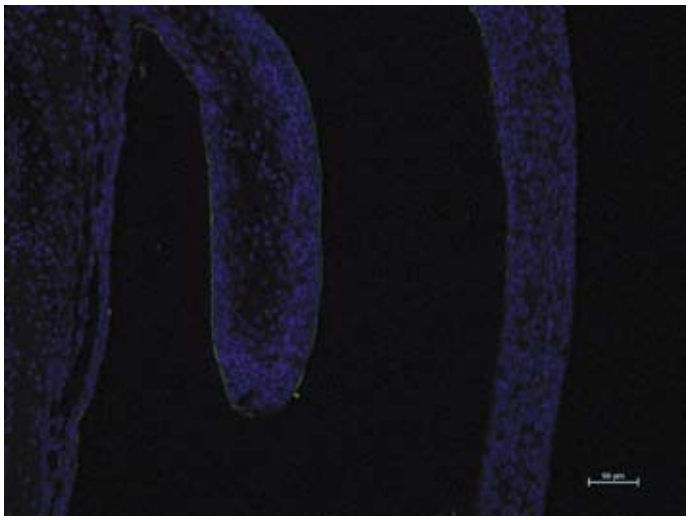

B

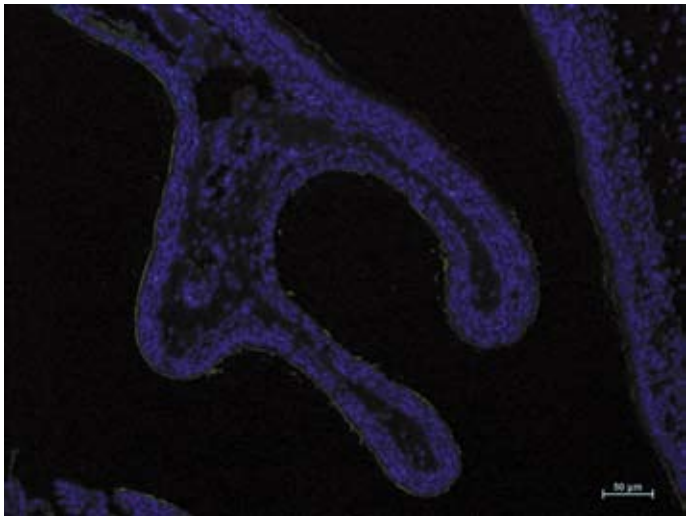

Figure 3. Representative picture of WIV-staining on the mucosal surfaces of the nasoturbinates when formulated with TMC-RA (A) and TMC (B) 20 minutes after administration (n=5 mice).

TMC-RA-WIV, mice were administered TMC-RA-WIV, TMC-WIV and nasal sections were stained to visualize the location of WIV. WIV-specific staining was found on the epithelial surfaces of the naso- and maxilloturbinates in all mice, for both TMC-WIV and TMC-RA-WIV (see Figure 3 for a representative example). This indicates that the degree of acetylation is unlikely to affect the contact between WIV with the mucosal surfaces. Furthermore, any difference between degradation of TMC-RA and TMC does not result in a different distribution of WIV in the nasal cavity.

Cell uptake studies

TMC and TMC-RA might differ in their influence on WIV uptake by nasal epithelial cells. As a surrogate test, the uptake by HeLa cells of fluorescent beads formulated with TMC solutions was

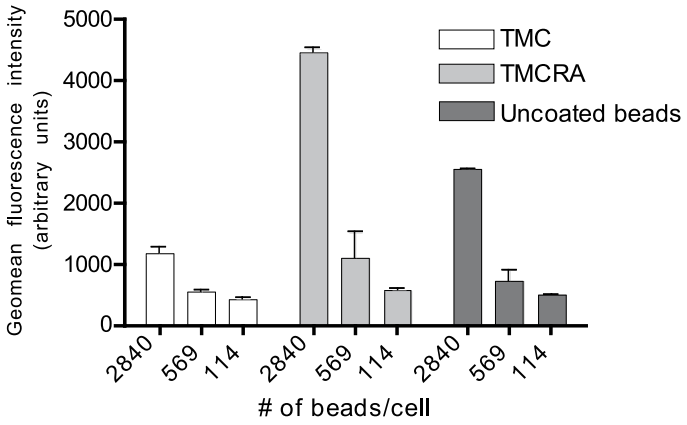

Figure 4: Uptake of fluorescently labeled beads, uncoated or coated with TMC or TMC-RA at a TMC/bead (w/w) ratio of 0.6:1, by HeLa cells when incubated in different concentrations. Error bars indicate standard deviations of three independent samples.

studied. Mixing the negatively charged fluorescent beads with TMC or TMC-RA yielded stable, positively charged nanoparticles with similar size and charge as the TMC-WIV formulations (data not shown). As shown in Figure 4, the uptake of beads by HeLa cells was strongly enhanced by formulation with any of the TMCs at a TMC/bead (w/w) ratio of 0.6:1. However, the uptake of TMC-RA-coated beads was significantly less than the uptake of the beads coated with TMC. Comparable results were obtained when HeLa cells were incubated with TMC-coated beads at a TMC:WIV (w/w) ratio of 1:1.

Initial studies with fluorescently labeled WIV and TMC-WIV formulations on 16-HBE14o cells, a human bronchial epithelial cell line of the upper respiratory tract, confirmed these data. TMC strongly enhanced the uptake of WIV, whereas TMC-RA only slightly enhanced the uptake (Figure 5). This may play a role in the decreased adjuvanticity of reacetylated TMC (TMC-RA). Further experiments should confirm these preliminary findings and provide more insight in the role TMC on the antigen uptake by epithelial cells.

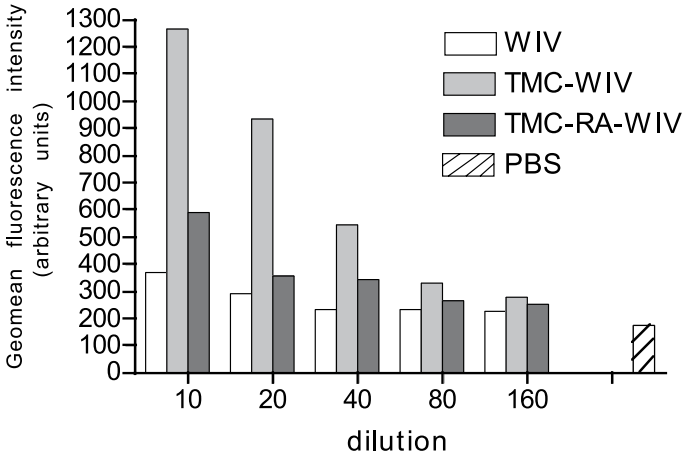

Figure 5: Uptake of fluorescently labeled WIV, uncoated or coated with TMC or TMC-RA, by 16-HBE14o human bronchial epithelial cells when incubated for 1 h in different dilutions

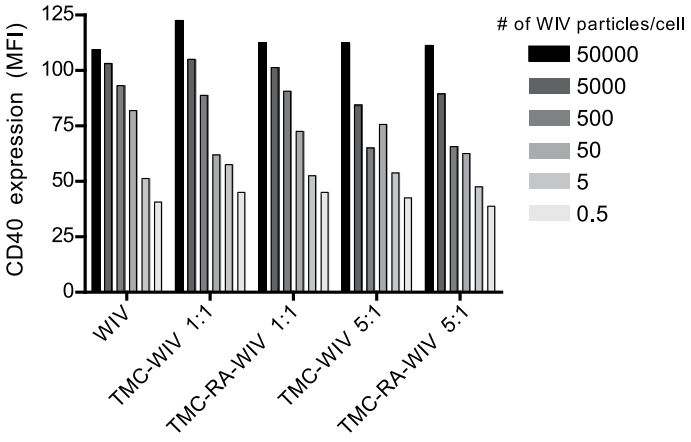

Figure 5: DC maturation by plain WIV, TMC-WIV and TMC-RA-WIV formulations at 1:1 and 5:1 TMC:WIV (w/w) ratios in different concentrations.

Maturation of and cytokine production by murine bone marrow derived dendritic cells

After the uptake through the epithelial cell layer, the antigens have to interact with DCs, thereby inducing maturation, antigen presentation and production of cytokines. To study the effect of the various TMCs on DCs, murine bone marrow-derived (BM)-DCs were incubated with various concentrations of plain WIV and WIV formulated with various TMCs. In an initial experiment, a clear concentration dependent CD40 expression, a marker for murine DC maturation, was found for all formulations, as shown in Figure 5, irrespective of the presence of TMC(-RA). This indicates that DC maturation was primarily induced by WIV and that the TMCs do not have a stimulating or inhibiting effect. Furthermore, none of the TMCs had a pronounced effect on the production of immunostimulatory cytokines like IL-10, IL-12, and TNFα, suggesting that the difference in adjuvant effect in mice is not due to a difference in BM-DC activation and maturation[1].

Maturation of and cytokine production by human monocyte derived dendritic cells

Additionally, the effect of TMC and TMC-RA on human monocyte derived DC maturation and cytokine production was studied. The only difference between TMC and TMC-RA is the DAc of 17% and 54%, respectively. The structure of the N-acetylated units within the polymers is called N-acetylglucosamine, or GlcNac. GlcNac has been described to bind several human C-type lectins, a family of lectins involved in the human innate immune response [9, 10]. This suggests that TMC-RA may have immunomodulatory effects on human DCs. In light of this hypothesis, we further explored the differences between the various TMCs in human monocyte derived (MD)-DCs. Incubation of human MD-DCs with TMC solutions and TMC-WIV formulations ((w/w) ratio 5:1) revealed a striking difference in CD86 expression, indicative of DC maturation, between TMC-RA and the other TMCs, as shown in Figure 6. TMC-RA induced a much higher CD86 expression than the other TMCs.

[1] Experiment should be repeated to draw final conclusions

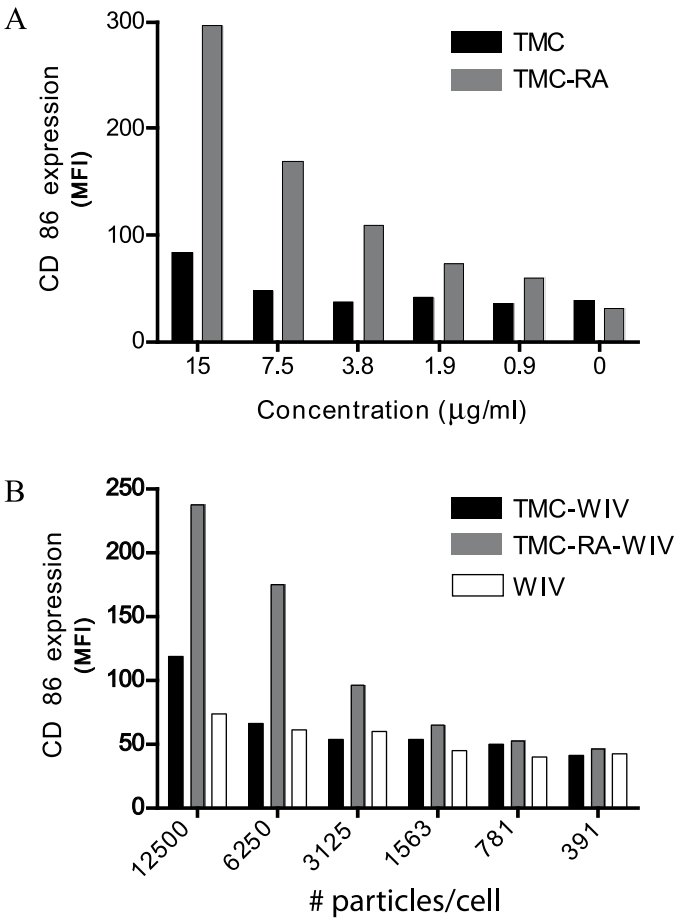

Figure 6: CD 86 expression by human MD-DCs after incubation with TMC and TMC-RA solutions (A) and by TMC-WIV and TMC-RA-WIV formulations (B). Results from one representative donor are shown. n=4.

Furthermore, TMC-RA-WIV also stimulated the secretion of proimflammatory cytokines IL-10; TNFα; IL12p40 and IL-12p70 more strongly than the other TMC-WIV formulations or WIV alone, as shown in Figure 7[2]. An endotoxin dose effect calibration on DCs verified that the observed effects on DCs cannot be attributed to the relatively low endotoxins levels in the TMCs (≤0.16 EU/µg TMC), as measured with a LAL test.

These results, combined with the results in mice, suggest that TMC-RA may activate human DCs by binding to a receptor that is not present on murine DCs. Further studies should be done to investigate this hypothesis in more detail.

[2] Experiments should be repeated with more DC donors to draw final conclusions.

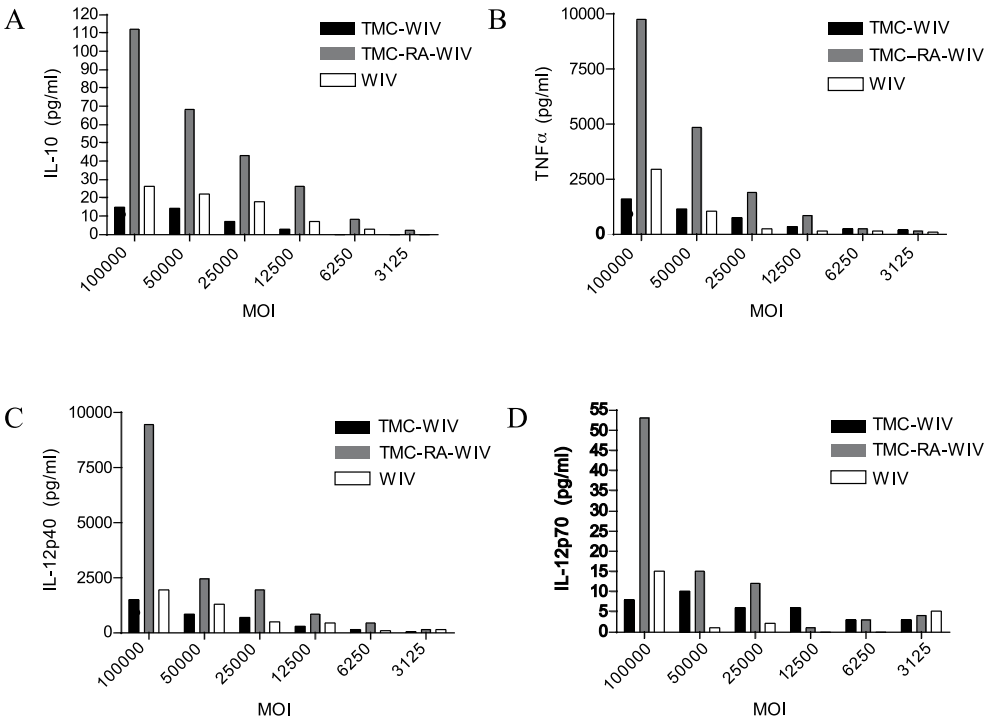

Figure 7: Expression of IL-10 (A); TNFα (B); IL-12p40 (C) and IL12p70 (D) by human MD-DCs after incubation with TMC-WIV formulations. The figure shows results from one representative donor. n=2.

Concluding remarks

In summary, we found that the degradation of TMC-RA in nasal washes was slightly faster than that of TMC. *In vivo* fluorescence imaging did not reveal a significant difference in nasal clearance of TMC-WIV and TMC-RA-WIV. Moreover, in nasal sections both TMC-WIV formulations were similarly distributed in the nasal cavity. The uptake of fluorescent beads in HeLa cells was less pronounced when coated with TMC-RA than with TMC (and TMC-OM). Similarly, TMC-RA could only slightly enhance the uptake of WIV in human bronchial epithelial cells whereas formulation with TMC strongly increased WIV uptake. Furthermore, preliminary experiments with murine BM-DCs suggested that WIV is the main inducer of DC maturation, measured as CD40 expression, and that TMC and TMC-RA do not have an additive effect on CD40 expression. In contrast, incubation on human MD-DCs revealed a strong effect of TMC-RA on DC maturation and cytokine production, when compared to the other TMCs and WIV.

In conclusion, these preliminary data suggest that the decreased adjuvant activity of TMC-RA for an i.n. vaccine in mice may be attributed to a faster degradation in the nasal cavity and a less efficient uptake by epithelial cells. Furthermore, we showed that the local distribution and the nasal clearance are not influenced by the DAc of TMC and thus cannot explain the decreased

adjuvanticity of TMC-RA when compared to TMC in mice. The preliminary studies in human and murine DCs suggest that TMC-RA has a different effect on human DCs than on murine DCs. TMC-RA induced enhanced DC activation and cytokine production with human MD-DCs compared to TMC. More studies should be done to further clarify the effect of TMCs and TMC-RA on human and murine DCs.
An i.m. vaccination study in mice with TMC-RA and TMC will reveal if the loss in adjuvant effect is specific for the i.n. route and M-cell uptake experiments should be done to reveal the role of M-cells in the adjuvant effect of TMCs.

Acknowledgements

The authors would like to thank Esmaeil Mortaz for providing us the 16-HBE14o cells for uptake studies.

References

[1] Hagenaars N, Mastrobattista E, Verheul RJ, Mooren I, Glansbeek HL, Heldens JG, et al. Physicochemical and Immunological Characterization of N,N,N-Trimethyl Chitosan-Coated Whole Inactivated Influenza Virus Vaccine for Intranasal Administration. Pharm Res 2009;26(6):1353-64.

[2] Verheul RJ, Amidi M, van der Wal S, van Riet E, Jiskoot W, Hennink WE. Synthesis, characterization and in vitro biological properties of O-methyl free N,N,N-trimethylated chitosan. Biomaterials 2008;29(27):3642-9.

[3] Verheul RJ, Amidi M, van Steenbergen MJ, van Riet E, Jiskoot W, Hennink WE. Influence of the degree of acetylation on the enzymatic degradation and in vitro biological properties of trimethylated chitosans. Biomaterials 2009;30(18):3129-35.

[4] Hagenaars N, Verheul RJ, Mooren I, de Jong PH, Mastrobattista E, Glansbeek HL, et al. Relationship between structure and adjuvanticity of N,N,N-trimethyl chitosan (TMC) structural variants in a nasal influenza vaccine. J Control Release 2009.

[5] Jiang X, van der Horst A, van Steenbergen MJ, Akeroyd N, van Nostrum CF, Schoenmakers PJ, et al. Molar-mass characterization of cationic polymers for gene delivery by aqueous size-exclusion chromatography. Pharm Res 2006;23(3):595-603.

[6] Bjerknes R, Bassoe CF. Phagocyte C3-mediated attachment and internalization: flow cytometric studies using a fluorescence quenching technique. Blut 1984;49(4):315-23.

[7] Sallusto F, Lanzavecchia A. Efficient presentation of soluble antigen by cultured human dendritic cells is maintained by granulocyte/macrophage colony-stimulating factor plus interleukin 4 and downregulated by tumor necrosis factor alpha. J Exp Med 1994;179(4):1109-18.

[8] Cole AM, Liao HI, Stuchlik O, Tilan J, Pohl J, Ganz T. Cationic polypeptides are required for antibacterial activity of human airway fluid. J Immunol 2002;169(12):6985-91.

[9] Zhang P, Snyder S, Feng P, Azadi P, Zhang S, Bulgheresi S, et al. Role of N-acetylglucosamine within core lipopolysaccharide of several species of gram-negative bacteria in targeting the DC-SIGN (CD209). J Immunol 2006;177(6):4002-11.

[10] Nadesalingam J, Dodds AW, Reid KB, Palaniyar N. Mannose-binding lectin recognizes peptidoglycan via the N-acetyl glucosamine moiety, and inhibits ligand-induced proinflammatory effect and promotes chemokine production by macrophages. J Immunol 2005;175(3):1785-94.

Chapter 8

Colloidal stability of *N,N,N*-trimethyl chitosan-whole inactivated influenza virus formulations

Niels Hagenaars, Pascal de Jong, Rolf Verheul, Enrico Mastrobattista, Wim Jiskoot

Manuscript in preparation

Abstract

Formulation of whole inactivated influenza virus (WIV) with N,N,N-trimethyl chitosan (TMC) as an adjuvant was previously shown to strongly enhance the immunogenicity and protective efficacy after intranasal (i.n.) vaccination in mice (chapter 4 and 5 of this thesis). The aim of the present study was to investigate the effect of TMC's structural properties, TMC:WIV ratio and salt concentration on the colloidal stability of liquid and freeze-dried TMC-WIV formulations. Using dynamic light scattering for particle size determination and zeta-potential measurements, the colloidal properties of these formulations were monitored over time at various TMC:WIV (w/w) ratios and salt concentrations. In 5 mM HEPES pH 7.4, all TMC-WIV formulations were stable for at least 2 weeks. Decreasing the TMC:WIV (w/w) ratio to 0.3:1 or lower resulted in an increase in particle size and polydispersity and a drop in zeta-potential, indicating aggregation of TMC-WIV. The higher the salt concentration, the less stable the TMC-WIV became. O-methylated TMC (TMC-OM) formed less stable formulations than TMC and partially reacetylated TMC (TMC-RA) was also less stable than TMC, but more stable than TMC-OM. At a higher TMC:WIV (w/w) ratio of 5:1, TMC-WIV samples were more stable. Freeze-drying of TMC-WIV formulations and subsequent rehydration with conservation of the particle size was feasible if 5 or 10% sucrose was used as a lyoprotectant. This feature may increase the shelf life of the vaccine.

Introduction

N,N,N- trimethylchitosan (TMC) has been tested as an adjuvant for several intranasal (i.n.) vaccines [1-3]. TMC is water soluble at neutral pH and relatively nontoxic *in vitro* and *in vivo* after i.n. administration. It can be characterized by several structural properties like the degree of quaternization (DQ); the degree of N-acetylation (DAc); and the degree of O-methylation (DOM). These properties had a profound effect on the i*n vitro* cytotoxicity of TMC and its ability to open tight junctions [4, 5]. It significantly enhanced the immunogenicity of whole inactivated influenza virus (WIV) after i.n. administration in mice [6]. In these studies, the colloidal TMC-WIV formulation was freshly prepared by simply mixing a solution of TMC with a WIV dispersion. The formulation was characterized as a dispersion of positively charged, nanoparticulate, TMC-coated WIV particles with TMC being partially bound and partially present in solution [6]. More recently, TMC-WIV formulations were prepared with TMCs with different structural properties to study their adjuvant effect in nasal vaccination [7] Vaccination studies in mice showed that TMC strongly enhances the immune responses against WIV, irrespective of the DQ and the DOM, but reacetylation of TMC almost completely abolishes TMC's adjuvant effect.

In addition to these *in vitro* and *in vivo* effects, the structural properties of TMC and the TMC:WIV (w/w) ratio may also influence the colloidal stability of these nanoparticulate vaccine formulations.

Colloidal instability can result in the formation of aggregates that could potentially lead to inactivation of the vaccine formulation, compromise its dosing accuracy or induce unwanted side effects. Although not much is known about the influence of aggregates on the immune response against i.n. WIV vaccines, there is evidence that aggregates can have an influence on the outcome of vaccination. Recently, an adverse effect called oculo-respiratory syndrome (ORS) was detected, in an i.m., inactivated split influenza vaccine from one manufacturer in Canada during the 2000-2001 flu season [8-10]. Upon further analysis of the product, large aggregates of up to 500 unsplit virions were found. A reduction in the amount of aggregates in the vaccine of 2001-2002 reduced the risks of ORS to comparable levels as the other vaccines on the market [11]. Mouse studies further suggested that the large aggregates induced a polarization of the immune response towards Th2, which is also associated with the clinical symptoms of ORS [12].

Influenza vaccine formulations are generally stored at 4°C as a liquid formulation and only need to be stable for 1 year, due to the annual change in influenza strain composition of the vaccine. A common approach for the stabilization of biologicals like therapeutic proteins and vaccines is drying the formulations into a powdered form using techniques like freeze drying and spray-freeze drying [13]. By using stabilizing sugars, the proteins can be protected against denaturation and/or aggregation and thereby the shelf life can be prolonged. Several dried influenza vaccine formulations have been described, including dried WIV formulations [14-16].

The aim of this study was to investigate the influence of the type of TMC, the TMC:WIV (w/w) ratio and the salt concentration the colloidal stability of TMC-WIV formulations. The possibility of freeze-drying the TMC-WIV formulations with preservation of their colloidal properties is also explored.

Materials and methods

Materials

Chitosan with a degree of acetylation of 17% (determined with 1H-NMR as described in [17] and a number average molecular weight (Mn) and weight average molecular weight (Mw) of 28 and 43 kDa, respectively, as determined by GPC as described in [4], was purchased from Primex (Siglufjordur, Iceland). Acetic acid (glacial 100%, anhydrous), acetic anhydride, ethanol, FluoroSafe™ (Calbiochem), formalin 37%, formic acid, glycin, sodium acetate, sodium borohydrate, and sodium chloride were purchased from Merck (Darmstadt, Germany). Bovine serum albumin (BSA), Cibacron brilliant red 3B-A, goat serum, rabbit serum, sucrose and Triton X-100 were obtained from Sigma-Aldrich (Steinheim, Germany). 10mM phosphate buffered saline (PBS) pH 7.4, was from Braun Melsungen (Melsungen, Germany) and xylene from J.T. Baker (Deventer, Netherlands). Citric acid was purchased from Fluka Biochemika (Darmstadt, Germany), HEPES and iodomethane from Acros Organics (Geel, Belgium). Purified, cell culture-grown, β-propiolacton-inactivated, influenza A/PR/8/34 virus (WIV) and rabbit anti-A/PR/8/34 serum were obtained from Nobilon International BV (Boxmeer, the Netherlands). Alexa488-labeled goat anti-rabbit IgG (H+L) and 4',6-diamidino-2-phenylindole dihydrochloride (DAPI) were purchased from Invitrogen (Breda, The Netherlands).

Synthesis and characterization of TMCs

Various TMC derivates were synthesized and characterized as described previously [4, 5]. The polymer characteristics are listed in table 1.

Preparation of vaccine formulations

WIV suspended in PBS (140 μg/ml) was concentrated by centrifugation at 22,000×g for 30 min at 4°C and resuspended in 5 mM HEPES (pH 7.4). The dispersion was subsequently dialyzed extensively against 5 mM HEPES using a Slide-A-Lyzer Dialysis Cassette (3,500 MWCO, Thermo scientific, Rockford, USA) and the concentration determined using the Dc Protein Assay from Bio-Rad (California, USA). BSA was used as a reference. The WIV dispersions were adjusted to 125 μg total protein/ml. The various TMC-WIV vaccines were prepared by simply adding a

Table 1: polymer characteristics of used TMC derivates.

Abbreviation	Mn (kDa)	Mw (kDa)	DQ (%)	DA (%)	DOM-6 (%)	DOM-3 (%)
TMC-OM45	32	49	45	11	25	16
TMC-OM86	29	44	86	9	76	72
TMC30	33	59	30	17	–	–
TMC43	36	75	43	17	–	–
TMC68	39	84	68	17	–	–
TMC-RA44	43	83	44	54	–	–

- = not applicable

volume of a TMC solution (in 5 mM HEPES buffer, pH 7.4) to an equal volume of WIV dispersion (in 5 mM HEPES, pH 7.4) using a Gilson pipette while gently mixing for 5 s. In the studies where the (w/w) ratio of TMC:WIV was varied (from 0.1:1 to 5:1), different TMC concentrations were added to the WIV dispersion while keeping the added volume the same. For the experiments with varying salt concentrations (0; 25; 50; 100 and 150 mM NaCl in 5mM HEPES buffer, pH 7.4), the salt concentration of the TMC solutions and the WIV dispersions (at (w/w) ratios of 1:1 and 5:1) were adjusted prior to the mixing of TMC and WIV.

Dynamic light scattering measurements

Particle size was determined by dynamic light scattering (DLS) measurements using a Malvern CGS-3 multi-angle goniometer (Malvern Instruments, Malvern, UK), consisting of a HeNe laser source (λ = 632.8 nm, 22 mW output power), temperature controller (Julabo Waterbath) and a digital correlator ALV-5000/EPP at a 90° angle. The provided ALV-60X0 Software V.3.X was used to analyze the autocorrelation functions, using the viscosity and refractive index of that specific sample (e.g. 5mM HEPES pH 7.4 (viscosity 0.89 cP, refractive index 1.333), 5% sucrose (viscosity 1.126 cP, refractive index 1.3403) or 10% sucrose (viscosity 1.287 cP, refractive index 1.3478). The runtime of each measurement was 40 seconds at a temperature of 25°C. DLS results are given as a z-average particle size diameter and a polydispersity index (PDI) from three independent measurements. The PDI can range from 0 (indicating monodisperse particles) to 1 (a completely heterodisperse system). All samples were prepared in triplicate at a final WIV concentration of 62.5 µg/ml.

Zeta-potential measurements

Immediately after the DLS measurements, the zeta-potential of salt-free samples were measured using a ZetaSizer Nano Z (Malvern Instruments, Malvern, United Kingdom), combined with the Dispersion Technology V.4.20 software. Each measurement is an average of 3 runs of 5 minutes. All measurements were conducted at 25 ^{0}C.

Sample storage

Samples that were freshly prepared were measured within 5 minutes after preparation. In between measurements, samples were initially stored on ice and after the 2 h time point, samples were stored in the refrigerator at 4°C.

Freeze drying

TMC43-WIV, TMC-OM45-WIV (see table 1 for TMC characteristics) and plain WIV formulations were freshly prepared by adding 1.6 ml of 125 µg/ml WIV dispersion in 5 mM HEPES pH 7.4 (without sucrose) to 1.6 ml 0%; 10% and 20% sucrose solutions in 5 mM HEPES pH 7.4 containing 125 µg/ml TMC43 or TMC-OM45 or no TMC, and mixing thoroughly with a pipette and vortexing for 5 s. This resulted in final sucrose concentrations of 0%; 5% and 10% respectively.

These formulations were freeze-dried using a Zirbus sublimator 400 (ZIRBUS technology, Bad

Grund, Germany). Samples were frozen within 10 minutes by cooling the shelf temperature to -60°C, followed by primary drying for 24 h at a product temperature of -30°C and a pressure of 0.45 mbar. Secondary drying was performed at a product temperature of 0°C for 12 h, followed by 6 h at 20°C. Lyophilization was terminated by automated closing of the rubber lids under vacuum. To study the colloidal stability, freeze-dried formulations were rehydrated with 1.0 ml distilled water and samples were mixed with a vortex for 5 s before they were transferred to glass tubes for DLS measurements.

Results and discussion

Influence of TMC type on the colloidal stability of TMC-WIV

WIV was formulated at a TMC:WIV (w/w) ratio of 1:1 with the various TMCs (see Table 1) that were used in the vaccination study, described in chapter 5 (Hagenaars and Verheul et al). The particle size (Figure 1a), polydispersity index (Figure 1b) and zeta-potential (Figure 1c) of each formulation was determined on day 0, 7 and 14.

Plain WIV in 5 mM HEPES buffer with an average particle size of 175 nm and PDI of 0.2 had a zeta-potential of -23 mV. Formulation of WIV with the various TMCs resulted in a slight increase in particle size independent of the TMC type, with an average particle size between 200 and 220 nm and a PDI between 0.2 and 0.26 (Fig 1a,b).

The zeta-potential of the TMC-WIV formulations was between +12 and +20 mV, as shown in Figure 1c. The zeta-potential of TMC-WIV increased slightly with a higher DQ. Upon storage at 4°C, all TMC-WIV formulations were stable over a period of at least 14 days, indicating that the type of TMC did not have a significant influence on the colloidal stability over this time-period.

Influence of TMC:WIV ratio on the colloidal stability of TMC-WIV

The influence of the TMC:WIV ratio on the colloidal stability was tested, using TMC43. The TMC43:WIV ratio was varied between 0 (only WIV) and 1, and the particle size, PDI and zeta-potential were measured over time. The particle size and zeta-potential of WIV without TMC did not change, indicating that WIV itself is colloidally stable (Fig. 1). For TMC-WIV, at all (w/w) ratios except for 0.1:1, positively charged particles were formed with similar particle sizes between 230 and 255 nm (Fig. 2a) and a PDI between 0.13 and 0.26 (not shown). However, the colloidal stability was highly dependent on the amount of TMC43 that was added. At (w/w) ratios of 1:1 and 0.6:1, the particle size and PDI were constant over a period of at least 7 days. At a (w/w) ratio of 0.3:1, the TMC-WIV formulation showed a stable particle size during the first 8 hours and then started to increase over time until large aggregates were formed after 5 days. At even lower (w/w) ratios of 0.2:1 and 0.15:1, particles were already aggregated after 1 h and the lowest (w/w) ratio of 0.1:1 resulted in instant aggregation after mixing of TMC and WIV. The zeta-potential of these particles also changed over time, depending on the (w/w) ratio, as shown in Figure 2b. At a (w/w) ratio of 1:1 or 0.6:1, the zeta–potential was fairly stable (18-20 mV) over time. At a (w/w) ratio of 0.3:1, the zeta-potential significantly decreased over a period of 7 days (from 15 to 8 mV).

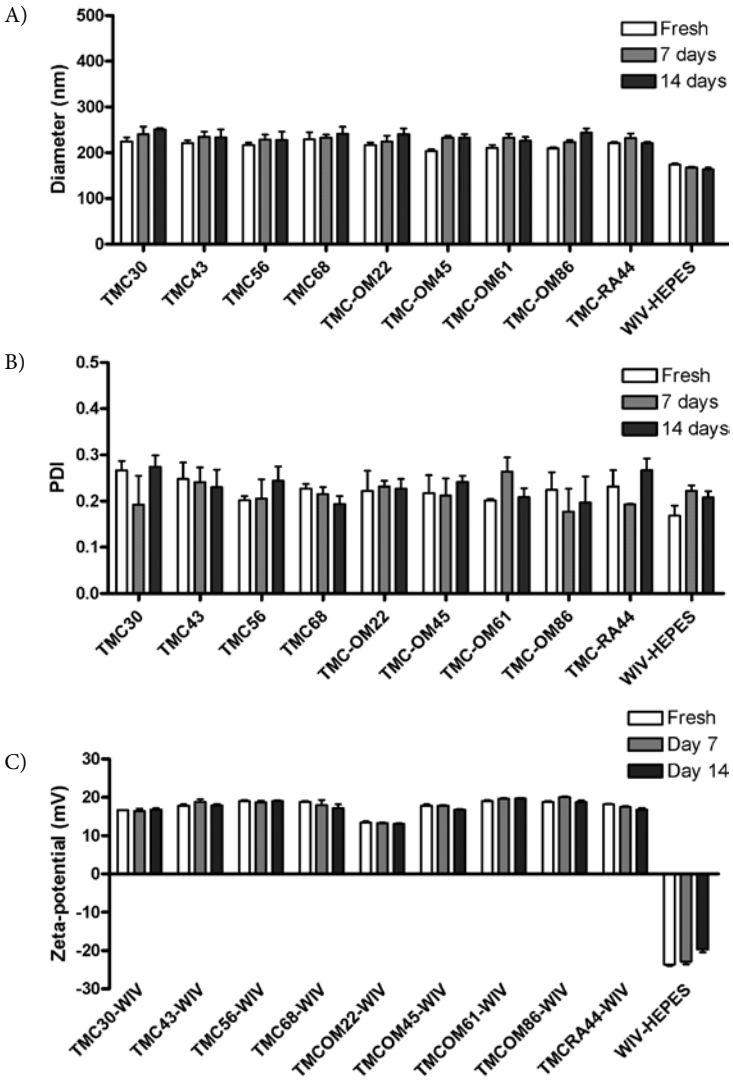

Figure 1: Particle size(A); Polydispersity index (B) and zeta-potential (C) of TMC-WIV formulations (TMC:WIV (w/w) ratio 1:1) with different TMCs in 5 mM HEPES buffer, freshly prepared and after storage at 4°C for 7 and 14 days. Error bars represent the standard deviation of three independent batches.

This observed decrease in zeta-potential went faster when a lower TMC:WIV (w/w) ratio is used, as evidenced by the rapid decrease in zeta-potential to neutral charge, observed at (w/w) ratios 0.2:1 and 0.15:1, respectively. The formulation with lowest (w/w) ratio of 0.1:1 that was measured already had a negative zeta-potential of -3mV that further decreased to -9 mV in 25 h.

Taken altogether, these results show that the zeta–potential decreases over time when the TMC:WIV (w/w) ratio is below 0.6:1. Furthermore, it appears that the observed aggregation is a result from this decrease. At zeta-potentials below +13mV, aggregation of the colloidal system was observed.

One explanation for the decrease in zeta-potential and induction of aggregation is the loss of TMC in solution due to handling. Positively charged TMC can potentially adhere to the negatively charged surfaces of the tubes, pipettes and cuvettes used to transfer and measure the particle size

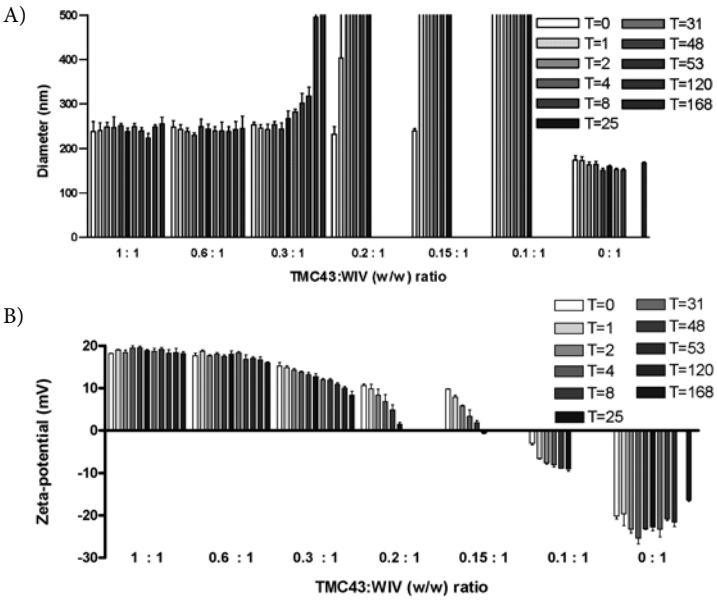

Figure 2: Particle diameter (A) and zeta-potential (B) of TMC43-WIV formulations at different TMC:WIV ratios in 5 mM HEPES over time. T represents time after preparation in hours and error bars represent the standard deviation of three independent batches.

and zeta-potential of these formulations. Logically, samples with higher (w/w) ratios, contained more free TMC [7] and were therefore better protected against the effects of a loss of an absolute amount of TMC compared to the formulations with low TMC content.
To check for this hypothesis, a freshly prepared TMC43-WIV formulation at a (w/w) ratio of 0.3:1 was transferred over 10 successive unused DLS glass tubes and 10 successive unused cuvettes to imitate the contact with glass and cuvette walls that all samples had during the stability experiment. The particle size and zeta-potential of this sample were measured before and after this procedure. No aggregation had occurred (data not shown). This indicates that the decrease in zeta-potential over time for TMC-WIV formulations at lower (w/w) ratios is not a result of a loss of free TMC due to adhesion of surfaces of pipette tips and glassware. It can further be concluded that the aggregation is not instant upon formulation and that the TMC:WIV ratio affects the speed of aggregation. This suggests that the aggregation is a result of an equilibrium shift between bound and free TMC in time.

Because the samples at (w/w) ratios 0.6:1 and 1:1 were stable for 14 days, their particle size and zeta-potential study was prolonged. Even 2 and 4 months after preparation, particle size, PDI and zeta-potential remained stable, as shown in figure 3. Further research should reveal whether these formulations will be stable for a longer period to be able to guarantee a 1-year shelf-life that is required for commercial development of a seasonal influenza vaccine.

Influence of salt concentration on the colloidal stability of TMC-WIV formulations
Several experiments were performed with TMC-WIV formulations in the presence of salt. Such studies may provide information on the influence of the structural properties of TMC, e.g. DQ,

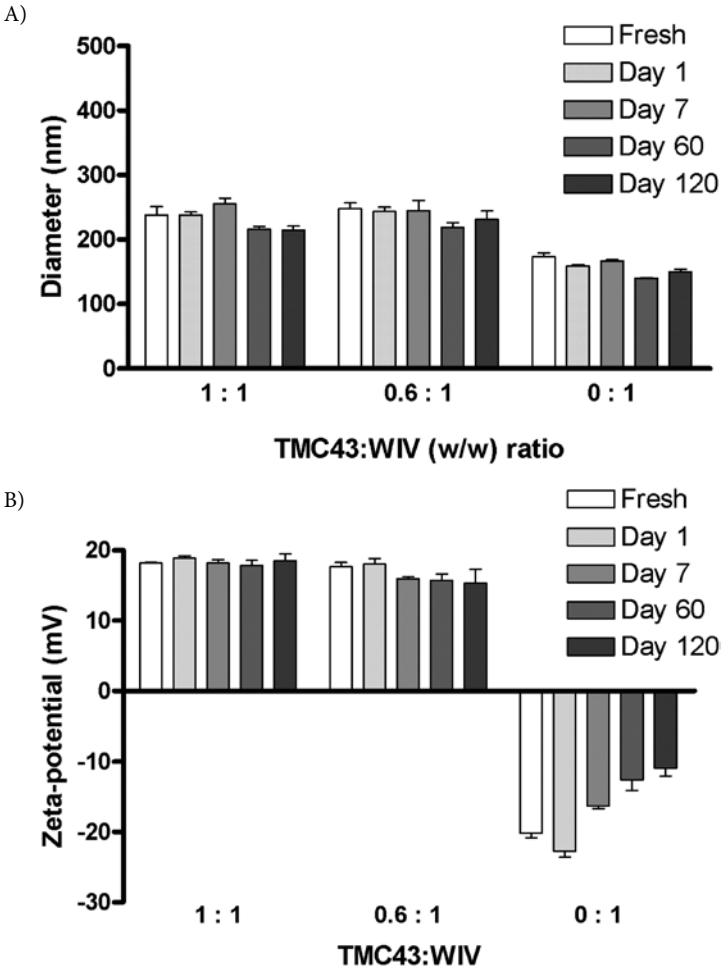

Figure 3: Particle size (A) and zeta-potential of TMC43-WIV formulations with different TMC:WIV (w/w) ratios in 5 mM HEPES over time. Error bars represent the standard deviation of three independent batches.

DOM and DAc, on its interaction with WIV in the presence of salt. This may predict the fate of these TMC-WIV formulations in *in vitro* assays that require incubation in ion-rich environment and after i.n. administration, although it is difficult to perfectly imitate the nasal milieu.

TMC43; TMC-OM45; TMC-RA44; TMC30 and TMC68 were formulated with WIV at a 1:1 and 5:1 (w/w) ratio in 5 mM HEPES, pH 7.4, at salt concentrations varying between 0 and 150 mM NaCl. The particle size and PDI were measured over time. The zeta-potential was not determined, because the salt concentration itself has a big influence on the zeta-potential which makes a comparison of formulations with different salt concentration impossible. Moreover, the sample conductivity becomes too high to measure the zeta-potential.

Uncoated WIV had a particle size of approximately 160 nm and the PDI remained constant between 0.14 and 0.22 for at least 1 h, regardless of the salt concentration. The influence of O-methylation and N-acetylation was studied by comparing TMC43-WIV, with TMC-OM45 and TMC-RA44, which have comparable DQ but different DOMs and DAcs (See Table 1). First, TMC43; TMC-

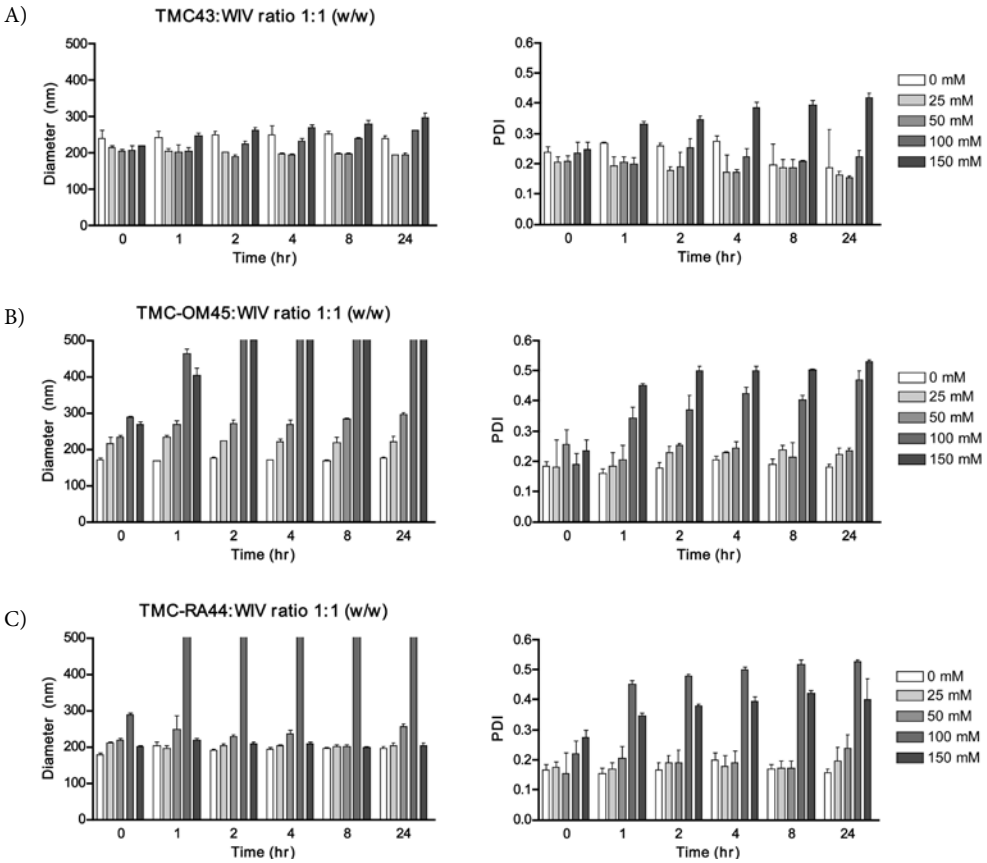

Figure 4: The influence of the type of TMC on the particle size (left panels) and PDI (right panels) of various TMC-WIV formulations at a TMC:WIV (w/w) ratio of 1:1 in different salt concentrations over time, with TMC43(A); TMC-OM45 (B); TMC-RA44(C). Error bars represent the standard deviation of three independent batches.

OM45 and TMC-RA44 were formulated with WIV at a (w/w) ratio of 1:1. As shown in Figure 4a, the average particle size of TMC43-WIV is similar and relatively stable over time in salt concentrations up to 100 mM. At higher concentrations, the particle size slowly increased over time and in 150 mM NaCl, the PDI also increased.

When WIV was formulated with TMC-OM45 at a (w/w) ratio of 1:1, the initial particle size varied more for the different salt concentrations, as shown in Figure 4b. On the other hand, the particle size and PDI were constant over 24 h at salt concentrations up to 50 mM. At higher salt concentrations, a strong increase in particle size and PDI were observed.

Figure 4c shows a similar trend for TMC-RA44-WIV formulations, where the particle size and PDI were also stable over 24 h in salt concentrations up to 50 mM. An increase particle size and PDI were observed at a concentration of 100 mM, whereas at 150 mM NaCl only the PDI increased and the particle size remained stable.

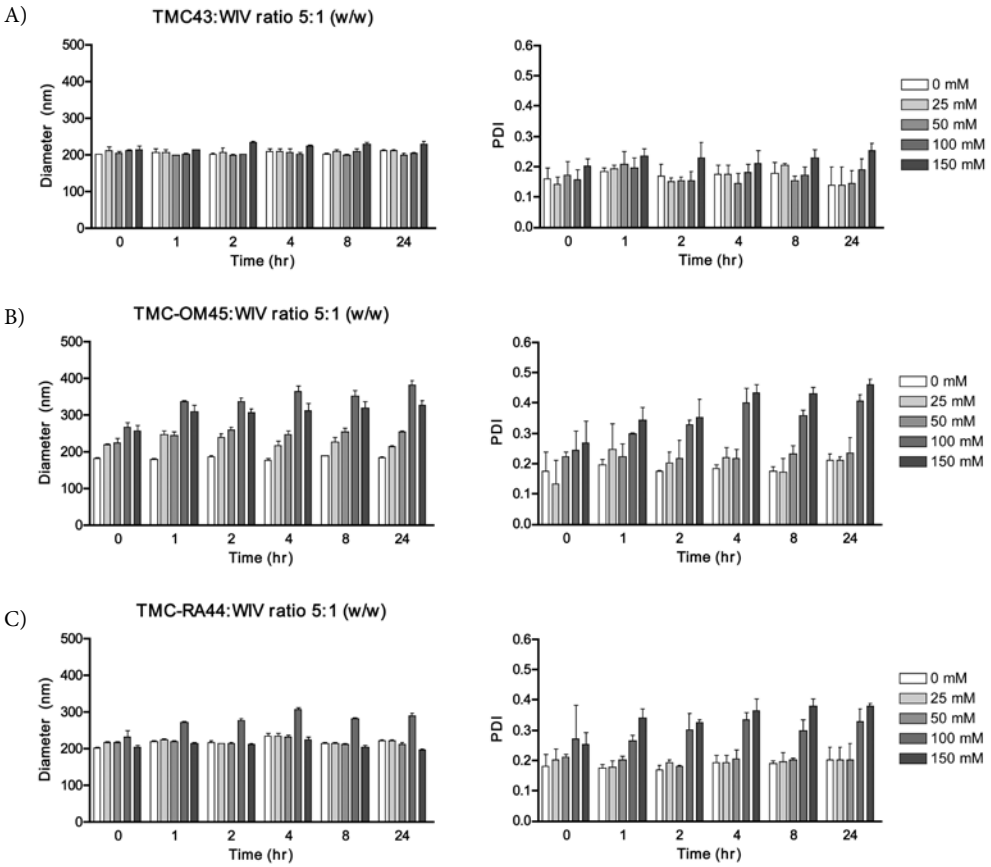

Figure 5: The influence of the type of TMC on the particle size (left panels) and PDI (right panels) of various TMC-WIV formulations at a TMC:WIV (w/w) ratio of 5:1 in different salt concentrations over time, with TMC43 (A); TMC-OM45 (B); TMC-RA44 (C). Error bars represent the standard deviation of three independent batches.

When these three TMC-WIV formulations are compared, the TMC43-WIV formulation appears to be the most stable at higher salt concentrations, which is most clear at a salt concentration of 100 mM.

The next step was to see whether in the presence of salt, a higher (w/w) ratio could improve the stability of TMC-WIV formulations. As shown in Figure 5, all formulations became more stable when a higher TMC:WIV (w/w) ratio was used. Figure 5a shows that the TMC43-WIV formulation had a salt concentration-independent particle size of approximately 200 nm that was stable over 24 h. Only at a salt concentration of 150mM, the size and PDI were slightly higher. The TMC-OM45-WIV, on the other hand, was not stable in 100 and 150 mM NaCl, as shown in Figure 5b. Both the particle size and the PDI increased over time, but less than for the TMC-OM45-WIV formulations at a 1:1 (w/w) ratio. TMC-RA44-WIV was also more stable when formulated at a higher (w/w) ratio, but the PDI still increased significantly at 100 mM and 150 mM salt concentration. Interestingly,

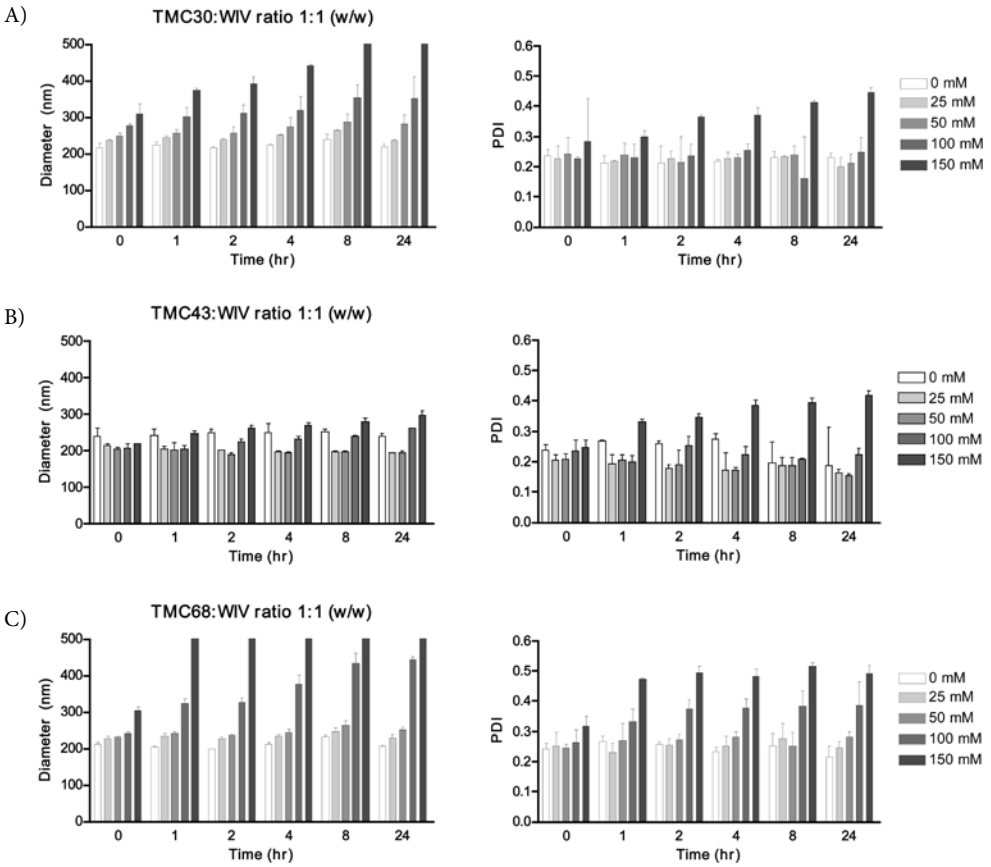

Figure 6: The influence of DQ on the particle size(left panels) and PDI (right panels) of various TMC-WIV formulations at a TMC:WIV (w/w) ratio of 1:1 in different salt concentrations over time, with TMC30(A); TMC43 (B); TMC68(C). Error bars represent the standard deviation of three independent batches.

unlike in 100 mM NaCl, the TMC-RA44-WIV formulations appeared to have a stable particle size in 150 mM NaCl solution. More experiments should be performed to explain this behavior.

Influence of DQ on the colloidal stability of TMC-WIV formulations

In addition to the influence of O-methylation and N-acetylation, the influence of DQ on the stability of TMC-WIV formulations in different salt concentrations was studied at (w/w) ratios of 1:1 and 5:1. Therefore, WIV was formulated with TMC30; TMC43 and TMC68 and the formulations were analyzed over time by DLS. As shown in figure 6, TMC30-WIV showed a salt concentration dependent particle size after preparation, and was relatively stable for 24 h at all tested salt concentrations except 150 mM. The particle size of TMC68-WIV was less salt concentration dependent, similar to TMC43-WIV. However, TMC68-WIV appeared to be the least stable of the three O-methyl free TMCs that were tested. The PDI and particle size increased more strongly than for TMC30-WIV and TMC43-WIV at salt concentrations higher than 50 mM.

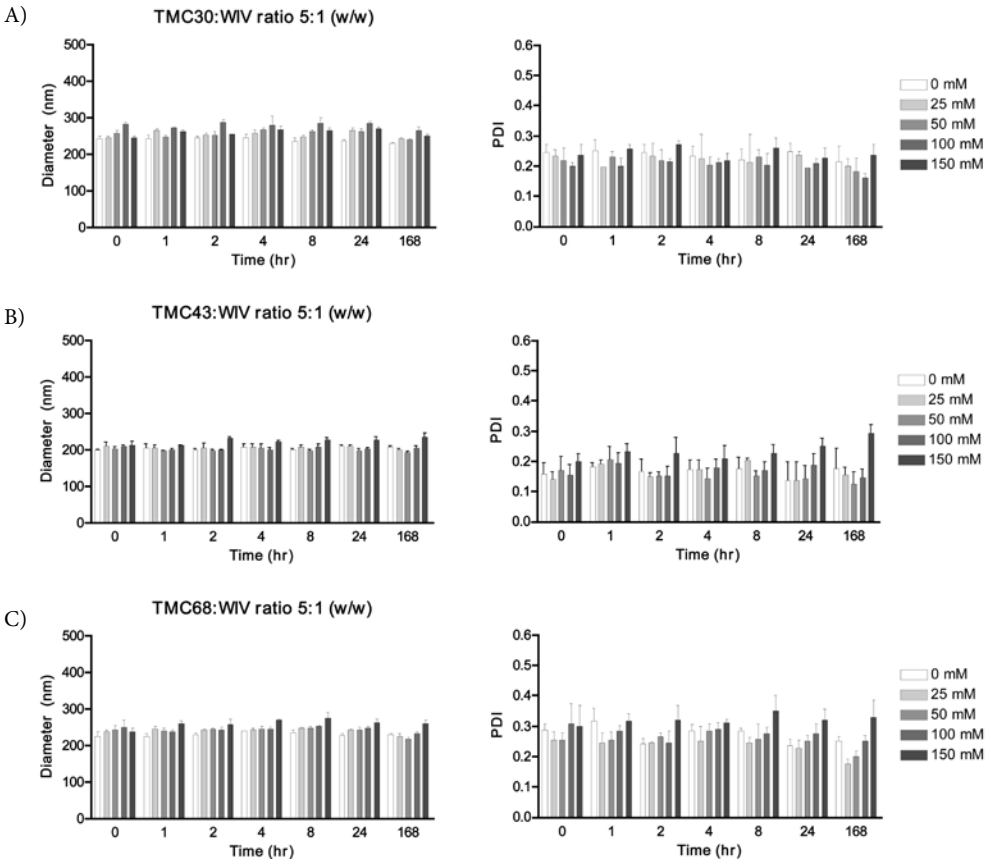

Figure 7: The influence of DQ on the particle size (left panels) and PDI (right panels) of various TMC-WIV formulations at a TMC:WIV (w/w) ratio of 5:1 in different salt concentrations over time, with TMC30(A); TMC43 (B); TMC68(C). Error bars represent the standard deviation of three independent batches.

Finally, when these formulations were prepared at a TMC:WIV (w/w) ratio of 5:1, stable particles were obtained for all three TMCs, as shown in Figure 7.

When combining these data with the results from the vaccination study with these formulations, described in chapter 5, it appears that the salt sensitivity of these formulations does not influence the immunogenicity of these vaccine formulation as TMC30-WIV, TMC43-WIV, TMC68-WIV and TMC-OM45-WIV induced comparable immune responses (chapter 5, [7]).

Influence of freeze drying on the colloidal stability of TMC-WIV formulations

The possibility to freeze dry these formulations while maintaining the nanoparticulate character was assessed. TMC43-WIV and TMC-OM45-WIV, being the most and least stable formulations in aqueous dispersion, respectively, were formulated at a 1:1 (w/w) ratio in 5 mM HEPES buffer containing 0%; 5% or 10% sucrose as a lyoprotectant.

As shown in Figure 12a, samples that were freeze-dried in the absence of sucrose showed an

A)

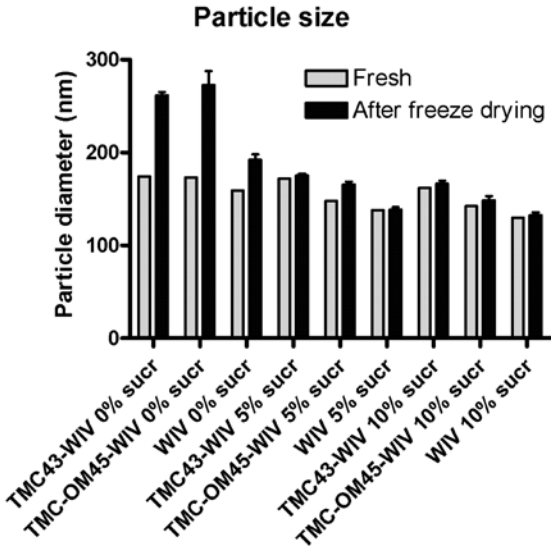

B)

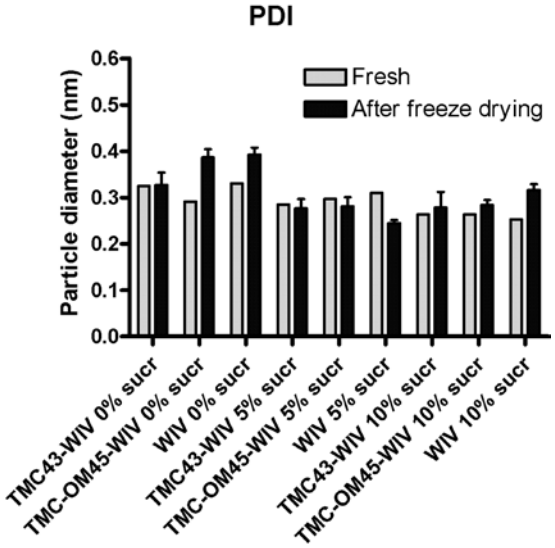

Figure 8: Particle size (A) and PDI (B) of various TMC43-WIV and TMC-OM45-WIV formulations (1:1 (w/w) ratio, 5 mM HEPES pH 7.4) prior to and after freeze drying. Error bars represent the standard deviation of three independent batches

increased particle size after rehydration, especially for the TMC43-WIV and TMC-OM45-WIV formulations. Furthermore, the PDI also increased when no lyoprotectant was included in the formulation (Figure 12b).

When TMC43-WIV, TMC-OM45-WIV and plain WIV formulations were freeze dried in the presence of 5% or 10% sucrose, the particle size and PDI did not change much after freeze-drying and rehydration when compared to the fresh sample (see Figure 12a and b), indicating that freeze-drying of TMC-WIV samples is feasible.

Concluding remarks

TMC-WIV formulations are stable in low salt concentration at TMC:WIV (w/w) ratios higher than 1:1, independent of the type of TMC. At higher salt concentrations, the formulations are less stable, especially with O-methylated TMC and, to a lesser extent, partially reacetylated TMC. Furthermore, the DQ appears to have some effect on the colloidal stability, but this effect is relatively small.

Additional studies have to be done to better understand the molecular interactions that drive the instability of TMC-WIV formulations. Based on the structural differences between the TMCs (Table 1), it is likely that several interactions may play a role. First of all, steric hindrance due to *O*-methylation and *N*-acetylation may decrease the strength of the electrostatic interactions between the TMC and WIV. Furthermore, a loss of hydroxyl groups, through *O*-methylation, may decrease the ability to form hydrogen bonds. The increase hydrophobic character of TMC-OM and TMC-RA could also play a role in the colloidal instability, especially at higher salt concentrations. In addition, studies should be performed to investigate the effect of chain length and concentration on the colloidal stability of TMC-WIV formulations.

Moreover, the importance of colloidal stability on the immunogenicity and toxicity of these i.n. vaccine formulations should be investigated for further development. In addition, the physicochemical stability of WIV, and of HA in particular, should be studied in more detail.

TMC-WIV formulations can be freeze dried without altering the particle size and PDI after rehydration. This shows that freeze drying is a feasible option, but the long term stability of freeze dried TMC-WIV formulations still has to be assessed.

Acknowledgements

The authors acknowledge Mies van Steenbergen for his help with the freeze-drying experiments.

References

[1] Amidi M, Romeijn SG, Verhoef JC, Junginger HE, Bungener L, Huckriede A, et al. N-trimethyl chitosan (TMC) nanoparticles loaded with influenza subunit antigen for intranasal vaccination: biological properties and immunogenicity in a mouse model. Vaccine 2007;25(1):144-53.

[2] Boonyo W, Junginger HE, Waranuch N, Polnok A, Pitaksuteepong T. Chitosan and trimethyl chitosan chloride (TMC) as adjuvants for inducing immune responses to ovalbumin in mice following nasal administration. J Control Release 2007;121(3):168-75.

[3] Baudner BC, Verhoef JC, Giuliani MM, Peppoloni S, Rappuoli R, Del Giudice G, et al. Protective immune responses to meningococcal C conjugate vaccine after intranasal immunization of mice with the LTK63 mutant plus chitosan or trimethyl chitosan chloride as novel delivery platform. J Drug Target 2005;13(8-9):489-98.

[4] Verheul RJ, Amidi M, van der Wal S, van Riet E, Jiskoot W, Hennink WE. Synthesis, characterization and in vitro biological properties of O-methyl free N,N,N-trimethylated chitosan. Biomaterials 2008;29(27):3642-9.

[5] Verheul RJ, Amidi M, van Steenbergen MJ, van Riet E, Jiskoot W, Hennink WE. Influence of the degree of acetylation on the enzymatic degradation and in vitro biological properties of trimethylated chitosans. Biomaterials 2009;30(18):3129-35.

[6] Hagenaars N, Mastrobattista E, Verheul RJ, Mooren I, Glansbeek HL, Heldens JG, et al. Physicochemical and Immunological Characterization of N,N,N-Trimethyl Chitosan-Coated Whole Inactivated Influenza Virus Vaccine for Intranasal Administration. Pharm Res 2009;26(6):1353-64.

[7] Hagenaars N, Verheul RJ, Mooren I, de Jong PH, Mastrobattista E, Glansbeek HL, et al. Relationship between structure and adjuvanticity of N,N,N-trimethyl chitosan (TMC) structural variants in a nasal influenza vaccine. J Control Release 2009.

[8] Boulianne N, De Serres G, Duval B, Shadmani R, Rochette L. Clinical manifestations and incidence of oculo-respiratory syndrome following influenza vaccination--Quebec, 2000. Can Commun Dis Rep 2001;27(10):85-90.

[9] Skowronski DM, De Serres G, Hebert J, Stark D, Warrington R, Macnabb J, et al. Skin testing to evaluate oculo-respiratory syndrome (ORS) associated with influenza vaccination during the 2000-2001 season. Vaccine 2002;20(21-22):2713-9.

[10] Skowronski DM, Strauss B, De Serres G, MacDonald D, Marion SA, Naus M, et al. Oculo-respiratory syndrome: a new influenza vaccine-associated adverse event? Clin Infect Dis 2003;36(6):705-13.

[11] De Serres G, Toth E, Menard S, Grenier JL, Roussel R, Tremblay M, et al. Oculo-respiratory syndrome after influenza vaccination: trends over four influenza seasons. Vaccine 2005;23(28):3726-32.

[12] Babiuk S, Skowronski DM, De Serres G, HayGlass K, Brunham RC, Babiuk L. Aggregate content influences the Th1/Th2 immune response to influenza vaccine: evidence from a mouse model. J Med Virol 2004;72(1):138-42.

[13] Amorij JP, Huckriede A, Wilschut J, Frijlink HW, Hinrichs WL. Development of stable influenza vaccine powder formulations: challenges and possibilities. Pharm Res 2008;25(6):1256-73.

[14] Garmise RJ, Mar K, Crowder TM, Hwang CR, Ferriter M, Huang J, et al. Formulation of a dry powder influenza vaccine for nasal delivery. AAPS PharmSciTech 2006;7(1):E19.

[15] Garmise RJ, Staats HF, Hickey AJ. Novel dry powder preparations of whole inactivated influenza virus for nasal vaccination. AAPS PharmSciTech 2007;8(4):E81.

[16] Huang J, Garmise RJ, Crowder TM, Mar K, Hwang CR, Hickey AJ, et al. A novel dry powder influenza vaccine and intranasal delivery technology: induction of systemic and mucosal immune responses in rats. Vaccine 2004;23(6):794-801.

[17] Sieval AB, Thanou M, Kotze AF, Verhoef JE, Brussee J, Junginger HE. Preparation and NMR characterization of highly substituted N-trimethyl chitosan chloride. Carbohydrate Polymers 1998;36(2-3):157-65.

Chapter 9

Summary and future perspectives

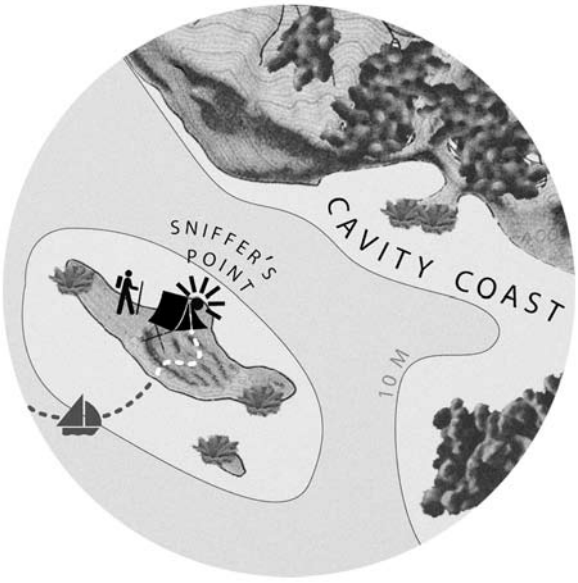

Summary

Seasonal influenza outbreaks are a significant burden on society, causing substantial morbidity and mortality each winter. In addition, potential pandemic influenza outbreaks have recently become a major concern due to the transmission of highly pathogenic H5N1 influenza virus from birds to humans in South-East Asia and the more recent spreading of the new H1N1 influenza to the human population (**Chapter 1**).

The best form of protection against influenza is vaccination, both by protecting individual vaccinees and by acquiring herd immunity when a large proportion of a population is vaccinated. Influenza vaccines are historically administered parenterally. Intranasal (i.n.) vaccination poses several advantages to the classical intramuscular (i.m.) route. These include easy, needle-free administration that no longer requires trained professionals and the potential induction of local sIgA levels on the mucosal surfaces of the airways, the port of entry for the influenza virus. A Live attenuated, cold-adapted influenza virus vaccine has successfully been introduced on the market and promising results have been made with adjuvanted inactivated i.n. influenza vaccines. However, the optimal balance between safety and efficacy in all target population, including the elderly, has not yet been found.

The principal aim of the research in this thesis was the rational design of an inactivated, i.n. influenza vaccine. To achieve this, the following sub-aims were defined:

- to elucidate the main physiological hurdles that limit the immunogenicity of i.n. vaccines;
- to explore the possibilities to overcome these hurdles by improving vaccine composition and delivery;
- to determine the mode of action of these improved formulations.

Chapter 2 gives a review on the current literature on i.n. delivery of inactivated vaccines and discusses the rational design of non-living i.n. vaccines. The main physiological hurdles in vaccine delivery via the nose are described and a roadmap to successful i.n. vaccination is laid out. After i.n. administration, the antigen should be delivered to the antigen-presenting cells (APCs) that can initiate an adaptive immune response, mainly present in the nasal-associated lymphoid tissue (NALT). To do so, the antigen must cross the nasal epithelium to reach the NALT before it is cleared from the nasal cavity by mucociliary clearance. The use of mucoadhesive polymers like chitosan and chitosan derivatives like N,N,N-trimethylchitosan (TMC) can enhance the immune responses against a variety of antigens, presumably by increasing the nasal residence time and/or increasing the contact area between the antigen and the mucosal surface. The uptake through the epithelium, especially by microfold cells (M-cells), can be improved by encapsulating soluble antigens into particles, preferably positively charged and with a submicron particle size. Furthermore, antigen can be more specifically targeted to M-cell by the use of targeting ligands.

After uptake through the epithelium, the antigen has to be taken up and processed by dendritic cells (DCs). The use of immunostimulatory adjuvants targeting the innate immune system via binding to pathogen recognition receptors (PRRs) like toll-like receptor (TLR) ligands, toxin-

based adjuvants and cytokines and co-stimulatory molecules can enhance and modulate immune responses elicited after intranasal vaccination. Furthermore, strategies to improve cytotoxic T-cell (CTL) induction are reviewed.

As described in **chapter 3**, there are four commonly used, nonadjuvanted, inactivated influenza vaccines: Whole inactivated influenza virus (WIV), split vaccine, subunit vaccine and virosomes. These different vaccine formulations can be differentiated by the antigen content and the antigen organization. WIV and split vaccine contain all viral components whereas subunit and virosomes only contain subunit components (mainly hemagglutinin (HA) and (NA)). On the other hand, both WIV and virosomes have an organized nanoparticulate structure, whereas split and subunit vaccines do not have their antigen present in organized nanosized vesicles. In **chapter 3** the immunogenicity and protectivity of these vaccines was compared in a vaccination-challenge study in mice via the i.m. as well as the i.n. route. It was shown that the i.m. route induces much stronger immune responses and better protection against homologous challenge. After i.n. vaccination, only split and WIV induced detectable serum humoral immune responses and partial protection. Vaccines containing all viral components clearly induced stronger immune responses than vaccines containing only part of the viral antigen repertoire (subunit and virosomal vaccines). Interestingly, subunit, virosomes and split vaccine exclusively induces IgG1 titers, an indicator that Th2 immune responses were elicited. On the other hand, WIV induced mainly IgG2a/c responses via both routes and also induced detectable mucosal sIgA responses, which was not induced by the other formulations.

From these results WIV was selected as the best candidate to further optimize intranasal inactivated influenza vaccines, because the mixed IgG1/IgG2a/c responses, indicative of a more balanced Th1/Th2 type cellular immune response, has been associated with improved protection against influenza. Illustrated by the strong immune responses elicited by non-adjuvanted WIV after i.m. vaccination, it appears that the relatively low immunogenicity after i.n. administration is likely the result of inefficient delivery of WIV via the i.n. route. The use of mucoadhesive polymers may overcome this problem by their interaction with the mucosal surfaces in the nasal cavity, potentially leading to an increased residence time and/or altered interaction with the mucosal surfaces that may lead to improved antigen uptake from the nasal cavity. TMC, a cationic, water-soluble derivative of chitosan has shown promising results as a mucoadhesive adjuvant in mucosal vaccinations. TMC is structurally characterized by its molecular weight, degree of quaternization (DQ), degree of O-methylation (DOM) and degree of N-acetylation (DAc).

In **Chapter 4**, the negatively charged WIV was formulated with 2 types of O-methylated TMCs (TMC-OM) to obtain positively charged nanoparticles with the TMCs being partially bound to WIV. Intranasal vaccination with these formulations revealed that TMC-WIV induced significantly stronger hemagglutination inhibition (HI) titers and IgG, IgG1 and IgG2a titers than plain WIV. Mice immunized with TMC-OM-WIV were protected against challenge, whereas mice vaccinated

with plain WIV were not. Furthermore, 2 groups of mice that received TMC-OM 2 h prior to WIV administration did not induce strong immune responses and were not fully protected, indicating that the adjuvant effect of TMC is mainly based on an improved i.n. delivery of WIV rather than on immunostimulatory effects.

Simultaneously, a novel synthesis method for TMC was developed by Verheul et al. [1], omitting O-methylation and chain scission, allowing a fair comparison of the influences of DQ and DOM on the biological properties of TMCs. In vitro experiments showed that these TMCs exerted a much stronger effect on the transepithelial electrical resistance (TEER) and induced more cell toxicity in epithelial Caco-2 cells than O-methylated TMCs. Furthermore, Verheul et al. showed in another paper that reacetylation of TMC improved its biodegradability and led to a loss of TEER effect and a significant decrease in cell toxicity [2]. In **Chapter 5** WIV was formulated with these different TMCs, varying in DOM, DQ and DAc, to assess the influence of these structural properties of TMC on their adjuvant effect for i.n. administration. All TMC-OM-WIV and TMC-WIV formulations showed comparable physicochemical characteristics. Moreover, they induced comparable immune responses, superior to those induced by WIV, and provided protection against challenge with live virus. Apparently, the role of O-methylation and degree of quaternization on the adjuvant effect were minimal, and the effect of these properties on *in vitro* TEER and cell toxicity are not correlated with their adjuvant effect (for i.n. administered WIV in mice).
Interestingly, reacetylated TMC (TMC-RA) formulated with WIV, induced significantly lower immune responses and could not protect mice against challenge. It appears that a high degree of acetylation abolished the *in vivo* adjuvant effect of TMC in mice. Additionally, the IgG1/IgG2a ratio was not influenced by the type of TMC. Only at higher TMC:WIV (w/w) ratios, increased IgG1 titers were observed after boost vaccination.

In chapter 6, the intranasal localization of WIV with and without TMC was visualized using *in vivo* fluorescence imaging and immunohistochemistry techniques in order to clarify the mechanism by which TMCs elicit their adjuvant effect. *In vivo* fluorescence imaging suggested that the improved immune responses of TMC-WIV formulations were not associated with a prolonged bulk nasal residence time. This was confirmed by immunohistochemical staining on nasal cross-sections. The latter experiments further revealed that formulation of WIV with TMC resulted in an altered distribution of the antigen in the nasal cavity after administration when compared to plain WIV. Plain WIV was mainly present in the nasal cavity, presumably in mucus blobs, but TMC-WIV was predominantly detected as a thin layer on the epithelial surfaces of the naso- and maxilloturbinates, having an increased contact area of the antigen with the mucosal surface. This increased contact with the epithelial surface may result in increased uptake of WIV and thus explain the improved immunogenicity of TMC-WIV. Additionally, the local toxicity of several TMC-WIV formulations was assessed, which is of paramount importance in the development of vaccine adjuvants. All TMC solutions and TMC-WIV formulations induced minimal local toxicity, comparable to plain WIV, which was significantly less than for polyethylenimine (PEI). Interestingly, the differences in

cell toxicity found *in vitro* between TMCs with various DQ and DOM could not be found after a single i.n. dose. Likely, the local toxicity is overestimated when using *in vitro* cell toxicity assays to predict the *in vivo* safety.

In the **Appendix to Chapter 6** additional experiments were performed to study the initial increase in fluorescence in the nose and later, even stronger, in the stomach after i.n. administration of IRDye800CW®-labeled WIV, as was observed in chapter 6. An increase in dye fluorescence after detergent disruption of IRDye800CW®-labeled WIV formulations or after trypsin treatment, but not by plain dilution, suggested that dequenching of the fluorescent label is responsible for an increase in fluorescence. It is likely that i.n. administered IRDye800CW®-labeled WIV is enzymatically degraded, explaining the enhanced fluorescence observed in the nose and in the stomach.

In **chapter 7**, various techniques were employed to find out why TMC-RA44 (TMC-RA) does not have adjuvant activity, in contrast to TMC43 (TMC) (see chapter 5).
In nasal washes TMC-RA was faster degraded than TMC. *In vivo* fluorescence imaging suggested that the clearance from the nasal cavity was similar for TMC-WIV and TMC-RA-WIV. Furthermore, immunohistochemical staining of these formulations showed that the location of TMC-RA-WIV and TMC-WIV were also comparable, leading to the conclusion that the distribution, retention and contact with the mucosal surface are not the cause of the observed difference between the adjuvanticity of TMC-RA and TMC. Formulation of fluorescently labeled beads with TMC or TMC-RA enhanced their uptake by HeLa cells. Moreover, formulation of WIV with these polymers improved its uptake by human bronchial epithelial cells (16-HBE14o). However, in both cases the uptake-enhancing effect was significantly less pronounced for TMC-RA, compared to TMC. Incubation of plain WIV, TMC-WIV and TMC-RA-WIV with murine bone marrow-derived dendritic cells (DCs) suggested that WIV had an immunostimulatory effect on DCs, which was not further increased by formulation with TMCs. So, the decreased adjuvanticity of TMC-RA in mice, as compared to TMC, may be due to reduced uptake by epithelial cells and/or enhanced biodegradation of TMC-RA.
These TMCs were also tested on human monocyte derived DCs, because the *N*-acetyl glucosamine structures in TMC-RA can potentially bind to innate immune receptors on human DCs and thereby act as an adjuvant. In contrast to the results with murine bone marrow-derived DCs, a striking difference in DC activation was observed between the effect of the various TMCs (in solution and when formulated with WIV). TMC-RA strongly induced DC maturation and production of proimflammatory cytokines IL-10, IL12p40, IL12p70 and TNFα, when compared to TMC. Further studies should be done to better understand the mechanisms behind the human DC-specific effect of TMC-RA44.

The type of TMC may have an influence on the colloidal stability of TMC-WIV formulations. Investigating the colloidal stability of TMC-WIV formulations is important for further

pharmaceutical development and for studying these formulations in *in vitro* cell studies. In **chapter 8**, the stability of TMC-WIV was investigated using zeta-potential measurements and dynamic light scattering to monitor the surface charge and particle size and polydispersity over time. The influence of the TMC-type and TMC:WIV ratio was tested at different salt concentrations.
A minimum TMC:WIV (w/w) ratio of 0.6:1 was necessary to obtain positively charged particles that are stable over time. At lower TMC:WIV w/w ratios, particles were unstable. Moreover, the unstable formulations showed a decrease in zeta potential and progressive aggregation over time.
At a 1:1 ratio, all formulations were stable for at least two weeks under refrigerated conditions. TMC43-WIV was monitored for a longer period and was still stable after 4 months. At higher salt concentrations, the formulations became less stable. TMC43-WIV was the most stable formulation, followed by TMC-RA-WIV. TMC-OM45-WIV was the least stable formulation. This indicates that O-methylation and N-acetylation have a negative effect on the colloidal stability of TMC-WIV formulations.

The research described in this thesis resulted in the rational design of an inactivated i.n. influenza vaccine, based on WIV with TMC as an adjuvant. The role of several potential physiological hurdles towards the induction of an immune response via i.n. vaccination, like mucosal clearance, antigen distribution in the nasal cavity and antigen uptake by epithelial cells and DCs were investigated. The possibilities to overcome these hurdles were explored and i.n. inactivated influenza vaccine based on TMC-WIV was formulated that shows promising results for further development. Finally, the mode of action of TMC as an i.n. vaccine adjuvant was studied.

Future perspectives

Further characterization and optimization of TMC-WIV formulations

Several aspects concerning TMC-WIV vaccine formulation have been studied in this thesis, like the influence of TMC:WIV ratio and the DQ, DOM and DAc of the TMCs on the formulation's physicochemical properties, stability, toxicity and efficacy. Taken altogether, both TMC and TMC-OM have good adjuvant properties, leading to effective TMC-WIV vaccines. The DQ plays a minor role in the stability, efficacy and in vivo toxicity of TMC-WIV. The mode of action of TMC in TMC-WIV i.n. vaccine is mainly an improved antigen delivery. Based on mouse studies, TMC-RA appears to be much less effective. An i.m. vaccination study in mice should be done to determine if this decreased adjuvant effect is specific for the i.n. route of administration.
Future experiments should be done to investigate whether the influence of DQ, DOM and DAc on the local toxicity and adjuvanticity is the same in other animal models and ultimately humans. The preliminary studies with TMC-RA on human DCs suggest an immunostimulatory adjuvant effect of reacetylated TMCs. The role of these structural properties on species specific innate immune responses should be investigated in more detail and the mode of action on human DCs should be identified.

Another structural property that has not been studied is the molecular weight of TMC, which may have an influence on the toxicity, efficacy and formulation stability of TMC-WIV vaccines.

In this thesis, we characterized the humoral immune responses that were elicited by the various TMC-WIV vaccines. For example, the potential of a single shot vaccine or the optimal interval between prime and boost vaccination is still unknown. Moreover, the potential of antigen sparing, e.g. through combination of TMC with other adjuvants, is still unexplored.
It would also be interesting to study the role of free TMC, not only in the formulation as stabilizer of the colloidal system, but also in the induction of immune responses. It is, however, difficult to separate the TMC-WIV particles from the free TMC without inducing aggregation (unpublished results). Therefore, it may be an interesting option to covalently link TMC with WIV, leading to a stronger interaction between antigen and adjuvant and hopefully stable TMC-WIV particles without free TMC.
One step further would be the coupling of targeting ligands to these TMC-WIV systems, like M-cell specific targeting ligands. Thiolation of TMC could also improve its adjuvant activity by increasing the mucoadhesive properties of the otherwise moderately mucoadhesive TMCs, which could lead in a further improvement of the close interaction between WIV and the mucosal surface (see chapter 6) and/or subsequent antigen transport through the epithelial barrier.
Because the formulation of TMC-coated WIV is based on electrostatic interactions between the cationic TMC and an anionic particulate antigen, this strategy can potentially be applied to vaccines against a wide variety of respiratory viruses, like parainfluenza virus, RSV, adenovirus, SARS and potentially also for other viruses like HIV and veterinary viral vaccines.
In addition to the exploration of other TMC-based WIV formulations and other infectious diseases, different routes of administration of these TMC-based vaccine formulations may be further explored. Especially the pulmonary route seems interesting, given the strong immune responses that can be induced via this needle-free route and the relative ease of administration. Potentially, TMC-WIV vaccines are safe and effective i.m. vaccines as well, but the adjuvanticity and thus potential antigen sparing of the various TMCs after i.m. vaccination has not yet been studied. The use of WIV for i.m. vaccination, however, has been linked to increased reactogenicity [3, 4]. Therefore, it is less likely that these vaccines will be developed as i.m. seasonal influenza vaccines.
There may be some concerns on the suitability of TMC for pharmaceutical development. As it is derived from a natural product there may be a risk of considerable batch-to-batch variability. Although TMC is derived from the natural polysaccharide chitin, it is feasible that TMCs can be reproducibly produced on large scale, using described synthesis routes [1], to obtain TMC with reproducible structural properties. The specifications for acceptable variations in structural properties like Mw, DQ, DAc and DOM have to be formulated for TMC in a later stage of the development of these vaccine formulations.

Bottlenecks in influenza vaccine development

In recent years the efforts to develop and produce new effective influenza vaccines has rapidly gained momentum, infused by the highly pathogenic avian H5N1 influenza outbreaks in Southeast Asia and more recently by the worldwide spreading of the 2009 H1N1 influenza virus of swine origin. It is likely that the increasing demand for influenza vaccines will continue during the next few years.

Licensing of pandemic and seasonal influenza vaccines that are based on production methods of already licensed products can undergo a fast track procedure due to the experience with the existing product that is on the market. In contrast, licensing a novel vaccine formulation with a new route of administration or adjuvant requires the full licensing procedure. As a result, these vaccines will only be developed when there is a strong demand for better vaccines from the public.

The major problem with a pandemic influenza vaccine is that the exact strain is not known until the pandemic has started. As a result, pandemic vaccine production can only start when the influenza pandemic is already spreading, putting an enormous pressure on the timeline of vaccine production. Therefore it is an enormous challenge to produce enough vaccines to accommodate the skyrocketing demands for pandemic vaccines in such a situation. To do so, increased production capacity, shortening of the time to market and antigen sparing vaccine formulations are critical for pandemic vaccination to be successful.

When there is enough momentum for the development of inactivated i.n. influenza vaccines, like TMC-WIV, several issues have to be discussed. The main hurdles for the development of an i.n. inactivated influenza vaccine are: understanding the vaccine-induced (mucosal) immunity; finding new correlates of protection; and developing predictive animal models. These issues are discussed in more detail in the following section.

Understanding the vaccine-induced (mucosal) immunity against influenza

Through the research presented in this thesis and a multitude of research done by others in the past few years, it has become clear that more research has to be done to understand the mucosal immune system. The induction of mucosal immune responses is a clear feature of i.n. vaccines that injectable vaccines do not have. More research should reveal the role of sIgA in protection against airway pathogens like influenza virus; their cross-protective properties in comparison to systemic IgG; and the induction of memory B-cells that can produce sIgA.

A better understanding of the physiological mechanisms involved in successful i.n. vaccine delivery, like the interaction between antigen and mucosal surfaces and the subsequent induction of an immune response will also greatly benefit vaccine development. The exact role of M-cells in the induction of immune responses is not clear. M-cells can take up particulate antigens and transport them to the underlying immune cells, but little is known about the processes that drive this uptake and about the importance of M-cells in vaccine induced immunity.

In conclusion, the role of mucosal immunity in protection against influenza, and in a broader sense to many other pathogens, should be further investigated to establish the added value of i.n. vaccines more firmly. At the same time, better i.n. vaccine formulations will be designed when it

becomes clear how the induction of mucosal sIgA responses, the main immunological advantage of mucosal over parenteral vaccine administration, can be optimized.
In addition to mucosal immune responses, other immune components that are involved in immunity against influenza should be investigated in more detail. Cell-mediated immunity against influenza, in the form of helper T-cell and cytotoxic T-cell responses, may provide a broader protection against influenza. This holds great promise for the development of better (i.n.) vaccines. Therefore it is crucial to better understand how cell mediated immunity can be optimally induced by vaccination. It may well be that the ideal i.n. influenza vaccine should induce immunity against influenza through a combination of CTL, mucosal sIgA and systemic IgG responses.

Finding new correlates of protection

One of the major hurdles for the development of i.n. vaccines is that HI titers are currently used as a correlate of protection by the regulating authorities. This correlate of protection was introduced with systemic humoral immunity in mind [5]. Neutralizing antibodies in the systemic circulation are the main protective immune component for parenterally administered subunit and split vaccines. Therefore, HI titers correlate well for these vaccines.
In the case of i.n. immunization, on the other hand, HI titers are less pronounced and protection may be likely provided by different immune components like mucosal sIgA titers. Additionally, the induction of CTL responses can also provide vaccine induced immunity. Vaccines that induce mucosal or cellular immunity may not fulfill the requirements set for i.m. split and subunit vaccines but may provide comparable or even superior protection, especially against heterologous influenza viruses. Due to a lack of proper correlates of protection, these vaccines are only licensed after protection has been shown in elaborate, time consuming and costly efficacy studies on a large number of individuals, so called clinical effectiveness studies.
The development of new, potentially better vaccines that are delivered via alternative routes and/or providing immunity via mucosal and/or cellular components of the immune system would be strongly facilitated by reliable correlates of protection that are specific for administration route and type of immune response. Only when this is realized, the full potential of new vaccine types will be exploited.

Developing predictive animal models

There has been an ongoing debate on which animal model to choose for the development of nasal influenza vaccines. As discussed recently in an excellent review by Van der Laan et al. [6], the use of mice has advantages and disadvantages. One should be careful in the extrapolation of murine data to the human setting, especially when concerning pathology and cross-protection, mainly because mice are not a natural host for influenza. On the other hand, the in depth-knowledge of the murine immune system, the availability of in-bred strains, the low costs and the availably immunological tools, make the mouse model suitable for preliminary adjuvant testing and more fundamentally, mechanistic studies about the role that certain factors play on the efficacy of vaccines. It should be noted however that some adjuvants can have species specific properties, especially when they

act on specific receptors of the immune system, as illustrated by the different immunostimulatory effects of TMC-RA44 on murine and human DCs (**chapter 7**). There will be differences between all animal models and humans and this will always hamper the predictability of animal studies. Therefore, there will always be a chance to find different results in humans than in animals, when moving forward from preclinical to clinical studies. Understanding the mechanism of action of an adjuvant is strongly desired in the search for an appropriate animal model and can help to reduce the chance of finding unexpected results in a progressed stadium adjuvant development.

Another animal that is ofter used for influenza vaccine testing is the ferret. The ferret is a better animal model regarding translation to humans because influenza susceptibility and pathology is comparable for humans and ferrets. It would be a great step forward if more immunological tools became available for the ferret and the development of a specific pathogen free (SPF) inbred ferret strain is desired. Also, more in depth knowledge of their immune system is absolutely necessary.
In the case of i.n. vaccination, developing the optimal animal model becomes even more difficult. In addition to the concerns about immunology, susceptibility, pathology and available tools, the nasal anatomy varies strongly between all animal models and humans. The importance of a comparable nasal anatomy in the predictive value of nasal vaccination studies in an animal model should be further studied. It is likely that there are significant differences between species concerning the immunological structures in the nasal cavity, like the presence, location and number of M-cells; the location and type of dendritic cells and other immune cells; and the sensitivity of the nasal route for inducing immune responses against antigens. Moreover, we should take into account factors influencing the delivery of antigens, such as the relative surface of the nasal mucosa, the properties of the excreted mucus and the mucociliary clearance. These properties will also differ between the various animals and humans and may play a role in the predictability of animal models. In light of these difficulties, it is better to investigate the mode of action in an early fase of development. This would help in the development of an appropriate animal model, reducing the amount of animals that are needed in preclinical evaluation.

Viability of TMC-WIV as a human influenza vaccine

To cope with a surge in pandemic vaccine demand when/if an influenza pandemic with high pathogenicicity has started, several antigen sparing strategies have been proposed by the WHO to increase vaccine production capacity by decreasing the required antigen dose per vaccine [7]. The use of i.m. WIV vaccines in the case of a pandemic, combined with licensed adjuvants has been indicated as the best approach for antigen sparing in vaccines.
At the same time, regulatory authorities enabled vaccine manufacturers with licensed seasonal influenza products on the market to short-track their pandemic vaccine licensing by using the same production methods. This leads to a preference for the development of "old-fashioned" pandemic influenza vaccines, and discourages vaccine producers to develop novel, potentially better vaccines.
In this light, it is unlikely that inactivated i.n. vaccines, like the TMC-WIV formulations described

in this thesis, will be developed for pandemic vaccination within the next few years, mainly because these vaccines still require more antigen than for the i.m. route, especially when HI is used as a correlate of protection.
To develop such influenza vaccines for pandemic as well as seasonal influenza, public awareness and understanding of the benefits of influenza vaccines is crucial, because this will provide the vaccine industry with solid demand for vaccines in the future. This, in turn, is an important incentive for vaccine producers to invest in development and licensing of novel influenza vaccines, like i.n. inactivated influenza vaccines.

If further research provides encouraging results in other animal models and, ultimately, in humans, i.n. inactivated influenza vaccines, like the TMC-WIV vaccines described in this thesis may become a useful addition to the current influenza vaccines. This requires definition of the right correlates of protection and an optimal safety/efficacy balance in the target populations, like the elderly.
Needle-free administration may increase vaccine intake in the communities and the simple administration no longer requires trained personnel, resulting in herd community and cost savings, respectively. Furthermore, evidence is accumulating that sIgA has the potential to provide a broad, heterosubtypic protection, a feature that is very helpful not only in protecting against seasonal, drifting influenza viruses, but also against pandemic strains that are still mutating or not exactly known. Ultimately, when worldwide seasonal influenza vaccine intake has increased, resulting in increased production capacity, i.n. influenza vaccines, like the TMC-WIV vaccines described in this thesis, may be used for pandemic vaccines as well.

References

[1] Verheul RJ, Amidi M, van der Wal S, van Riet E, Jiskoot W, Hennink WE. Synthesis, characterization and in vitro biological properties of O-methyl free N,N,N-trimethylated chitosan. Biomaterials 2008;29(27):3642-9.

[2] Verheul RJ, Amidi M, van Steenbergen MJ, van Riet E, Jiskoot W, Hennink WE. Influence of the degree of acetylation on the enzymatic degradation and in vitro biological properties of trimethylated chitosans. Biomaterials 2009;30(18):3129-35.

[3] Kunz C, Hofmann H, Bachmayer H, Liehl E, Moritz A, SchmidtG. [A new influenza subunit vaccine: reactogenicity and antigenicity in comparison to split and whole virus vaccines (author's transl)]. Infection 1976;4(2):73-9.

[4] Gross PA, Ennis FA, Gaerlan PF, Denson LJ, Denning CR, Schiffman D. A controlled double-blind comparison of reactogenicity, immunogenicity, and protective efficacy of whole-virus and split-product influenza vaccines in children. J Infect Dis 1977;136(5):623-32.

[5] Hobson D, Curry RL, Beare AS, Ward-Gardner A. The role of serum haemagglutination-inhibiting antibody in protection against challenge infection with influenza A2 and B viruses. J Hyg (Lond) 1972;70(4):767-77.

[6] van der Laan JW, Herberts C, Lambkin-Williams R, Boyers A, Mann AJ, Oxford J. Animal models in influenza vaccine testing. Expert Rev Vaccines 2008;7(6):783-93.

[7] World Health Organization. Global pandemic influenza action plan to increase vaccine supply. 2006.

Affiliations of collaborating authors

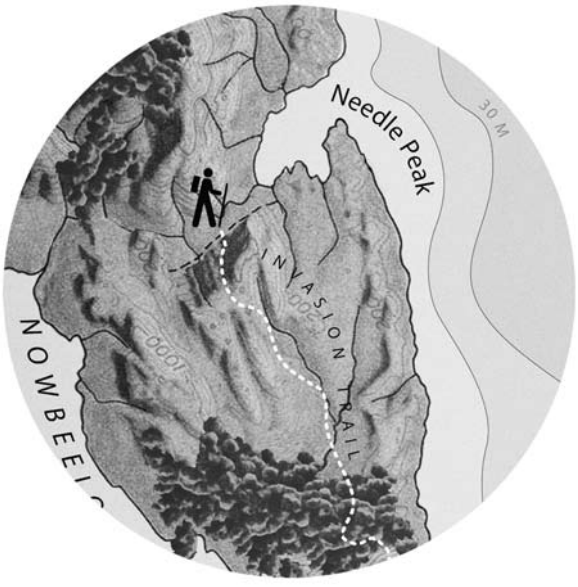

In alphabetical order:

Didier Betbeder
Laboratoire de Physiologie, Faculté de Médecine, Université de Lille 2, Lille, France

Han van den Bosch
Nobilon, part of Schering Plough, Boxmeer, The Netherlands

Sven Bruijns
Department of Molecular Cell Biology and Immunology, Vrije University Medical Center, Amsterdam, The Netherlands

Thomas van Es
Department of Molecular Cell Biology and Immunology, Vrije University Medical Center, Amsterdam, The Netherlands

Ethlinn van Gaal
Department of Pharmaceutics, Utrecht Institute for Pharmaceutical Sciences, Utrecht University, Utrecht, The Netherlands

Harrie Glansbeek
Nobilon, part of Schering Plough, Boxmeer, The Netherlands

Jacco Heldens
Nobilon, part of Schering Plough, Boxmeer, The Netherlands

Wim Hennink
Department of Pharmaceutics, Utrecht Institute for Pharmaceutical Sciences, Utrecht University, Utrecht, The Netherlands

Wim Jiskoot
Division of Drug Delivery Technology, Leiden/Amsterdam Center for Drug Research, Leiden University, Leiden, The Netherlands

Pascal de Jong
Department of Pharmaceutics, Utrecht Institute for Pharmaceutical Sciences, Utrecht University, Utrecht, The Netherlands

Eric Kaijzel
Department of Endocrinology and Metabolic Diseases, Leiden University Medical Center, Leiden, The Netherlands

Yvette van Kooyk
Department of Molecular Cell Biology and Immunology, Vrije University Medical Center, Amsterdam, The Netherlands

Clemens Löwik
Department of Endocrinology and Metabolic Diseases, Leiden University Medical Center, 2300 Leiden, The Netherlands

Marta Mania
Department of Pharmaceutics, Utrecht Institute for Pharmaceutical Sciences, Utrecht University, Utrecht, The Netherlands

Enrico Mastrobattista
Department of Pharmaceutics, Utrecht Institute for Pharmaceutical Sciences, Utrecht University, Utrecht, The Netherlands

Imke Mooren
Animal services department, Intervet Schering-Plough Animal Health, Boxmeer, The Netherlands

Rob Nieuwland
Department of toxicology Intervet Schering-Plough Animal Health, Boxmeer, The Netherlands

Ivo Que
Department of Endocrinology and Metabolic Diseases, Leiden University Medical Center, Leiden, The Netherlands

Virgil Schijns
Nobilon, part of Schering Plough, AH Boxmeer, The Netherlands

Bram Slütter
Division of Drug Delivery Technology, Leiden/Amsterdam Center for Drug Research, Leiden University, RA Leiden, The Netherlands

Rolf Verheul
Department of Pharmaceutics, Utrecht Institute for Pharmaceutical Sciences, Utrecht University, Utrecht, The Netherlands

Herman Vromans

Department of Pharmaceutics, Organon, part of Schering Plough, Oss, the Netherlands

Department of Pharmaceutics, Utrecht Institute for Pharmaceutical Sciences, Utrecht University, Utrecht, The Netherlands

Nederlandse samenvatting

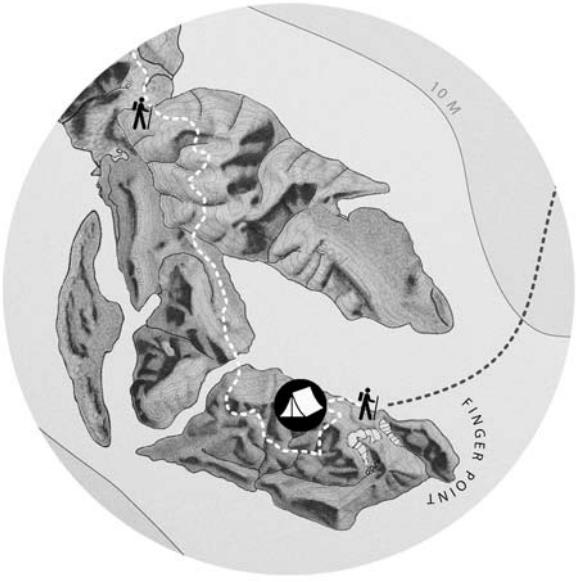

Ieder winterseizoen veroorzaken influenza A en B virussen een griepepidemie waarvan de hevigheid kan variëren. De griep –of influenza– wordt veroorzaakt door besmetting met het griepvirus of influenzavirus. Het griepvirus bestaat uit een klein deeltje dat is opgebouwd uit verschillende eiwitten en de genetische codering van het virus in de vorm van RNA –vergelijkbaar met DNA-Besmetting met een griepvirus leidt tot een infectie van de luchtwegen die meestal zonder complicaties na een aantal dagen overgaat. Bij mensen met een verhoogd risico, zoals ouderen en chronisch zieken, kan de griep echter leiden tot ernstige complicaties, zelfs met de dood als gevolg. Zodoende zijn griepepidemieën een substantiële belasting voor de maatschappij. Naast deze jaarlijkse griepuitbraken ontstaat er iedere 10-30 jaar een grieppandemie, een wereldwijde uitbraak van de griep, waarbij een nieuw griepvirus wordt geïntroduceerd in de menselijke populatie. Afhankelijk van de eigenschappen van zo'n virus kan een pandemie desastreuze gevolgen hebben voor de wereldbevolking, zoals het geval was bij de Spaanse griep tijdens de eerste wereldoorlog. De huidige Mexicaanse griep is ook zo'n pandemische griep, maar lijkt tot nu toe mild van aard. De H5N1 vogelgriep die eind jaren negentig in zuidoost Azië is opgedoken, is daarentegen zeer dodelijk maar is nog niet in staat zich gemakkelijk van mens tot mens te verspreiden.
De beste bescherming tegen griep is vaccinatie. Vaccinatie is het opwekken van een afweerreactie tegen een bepaalde stof (antigeen), vaak een eiwit. Het menselijk lichaam herkent dit antigeen als lichaamsvreemd –d.w.z. als een soort indringer– en gaat vervolgens antistoffen –ook wel antilichamen genoemd– aanmaken. Deze antilichamen herkennen vervolgens het antigeen wanneer ze daar in een later stadium –dit kan variëren van een paar dagen tot soms jaren later– mee in contact komen. Het immuunsysteem ruimt de indringer dan op voordat deze gevaarlijk kan worden. Door toediening van geïnactiveerde (dode) griepvirussen of eiwitten (antigenen) afkomstig van het griepvirus kan iemand op deze manier in het vervolg beschermd worden tegen besmetting met dat virus. Ook worden soms verzwakte, levende virussen gebruikt waar je niet ziek van wordt maar die wel antilichamen opwekken.

Griepvaccins worden al gebruikt sinds de 40er jaren van de vorige eeuw. Tot op heden worden bijna alle griepvaccins geproduceerd door het kweken van griepvirussen op bevruchte kippeneieren en de virussen vervolgens te oogsten, eventueel te inactiveren, te zuiveren en de virusdeeltjes of daaruit gezuiverde eiwitten (antigenen) in de juiste dosis in een injectiespuit te stoppen. Bijna alle geregistreerde griepvaccins worden via een intramusculaire (i.m.; in de spier) injectie toegediend. Toediening van griepvaccins via de intranasale (i.n.; in de neus) route biedt een aantal voordelen boven de traditionele route in de spier. Zo is voor de toediening geen naald nodig maar kan eenvoudig plaatsvinden in de vorm van neusdrupels of een neusspray, waardoor het vaccin niet langer door een arts of verpleegkundige hoeft te worden toegediend. Bovendien biedt de i.n. toedieningsroute het voordeel dat naast het opwekken van antilichamen in het bloed ook antilichamen worden uitgescheiden op de slijmvliezen in de neus en longen. Dit is de natuurlijke infectieroute van het griepvirus en zo kan het virus dus direct bij binnenkomst aangepakt worden voor het zich verspreidt in het lichaam.
Vaccins die via de neus worden toegediend zijn slechts gedurende een korte periode in de neus

aanwezig voordat ze door trilhaartjes naar de keel en uiteindelijk de maag worden afgevoerd. Eenmaal in de maag aangekomen worden ze afgebroken door het maagzuur en daarin aanwezig enzymen, waardoor ze niet meer werken. De grote uitdaging is er voor te zorgen dat het vaccin, in de korte tijd dat ze in de neusholte aanwezig zijn, opgenomen wordt door het neusslijmvlies en vervolgens een immuunreactie opwekt.

De griepvaccins die worden toegediend via de neus zijn onder te verdelen in levende, verzwakte griepvirussen en geïnactiveerde (dode) griepvirussen of bepaalde eiwitten daarvan. Er zijn reeds via de neus toegediende griepvaccins op de markt in de Verenigde Staten en Rusland. Deze vaccins bevatten levende, verzwakte griepvirussen. Van de geïnactiveerde (dode) vaccins zijn nog geen i.n. vaccins beschikbaar, maar er zijn wel positieve resultaten bereikt in preklinisch onderzoek. Echter, voor beide typen i.n. griepvaccins geldt dat de optimale combinatie van veiligheid (geen bijwerkingen) en effectiviteit (bescherming) nog niet voor alle doelgroepen, inclusief ouderen, gevonden is. Voor de geïnactiveerde i.n. influenzavaccins geldt eigenlijk dat deze een hulpstof, ook wel een adjuvans genoemd, nodig hebben die de immuunrespons versterkt.

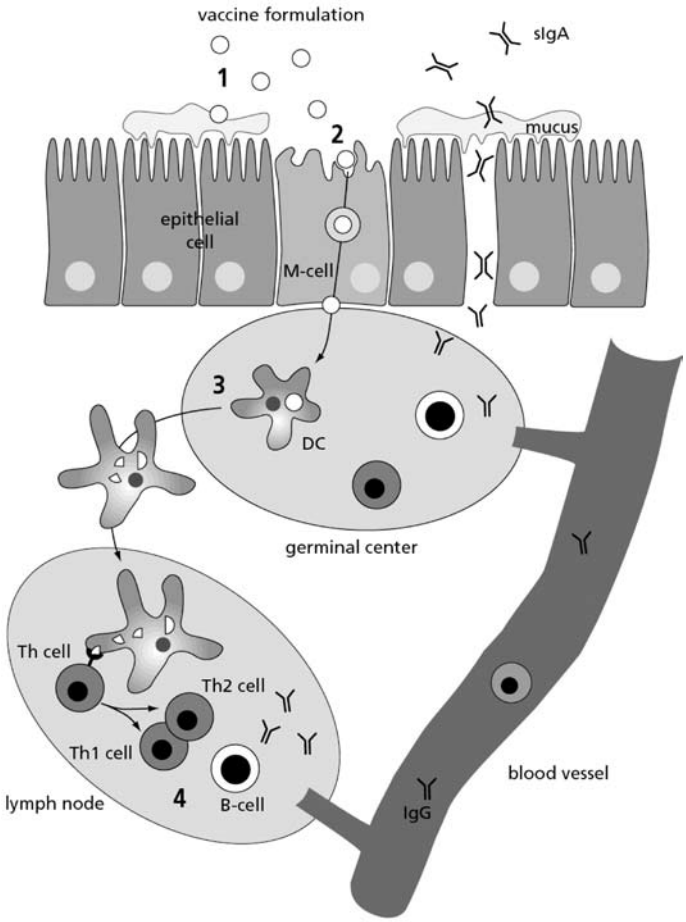

Figuur 1. Schematische weergave van de geplande route naar een immuunrespons na vaccinatie via de neus. 1) Na toediening moet het vaccin in contact komen met de oppervlaktes van het neusslijmvlies; 2) Vervolgens moet het antigeen worden opgenomen; 3) Transport naar en activatie van DC's; 4) Het aanmaken van antilichamen.

Het kerndoel van het in dit proefschrift is beschreven onderzoek is het ontwerpen van een geïnactiveerd i.n. griepvaccin. Om dit te bereiken, is het van belang eerst helder te krijgen welke fysiologische factoren een rol spelen bij de effectiviteit van i.n. griepvaccins. Vervolgens moet onderzocht worden of het mogelijk is om het vaccin effectiever te maken, door te sleutelen aan de samenstelling, zodat deze fysiologische factoren de effectiviteit niet meer begrenzen. Daarna is het interessant om uit te zoeken wat het achterliggende mechanisme is van de verbeterde effectiviteit van deze vaccins.

In hoofdstuk 2 wordt aan de hand van een literatuurstudie een "routeplanning" voor succesvolle i.n. vaccinatie beschreven (zie Figuur 1).

Na toediening via de neus zal het antigeen moeten worden afgeleverd bij antigeen-presenterende cellen, zoals dendritische cellen (DC's), die vervolgens een immuunrespons kunnen initiëren. Alvorens het antigeen bij de DC's terechtkomt, zal het na toediening eerst in contact komen met het neusslijmvlies, ook wel mucosa genoemd. Vervolgens zal het antigeen opgenomen moeten worden door de neusepitheelcellen of gespecialiseerde M-cellen, voordat het is afgevoerd door trilhaartjes naar de keelholte. M-cellen bemonsteren de neusholte voor potentieel gevaarlijke indringers zoals virussen. Ze zijn daarom ook gespecialiseerd in het opnemen van deeltjes uit de neus die de grootte hebben van virussen, die hen vervolgens aan het immuunsysteem aanbieden zodat ze kunnen worden opgeruimd.
De effectiviteit van vaccins via de neus zou kunnen worden verbeterd door de verblijftijd van het antigeen in de neus te verlengen, waardoor het meer kans heeft te worden opgenomen. Er zijn grote moleculen die zich sterk aan mucus en slijmvliezen binden, genaamd mucoadhesieve polymeren, zoals chitosan en het daarvan afgeleide *N,N,N,*-trimethylchitosan (TMC). Deze stoffen kunnen als adjuvans aan vaccins worden toegevoegd om de immuunreactie na toediening via de neus te versterken. Het idee is dat TMC als een soort moleculaire lijm werkt waardoor de verblijftijd van het antigeen in de neus langer wordt en het contact tussen het antigeen en het neusslijmvlies wordt verbeterd, waardoor meer antigeen wordt opgenomen door het neusslijmvlies. De opname door het neusslijmvlies, in het bijzonder door M-cellen, is groter voor deeltjes met de grootte van een virusdeeltje, zo tussen de 50 en 500 nanometer (1 nanometer = 1 miljoenste millimeter), genaamd nanodeeltjes.
Na opname door het epitheel moet het antigeen opgenomen worden door de DC's die achter het slijmvliesoppervlak liggen. Deze cellen zijn de grote schakel in het starten van de immuunrespons. De DC's moeten dus worden gestimuleerd, anders gebeurt er niet veel. Daarnaast zullen de DC's geïnstrueerd moeten worden welke signalen ze moeten doorgeven aan andere immuuncellen, zodat een optimale, beschermende immuunrespons wordt opgewekt. Het stimuleren en instrueren van DC's kan bevorderd worden door bepaalde adjuvantia toe te voegen aan het vaccin.
Er zijn 4 soorten geïnactiveerde griepvaccins die veel gebruikt worden: Geïnactiveerd virusvaccin (in het Engels whole inactivated virus (WIV) vaccine), split-vaccin, subunit-vaccin en virosomen (zie Figuur 2).

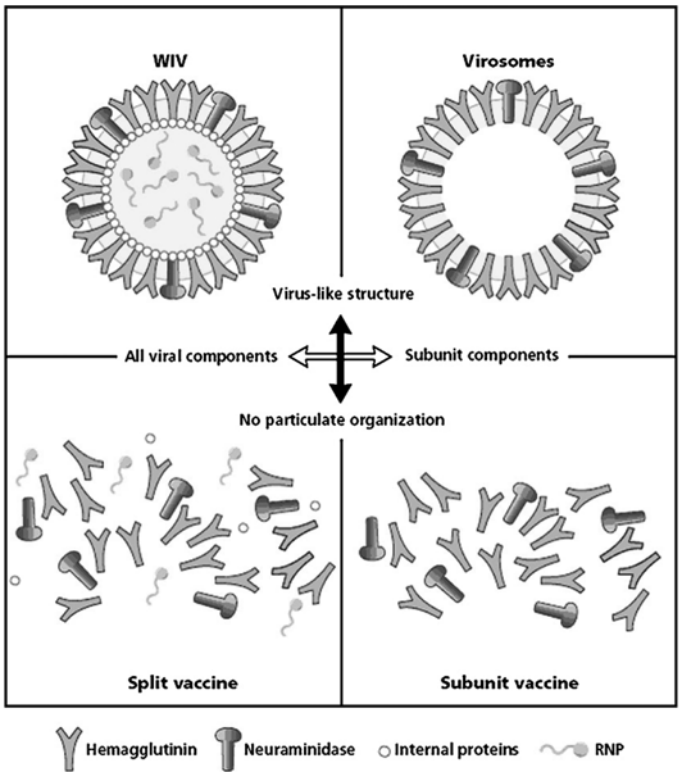

Figuur 2: Schematische weergave van de samenstelling (vergelijk de linker helft met de rechter helft) en ruimtelijke organisatie (vergelijk de bovenste helft met de onderste helft) van antigenen in WIV-, split-, subunit- en virosomale vaccins.

Deze formuleringen verschillen onderling in de samenstelling van de viruscomponenten en de ruimtelijke organisatie van de antigenen, zoals weergegeven in figuur 1. WIV- en split-vaccin bevatten allebei alle virale componenten, terwijl subunit-vaccin en virosomen alleen de buitenste eiwitten van het griepvirus bevatten (de interne eiwitten en de genetische informatie –weergegeven als bolletjes en sliertjes– zijn verwijderd). Daarnaast hebben WIV en virosomen een georganiseerde structuur van de antigenen in nanodeeltjes, terwijl in split- en subunit-vaccins de antigenen in opgeloste vorm aanwezig zijn.

In **hoofdstuk 3** is de invloed van deze onderlinge verschillen in vaccinformulering op de effectiviteit bestudeerd door muizen te vaccineren via de neus en de spier. In dit soort studies worden muizen eerst gevaccineerd en wordt na enige tijd –hier 3 weken na de vaccinatie– bloed afgenomen om te kijken of de muizen antilichamen in hun bloed hebben. Een aantal muizen wordt opgeofferd voor het doen van een neuswassing om naar de lokale antilichaamproductie in de neus te kijken. Vervolgens worden de nog levende muizen met verneveld levend griepvirus in contact gebracht waardoor ze het virus inademen. Als het vaccin goed heeft gewerkt dan zijn muizen beschermd en worden niet ziek, terwijl een slecht vaccin de muizen niet kan beschermen waardoor ze ziek worden en gewicht beginnen te verliezen.
Vaccinatie via de spier wekte met alle vaccins veel hogere antilichaamconcentraties in het bloed en

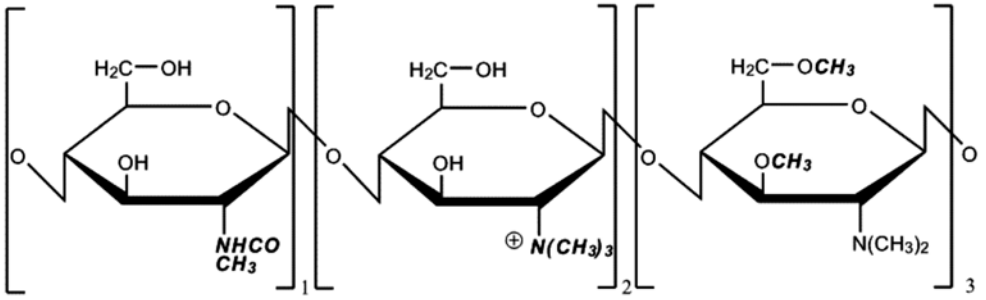

Figuur 3. TMC is een hele lange keten van 3 soorten blokken zoals hierboven weergegeven. TMC's kunnen verschillen in ketenlengte (het aantal blokken achter elkaar), ladingsdichtheid (hoeveel procent is blok 2 aanwezig), O-methylering (hoeveel procent is blok 3 aanwezig) en acetylering (hoeveel procent is blok 1 aanwezig).

betere bescherming tegen levend virus op dan vaccinatie via de neus. Na toediening via de neus werden er alleen antilichaamspiegels gemeten na vaccinatie met WIV- of split-vaccin, die slechts gedeeltelijke bescherming boden. Vaccins die alle virale componenten bevatten (WIV- en split-vaccin), bleken dus effectiever dan vaccins die slechts een deel van de virale componenten bevatten (subunit vaccin en virosomen). Interessant genoeg wekte WIV, ongeacht de toedieningsroute, een ander type antilichamen op in het bloed dan de andere vaccins. Daarnaast was WIV als enige in staat na toediening via de neus een lokale afweerreactie in de neusholte op te wekken.

deze resultaten werd WIV gekozen als de meest veelbelovende kandidaat voor verdere ontwikkeling als vaccin voor toediening via de neus. Gezien de grote verschillen in immuunresponsen tussen de toedieningsroutes, lijkt de effectiviteit vooral verminderd te worden na toediening via de neus. Blijkbaar is het dus moeilijk voor het antigeen om de immuuncellen via de neus te bereiken. Zoals al eerder werd uitgelegd zou de korte verblijftijd van het antigeen in de neus en de opname door het neusslijmvlies wel eens de bottleneck kunnen zijn. Door gebruik te maken van mucoadhesieve polymeren zou het antigeen mogelijk via de neus ook een goede immuunrespons kunnen opwekken omdat het dan wl de immuuncellen bereiken.
TMC, een positief geladen wateroplosbaar en mucoadhesief polymeer is in eerdere studies veelbelovend gebleken als adjuvans in vaccins die via de neus worden toegediend. TMC is een verzamelnaam voor een groep polymeren met veel overeenkomsten in chemische structuur maar met specifieke verschillen (bijvoorbeeld de ketenlengte, ladingsdichtheid, methylering en acetylering)(Zie figuur 3).

Zoals beschreven in **hoofdstuk 4**, werden er positief geladen nanodeeltjes gemaakt door het negatief geladen WIV te mengen met TMC. Hierdoor wordt een deel van de TMC-moleculen gebonden aan WIV als een soort coating, terwijl andere TMC-moleculen vrij in oplossing blijven (Zie figuur 4). Deze deeltjes noemen we TMC-WIV.

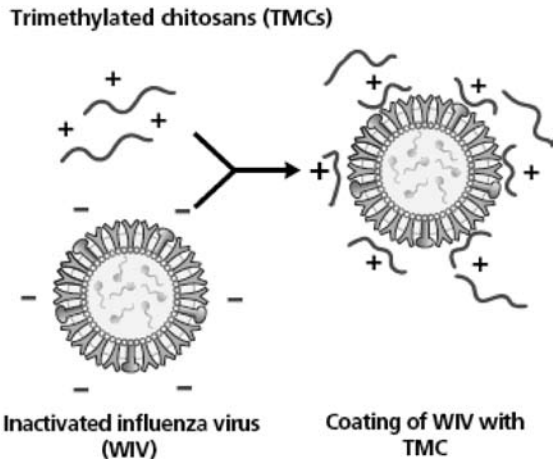

Figuur 4 Door negatief geladen, geïnactiveerde virusdeeltjes te mengen met positief geladen TMC moleculen, worden de virusdeeltjes met een laagje TMC-moleculen bedekt en krijgen ze een positieve lading. De niet gebonden TMC-moleculen zijn vrij in oplossing.

Vaccinatie via de neus met TMC-WIV wekte significant sterkere immuunresponsen op en gaf betere bescherming dan vaccinatie met WIV alleen.

In **hoofdstuk 5** hebben we verder uitgezocht welke van de in figuur 3 beschreven structuureigenschappen van TMC invloed hebben op de effectiviteit van TMC-WIV-vaccins. Om dit te onderzoeken werden er TMC-WIV-vaccins gemaakt met verschillende TMC's. Alle TMC–WIV-deeltjes waren positief geladen en ongeveer even groot, ongeveer 200 nm in diameter.
De immunogeniciteit van de TMC-WIV-vaccins –dit is de mate waarin het vaccin een immuunrespons opwekt– was vergelijkbaar voor de meeste TMC's en significant beter dan WIV zonder TMC. Bovendien waren de gevaccineerde muizen beschermd tegen infectie met levend griepvirus. Hieruit bleek dat de ladingsdichtheid en de methylering van TMC amper invloed hebben op de activiteit van TMC als adjuvans. Daarentegen bleek dat een verhoogde acetylering van TMC –dus een hoger percentage van blok 1 uit figuur 3 in de polymeerketen– een negatief effect had op het adjuvanseffect. Dit bleek uit lagere antilichaamtiters en matige bescherming na blootstelling aan levend virus.

In **hoofdstuk 6** werd verder uitgezocht waarom de TMC-WIV-formuleringen nu beter werkten dan het kale WIV vaccin. De verblijftijd van het TMC-WIV-vaccin, zichtbaar gemaakt met behulp van fluorescentie, bleek vergelijkbaar met die van kaal WIV. Deze bevinding werd bevestigd in weefselkleuringen van dwarsdoorsneden van de neusholtes van muizen. Blijkbaar is de verbeterde immuunrespons van TMC-WIV-vaccins niet het gevolg van een verlengde nasale verblijftijd.
Deze experimenten lieten ook zien dat de TMC-WIV-vaccins een andere distributie in de neusholte hadden dan WIV. WIV werd voornamelijk teruggevonden in de neusholte in losse klodders (vermoedelijk mucus), terwijl TMC-WIV vooral op de oppervlaktes van het neusepitheel aanwezig was. TMC-WIV had dus een groter contactoppervlak met het epitheel. Dat zou kunnen leiden tot

een verhoogde opname van het antigeen door het epitheel, wat de toegenomen immunogeniciteit zou kunnen verklaren.
Zoals eerder genoemd, staat de veiligheid van vaccins voorop en daarom werd de toxiciteit van verschillende TMC-WIV-vaccins in de neus getest. Alle TMC-WIV-vaccins wekten een minimale lokale toxiciteit op, die vergelijkbaar is met het kale WIV-vaccin, wat aangeeft dat er van TMC weinig lokale bijwerkingen zijn te verwachten.

Met behulp van verschillende technieken is in **hoofdstuk 7** onderzocht waarom TMC met een verhoogde acetyleringsgraad (TMC-RA) minder goed werkt als adjuvans dan de andere TMC's. In neuswassingen van muizen bleek TMC-RA sneller te worden afgebroken dan TMC, terwijl geen verschil waargenomen kon worden tussen de verblijftijd in de neus van TMC-WIV en TMC-RA-WIV. De locatie van het antigeen in de neusholte was ook vergelijkbaar tussen TMC-WIV en TMC-RA-WIV. De verhoogde acetyleringsgraad lijkt dus geen effect te hebben op de distributie, de nasale verblijftijd en het contactoppervlak met het neusslijmvlies. Zodoende kunnen deze factoren het verminderde adjuvantseffect van TMC-RA niet verklaren. De opname van WIV door epitheelcellen bleek door TMC en TMC-RA versterkt te worden, maar de opname was duidelijk minder na formulering met TMC-RA in vergelijking met TMC. Onlangs is ook een aantal initiële studies gedaan met DC's uit het beenmerg van muizen en DC's uit mensenbloed om er achter te komen of de TMC's ook een stimulerend effect hebben op DC's; de cellen die de uiteindelijke immuunrespons grotendeels "regisseren". De verschillende TMC's bleken op muizen DC's geen sterk stimulerend effect te hebben. Op grond van deze studies lijkt het er dus op dat de snellere afbraak en de verminderde opname door epitheelcellen het verminderde adjuvanseffect van TMC-RA zouden kunnen verklaren.
In tegenstelling tot de resultaten op de muizen DC's, had TMC-RA op DC's van mensen een veel sterker activerend effect in vergelijking tot de andere TMC's of WIV zelf. Het is opmerkelijk dat het TMC-RA op DC's van mensen juist het meest immuunstimulerend werkte, terwijl het in muizen juist minder hoge immuunresponsen opwekte. Er moeten nog meer studies worden gedaan om de ware toedracht van deze waarnemingen te achterhalen.

Een ander belangrijk aspect in de ontwikkeling van deze vaccins is de stabiliteit van de TMC-WIV-deeltjes. In **hoofdstuk 8** werd de invloed van verschillende TMC-varianten op de lading en grootte van de TMC-WIV-deeltjes onderzocht met behulp van zeta-potentiaalmetingen en dynamische-lichtverstrooiingsmetingen. Een minimale hoeveelheid TMC was nodig om stabiele positief geladen deeltjes te krijgen. Bij lagere TMC/WIV-verhoudingen nam de lading af en klonterden de deeltjes na verloop van tijd samen. Bij een 1:1 gewichtsverhouding van TMC/WIV waren de TMC-WIV-deeltjes stabiel over een periode van 2 weken, ongeacht het type TMC dat werd gebruikt. Een aantal formuleringen was na 4 maanden nog stabiel. In aanwezigheid van zout waren de TMC-WIV-vaccins minder stabiel, afhankelijk van de TMC-variant.
Het onderzoek dat in dit proefschrift staat beschreven heeft geresulteerd in een rationeel ontworpen, geïnactiveerd griepvaccin voor toediening via de neus gebaseerd op WIV en geadjuveerd met

TMC. De rol van verschillende fysiologische processen op het pad naar succesvolle immunisatie via de i.n. route zijn onderzocht, waaronder mucociliaire klaring, distributie van het antigeen in de neusholte, opname door epitheelcellen en activatie van dendritische cellen. Mogelijkheden om het vaccin te verbeteren door te sleutelen aan de antigeensamenstelling en de toevoeging van TMC als adjuvans, werden bestudeerd. Daarnaast is het werkingsmechanisme van TMC als i.n. vaccinadjuvans onderzocht. Tot slot is een verkennende studie gedaan naar de stabiliteit van TMC-geadjuveerde WIV-vaccins. Er is een geïnactiveerd influenzavaccin ontwikkeld dat veelbelovende resultaten heeft laten zien, welke aanleiding geven tot verdere preklinische en klinische ontwikkeling.

Curriculum vitae

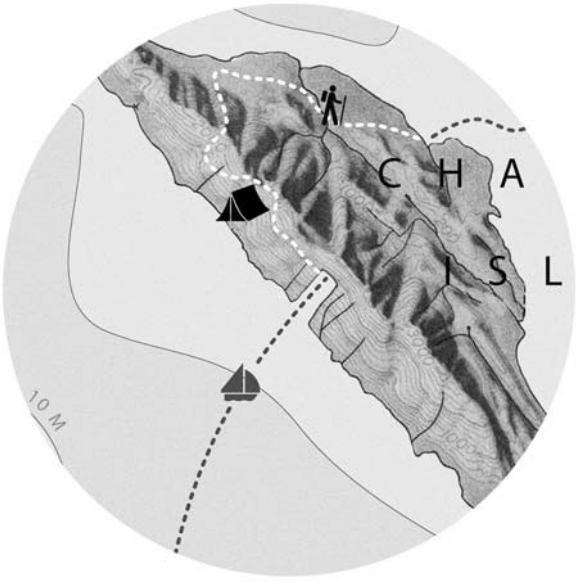

Niels Hagenaars was born on September 1st 1980 in Delft, the Netherlands. After graduating from the gymnasium in 1998 at Sint Stanislascollege in Delft, the Netherlands, he started his study pharmacy at Utrecht University, The Netherlands. In 2001 he visited the British Columbian Cancer Research Center in Vancouver, Canada, for a 6-month research project on doxorubicin-loaded, thermosensitive liposomes for cancer therapy under the supervision of Ludger Ickenstein and Lawrence Mayer. Between 2003 and 2005, Niels did internships at several community and hospital pharmacies and Octoplus BV for his masters degree. In April 2005 he became a licensed pharmacist (Pharm. D.) and in September of the same year he started his PhD project, under the supervision of prof dr. Wim Jiskoot, prof. dr. Herman Vromans and dr. Enrico Mastrobattista. This project was a collaboration with Nobilon International, part of Schering-Plough, Boxmeer, The Netherlands and resulted in this thesis. Recently, Niels started as a strategy consultant at Gupta strategists, which focuses on the health care sector in the Netherlands.

List of publications

List of publications

Hagenaars N, Slütter B, Jiskoot W. Rational design of nasal vaccines. J Drug Target. 2008 Jan;16(1): 1-17. Review

Hagenaars N, Mastrobattista E, Glansbeek H, Heldens J, van den Bosch H, Schijns V, Betbeder D, Vromans H, Jiskoot W. Head-to-head comparison of four nonadjuvanted inactivated cell culture-derived influenza vaccines: effect of composition, spatial organization and immunization route on the immunogenicity in a murine challenge model. Vaccine. 2008 Dec 2;26(51):6555-63.

Hagenaars N, Mastrobattista E, Verheul RJ, Mooren I, Glansbeek HL, Heldens JG, van den Bosch H, Jiskoot W. Physicochemical and immunological characterization of N,N,N-trimethyl chitosan-coated whole inactivated influenza virus vaccine for intranasal administration. Pharm Res. 2009 Jun;26(6):1353-64. Epub 2009 Feb 18.

Hagenaars N, Verheul RJ, Mooren I, de Jong PH, Mastrobattista E, Glansbeek HL, Heldens JG, van den Bosch H, Hennink WE, Jiskoot W. Relationship between structure and adjuvanticity of N,N,N-trimethyl chitosan (TMC) structural variants in a nasal influenza vaccine. J Control Release. 2009 Aug 25. [Epub ahead of print]

Dankwoord

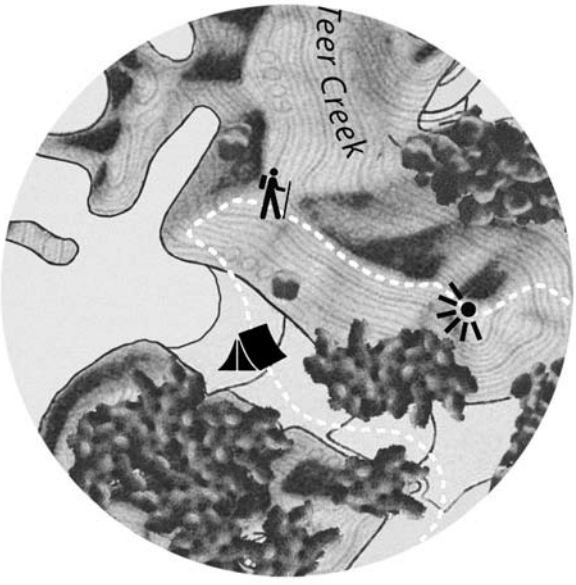

Dankwoord

Het begon allemaal met een sollicitatiegesprek bij de twee initiatoren achter deze fantastische ontdekkingsreis, Herman Vromans en Wim Jiskoot. Hoeven hier geen achternamen bij? Sindsdien is er het een en ander veranderd en verschoven.

Wim, snel nadat ik was begonnen wist je jouw rol van hoofdgids in te ruilen voor die van expeditieleider van je eigen ontdekkingsreizen. Je kreeg het daardoor stukken drukker en ons contact werd minder frequent, maar zeker niet minder waardevol. Het vertrouwen en de vrijheid die je me gaf om mijn eigen wegen te bewandelen en de betrokkenheid die je liet zien wanneer ik het nodig had, hebben veel voor me betekend. Zeker in de laatste periode ben ik er achter gekomen hoe geweldig het is om een begeleider te hebben waar je op kan terugvallen en die de verslaglegging altijd snel en scherp van commentaar voorziet. Heel erg bedankt daarvoor.

Herman, de verschuivingen in ons team hebben er toe geleid dat jij mijn verkenningstochten meer van een afstand bent gaan bekijken. Je mensenkennis, je non-conformistische no-nonsense instelling en wetenschappelijke nieuwsgierigheid heb ik altijd zeer bewonderd en hebben me in veel situaties geholpen.

Al gauw kwam er een nieuwe hoofdgids in het team. Enrico, je bent een creatieve geest die altijd nieuwe onbewandelde wegen in wil slaan. Daarnaast was je altijd een laagdrempelige vraagbaak waar ik mijn geplande routes mee doornam en verslagen mee besprak. Bedankt voor al je hulp.

Ik heb ontzettend veel hulp gehad van de professionele expeditie uit Boxmeer. Zonder jullie had ik geen schijn van kans gehad om mijn einddoel te halen. Jullie zijn een fantastische groep mensen waar ik me heel erg thuis voelde en heel veel van heb geleerd. Zonder iemand tekort te willen doen: Han, bedankt voor je betrokkenheid. Jacco, je kennis van het terrein en je visie op wat mij nog te wachten stond hebben mij telkens vooruit gebracht. Je was er altijd als ik je nodig had. Harrie, bedankt voor de tijd die je altijd voor me had, je enthousiaste meedenken en hulp bij het maken van nieuwe plannen. Imke en Rob, jullie zijn geweldig! Lizzy, Stephanie Basten en Stephanie de Weert, Lisette, Teun, Jeroen, Mike, Geert, Marien, Mark, Willem, Rinus, Paul en alle andere mensen van Nobilon R&D, Intervet ASD en pathologie: Hoiiè en bedankt!

Nadat ik op weg ging kwam ik al gauw Bram tegen. Samen hebben wij het terrein van ons onderzoek in kaart gebracht. Succes met de afronding van jouw onderzoek en bedankt voor je hulp.

Gaandeweg raakte ik dieper en dieper in nieuwe gebieden verzeild die onbegaanbaar zouden zijn voor mij alléén. Gelukkig heb ik veel hulp gehad van geweldige mensen die mij door het soms lastige terrein wisten te loodsen:

Didier: Thanks a lot for your help during the first year of my journey. Alice, Dietmar, Marij : Helaas geen mooie resultaten maar ik ben zeer dankbaar voor jullie hulp. Anne Marie van Ederen, Frits en Yanling: Dank voor jullie hulp en kennis. Ivo, Eric en Clemens: bedankt voor de mogelijkheden en hulp bij de omzwervingen in Leiden. Thomas en Sven: ik ben jullie erg dankbaar voor onze samenwerking tijdens het hectische laatste deel van mijn tocht.

Daarnaast heb ik natuurlijk heel erg veel gehad aan iedereen van het basiskamp in het Wentgebouw. De vele sociale activiteiten, behulpzaamheid, vrijheid, vriendschappen, goed onderzoek en congresbezoekjes zal ik gaan missen. Wim, ik wil je complimenteren met de manier waarop je leiding geeft aan deze groep enthousiastelingen. Ik wil je bedanken voor de vele leuke momenten die ik met je heb beleefd.

Binnen deze groep heb ik veel hulp gehad van een aantal jonge nieuwsgierige studenten. Marie, I truly enjoyed your company here and in Göteborg. Thanks for all the hard work. You are a great person. Marta, your curiosity and perseverance and talent have really pushed my research forward. I hope you will be successful in your own explorations. Pascal, je bent een gemotiveerde, zelfstandige, hard werkende en gezellige aanwinst geweest tijdens dit avontuur. Zonder jou was dit verslag een stuk minder mooi geworden. Heel veel succes in je eigen omzwervingen in de toekomt!

Verder heb ik met veel collega's mooie momenten beleefd, waaronder Mies, MarCEL, Ghassi, Sabrina, Wouter, Joris, Ellen, Bart, Marina, Maryam en natuurlijk Ethlinn. Jullie gaven kleur aan mijn onderzoekstijd.

In het bijzonder wil ik iedereen bedanken van advanced base camp Z609: Sophie, Marion, Nataša, Albert, Marcus, Albert, Laura, Abdul. Dankzij jullie voelde ik me thuis op ons lab.

Frank, we zijn tegelijk gestart en tegelijk komen onze tochten tot een eind. Je hebt me, vooral in de laatste periode, scherp gehouden en geïnspireerd. Je bent een gouden vent. Bedankt voor je steun en heel veel succes met alle reizen die de toekomst je biedt. Het ga je goed.

Rolf, mooie jongen, na alle avonturen die wij met elkaar hebben meegemaakt van sunshine coast, vreemde dansrituelen, filosofische gesprekken, een voorliefde voor het buitenleven en muzikale gedeelde noemers, hebben we uiteindelijk ook nog samengewerkt. In alle gevallen heeft het tot mooie momenten geleid. Je bent een goede collega en vriend.

Tween81; Superpikey; Mr DT10 in parrot; Whitest boy alive; Imitatie-Wim H, -Ton T. en -Bertus R; Planerbouwen; Niels, kijk eens hoe ver ik kan gooien!; Henk van Velde 1; Skinny jeans; Knut; Tetrameerstaining; Ze komen hem wel halen! Joost, de glimlach die bij het schrijven van deze ogenschijnlijk vreemde opsomming van woorden op mijn gezicht verschijnt, heb ik aan jou te danken! Dank voor je vriendschap.

Naast de wereld van ontdekkingen heb ik ook altijd een kans gehad om even niet aan alle ontberingen te denken. Familie, goede vrienden uit Pijnacker, Boys van de Reigerstraat en huize Boyo, JC Diesel, visvrienden, studiegenoten: bedankt voor alle mooie tijden die ik met jullie heb gehad de afgelopen jaren. Familie Tolboom, bedankt voor het vertrouwen en de leuke tijden die we de afgelopen 4 jaar hebben gehad.

Lieve Tanno, je onvoorwaardelijke trouw, je humor en je gezelligheid maken van jou een kei van een broer. Ik kan niet wachten je in pak te zien! Lieve pap en mam, Beetje en Rinus. Jullie hebben me al meer dan 29 jaar overspoeld met liefde, vertrouwen, energie, medeleven, vrijheid en plezier. Meer kan ik me niet wensen. Ik heb niet veel met jullie over mijn werk gesproken, maar jullie zijn van onschatbare waarde geweest.

Lieve Nelleke, jij bent mijn grootste ontdekking van de afgelopen jaren. Gaandeweg ben je een onmisbare steunpilaar geworden waar ik lief en leed mee kan delen. Je vrolijkheid, gevoel voor humor, gedrevenheid, medeleven, structuur en liefde halen in mij het beste naar boven. Wat moet ik zonder jou?